NEW YORK STATE GEOLOGICAL ASSOCIATION (NYSGA)

86th ANNUAL MEETING

October 10-12th, 2014

Aerial view of Bonnie Castle Resort located in beautiful downtown Alexandria Bay, Thousand Islands.

GEOLOGY OF THE NORTHWESTERN ADIRONDACKS AND ST. LAWRENCE RIVER VALLEY

Hosted by the St. Lawrence University Department of Geology
and
Bonnie Castle Resort

Organized by J. Chiarenzelli and D. Valentino

TABLE OF CONTENTS

OVERVIEW OF EVENTS

FRIDAY OCTOBER 10TH

Registration 4-6 pm

Welcoming Reception 5-6 pm

Friday Evening Kick-off Lecture: 7:00 pm "THE BALMAT ZN DEPOSITS OF NORTHERN NYS: GRENVILLIAN AGE, UPPER AMPHIBOLITE GRADE POLYDEFORMATION AND KM-SCALE MOBILIZATION OF WORLD CLASS ZINC OREBODIES" **Mr. William deLorraine** (St. Lawrence Zinc Corporation)

SATURDAY OCTOBER 11TH

BREAKFAST 7:00-9:00 am

SATURDAY FIELD TRIPS

A-1 LOWER PALEOZOIC SEDIMENTARY SUCCESSION OF THE ST. LAWRENCE RIVER VALLEY, NEW YORK AND ONTARIO: **A. Husinec and J. A. Donaldson** ..... p. 1-28.

A-2 MILITARY GEOLOGY OF THE BATTLE OF SACKETT'S HARBOUR (28 MAY 1813), LAKE ONTARIO, NY: **A. Stewart and R. Kleptko** ..... p. 29-55.

A-3 GEOCHEMISTRY OF TOURMALINE FROM SOME ADIRONDACKS LOCATIONS: INDICATOR OF THE HOST ENVIRONMENT: **M. Lupulescu and J. Chiarenzelli** ….. p. 56-70.

A-4 MESOPROTEROZOIC MAGMATISM OF THE ADIRONDACK LOWLANDS: THE RESULT OF CLOSURE OF THE TRANS-ADIRONDACK BACKARC BASIN: **S. Regan, W. Peck, B. Selleck, M. Wong, and J. Chiarenzelli** ….. p. 71-90.

A-5 GEOLOGY OF THE BALMAT ZINC REGION: **W. deLorraine** ….. p. 91-97.

A-6 THREE AND A HALF SKARNS: **G. Robinson and S. Chamberlain** ….. p. 98-112.

SELF-GUIDED FIELD TRIP GEOLOGY OF THE CAMBRIAN NONCONFORMITY AT THE WELLESLEY ISLAND STATE PARK NATURE CENTER: **D. Valentino** ..… p. 264-268.

Cocktail Hour: 6-7 pm

Banquet: 7-10 pm

Saturday Evening Key Note Address: **8:30 pm "**FROM ENIGMATIC STRUCTURES IN THE WESTERN DESERT OF EGYPT TO TRAINING NASA ASTRONAUTS: USING GOOGLE EARTH AS A TOOL FOR RESEARCH AND TEACHING" **Dr. Barbara Tewksbury** (Hamilton College)

SUNDAY OCTOBER 12TH

BREAKFAST 7:00-9:00 am

SUNDAY FIELD TRIPS

LIST OF FIELD TRIPS, SHORT COURSE, AND SELF-GUIDED TRIP

Saturday, October 11th

Sunday, October 12th

LOCATION AND TIMING OF EVENTS AT BONNIE CASTLE RESORT

Friday, October 10th

4:00 pm Registration table opens (Riverside Sports Bar)

5:00 pm Welcoming Reception (Riverside Sports Bar)

7:00 pm William deLorraine presentation (Holland Room)

Saturday. October 11th

7-9 am Breakfast Buffet (Manor House Restaurant)

8-9 am Pickup boxed lunches (Riverside Sports Bar)

Depart for field trips (check time and location below)*

6-7 pm Cocktail Hour (Holland Room)

7-10 pm Banquet (Holland Room)

~8:30 pm Key note address by Dr. Barbara Tewksbury (Holland Room)

Sunday, October 12th

7-9 am Breakfast Buffet (Manor House Restaurant)

Depart for field trips (check time and location below)*

***TRIP DEPARTURE TIMES AND RENDEZVOUS LOCATIONS**

A-1 9:00 am , Bonnie Castle Resort parking lot

A-2 11:00 am, Bonnie Castle Resort parking lot

A-3 9:00 am, MacDonald's parking lot in Gouverneur

A-4 8:00 am, Price Chopper Parking Lot intersection I81 and Rt. 12 Alexandria Bay

A-5 10:00 am, Aubuchon Hardware parking lot in Gouverneur across from Kinney Drugs

A-6 9:30 am , Along Rt.3 at the intersection of Richter Rd. across from church at east end of the village of Natural Bridge

A-7 Cancelled

B-1 8:30 am, Bonnie Castle Resort parking lot

B-2 9:00 am, Alexandria Bay Big M Parking lot, ~0.5 miles west of traffic light on Rt. 12

B-3 8:00 am, Bonnie Castle Resort parking lot

B-4 9:00 am, Price Chopper Parking Lot intersection I81 and Rt. 12 Alexandria Bay

B-5 9:00 am, Pierrepont Highway Department parking lot, intersection of CR 24 and 29

B-6 9:00 am, Price Chopper Parking lot in Gouverneur, 389 E. Main Street

B-7 8:30 am, 135 Nevaldine Hall (Rm. NS-135), SUNY Canton Campus, 34 Cornell Drive, Canton

Self-guided geology tour: Anytime dawn to dusk, Wellesley Island State Park, Wellesley Island (must cross bridge onto the island), Minna Anthony Common Nature Center

FRIDAY NIGHT KICK OFF LECTURE

THE BALMAT ZN DEPOSITS OF NORTHERN NYS: GRENVILLIAN AGE, UPPER AMPHIBOLITE GRADE POLYDEFORMATION AND KM-SCALE MOBILIZATION OF WORLD CLASS ZINC OREBODIES

by **WILLAM deLORRAINE** (ST. LAWRENCE ZINC CO.)

Abstract

Multiple lines of evidence suggest differentiation of sphalerite from stratiform massive sulfide ore lenses followed by cross-stratal mobilization as sulfide dikes over distances of several kilometers in rocks of the NW Adirondack Lowlands during the Upper Amphibolite facies Shawinigan (Grenville) Orogeny (ca. 1.20-1.15 Ga). This occurred within the siliceous dolomitic carbonate-evaporite sequence of upper marble prior to development of the host Sylvia Lake Syncline. "Daughter" orebodies formed when sphalerite "dikes" intruded syntectonic D2 macrofractures where they intersected stratiform massive "parent" lenses. Several daughter orebodies retain linkage to parents via thin, refolded, "durchbewegt" ore sheets traversing both stratigraphy and metamorphic fabrics. Long after intrusion of sphalerite dikes, recurrent strains partitioned along macrofracture surfaces tectonically milled, abraided and rounded admixed xenolithic fragments of wall rock contained within them. Daughter orebodies thereby acquired distinctive durchbewegung textures concomittantly nearly doubling their thicknesses while halving their tenors as macrofractures evolved into tectonic slides -- some with km-scale displacements.

Geochemical groupings of orebodies are consistent with three "SEDEX" source bed horizons. Each of these occurs a short distance stratigraphically above thick anhydrite layers of evaporite provenance. Parent sulfide lenses at these horizons are the progenitors of nearby constellations of metamorphic/metamorphosed daughter orebodies some of which occur along tectonic slides in other stratigraphic units. Lateral propagation of daughter sulfide was limited by intersection of macrofractures with anhydrite horizons wherein they dead-end. D3 tectonic dislocations on tectonic slides resulted in several daughter orebodies' dismemberment into halves offset by distances ranging up to 4000 feet/1.25km. Superposition of the nappe-scale Sylvia Lake syncline largely culminated polyphase deformation and overturned parent-daughter ore complexes on its upper limb. Long thought to have been the driving force or "tectonic engine" responsible for large scale sulfide mobilization to dilatent sites within its major and minor fold hinges, the Sylvia Lake syncline is now known to refold durchbewegt "daughter" ore sheets and thus is a relatively late stage feature in the evolution of orebodies in the district. Recognition of its status as a late stage regional isocline caused a shift in exploration focus for an undiscovered "Parent" or source bed orebody from the axial region to the upper limb of the Sylvia Lake syncline.

SATURDAY NIGHT KEY NOTE ADDRESS

FROM ENIGMATIC STRUCTURES IN THE WESTERN DESERT OF EGYPT TO TRAINING NASA ASTRONAUTS: USING GOOGLE EARTH AS A TOOL FOR RESEARCH AND TEACHING

DR. BARBARA TEWKSBURY

(HAMILTON COLLEGE)

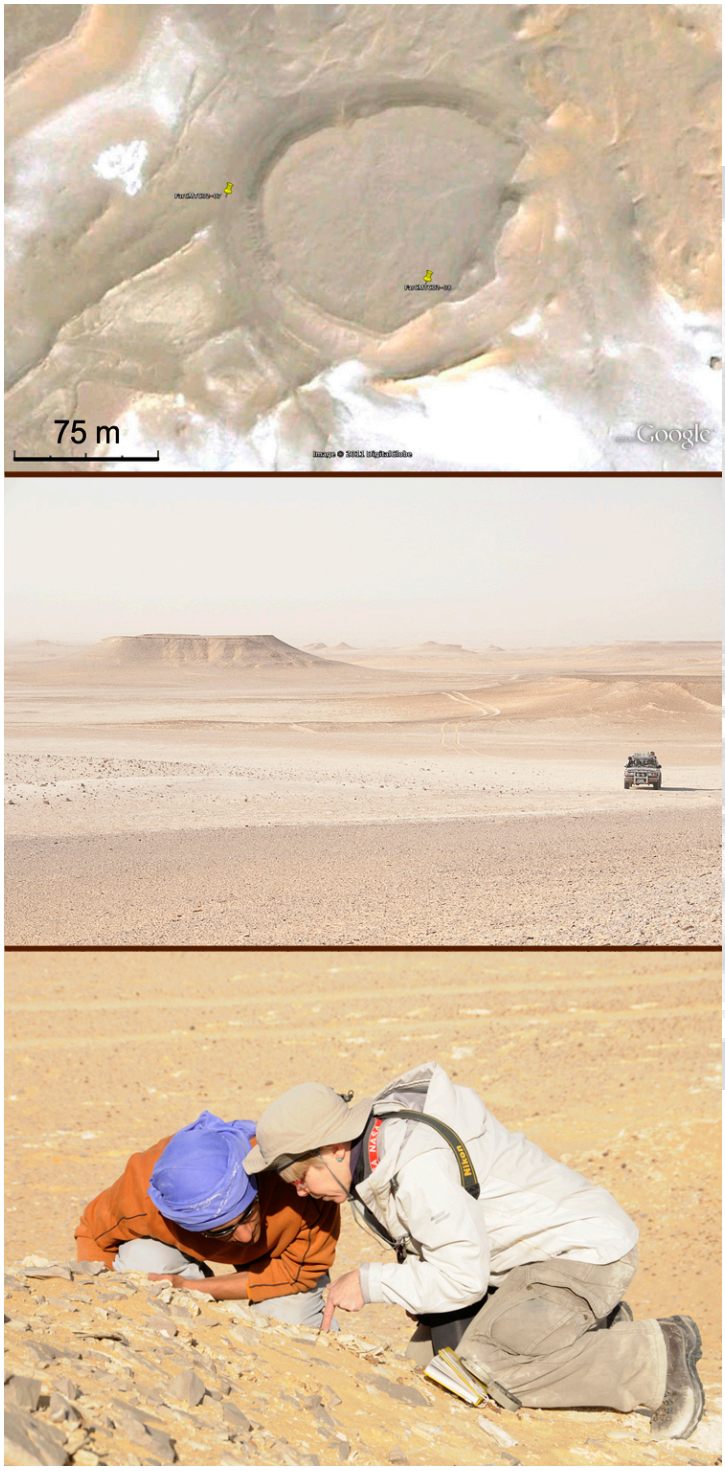

LOWER PALEOZOIC SEDIMENTARY SUCCESSION OF THE ST. LAWRENCE RIVER VALLEY, NEW YORK AND ONTARIO

ANTUN HUSINEC
Department of Geology, St. Lawrence University, Canton, NY 13617

J. ALLAN DONALDSON
Department of Earth Sciences, Carleton University, Ottawa, Ontario, Canada K1S 5B6

INTRODUCTION

Our fieldtrip to the St. Lawrence River valley in New York and Ontario will showcase the two Lower Paleozoic formations outcropping along the river (Fig. 1.), the middle to upper Cambrian Potsdam Sandstone, and lower-middle Ordovician Theresa (March in Ontario) Sandstone. We will be able to examine the non-conformable contact between Potsdam Sandstone and the underlying Proterozoic basement of the Grenville orogeny, the disconformable contact between Theresa and Potsdam Sandstones, different primary sedimentary structures, trace fossils, and microbial structures preserved within the formations.

Figure 1. Map showing locations of field trip stops in St. Lawrence Lowlands.

Potsdam Formation represents the earliest marine onlap of the Proterozoic Grenville basement and is exposed in the circum-Adirondack region of New York, and bordering areas of Quebec and Ontario (Landing, 2012) (Figs. 2, 3). The timing of the onlap is problematic due to general lack of macrofossils in the lower part of the formation (Ausable Member); the upper age bracket of this member is the Middle Cambrian based on the *Crepicephus* Zone trilobites reported from the overlying basal Keeseville Member (Lochman, 1968, Landing et al., 2009). In addition to trilobites recorded in the lowermost Keeseville Member, the Middle to Upper Cambrian age of the upper Potsdam Formation is indicated by abundant findings of trace fossils (e.g., Bjerstedt and Erickson, 1989; Erickson, 1993a, b; Erickson and Bjerstedt, 1993; Erickson et al., 1993; MacNaughton et al., 2003; Hoxie and Hagadorn, 2005; Getty and Hagadorn, 2006; Landing et al., 2007) and locally stranded medusae (Hagadorn et al., 2007).

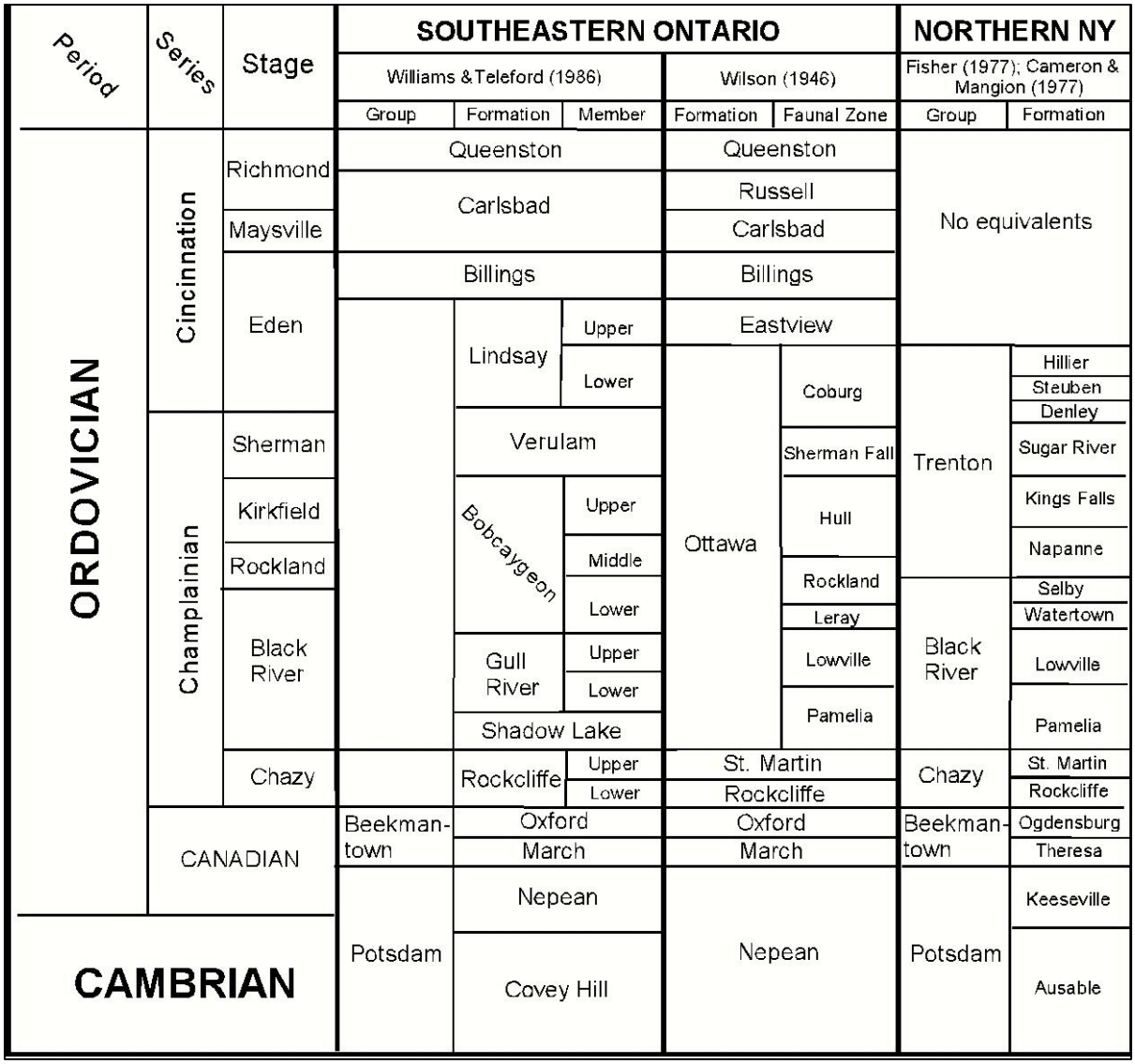

Figure 2. Nomenclature and correlation of Cambro-Ordovician lithostratigraphic units in southeastern Ontario and northern New York after Williams et al. (1992).

The basal, lower part of the Potsdam Formation (Ausable Member, not visited on this trip) is characterized by four non-marine lithofacies (McRae, 1985), including massive matrix-supported conglomerate, bedded grain-

supported conglomerate, conglomerate-arkose, and pebble conglomerate-arkose fining-upward sequences, interpreted to represent debris flows, proximal gravelly braided-stream deposits, intermediate-to-distal gravelly braided-stream deposits, and proximal sandy braided-stream deposits, respectively. These basal, arkosic deposits are both compositionally and texturally immature and contain detritus derived from the underlying weathered Proterozoic surface (McRae, 1985; Selleck, 1997). The terrestrial, braided-stream and braided alluvial plain deposition was terminated by the subsequent (Middle?) Cambrian cratonic transgression that deposited the "classic", upper Potsdam quartz arenites of the Keeseville Member. At Alexandria Bay and its vicinity (stops 1-4 of this field trip), as well as in the Redwood-Hammond area, the extreme textural maturity, lack of terrigenous silts and clays, lack of fossils, large scale of bedding, presence of silcreted sandstone breccias, and the sharp, clast-free contact with the underlying basement all suggest subaerial, possibly eolian, beach-berm-coastal dune depositional environment (Selleck, 1975) (Fig. 3). McRae (1985) argues that the provenance, compositional and textural maturity, large-scale high-angle planar cross-bedding, absence of fossils, and close association with braided fluvial deposits were consistent with interpreting these strata in the vicinity of Alexandria Bay and in Hannawa Falls as eolian. Based on provenance analysis of detrital zircon (Gaudette et al., 1981) and basal conglomerate clasts of the lower Potsdam Formation (Kirschgasser and Theokritoff, 1971; McRae, 1985; Blumberg et al., 2008), the framework grains originated from Adirondack, Superior, and Grenville provinces (Hagadorn et al., 2013). Contrary to the lower part of the Keeseville Member in the St. Lawrence Lowlands, the upper part of this member, composed of medium- to very thin-bedded, calcite- and silica-cemented fine-to-medium grained quartz arenite, clearly indicates subaqueous, nearshore, tidal deposition (Bjerstedt and Erickson, 1989). This is indicated both by presence of current ripples, herringbone cross bedding, mudcracks, soft sediment deformation, trace fossil assemblages of low-level suspension feeders of the *Skolithos* ichnofacies (*Diplocraterion sp.*, *Monocraterion* sp., *Skolithos* sp.) (Bjerstedt and Erickson, 1989), as well as by rare presence of the inarticulate brachiopod *Lingulepis acuminate* (Selleck, 1984). The Potsdam Formation varies in thickness from a few tens of meters at southern localities of the New York promontory region, to more than 650 m north of Plattsburg, New York (Landing, 2012).

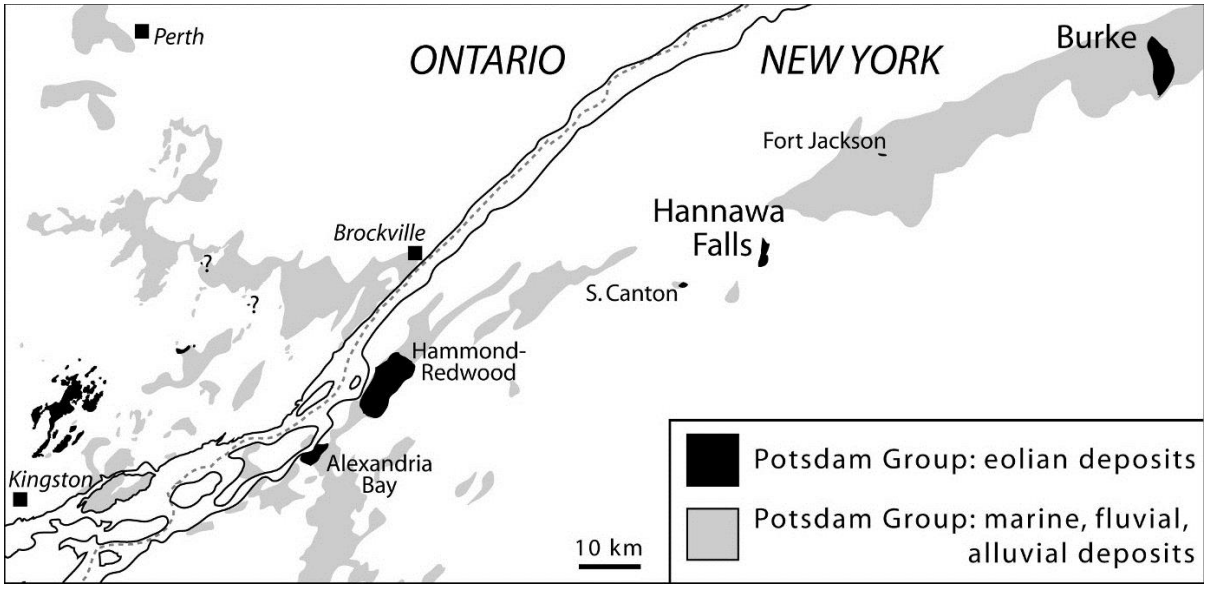

Figure 3. Map showing all Potsdam Fm. outcrops in St. Lawrence Lowlands. Modified from Hagadorn et al. (2011).

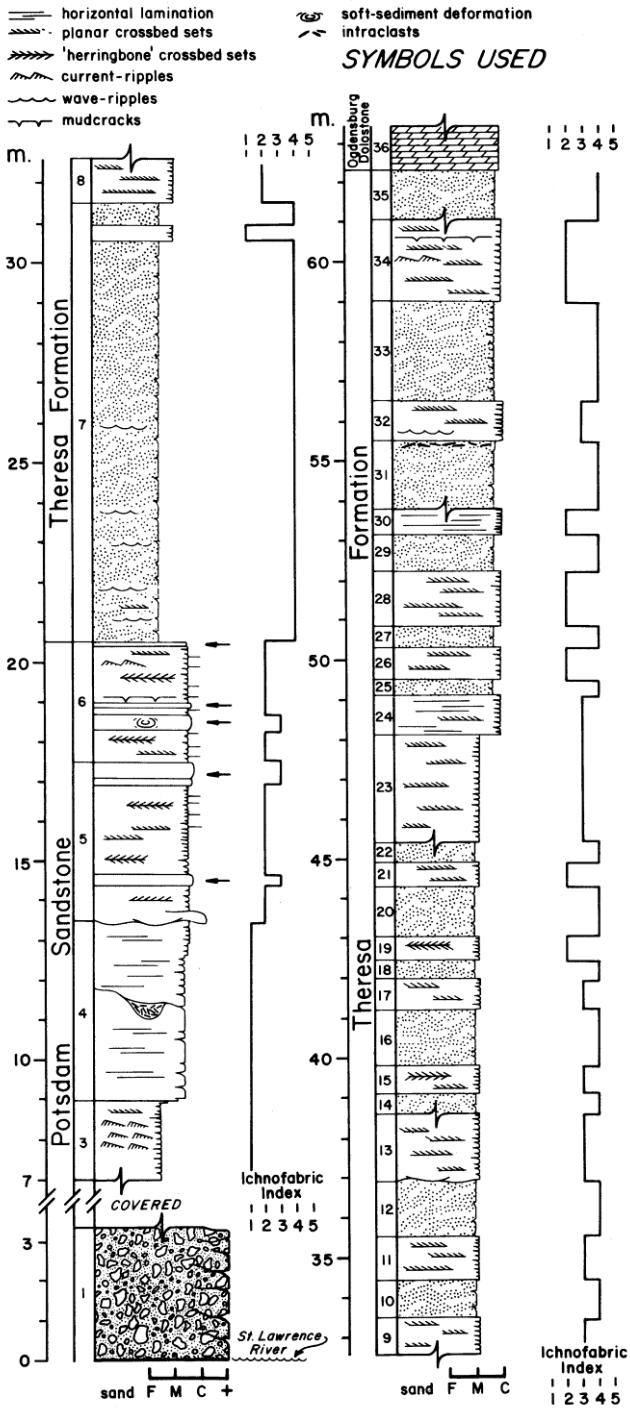

Figure 4. Composite section of the Potsdam and Theresa Formation in the St. Lawrence River valley in New York after Bjerstedt and Erickson (1989). Ichnofabric index indicates endobenthic disruption of primary sedimentary lamination (Droser and Bottjer, 1988); it is low (1-2) in white cross-bedded sandstone, and increases in burrowed gray quartz arenite (index 4-5). Arrows indicate presence of Diplocraterion burrows in upper Potsdam Formation.

Uppermost Cambrian and lowermost Ordovician strata are absent in the St. Lawrence River valley, indicating a long hiatus between the Potsdam and Theresa Formations (Landing, 2012) (Fig. 4). This contact is indicated by an abrupt increase in carbonate content, and a shift from sandy, tidal-flat facies to subtidal shelf/lagoon facies (Selleck, 1984; Woodrow et al., 1989). The middle Early Ordovician age of the lower Theresa Formation is indicated by Stairsian (*Macerodum dianae* Zone) conodonts (Salad Hersi et al., 2003). The formation is informally subdivided into lower, middle, and upper parts. The lower part is thoroughly bioturbated fine-grained quartz arenite cemented by calcite. The middle and upper parts of the formation are characterized by two sharply defined lithofacies that alternate in vertical sequence. These include gray, thick-bedded to massive, intensely burrowed, poorly sorted medium-to-coarse grained calcareous quartz arenite, and white to pale tan thin-to-medium bedded, fine-to-medium grained, siliceous to calcareous, planar and herringbone cross-bedded quartz arenite (Bjerstedt and Erickson, 1989). The maximum estimated thickness of the Theresa Formation in northwest New York varies from 28 m (Selleck, 1984) to 43 m (Cushing, 1916). In Ontario, its equivalent March Formation is up to 45 meters thick (Greggs and Bond, 1971).

In the St. Lawrence River Valley of New York, the Theresa Formation yields an association of peritidal facies characterized by a poor body fossil assemblage but rich biogenic structures. Road-cut stratigraphy is complicated due to the patchy character of exposed sections, but a characteristic vertical sediment sequence of lower, middle, and upper Theresa can be recognized. Bioturbated facies of the gray calcareous sandstone contains a *Cruziana* ichnofacies of abundant deposit feeders (Bjerstedt and Erickson, 1989). *Scolithos* ichnofacies is present in the white cross-bedded sandstone. The white sandstone in the upper Theresa Formation is also characterized by wave ripples, herringbone cross-stratification and horizontal lamination. Microbial structures distinguished by wavy laminated stromatolite growth structures are common in the white quartz sandstones of the middle Theresa Formation (Donaldson and Chiarenzelli, 2007; Husinec et al., 2008). Vertical sections of stromatolites exhibit predominantly space-linked hemispheroids with close-linked hemispheroids as a microstructure in the constituent laminae. Hemispheroids vary both in amplitude and in shape, i.e. from low-amplitude (5-10 cm) and gently convex, to higher-amplitude (up to 20 cm), steeply convex to slightly rectangular, vertically stacked hemispheroids. Subcircular, concentrically stacked spheroids up to 30 cm in diameter, with laminae composed of close-linked hemispheroids are observed in plan view. The facies stacking pattern observed within the microbial structure-rich part of the Theresa Formation likely represents shallowing-upward parasequences composed of gray, intensely bioturbated, restricted subtidal facies, capped by microbial laminites of tidal flats. Some parasequences are capped by thin breccia-conglomerate horizons suggesting periodic subaerial exposure of tidal flats. The alternating vertical stacking pattern of the two facies is complicated by their common interfingering in the upper Theresa, suggesting facies mosaics. In the Thousand Islands region, Theresa Formation is unconformably overlain by the Ogdensburg dolomite. Near Morristown, NY, Selleck (1984) recorded wavy-bedded, rather pure dolomite overlying the quartz arenite, and mapped it as contact between the Ogdensburg and Theresa Formations. The Ogdensburg Dolomite is best preserved in local quarries, where it commonly contains stromatolites (Kerans, 1977; Selleck, 1984; Van Diver, 1976) formed in upper intertidal to supratidal setting (Kerans, 1977).

STOP 1. NONCONFORMITY BETWEEN PROTEROZOIC BASEMENT AND POTSDAM SANDSTONE AT ALEXANDRIA BAY, NEW YORK

Latitude 44°20'42.54"N; Longitude 75°52'38.82"W

Road Log

Cumulative Mileage	Mileage from Previous Point	Route Description
0.0	0.1	Meet at Bonnie Castle Resort parking lot (31 Holland St, Alexandria Bay). Head south on Holland St
0.1	0.1	Continue onto 2nd St
0.2	0.4	Turn left onto Walton St
0.6	0.2	Continue onto Old Goose Bay Rd
0.8	1.4	Turn left onto NY-12 N. Stop 1 will be on the left. Park on the right shoulder and use caution when crossing on the left (north) side of NY-12 N.

Estimated driving time: 4 minutes

One of the best exposures of the non-conformable contact between the Potsdam Formation and the underlying Proterozoic basement in northwestern New York is in a road cut located approximately 1.5 miles northeast of Alexandria Bay, where New York State route 12 (NY-12), a two-lane undivided roadway cuts into a hill some 360 m (1,180 ft) west of the Cranberry Creek bridge (Fig. 5). The basal Potsdam Formation is in sharp contact with the Proterozoic gneiss that shows signs of alteration (illite, Fe-chlorite, and siderite; Selleck, 1993). The basal ~2 meters of Potsdam Sandstone weather into thin and friable slabs that are composed of low-angle cross-laminated (Fig. 6), non-arkosic and non-conglomeratic quartz arenite that is overall moderately sorted and contains some coarse grains within the predominantly fine- to medium-grained framework. Sorting increases up-section, and the sandstone becomes more massive. No body fossils or trace fossils are present in the Potsdam Formation at this stop.

Figure 5. South face of a road cut showing nonconformable contact (red dashed line) between Proterozoic basement and the overlying Potsdam Formation. Stop 1, Alexandria Bay, New York.

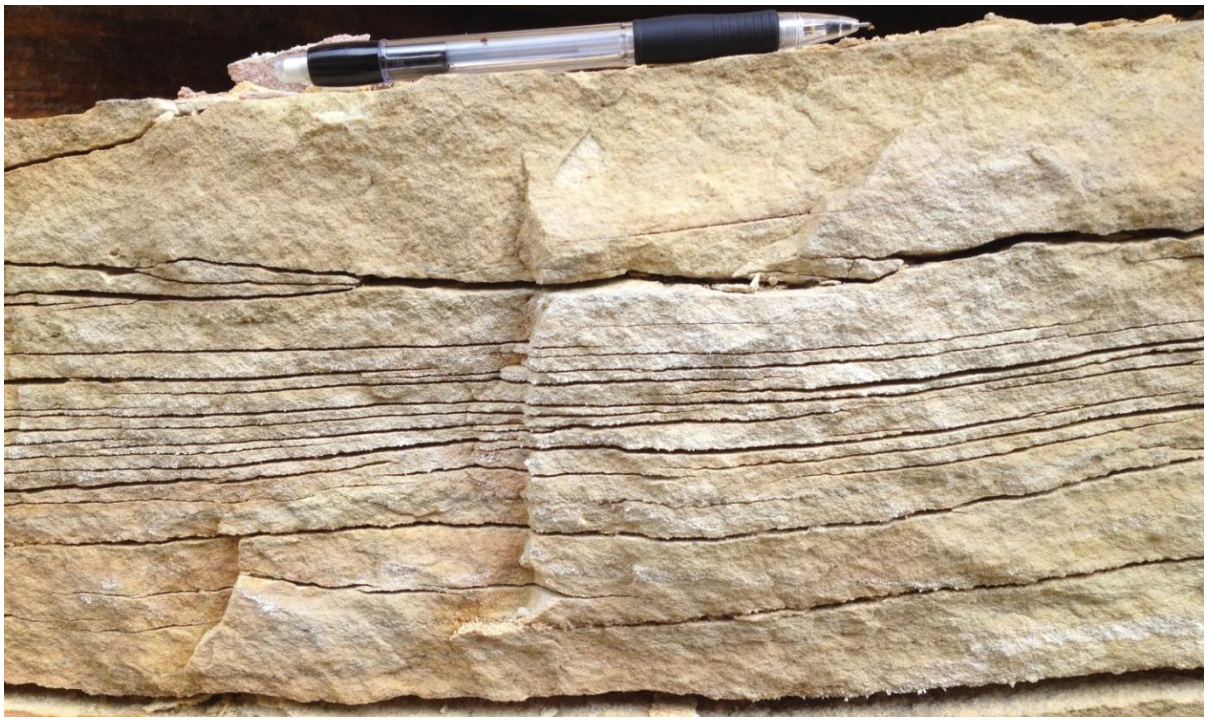

Figure 6. Low-angle cross-lamination in lower Potsdam Formation. Pencil for scale is 6 in (15cm) in length. Stop 1, Alexandria Bay, New York.

STOP 2: PRIMARY SEDIMENTARY STRUCTURES IN BASAL POTSDAM SANDSTONE, GOOSE BAY, NEW YORK

Latitude 44°21'23.39"N; Longitude 75°51'22.67"W

Road Log

Cumulative Mileage	**Mileage from Previous Point**	**Route Description**
2.2	1.4	Head east on NY-12 N toward Log Hill Rd. Stop 2 will be on the right.

Estimated driving time: 2 minutes

The northwest face of this road cut nicely exposes lowermost approximately 2.5 meters of Potsdam Sandstone (Fig. 7). The basal ~1.5 meters is a cross-laminated medium- and fine-grained quartz arenite showing tabular cross-bedding with curved bases and sharp erosive tops. The overlying ~40-cm-thick tabular quartz-arenite bed is characterized by planar to very low-angle cross lamination. The topmost set exhibits discontinuous, faint wavy (possible erosive bases) and parallel stratification, and becomes more massive updip. The exposed section is barren of body and trace fossils and contains no obvious microbially formed structures.

Figure 7. Planar cross-lamination (bed A) and parallel stratification (beds B and C) in lower Potsdam sandstone. Note curved base and sharp erosive top of bed A, flow to the right. Stop 2, Goose Bay, New York.

STOP 3: NONCONFORMITY BETWEEN PROTEROZOIC BASEMENT AND POTSDAM SANDSTONE AT GOOSE BAY, NEW YORK

Latitude 44°22'5.69"N; Longitude 75°50'20.93"W

Road Log

Cumulative Mileage	Mileage from Previous Point	Route Description
3.6	1.2	Head northeast on NY-12 N toward Goose Bay. Stop 3 will be on the right.

Estimated driving time: 1 minute

The road cut on the southeast side of the road exposes the nonconformity between Potsdam Sandstone and the underlying Grenville basement rock (Fig. 8). The contact is sharp but irregular, and displays heavily weathered, friable Proterozoic basement rock below the unconformity. Basal Potsdam Sandstone is a quartz arenite composed of poorly sorted and angular grains without any fossils. The lower 50-60 cm is white to light gray in color; the color changes in the upper part of the outcrop to pink and red. The reddish color around detrital grains and within secondary silica and illite cements is due to presence of finely crystalline hematite, goethite and anatase that formed by breakdown of detrital magnetite and ilmenite grains (Selleck, 1993). This basal, low-angle cross-laminated sandstone weathers more easily than the overlying, more massive quartz arenite that we observed at Stop 1, but is missing at this outcrop.

Figure 8. Nonconformable contact (red dashed line) between Proterozoic basement and the overlying Potsdam Formation. Stop 3, Goose Bay, New York.

STOP 4: POTSDAM SANDSTONE AT SCHERMERHORN HARBOR, HAMMOND, NEW YORK

Latitude 44°24'36.20"N; Longitude 75°47'14.94"W

Road Log

Cumulative Mileage	**Mileage from Previous Point**	**Route Description**
4.8	3.9	Head northeast on NY-12 N toward Shannon Rd. Stop 4 will be on the right. Stop 4 will be on the left. Park on the right shoulder and use caution when crossing on the left (northwest) side of NY-12 N.

Estimated driving time: 4 minutes

Note that between this stop and Alexandria Bay, all the outcrops are either Proterozoic Grenville basement or Potsdam Sandstone, indicating that Potsdam Formation blanketed topographic lows of the Proterozoic surface. Topographically higher areas likely were not sites of Potsdam deposition, or alternatively, sandstone was subsequently eroded from these areas. At this an unconformity within Potsdam Sandstone is exposed, (Fig. 9). The basal 3 meters above the unconformity is characterized by cross bedding (Fig. 10), with alternating poorly sorted, coarse- (up to very coarse in places) to medium-grained quartz arenite. This basal sandstone characteristically weathers into thin slabs. Upward in the section, the sandstone becomes more massive.

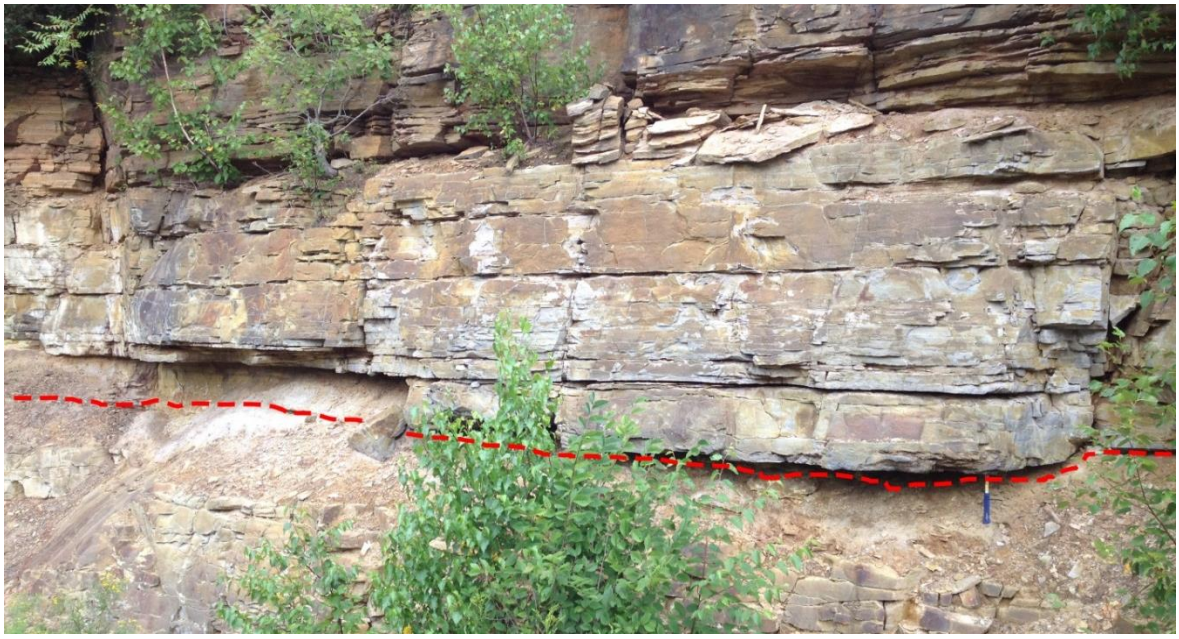

Figure 9. Unconformity within Potsdam sandstone (red dashed line). Stop 4, Schermerhorn Harbor, Hammond, New York.

Figure 10. Cross-laminated basal Potsdam Formation showing tabular cross-bedding. Pencil for scale is 6 in (15cm) in length. Stop 4, Schermerhorn Harbor, Hammond, New York.

STOP 5: DISCONFORMITY BETWEEN POTSDAM SANDSTONE AND THERESA FORMATION AT CHIPPEWA BAY, NEW YORK

Latitude 44°28'2.44"N; Longitude 75°45'48.70"W

Road Log

Cumulative Mileage	Mileage from Previous Point	Route Description
8.7	5.0	Head northeast on NY-12 N toward Factory Rd. Stop 5 will be on the right.

Estimated driving time: 5 minutes

The disconformity between the Theresa Formation and Potsdam Sandstone is spectacularly exposed near Chippewa Bay, New York (Fig. 11). An unconformity without angular discordance (dashed line in Figure 11) is marked by a thin, vegetated interval on top of the Potsdam Formation. The contact between two formations is sharp and indicated by a change in color from white to pale tan silica-cemented Potsdam below, to carbonate-cemented dark gray Theresa sandstone above. Unlike the lower part of the Potsdam Formation that on previous stops is devoid of any biogenous structures, its uppermost part exposed at this stop contains abundant *Diplocraterion* and *Skolithos* trace fossils (Fig. 12), clearly indicating a shallow-marine setting. The basal part of Theresa is extensively burrowed, and most primary sedimentary structures are completely obliterated. In addition to biogenous structures, Selleck (1993) recorded numerous fragments of the brachiopod *Lingulepis* in both the upper Potsdam and lower Theresa at this location.

Figure 11. Southwest face of a road cut showing disconformable contact (red dashed line) between Proterozoic basement and the overlying Potsdam Formation. Stop 5, Chippewa Bay, New York.

Figure 12. Abundant "U"-shaped Diplocraterion burrows in an ~30 cm (1 ft) thick quartz arenite bed in uppermost Potsdam Formation. Stop 5, Chippewa Bay, New York.

STOP 6: LOWER THERESA FORMATION NORTH OF CHIPPEWA BAY, NEW YORK

Latitude 44°30'10.21"N; Longitude 75°45'22.62"W

Road Log

Cumulative Mileage	Mileage from Previous Point	Route Description
13.7	2.7	Head northwest on NY-12 N toward Dubois Rd. Stop 6 will be on the right.

Estimated driving time: 3 minutes

The road cut on the northeast side of the NY-12 exposes extensively burrowed lower Theresa Formation (Fig. 13). Individual burrows, and possible pseudomorphs after evaporite minerals, are clearly visible as molds on weathered face of the oucrop (Fig. 14), and contribute to overall high porosity of this facies. Medium-grained quartz arenite is cemented by carbonate and is moderately to well sorted. The dark gray color is typical for the lower Theresa, with rare thin yellowish intervals that follow the bedding.

Figure 13. Southwest face of a road cut showing planar bedding in dark gray quartz arenite in the lower Theresa Formation. Stop 6, Chippewa Bay, New York.

_

Figure 14. Vuggy, highly burrowed sandstone of the lower Theresa Formation. Pencil for scale is 6 in (15cm) in length. Note probable molds of halite crystals (arrows point to a few of the largest ones).

STOP 7: MICROBIAL STRUCTURES IN THERESA FORMATION NORTH OF CHIPPEWA BAY, NEW YORK

Latitude 44°32'59.22"N; Longitude 75°41'58.60"W

Road Log

Cumulative Mileage	Mileage from Previous Point	Route Description
16.4	4.4	Head northwest on NY-12 N toward Riverledge Rd. Stop 7 will be on the right.

Estimated driving time: 5 minutes

The road cuts at this stop expose microbial structures preserved within the white, medium-grained quartz arenites of the middle Theresa Formation. These structures are exposed on both sides of NY-12, and are distinguished by wavy-laminated stromatolite growth structures that are common in the white quartz sandstones of the middle Theresa Formation. Vertical sections of stromatolites exhibit predominantly space-linked hemispheroids with close-linked hemispheroids as a microstructure in the constituent laminae (Fig. 15). Hemispheroids vary both in amplitude and in shape, i.e. from low-amplitude (5-10 cm) and gently convex, to higher-amplitude (up to 20 cm), steeply convex to slightly rectangular, vertically stacked hemispheroids. Subcircular, concentrically stacked spheroids up to 30 cm in diameter, with laminae composed of close-linked hemispheroids are observed in plan view (Fig. 16). Their shape closely resemble intertidal forms from Shark Bay (cf. Tucker & Wright 1990, p. 150, fig. 4.50B).

Figure 15. Vertical sections of stromatolites in the middle Theresa Formation. Stop 7, Chippewa Bay, New York.

Figure 16. Glacially polished outcrop of quartz arenite showing a bedding-parallel section of well-preserved circular to sub-circular stromatolites. Pencil for scale is 6 in (15cm) in length. Stop 7, Chippewa Bay, New York.

STOP 8: UPPER THERESA FORMATION AT MORRISTOWN, NEW YORK

Latitude 44°34'57.11"N; Longitude 75°38'19.63"W

Road Log

Cumulative Mileage	**Mileage from Previous Point**	**Route Description**
20.8	3.5	Head northeast on NY-12 N toward Worden Rd.
24.3	0.5	Continue onto NY-37 E. Park on the right shoulder. We will first focus on the right (east) and then on the left (west) side of the road. Use caution when crossing NY-37 E.

Estimated driving time: 4 minutes.

The upper Theresa is nicely exposed in road cuts on both sides of NY-37 immediately south of its intersection with High Street at Morristown, New York. The formation is characterized by thin beds of dark gray and white-yellowish calcareous quartz arenite that irregularly alternate, interfinger and pinch out. Dark gray sandstone is

thoroughly burrowed; extensive bioturbation resulted in complete obliteration of primary structures in this subtidal facies. On the contrary, although locally burrowed, the white to yellowish sandstone is characterized by well-preserved sedimentary structures indicating intertidal sand-flat setting with channel fills. Sedimentary structures include ripple cross-lamination, erosional (reactivation) surfaces, herringbone cross bedding, and local conglomerate-filled scours.

Figure 17. Bedding plane view of round-crested symmetrical wave ripples preserved on surface of quartz arenite, upper Theresa Formation. Pencil for scale is 6 in (15cm) in length. Stop 8, Morristown, New York.

Figure 18. Small-scale (ripple) cross-lamination in upper Theresa Formation characterized by thin (<10 cm), planar to slightly curved sets of cross laminae. Pencil for scale is 6 in (15cm) in length. Stop 8, Morristown, New York.

Figure 19. Cross-laminated quartz arenite (upper Theresa Fm.) showing two low-angle erosional (reactivation) surfaces indicated by dashed black lines. Pencil for scale is 6 in (15cm) in length. Stop 8, Morristown, New York.

Road Log to Canada

Cumulative Mileage	**Mileage from Previous Point**	**Route Description**
24.8	13.6	Head north on NY-37 toward High St.
38.4	0.9	Turn left onto Trooper Shawn W. Snow St.
39.3	1.5	Continue onto Ogdensburg-Prescott International Bridge. Entering Ontario. Toll Road.

Estimated driving time: 20 minutes.

STOP 9: NONCONFORMITY BETWEEN PRECAMBRIAN BASEMENT AND POTSDAM SANDSTONE AT LYN VALLEY CONSERVATION AREA, ONTARIO

Latitude 44°34'35.21"N; Longitude 75°46'30.98"W

Road Log (Odometer reset at Canadian Customs in Johnstown, Ontario; distance in kilometers)

Cumulative Distance (km)	Distance from Previous Point (km)	Route Description
0	0	Depart from Canadian Customs
2.0	2.0	Cross over Hwy 401 and turn right to enter cloverleaf for Hwy 401 west
25.0	27.0	Exit Hwy 401 on Stewart St. North in Brockville
0.5	27.5	Left on Parkedale (becomes Old Red Road)
3.5	31.0	Right on Road 46; left at junction with Cty. Rd. 27
2.0	33.0	Left on Cty. Rd. 27 in village of Lyn at intersection with Perth St.
0.2	33.2	Left on Lyn Valley Road
0.2	33.4	Lyn Valley Conservation Area, north side of road

Estimated driving time: 30 minutes.

From the parking area follow the gravel road northward to the start of a footpath that leads eastward through bushes and trees to the base of a 20-metre vertical section of Potsdam sandstone (Fig. 20). This cliff displays almost flat-lying beds with pebble interbeds (clasts of quartz sandstone), ripple marks and low-angle crossbedding that reflect deposition in water rather than by wind. Elsewhere within the Potsdam, large-scale steeply inclined crossbedding in pebble-free Potsdam sandstone in areas to the west reflects eolian transport. Trace fossils plus a wide range of directions of crossbed inclination indicate a shallow-water marine environment. Curled biofilm structures (Fig. 21) plus desiccation cracks reflect occasional subaerial exposure. Surface patches of gravel and sand cemented to the outcrop surface mark places where crossbedded Pleistocene outwash was once in contact with this Paleozoic cliff, reflecting the rapid rate at which unconsolidated deposits can be locally lithified.

Figure 20. Horizontally bedded quartz sandstone in the lower part of the Potsdam Group, exposed in a cliff north of the entrance gate to the Lyn Conservation Area.

Figure 21. Close-up view of the western end of the cliff exposure shown in Fig. 20, showing prominent wavy biofilm structures above (and a few below) the coin.

Figure 22. View looking southward at array of boulders and blocks derived from nearby glacial till. They provide a sampling of rocks to the north: mainly Paleozoic sandstone, limestone and dolomite plus Proterozoic igneous and metamorphic rocks from the Grenville Province, although a few have come from Archean terrain of the Superior Province.

Distinctive roll-up structures, especially prominent near the western end of this outcrop (Fig. 21), record the curling of sheets of sand grains bound by tenacious films of cyanobacteria in response to desiccation. Although the sands were deposited in water, the presence of such structures indicates intermittent episodes of subaerial exposure sufficiently long to allow drying, shrinking and curling of such coherent thin sheets of biofilm-bound sand. Elsewhere in eastern Ontario and northern New York State, similar curled biomats are overlain by sequences of continuous biomat layers that trapped successive interlayers of quartz sand to form distinctive domal stromatolites, indicating more persistent subaqueous conditions. Impressive examples occur within the city limits of Ottawa, Ontario (Hilowle et al., 2000, Donaldson et al., 2002)

On the return trip to the bus, check a few of the numerous boulders and blocks (Fig. 22) arrayed along the west side of the gravel roadway. Extracted from nearby outwash deposits, they provide examples of Precambrian igneous and metamorphic rocks from the Canadian Shield in addition to samples from the Paleozoic cover. The Precambrian boulders display pegmatite dykes, crosscutting relationships, inclusions, foliation, lineation and fractures (some with minor fault offsets).

Figure 23. Glacially striated and polished outcrop, one of several adjacent to telephone pole shown in Figure 22.

Between the margin of the gravel road and the telephone pole in Figure 22, immediately north of the largest boulder, a cluster of small glacially polished and striated outcrops of Grenville basement rock displays near-vertical foliation (Fig. 23). Distinct lithologic interlayers suggest a sedimentary provenance for these Precambrian rocks, with the compositional layering probably marking original bedding.

STOP 10: HERITAGE STONE BUILDING ON WEST MAIN ST., LYN VILLAGE, ONTARIO

Latitude 44°34'36.53"N; Longitude 75°47'4.11"W

Road Log

Cumulative Distance (km)	Distance from Previous Point (km)	Route Description
33.4	0.4	From Conservation Area, return to Lyn Village via Lyn Valley Road, turning right on West Main Street. Just before the intersection with Perth St., turn left into the parking on the north side of a small stone building, one of many in this region. This one houses a public library and the meeting room for the local Masonic Lodge.

Estimated driving time: 2 minutes.

Its walls of Potsdam sandstone are replete with an impressive array of trace fossils, with *Diplocraterion* and *Skolithos* predominating. A few blocks, especially those in the north wall, show syndepositional deformation of these trace fossils in vertical section, comparable to the syndepositional overturn of crossbeds.

Figure 24. Historic building currently used as a meeting hall and public library in Lyn Village. It is on the west side of Main St., about 50 metres south of a T-junction with Perth St.

Figure 25. Close-up view of Potsdam sandstone blocks in north wall of building shown in Fig. 24. Most show excellent examples of Diplocraterion (note that some blocks have been installed upside down). Some blocks installed with bedding parallel to the wall reveal solitary ichnotraces of Monoocraterion and Skolithos as well as the characteristic paired tubes of Diplocraterion.

STOP 11: PALEOZOIC-PRECAMBRIAN UNCONFORMITY, QUABBIN HILL

Latitude 44°28'20.50"N; Longitude 75°54'52.41"W

Road Log

Cumulative Distance (km)	Distance from Previous Point (km)	Route Description
33.8	8.2	Follow Hwy. 27 through Yonge Mills to junction with Hwy. 2.
41.0	6.0	Turn right on Hwy. 2
47.0	3.0	Turn right on Quabbin Road (Hwy. 4) Drive through the village of Mallorytown, site of former glass-making factory that utilized high-quality Potsdam sandsone. Park on north shoulder of Hwy. 4, just beyond intersection with Quabbin Hill Road (road on south side of Hwy. 4 at start of hill)

Estimated driving time: 15 minutes.

The rock cut on the north side of the highway on Quabbin Hill directly exposes the regional nonconformity between Potsdam sandstone and the underlying Grenville basement rock. The latter displays excellent spheroidal weathering of the basement (Fig. 26, 27), which here is a massive intrusive mafic rock. The Potsdam contains trace fossils perpendicular to bedding, just like those seen at STOPS 9 and 10, but the underside of beds on the south side of the highway display a different variety of trace fossils: sinuous trails parallel to bedding (Fig. 28).

Figure 26. Looking north across Quabbin Hill Road at the nonconformity between Potsdam sandstone and underlying Grenville basement rock.

Figure 27. Close-up view of spheroidal weathering in mafic intrusive rock beneath the nonconformity. This 3 m wide by 2 m high view is immediately left of the white signpost bar, lower right side of Figure 26.

Figure 28. Sinuous tubular traces, their patterns accentuated by weathering of the underside of an overhanging bed, mark the paths of soft-bodied vermiform organisms that browsed on bedding-parallel organic mats.

Of particular interest in the south-side roadcut are two independent indications of repeated subaerial exposure: bedding-parallel nodular zones within bioturbated silty layers that probably represent tropical soil horizons (Fig. 29), and desiccation patterns on several bedding surfaces. The unconformity surface marks a gap in the geological record of at least half a billion years. During this time, the land may have been elevated so that no rock record accumulated, although it is possible that post-Grenville Proterozoic strata were indeed deposited, but subsequently removed by erosion before the onset of Paleozoic sedimentation.

Figure 29. Highly bioturbated silty sandstone beds with prominent stylolites probably initiated along biomat layers. Sporadic nodular patches are inferred to represent thin paleosols.

STOP 12: PRECAMBRIAN BASEMENT EXPOSURE WITHIN COMMUNITY AT ROCKPORT BOAT LINE, ROCKPORT

Latitude 44°22'51.67"N; Longitude 75°55'55.26"W

Road Log

Cumulative Distance (km)	**Distance from Previous Point (km)**	**Route Description**
50.0	8.0	Turn left on Blue Mountain Road.
58.0	4.0	Turn left on Hwy 2. Drive eastward.
62.0	5.0	Turn right on Mallorytown Road (Hwy 5).
67.0	2.0	Cross Hwy 401.
69.0	2.0	Left on Parkway.
71.0	4.0	Turn right at entrance to "Rockport Boathouse". Turn left between Boathouse and parking lot. Follow paved road parallel to St. Lawrence River.
75.0	1.0	Stop 12.

Estimated driving time: 17 minutes.

This outcrop displays lit-par-lit sills of pink to white granite pegmatite and aplite that were injected parallel to the foliation of fine-grained gray to black gneiss and schist of presumed sedimentary provenance (Figure 30). Similar magmatic fluids were injected along crosscutting dykes during multiple episodes that can be put in sequence by observing crosscutting relationships. The metamorphic foliation of the host rock for these intrusions may have developed along the bedding of an original clay-rich sedimentary rock, such as mudstone or siltstone. Although foliation is typically vertical or dips steeply in most exposures or Grenville metamorphic rocks, it here is almost horizontal, perhaps due to location along the hinge of a fold, or to low-angle thrust faulting. The pinch-and-swell morphology of some lit-par-lit injections indicates lateral extension that was locally sufficient to form several boudinage (Figure 31). Note also the prominent sub-ice hydraulic scouring that created sculpted and polished benches along the outcrop during deglaciation.

Figure 30. Outcrop of Grenville gneiss on north side of paved road east of Rockport Boathouse.

Figure 31. Close-up view of boudinage in central lower part of Grenville gneiss shown in Figure 30.

Road Log back to USA

Cumulative Distance (km)	Distance from Previous Point (km)	Route Description
76.0	1.0	Return to Rockport Boathouse entrance; turn left on Thousand Islands Parkway.
77.0	3.0	Turn left at Selton to access International Bridge for our return to New York State via Hwy 81.

Estimated driving time: 3 minutes.

References:

Bjerstedt, T. W., and J. M. Erickson, 1989, Trace fossils and bioturbation in peritidal facies of the Potsdam-Theresa Formations (Cambrian–Ordovician, northwest Adirondacks): Palaios, v. 4, p. 203–224, doi:10.2307/3514770.

Blumberg, E., Chiarenzelli, J.R., Husinec, A., and Rygel, M., 2008, Insight from cores in the Potsdam Group, northern New York: Geological Society of America, Abstracts with Programs, Northeastern Section, v. 40, p. 82.

Cushing, H.P., 1916, Geology in the vicinity of Ogdensburg: New York State Museum Bulletin, no. 191, 64 p.

Donaldson, J.A., and J.R. Chiarenzelli, 2007, Disruption of mats by seismic events, *in* Schieber, J., Bose, P.K., Eriksson, P.G., Banerjee, S., Sarkar, S., Altermann, W., and Catuneanu, O. (Eds.), Atlas of microbial mat features preserved within the siliciclastic sedimentary rock record. Amsterdam, Elsevier, p. 245-247.

Donaldson, J.A., Munro, I., and Hilowle, M.A., 2002, Biofilm structures, trace fossils and stromatolites in Early Paleozoic quartz arenites and carbonates of the Ottawa region, Ontario: Twelfth Canadian Paleontology Conference, Program and Abstracts, 12.

Erickson, J. M., 1993a, Cambro–Ordovician stratigraphy, sedimentation and ichnobiology of the St. Lawrence lowlands–Frontenac Arch to the Champlain valley of New York, in New York State Geological Association 65th Annual Meeting, Field Trip Guidebook: New York State Geological Association, p. 68–95.

Erickson, J. M., 1993b, A preliminary evaluation of dubiofossils from the Potsdam Sandstone, in New York State Geological Association 65th Annual Meeting, Field Trip Guidebook, NewYork State Geological Association, p. 121–130.

Erickson, J. M., and T. W. Bjerstedt, 1993, Trace fossils and stratigraphy in the Potsdam and Theresa Formations of the St. Lawrence lowland, New York, in New York State Geological Association 65th Annual Meeting, Field Trip Guidebook: New York State Geological Association, p. 97–119.

Erickson, J. M., P. Connett, and A. R. Fetterman, 1993, Distribution of trace fossils preserved in high energy deposits of the Potsdam Sandstone, Champlain, New York, in New York State Geological Association 65th Annual Meeting, Field Trip Guidebook: New York State Geological Association, p. 133–143.

Gaudette, H.E., Vitrac-Michard, A., and Allegre, C.J., 1981, North American Pre-Cambrian history recorded in a single sample: High resolution U-Pb systematics of the Potsdam sandstone detrital zircons, New York State: Earth and Planetary Science Letters, v. 54, p. 248–260.

Getty, P. R., and J. W. Hagadorn, 2006, Producing and preserving Climactichnites (abs.): Geological Society of America, Abstracts with Programs, v. 38, no. 1, p. 23.

Greggs, R., and Bond, I., 1971, Conodonts from the March and Oxford Formations in the Brockville area, Ontario: Canadian Journal of Earth Science, v. 8, p. 1455-1471.

Hagadorn, J.W., Collette, J.H., and Belt, E.S., 2011, Eolian-aquatic deposits and faunas of the middle Cambrian Potsdam Group. Palaios, v. 26, p. 314-334.

Hilowle, M.A., Donaldson, J.A., Arnott, R.W.C., 2000, Biofilm-mediated structures in quartz arenites of the Cambro-Ordovician Nepean Formation. GeoCanada2000 -The Millenium Geoscience Summit, Calgary, conference CD, [www.ironleaf.com, abstract 868].

Husinec, A., Donaldson, J.A., Chiarenzelli, J.R & Erickson, J.M., 2008, Occurrence and features of microbial structures of the Theresa Formation, Cambro-Ordovician, New York, in GSA Northeastern Section – 43rd Annual Meeting, Abstracts with Program, p. 15-16, Buffalo, NY, USA.

Hoxie, C. T., and J. W. Hagadorn, 2005, Late Cambrian arthropod trackways in subaerially exposed environments (abs.): Geological Society of America, Abstracts with Programs, v. 37, no. 1, p. 12.

Kerans, C., 1977, Stromatolites, lithofacies and proposed depositional model for the Ogdensbura Dolostone (Lower Ordovician). St. Lawrence County, G.Y.: [unpub. B.S. thesis], St. Lawrence University, Canton, New York, 85 p.

Kirschgasser, W., and Theokritoff, G., 1971, Precambrian and lower Paleozoic stratigraphy, northwest Saint Lawrence and north Jefferson counties, New York: New York State Geological Association, Annual Meeting, Field Trip Guidebook, p. B1–B24.

Landing, E., 2012, The Great American Carbonate Bank in Eastern Laurentia: Its Births, Deaths, and Linkage to Paleooceanic Oxygenation (Early Cambrian-Late Ordovician), *in* J. R. Derby, R. D. Fritz, S. D. Longacre, W. A. Morgan, and C. A. Sternbach (Eds.), The Great American Carbonate Bank: The Geology and Economic Resources of the Cambrian: AAPG Memoir 98, p. 451-492.

Landing, E., L. Amati, and D. A. Franzi, 2009, Epeirogenic transgression near a triple junction: The oldest (latest Early–Middle Cambrian) marine onlap of cratonic New York and Quebec: Geological Magazine, v. 146, p. 552–566

Landing, E., D. A. Franzi, J. W. Hagadorn, S. R. Westrop, B. Kröger, and J. Dawson, 2007, Cambrian of east Laurentia: field workshop in eastern New York and western Vermont, in E. Landing, ed., Ediacaran–Ordovician of east Laurentia: S. W. Ford memorial volume: New York State Museum Bulletin, v. 510, p. 25–80.

Lochman, C. 1968. *Crepicephalus* faunule from the Bonneterre Dolomite (upper Cambrian) of Missouri. Journal of Paleontology, v. 42, p. 1153–62.

MacNaughton, R. B., J. W. Hagadorn, and R. H. Dott Jr., 2003, Did the Climactichnites organism leave the water? Paleoecological insights from the Upper Cambrian of central Wisconsin: Canadian Paleontology Conference Proceedings, Geological Association of Canada, no. 1, p. 26-27.

McRae, L.E., 1985, Sedimentology and paleomagnetics of the basal Potsdam Sandstone in the Adirondack border region, New York State, southwestern Quebec, and southeastern Ontario: Unpublished Ph.D. thesis, Dartmouth College, Hanover, New Hampshire, 178 p.

Salad Hersi, O., D. Lavoie, and G. S. Nowlan, 2003, Reappraisal of the Beekmantown Group sedimentology and stratigraphy, Montre´al, southwestern Quebec: Implications for understanding the depositional evolution of the Lower–Middle Ordovician Laurentian passive of eastern Canada: Canadian Journal of Earth Sciences, v. 40, p. 149–176.

Selleck, B.W., 1975, Paleoenvironments and petrography of the Potsdam Sandstone, Theresa Formation and Ogdensburg Dolomite (U. Camb.–L. Ord.) of the southwestern St. Lawrence Valley, New York: Unpublished Ph.D. thesis, University of Rochester, New York, 210 p.

Selleck, B.W., 1984, Stratigraphy and sedimentology of the Theresa Formation (Cambro-Ordovician) in northwestern New York. Northeastern Geology, v. 6, p. 76-88.

Selleck, B.W., 1993, Sedimentology and diagenesis of the Potsdam Sandstone and Theresa Formation, southwestern St. Lawrence Valley, *in* NYSGA Fieldtrip Guidebook, 65th Annual Meeting, p. 219-228.

Selleck, B.W., 1997, Potsdam Sandstone of the southern Lake Champlain Valley: Sedimentary Facies, environments and diagenesis, *in* 1997 NEIGC Fieldtrip Guidebook, p. C3-1 - C3-16

Tucker, M.E., and Wright, V.P., 1990, Carbonate Sedimentology. Blackwell, 482 p.

Van Diver, B.B., 1976, Rocks and routes of the North Country, New York: W.F. Humphrey Press Inc., Geneva, New York, 204 p.

Woodrow, D.L., Brett, C.E., Selleck, B.W., Baurd, G.C., 1989, Sedimentary Sequences in a Foreland Basin: The New York System - Cambrian and Ordovician Strata in Northeastern New York; 28th Int. Geol. Congress Guidebook T156, p. 1-6

MILITARY GEOLOGY OF THE BATTLE OF SACKETT'S HARBOUR (28 MAY 1813), LAKE ONTARIO, NY

ALEXANDER K. STEWART
Department of Geology, St. Lawrence University, Canton, New York 13617

ROSS W. KLEPETKO
Storefront Academy Harlem, New York, New York 10035

INTRODUCTION

Geology has shaped warfare since its inception; however, it was not until the end of the 18th century that geologists shaped warfare (cf., Guth, 1998; Kiersch and Underwood, 1998). For thousands of years, the idea that a hilltop position or fortification would provide the tactical advantage was considered "common sense." Those who held the high ground were more likely to survive the fight and promulgate their ideals and to prosper. With the inception of the discipline of geology, these common-sense notions were turned into well-thought and planned military-geology strategies. There are many examples of the science of geology dictating tactical and strategic outcomes in war, from Napolean's invasion of Egypt (1798) to recent counterinsurgency operations in Afghanistan (Stewart, 2014).

For the Battle of Sackett's Harbour (1813), engineer siting of Fort Tompkins and anticipated defense of the mainland by Brigadier General Brown, New York Militia were "common-sense" approaches to dealing with the tactics of the day. For this field trip, we propose to highlight these "common-sense" notions as geological controls on the battle. If it were not for the inadvertent recognition of geological processes at the main naval base on Lake Ontario, this United States tactical victory would have allowed the United Kingdom complete control of Lake Ontario and their primary supply route, the St. Lawrence River.

Portions of this field trip are the result of Ross Klepetkos' senior project (2011) at St. Lawrence University where he synthesized his love of history with geology. The purpose of this trip is to provide an enjoyable recounting of the Battle of Sackett's Harbour (1813) by following the path of the advancing British Regulars while highlighting the local geology and its unintended controls on the battle. Had the geology of Sackett's Harbour been different, there would have been no rebounded cliff, spit and protected harbor, tombolo and island–no naval stronghold and no battles–no Sackett's Harbour.

WAR OF 1812

In the short, but rich history of the United States of America, the War of 1812 (1812-1815) is often a forgotten conflict in the midst of the American Revolutionary War (1775-1783) and the War Between the States (1861-1865). Considering the wide geographic reach of the War of 1812, from the Battle of New Orleans to the burning of the White House and naval skirmishes off the coast of South America, it is odd that it would be "forgotten."

President James Madison signed Congress' official declaration of war against the United Kingdom on June 18th, 1812 as the result of 1) imposed trade restrictions with France (the UK was involved in the Napoleonic Wars), 2) UK impressment of US sailors, 3) UK support of native tribes against US westward expansion and 4) possible insults to national honor on the high seas and potential annexation of Canada to the USA (Latimer, 2010). Politicians in Washington City were of the mind that the USA could win a quick victory by an easy capture of British Canada; thereby, making British acquiesce to demands before she could send troops to take action (Katcher and Fosten, 1990). This, of course, was not the case. Instead, the war was fought on both sides with military incompetence and internal dissent leading to over 6,700 US casualties and over 5,200 UK casualties at the cost of approximately $105 million (£25 million) or, in today's values, approximately $1.4 trillion (£1.4 trillion).

After almost three years of land and sea warfare, the peace Treaty of Ghent (Belgium) was signed December 24th, 1814 with the final US victory occurring at the Battle of New Orleans, thanks to the speed of news, on January 8th, 1815. The result of nearly three years of fighting was a *status quo antebellum* where impressment was a moot point after the defeat of Napolean (1815). A significant US gain was the Treaty of Rush-Bagot (1818), which initiiated the longest (chronologically and spatially) peaceful border in the world between the USA and Canada.

BATTLE OF SACKETT'S HARBOUR (29 MAY 1813)

The history of Sackett's Harbour (currently spelled Sackets Harbor) is what defines the town and provides its character (Figure 1). Driving around modern day Sackett's Harbour, one can see that history lives on, from the battlefield memorials to the numerous buildings that date back to the earliest parts of the 19th century. These buildings are a reminder of when this summer lake town was *the* major naval and military outpost on Lake Ontario; responsible for controlling its treacherous waters, as well as the supply lines to Upper Canada via the St. Lawrence River. Twice, the Americans were required to fight for its protection, first a naval battle on July 19th, 1812 where American sailors repulsed a British attack and second, the focus of this trip, on May 29th, 1813, the amphibious assault, land and naval battle.

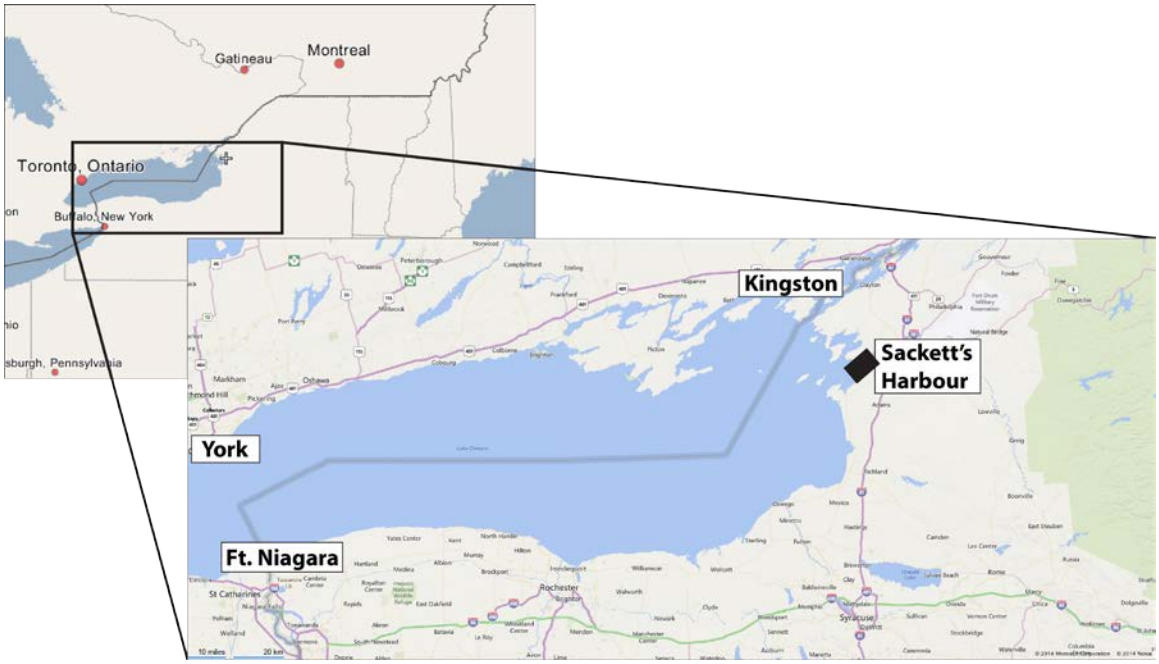

Figure 1. Regional map and Lake Ontario blowout map. Black polygon represents approximate area of subsequent Sackett's Harbour figures.

This second Battle of Sackett's Harbour was a result of local anxieties, as well as the tensions that led to the War of 1812. In the years before the war, the British were engaged with their enemies in the Napoleonic Wars. During this time, Americans took advantage of both the British and French need for American goods and services by trading with both. The British, upset by this, embargoed American trade with the French by a blockade and boarded American merchant ships looking for Royal Navy deserters who had signed on with the merchant ships for better pay. One such instance occurred when the Royal Navy fired upon the merchant ship USS *Chesapeake* off the coast of Virginia, killing and wounding members of the crew in order to board the ship and search for British deserters. International incidents like this one, as well as political pressure from a group of congressmen known as the "War Hawks," led to a declaration of war on June 1st, 1812.

Prior to the War of 1812, Sackett's Harbour and the surrounding area were primarily supported by agriculture, with town residents actively engaged in trade with their Canadian neighbors across the St. Lawrence River.

Town founder, Augustus Sackett, came north from New York City as a land speculator, and found the area to be quite advantageous due to its relatively deep and protected harbor. Thus, the town grew from a small farming town into one of the more important towns on Lake Ontario. Close by in soon-to-be named Brownsville, NY, future militia commander Jacob Brown settled a community and emerged as a local leader. Brown was also known for taking advantage of the tensions between the Americans and the British across the lake and river, as he became an avid smuggler of potash. In fact, Brown became known as "Potash" Brown for his ability to smuggle the valuable fertilizer. When war broke out, however, this all changed when the military recognized the strategic value of Sackett's and decided to make it the major base of operations on Lake Ontario.

The base of operations contained three groups, the U.S. Navy commanded by Commodore Issac Chauncey, the U.S. Army regulars commanded by Major General Henry Dearborn, and the New York Militia commanded by local Brigadier General Jacob Brown. Dearborn and Chauncey conferred and decided that there were too many British stationed at Kingston, British Canada and, therefore, decided to attack York. Chauncey and the U.S. Navy had recently outfitted local merchant boats with cannon, so they sailed to York, capturing it with some ease, for the American forces at Sackett's Harbour outnumbered that of any British post on Lake Ontario. They burned York, and, riding high off their victory, decided to sail to the mouth of the Niagara River and attack Fort George in Ontario (Figure 1).

With Isaac Chauncey and General Dearborn engaged across the lake, a depleted force was left to protect Sackett's Harbour. The ranking officer in the British Army, Sir George Prevost, recognized this weakness– thanks to information provided by a loyalist. Taking into account that the American ship, the USS *General Pike* was nearing completion, it would not be long before the British lost their advantage on the vicious waters of Lake Ontario and become more vulnerable to attack. Prevost consulted with the newly arrived and celebrated naval Commodore, James Lucas Yeo, and ultimately decided that the time was right to attack Sackett's Harbour. They did not want to risk Chauncey and Dearborn returning from their attack on Fort George, and also recognized that, given the weather and unpredictable waters of Lake Ontario, a good opportunity for an attack could not be wasted.

After Yeo and the Prevost decided to attack, the newly appointed Commander Yeo sailed his fleet the short distance across the lake from Kingston stopping on the far side of the concealing Horse Island on the night of May 28th 1813 (Figures 1 and 2). Yeo and the Prevost decided that, based on the less than ideal conditions, they would hold their attack until the next morning. By doing so, the British gave the Americans more than enough time to prepare and the next morning, May 29th, 1813, Americans fired on the British as they neared land and were close enough for effective shots. After this initial attack, the New York Militia (NYM) retreated to the beach opposite Horse Island. This gave the British time to gather and rearm. The British were then forced to cross the knee-deep water atop the slippery shoal rocks from Horse Island onto the small beach where the militiamen were stationed, as this was the only point the British could get onto the mainland. This forced the British advance into a kill zone, but the defending NYM had not been battle tested and were afraid of the much more advanced British regulars. At this point, one of the NYM stated, "I fear we shall be compelled to retreat…. I know we shall, and as I am a little lame, I'll start now" (quoted in Wilder, 1994). The militia retreated into the woods against Brown's orders. Still, Brown gathered as many of the fleeing men as possible and attempted to make one last stand (Figure 3). Again, the Americans withdrew, providing yet another opportunity for the British to reorganize and revise plans for their struggling main assault.

Figure 2. Reconstructed battle sequence highlighting the UK amphibious assault on the windward side of Horse Island. At this point, NY militia (NYM) were in defensive positions on the island; despite the British Regulars disembarking their bateaux and crossing knee-deep waters atop slippery limestone pavement, the NYM failed to repel the invasion.

Most of the British regulars marched down the road that ran along the shore toward the main fortifications near Fort Tompkins (Figure 4). The Voltigeurs (British Army) under the command of Captain Jacques Viger flanked right, trying to get around the American defenses. A remaining group of British forces, who had accompanied the assault, chased the retreating NYM into the forest that separated the village from the assault point (Figure 4). As the British marched down the road, an American marksman spotted Major Drummond (British Army) who was the second in command under Prevost, and waiting until he was in range, took a shot. Drummond dropped to the ground, but was only wounded. Earlier, at the encouragement of his men, Drummond had removed his epaulets, storing them inside of his shirt. When the marksmen fired his weapon, the bullet hit the epaulets, saving the major's life, and, unfortunately for the Americans, allowing him to resume his command.

As Major Drummond and the British marched forward, joined by the Voltigeurs, the British were again too much for the Americans. American military leaders Colonel Electus Backus, Major Jacint Laval, and Major Thomas Aspinwall retreated 200 meters toward Fort Tompkins and made their stand. It was the 32-pound gun inside Fort Tompkins, however, that was doing the most damage (Figure 5). Yet, the damage was mostly psychological because the British knew they stood little chance of success if they did not take or somehow dismantle the gun.

Patrick A. Wilder (1994) describes the scene in his book *The Battle of Sackett's Harbour*, "The American artillerists toiling in Fort Tompkins repeatedly discharged the 32-pounder into the woods toward the oncoming British. A deluge of cannon balls, grapeshot, and bullets lopped off treetops and branches, which flew in every direction. One nearly killed Captain Jacques Adhimar [British Army]." After seeing the significant damage the cannon was doing, Colonel Baynes of the Royal Army approached Prevost and said that his men would not be able to take the fort. British forces reorganized and made another attack on the American fortifications, yet by this time the British forces were reduced in number to approximately 300 men (Figure 6). In addition, Prevost received the news that all the other field officers, except for one, were wounded.

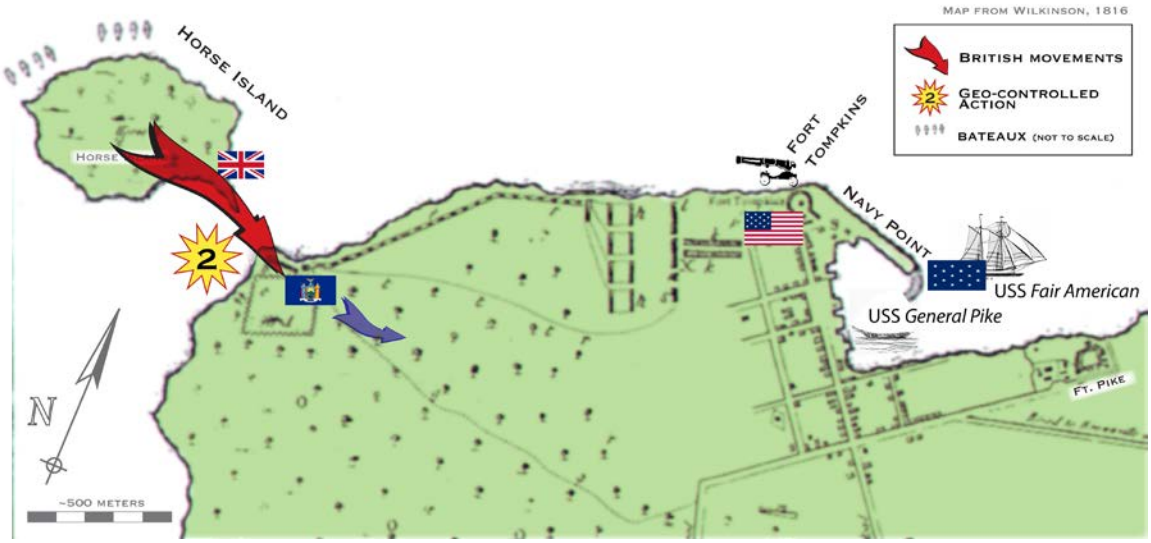

Figure 3. Reconstructed battle sequence highlighting the retreat of the NYM across the tombolo and their straggled defense behind the mainland beach berm. British regulars advanced across the same knee-deep, mossy-boulder-and-cobble tombolo toward the NYM defensive "kill zone." This should have been (the second, see Figure 2) guaranteed end to the battle because the British would have only been five to ten abreast as they advanced across the tombolo, for the water depths increase to above waist deep just meters away from the tombolo's centerline.

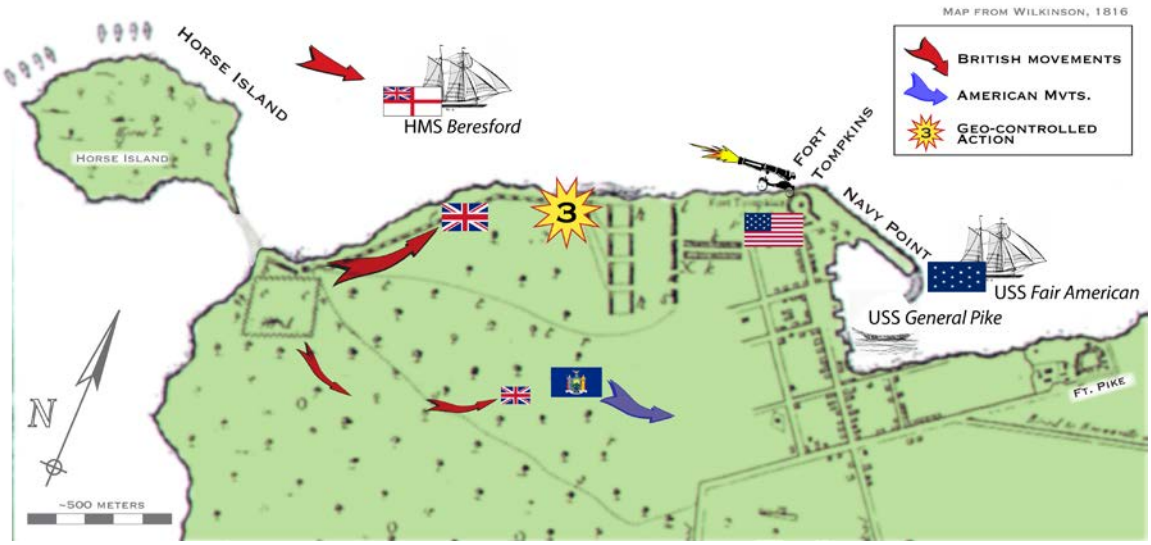

Figure 4. Reconstructed battle sequence highlighting the confused retreat of NYM back toward Forts Tompkins and Pike. After the main British force made the mainland, they continued along the lakeshore through abatis and direct fire from the 32# gun at Fort Tompkins. The British Voltigeurs split from the main group to follow some retreating NYM and to flank the cantonment. During this time, the HMS Beresford, the only British ship able to maneuver in these calm, shallow waters began rowing in to support her infantry.

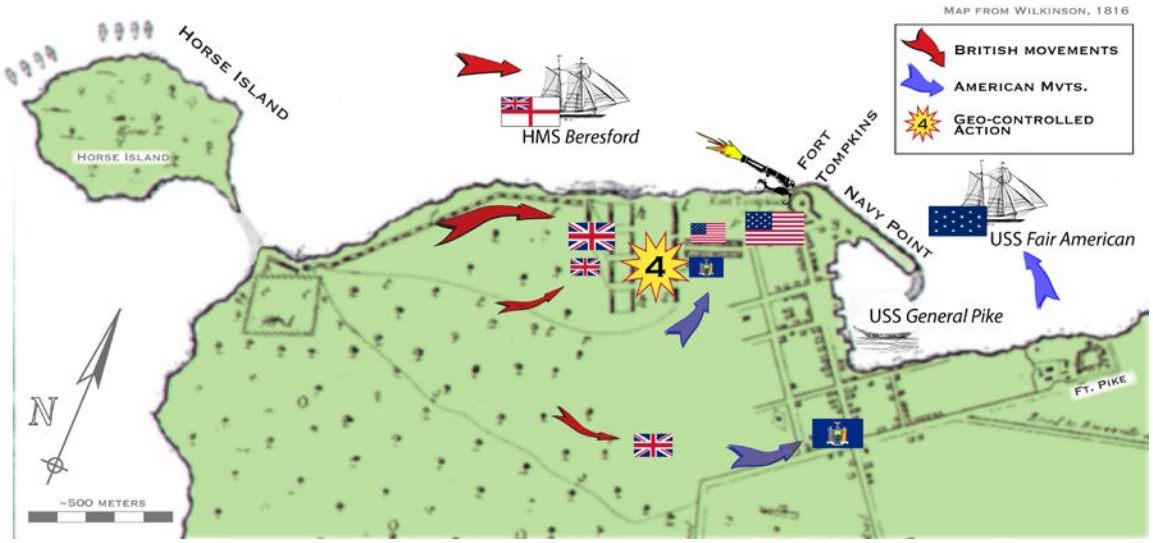

Figure 5. Reconstructed battle sequence highlighting the in-line, infantry firefight at the Smith (Basswood) Cantonment with the movement of the USS Fair American into position to ward off the HMS Beresford.

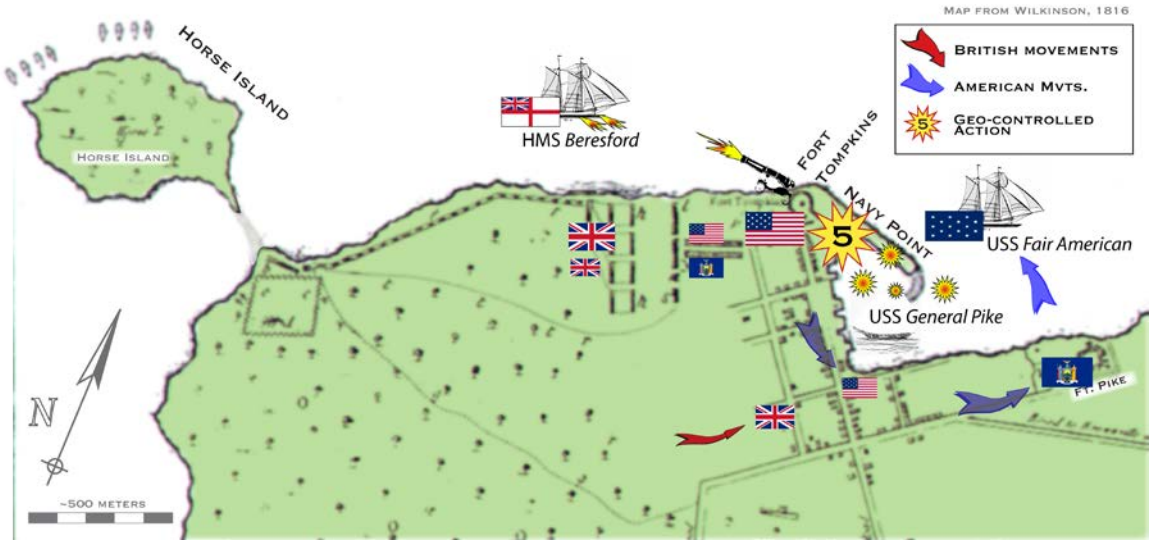

Figure 6. Reconstructed battle sequence highlighting the exchange of fire between the 32# cannon at Fort Tompkins and the HMS Beresford. Because of keen placement of Fort Tompkins, fire from the Beresford either smashed into the 7-meter cliff face below the fort, or overshot into and around the harbor. US sailors and soldiers on Navy Point misinterpreted this as fire from an over-run (British taken) Fort Tompkins (which was not the case). Because of confusion, the Americans set the USS General Pike and stores on Navy Point ablaze.

British Naval commander Yeo favored supporting the land attack by going ashore and leaving the naval support in the hands of the ships' various captains. Meanwhile, most of the ships remained in their positions, out of range and ineffective at providing naval support. The HMS *Beresford*, the only British ship outfitted with sweeps (long oars), zigzagged into the unknown depths to provide support (Figure 6), but was met by the USS *Fair American* commanded by LT Wolcott Chauncey, USN. The ships fired on each other until Chauncey cut his cables and retreated, leaving Navy Point and Fort Tompkins.

Chauncey's departure was a key event. He had been left in charge of the base's naval operations, while his senior officer and brother, along with portions of the army, were in the western part of the Lake, fighting at Fort Niagara. Earlier in the morning, before the start of the battle, LT Chauncey had given the order that if his ship was on fire and/or Fort Tompkins was taken, he would fly a red flag from his ship. This was the signal for the remaining men to set ablaze the stores at Navy Point and the recently laid-down USS *General Pike*, thus averting their capture by the British (Figure 7).

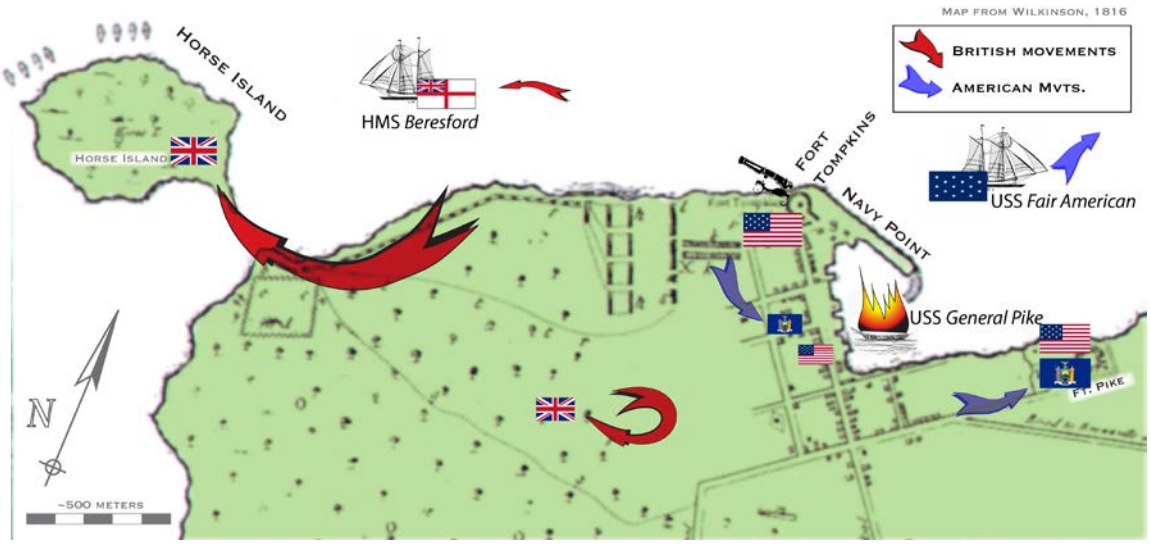

Figure 7. Reconstructed battle sequence highlighting the burning of the USS General Pike and the general retreat of both the USS Fair American, HMS Beresford and the US regulars, NYM and the British main assault. At this point, neither side was "winning," but because the British force was retreating to their ships, the Americans held the day.

Confusion was running rampant at Navy Point because of mixed signals and general loss of command and control. For example, the Americans at Navy Point thought that the British took the 32-pound cannon at nearby Fort Tompkins. Instead, the firing from the HMS *Beresford* had forced the artillerists of the 32-pound, main gun at Fort Tompkins to take cover; it was these *Beresford* volleys that were overshooting the fort and hitting around the harbour. American sailors thought that this fire was coming from the "captured" Fort Tompkins, but in fact they were shots intended for Fort Tompkins from the *Beresford.* Because of the confusion and the insistence of some that Chauncey's order be followed, sailors decided to burn the USS *General Pike* and the stores and retreat to Fort Volunteer across the river from Navy Point and Fort Tompkins (Figure 7).

Simultaneously, the U.S. Army was also retreating to Fort Volunteer where Colonel Backus was mortally wounded, leaving Major Laval, USA of the Dragoons, in charge. Major Laval also sent his men back to Fort Volunteer, leaving Major Aspinwall and his men to protect Fort Tompkins (Figure 7).

It appeared the momentum was shifting. Major Aspinwall held Fort Tompkins, the burial site of General Pike, and repelled the British advance. By this time, the HMS *Beresford* continued firing on Fort Tompkins, but she was unable to communicate with her land forces, as Yeo had not set up any signals in advance. Aspinwall and his men took full advantage of the situation, continuing to successfully defend Fort Tompkins, and, in the process, killing many British troops.

Thinking he had a clear advantage, Major Drummond suggested the British approach the Americans, demanding their surrender. Major Laval refused, telling Drummond, "Then tell Sir George Prevost we will wait the issue of his [next] attack" (quoted in Wilder, 1994). It was decision time for Prevost and he chose retreat (Figure 7). Prevost feared that Isaac Chauncey and his fleet could return and cut them off at any minute, unaware that American troops, in fact, were quite fearful of the British and had low morale. Meanwhile, Viger

and the Voultigers, unaware of the retreat, had made their way into the village and, as a result, were among the last ones to sail back to Kingston.

While the battle at Sackett's Harbour is an American victory, the British were able to accomplish something during their invasion. In the midst of the confusion on Navy Point, and the apparent signal by Wolcott Chauncey to burn the naval stores, the British were able to maintain superiority on the Lake as the USS *General Pike's* construction was delayed by two months–keeping the U.S. Navy from ascending to power on Lake Ontario until much of the sailing season of 1813 was over.

After the battle, Sackett's Harbour increased its military strength, adding Fort Kentucky and by building up Fort Volunteer, now known as Fort Pike. The harbor held it's key position until railroads became more commonplace and bypassed Sackett's Harbour. Still, Sackett's Harbour maintained a luster given that it was a posting for military luminaries, including Ulysses S. Grant before the start of the War Between the States.

Clearly, Sackett's Harbour was at its prime during the War of 1812 as American forces were able to fend off two British invasions. Thanks to several key victories, including those at Sackett's Harbour, the U.S. maintained a strong presence on the lake as the USS *General Pike* was eventually restored and completed. The U.S. also made a statement to the British about their strength in the war as a whole. Yet, as one drives through the modern day summer community of Sackett's Harbour and its colorful history is celebrated, it is hard to imagine its fields bloodied and its coastline bombarded with fire.

GEOLOGICAL OVERVIEW OF SACKETT'S HARBOUR

Sackets Harbor, New York is rich with history, evident by a drive down the main street; they have truly embraced their War-of-1812 history. There is a history, however, that predates any war or people on the land–the geologic history. From the building stones to the cliff that protects the historic battle site from the rough waters of Lake Ontario, geology plays an essential role in the village of Sackets Harbor. The geology of the area ties in with several geologic events, including an eperic sea over 400 million years ago and a great ice sheet that covered the area "just" 15,000 years ago. The best way to get insight into that ancient ocean is through the limestone cliff that lines the shore of the lake; for evidence of the massive continental-sized glacier, you only have to look at that same cliff, the rolling topography and the lake.

The cliff along the eastern shore of Lake Ontario is comprised of up to seven meters of Ordovician-aged, shallow-ocean-water sedimentary rocks; part of the Lake Ontario Homocline (Kay, 1942) with a dip of approximately 8m/km to 222^{o} (Wallach and Rheault, 2010). These limestones and shales are evidence of fluctuating sea levels, or eustatic changes, during a time when nascent North America was about 25^{o} south of the equator. The shales were deposited in quiet, deeper water environments (10's of meters) while the interbedded limestones represent shallow-water carbonate factories. The deposition of these beds, along with the sea-level transgressions (local deepening) and regressions (local shallowing) would have taken many thousands of years, a long period of time, but relatively insignificant in geologic time. These limestones and shales have been identified as part of the Trenton Group's, "Shoreham interval." These limestones are analogous to modern-day Bahamian environments–places where little ocean critters, such as foraminifera, multiply in shallow, warm, sun-rich ocean waters. These creatures live and die by the trillions, accumulating only millimeters every thousand years or so, turning to limestone over time. At varying times, mountain-building events on the eastern edge of the continent affected the local depth of ocean water (by raising/lowering the land). When the land was depressed, deeper water sediments prevailed. In these deep, dark regions, forams are not able to proliferate; as a result, fine-grained sediments settle in this quiet environment–one way of making shaley units.

There are several prominent features associated with this cliff. First, while walking atop the cliff, one notices the jagged nature of the cliff edge and numerous depressions next to it. These features are places where the cliff has been weathered and eroded underneath, causing subsidence and cliff-face retreat. This erosion is caused by wave action constantly beating the cliffs until eventually the cliff is weakened to the point that it falls into the lake. The reason the waves are so effective at eroding the cliff is because wave action is concordant to the joints in the rock. These joints are weaknesses, allowing the waves to be more successful with their weathering and erosion, causing faster cliff retreat. In fact, there are multiple instances where the cliff face has already been

sapped, separated and tilted toward the lake. In another instance, wave action has worked antithetic joint sets making a small cavern beneath the cliff edge. This erosion has caused the cliff to retreat over time; possibly, two to five meters since the battle.

The surrounding area was also impacted by the Quaternary continental glaciers, which advanced and retreated multiple times in the past two million years. While the last glaciation maxed out around 15,000 years ago, evidence of the advance and retreat of these glaciers can be found in the area. There are numerous glacial features, including drumlins and moraines, which can be seen to the east in Watertown. Also, the area that Lake Ontario currently occupies was once covered by another, larger lake known as glacial Lake Iroquois. This lake formed as meltwater from the Laurentide Ice Sheet was prevented from flowing out the St. Lawrence River Valley by the retreating ice to the north, and geographic boundaries like the Adirondack Mountains to the east. Eventually however, the ice melted farther north and the water from the lake drained through the St. Lawrence River.

Wave refraction also played a part in shaping not just the cliff, but Horse Island. Horse Island is an island in Lake Ontario adjacent to mainland Sackets Harbor and nearby Gilmore Point. Before it was an island, however, it was likely an extension of Gilmore Point. Today, Horse Island is probably a "lake stack." The bathymetry of the lake near Horse Island helped focus wave-refracted energy, which eventually cut Horse Island off from the mainland. This same process is responsible for maintaining the thin tendril that connects Horse Island to the mainland–a tombolo. The tombolo, currently known as Gilmore Shoal, is covered with shallow water and was the route taken by the British invasion force when attacking Sackets.

Several lake-coast, geologic processes, including longshore drift and wave refraction, are the modern modifiers of the Sackets Harbor area. Longshore drift is the process by which sediment is transported along the coast. Depending on the prevailing wind direction, sediment is eroded and deposited continuously along the coast by swash and backwash. At Sackets Harbor, westerly winds generate waves that move sediment from the Horse Island area towards the village of Sackets Harbor. These drifting particles are carried to the harbor and then deposited as a spit of land, which projects from the mainland and protects the harbor. This spit is known as Navy Point, where the U.S. Navy was stationed during the War of 1812 and after. These protected harbor waters were crucial for ship building operations as well as stationing naval vessels. Today, these same protected waters are used for the same protective purpose, but only for pleasure craft.

Wave refraction is the process by which the limestone cliff that lines the coast is weathered and eroded. Waves are altered by the bathymetry of the lake floor. As a linear wave crest makes its way toward the shore, the shore end will encounter a shallowing bathymetry before elsewhere along its crest length (due to the angle of impingement). As this portion of the wave enters the shallower water, it slows down while the deeper, farther removed portion along the same crest continues at a now, relatively faster rate causing the wave crest to "bend" toward the shore. This process is undercutting the cliff along the joints, causing the weathering and, ultimately, the cliff erosion and retreat. This is an important process relative to the battle, for the cliff provided natural protection to the American fortifications at Sackets Harbor.

WALKING TOUR LOG AND NOTES FOR TRIP A-2

This tour will leave from the Bonnie Castle Resort, 31 Holland Street, Alexandria Bay, NY 13607 at 1100hrs taking about 45 minutes to arrive at the Sacket's Harbor Battlefield State Historic Site (SHB), 500 W. Main Street, Sacket's Harbor, NY 13685 and return to Bonnie Castle Resort by 1700hrs.

NOTE 1. If you are driving separately, please plan to arrive at the SHB (start, see below) by 1145hrs; we will be taking NY12 south from Bonnie Castle Resort to I-81 south to NY3 (Arsenal Street) west to the SHB.

NOTE 2. This is a walking tour of approximately 4.5 kilometers in length (Figure 8). The first portion of this trip will be a visit to Horse Island (private), which is connected to the mainland by a 250-meter, narrow strip of mossy cobbles and boulders submerged in upto 0.5 meters of water. Access to the island will require knee-deep wading with sandals (and dry shoes to change, if you choose). There will be a gazebo available on the island to change sandals/shoes (and vehicles on the mainland).

NOTE 3. The formal portion of this trip will terminate at the SHB proper, hopefully, allowing approximately 30 minutes to follow the official signed trail of the battlefield or visit the village.

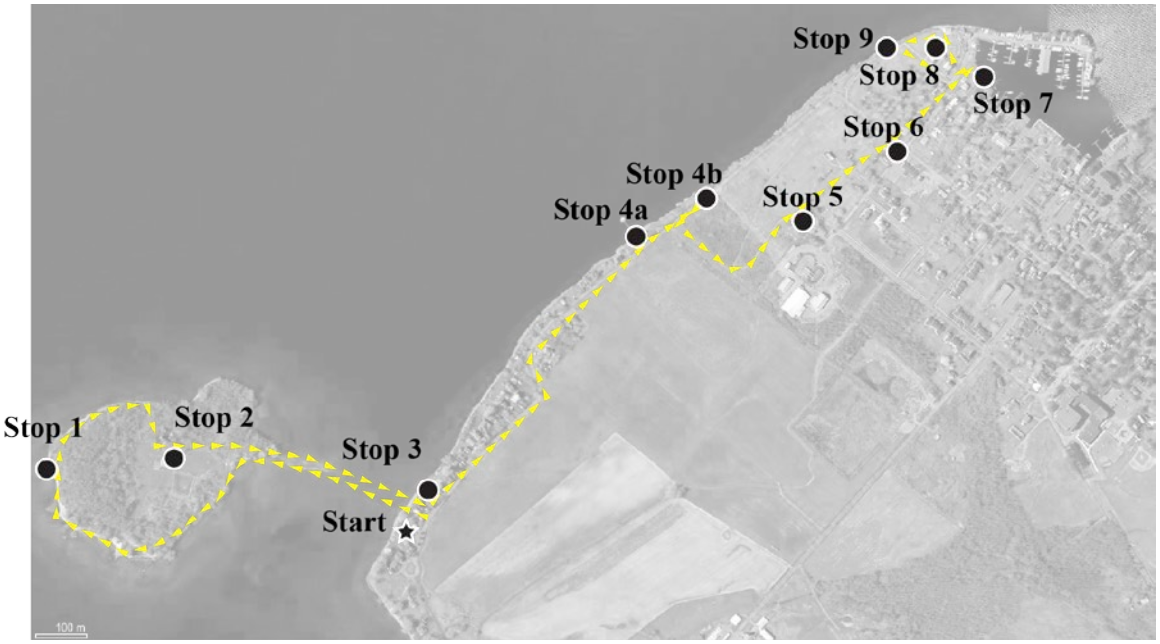

Figure 8. Overview map of the Sackets Harbor area showing the walking tour and stops. Start to Stop #3 is private property (see Table 1 for stop details).

CUMULATIVE KM (MILES)	KM (MILES) FROM LAST POINT	ROUTE DESCRIPTION
0.0 (0.0)		*PRIVATE*. Park at 444 Ontario Street to access Horse Island. Using care, cross tombolo to Horse Island.
0.4 (0.25)	0.4 (0.25)	At gazebo, change sandals/shoes for tour of island.
1.0 (0.6)	0.6 (0.35)	Walk counterclockwise the circumference of the island. There will be occasional, unofficial stops looking at limestone bedrock, joint patterns, glacial erratics and striations. **STOP 1** is on the western edge of the island.
1.4 (0.85)	0.4 (0.25)	Continue along the circumference of the island to the north; head south to SH lighthouse and **STOP 2** (led by Mrs. Diane Cozad, owner).
1.65 (1.1)	0.15 (0.1)	Continue south to gazebo. Change shoes/sandals.
2.0 (1.3)	0.35 (0.2)	Continue easterly across tombolo to mainland. Change sandals/shoes. **STOP 3.**
2.8 (1.8)	0.8 (0.5)	Continue northeast on Ontario Street to **STOP 4a** at the derelict oil-transfer mooring dolphin.
2.95 (1.9)	0.15 (0.1)	Continue northeast along lakeshore exposure to **STOP 4b** at the memorial-cross vista.
3.2 (2.0)	0.25 (0.15)	Backtrack on Ontario Street approximately 80 meters to access road heading landward to the east-southeast. Continue 150 meters to SHB trail access where we will pickup the USA retreat/UK advance.
3.35 (2.1)	0.15 (0.1)	Continue northeast on right fork of trail to Fort Kentucky (**STOP 5**).
3.55 (2.2)	0.2 (0.1)	Continue northeast on trail, through parking lot and into the grassy quadrangle amongst buildings (**STOP 6**).
3.8 (2.4)	0.25 (0.15)	Continue approximately 25 meters northeast to pickup the trail, continue along trail, across road, another 150 meters to the lieutenant's house (smaller yellow brick structure) and continue 75 meters toward the gated road access to the harbor (**STOP 7**).
3.9 (2.5)	0.1 (0.05)	Access fenced, park area by using gate on the east side of the lieutenant's house and proceed to open grassy area by boathouse (do not follow boardwalk) (**STOP 8**).
4.0 (2.6)	0.15 (0.1)	Continue to lakeshore and walk approximately 75 meters to the west-southwest along rocky coast (**STOP 9**).
4.25 (2.75)	0.25 (0.15)	Return to parking lot and vans by lieutenant's house (take boardwalk).

Table 1. List of stops, locations and highlights.

Stop (#, name)	Location	Highlights
Start	N 43.941448°, W 76.138362°	*Private Residence*, 440 Ontario Street, 13685
1—Amphibous assault	N 43.942376°, W 76.147381°	Amphibious assault point at greatest concealment; primary impact of lake waves, rolled and concentrated glacial erratics
2—Lighthouse	N 43.942944°, W 76.144514°	Horse Island (Sackets Harbor) Lighthouse (1870)
3—Beach berm defense	N 43.941664°, W 76.138352°	USA-defensive killzone; convergent longshore drift (tombolo) and storm-wave-deposited beach berm.
4a—Cliff retreat @ oil-transfer mooring dolphin	N 43.946724°, W 76.132373°	(1 of 2) exposure of joint-controlled cliff-face retreat due to coincident impingement of wavefronts.
4b—Cliff retreat @ memorial cross	N 43.947352°, W 76.131250°	(2 of 2) “lake stack” in progress
5—Ft. Kentucky (c. 1814)	N 43.947241°, W 76.128554°	Remnant, post-battle earthwork of Ft. Kentucky with 32” cannon.
6—Barracks assault	N 43.948224°, W 76.126645°	Center of barracks where fighting in-line occurred (surrounded by post-war structures)
7—Navy Point/Harbour view	N 43.950032°, W 76.123795°	Protective spit and harbor, location of the USS *General Pike*, which was prematurely burned during the battle
8—Ft. Tompkins	N 43.950280°, W 76.125050°	Location of Ft. Tompkins, the primary blockhouse-style fort that successfully defended the harbor
9—Lake view and cliff face	N 43.950313°, W 76.125742°	A lake-side exposure view of the 7+-meter cliff that protected Ft. Tompkins from shelling
End	N 43.949700°, W 76.124362°	

STOP 1 – UK AMPHIBIOUS ASSAULT LOCATION/WINDWARD SIDE OF HORSE ISLAND (private)/ JOINT-CONTROLLED "BIOSTROME" (ORDOVICIAN)

N 43.942376°, W 76.147381°

At this location you are in the most concealed position with respect to Forts Tompkins and Pike near Sackett's Harbour. This windward side of Horse Island was a "natural" place for Commanders Yeo and Prevost to make an amphibous assault (Figure 2). General Brown, NYM, however, had set up defensive positions in the treeline along this edge of the island. Upon dismounting, the UK troops were under fire from 6-pound field guns and the 32-pound gun, firing long range, from Fort Tompkins. Because the NYM were untrained, completely untested and feared the regular British troops, they retreated back across the shoal (tombolo) to the mainlaind where they set up another defensive position behind the storm-deposited beach berm (Figures 3 and 9).

> **"The militia soon began to assemble, and as fast as they arrived they were armed and sent to Horse Island, which was the point at which the enemy was expected to bind."** (Rodgers, 1897)

Figure 9. Photograph looking northeasterly at the mainland edge of the tombolo. It was along this storm-deposited beach berm that NYM Brigadier General Brown rallied some retreating militia to "defend" the mainland from the advancing British. With British advancing a few men abreast across knee-deep water and mossy cobbles, this should have been a guaranteed "kill zone" sending the British in retreat. The untested NYM, however, retreated despite their significant advantage.

Geologically, Horse Island is a joint-bounded (Figure 10), biostrome-like, coarse-grained limestone with well-exposed orthocone nautaloids at lake level. This coarse unit is overlain by approximately 0.5 meters of nodular calcisiltites in 5-10-centimeter beds interbedded with silts and shales. As you walk the perimeter of the island to this location you will notice an excellent assortment of glacial erratics, which have been storm-wave concentrated into piles and mantling the northern shore. These erratics, gabbros, gneisses, Potsdam sandstone, pegmatic granites and porphyritic gabbros, likely rolled out of the glacial drift covering the island. On the

western-most lake-level exposure are a series of glacial striations with a mean vector of 196° (n=8, σ=3.8°; Figure 11).

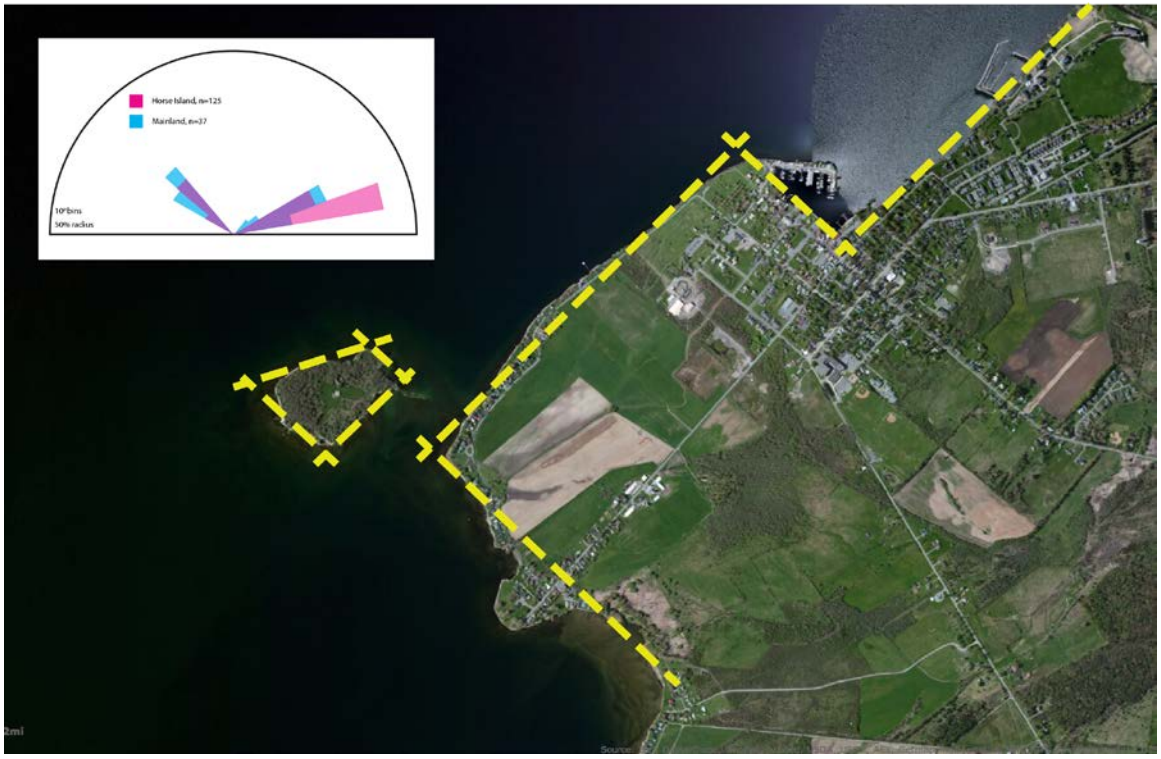

Figure 10. Satellite image of the Sackett's Harbour area highlighting the joint-controlled lakeshore and Horse Island (dashed lines). Inset is a rose diagram of both mainland and Horse Island joint data.

STOP 2 – HORSE ISLAND (SACKETS HARBOR) LIGHTHOUSE (c. 1870)(private)/INITIAL USA DEFENSIVE POSITIONS

N 43.942944°, W 76.144514°

The Horse Island lighthouse (Sackets Harbor, ARLHS USA-380) was originally emplaced in 1831 approximately 100 meters northwest of this location after Congress appropriated $4,000 for the building of a 1.5-story keeper's dwelling and tower (LHF, 2014). By 1869, the lack of upkeep resulted in conditions beyond repair; therefore, Congress appropriated more funds for a new Queen Anne/Italianete brick lighthouse and keeper's dwelling (Figure 12). In 1899, the tower received a ten-foot addition raising its height to 55.5 feet (LHF, 2014). This light was decommissioned in 1957 and replaced by a modern, steel tower.

Figure 11. Perspective photograph of glacier striations on Horse Island. North arrow is oriented correctly.

Because Commanders Yeo and Prevost decided to await calmer waters after their arrival to the Sackett's area on the evening of 27MAY (and a bungled attempt at attack that day), Brigidier General Brown, NYM was able to set up hasty defensive positions in and around this location. Most likely, positions would have been naturally made beach-berm positions during the initial amphibous assault. As the NYM retreated through the woods at this location, the British Regulars were able to reform and be supported by their naval comrades. To the east of this location, there is a thought-to-be entrenchment used by the NYM during the assault; however, it is coincident with the jointing in the area and is most likely mass wasting in progress (similar to Stop #4).

> **"…separated from the mainland by a shallow strait, which is always fordable and sometimes almost dry. This strait, which, with the approach, formed a causeway 400 yards in length, had to be traversed by the attacking column…"** (Hannay, 1903)

The military-geology of this island is limited to its ability to provide concealment to the amphibious landing party. This concealment was provided by trees growing atop a joint-controlled limestone "biostrome" that has withstood millenia of direct impingement of waves and storm waves. This energy was maximal on the western side of the island and wave refration wrapped around the island providing sediment for deposition due to lack of competence in the leeward side of the island making the tombolo used for the mainland assault. Along the eastern edge of the island there is an elongated "entrenchment," thought to be made/used by the NYM during the battle (and thereafter). Unfortunately, the structure is not man-made, but the intermediate phase of a block slump (similar to what can be seen at Stop #4). The strike of the feature is the same as the northwest-southeast joint set affecting the area. As far as its use by NYM during the War of 1812, that too is unlikely, for its orientaion and location is on the Fort Tompkins/garrison side providing little defensive or offensive purpose.

STOP 3 – TOMBOLO/MAINLAND/USA-HELD KILLZONE FOR ADVANCING UK FORCE/STORM-DEPOSITED BEACH BERM

N 43.941664°, W 76.138352°

At this point, NYM had retreated after a perfect opportunity to "shoot fish in a barrel" on the island. After their splashy retreat across the tombolo, what militia remained were rallied by Brown, NYM to take defensive positions behind these storm-deposited beach berms. This defensive action is best summarized by a retreating NYM, "I fear we shall be compelled to retreat … I know we shall, and as I am a little lame, I'll start now" (quoted in Wilder, 1994). Despite this natural, 250-meter, amphibious "killzone," the British regulars were able to cross the tombolo and make the mainland with little resistance and move northward along the shoreline to Fort Tompkins; CPT Viger of the British Voltigeurs (skirmish unit) flanked to the east trying to get around the US defenses (Figures 3 and 4).

Figure 12. Photograph of the Horse Island Lighthouse.

"The beach is of very limited extent, and bounded on the land side by a bank of sand several feet high, which had been thrown up by the current, as it rushed through the narrow channel separating Horse Island from the main. Behind this natural embankment, General Brown had formed a battalion of militia of 500 men" (Brown, 1827)

Figure 13. Satellite image of Horse Island with primary, secondary and tertiary wave crests highlighted. This image highlights well the wave-refraction and long-shore drift processes that accentuate the joint-controlled Horse Island and maintain the tombolo. During stormy times, these processes are magnified and provide most of the destructive and constructive events.

Figure 14a. View of Horse Island and tombolo from the mainland. This photograph was taken in April with relatively low water levels, thus showing the mossy, boulder-rich tombolo.

Figure 14b. View of Horse Island and tombolo from the mainland. This photograph was taken in October with relatively high water levels; likely the approximate water levels of late May in 1813 before lake-level management by the series of dams and locks on the St. Lawrence River.

This tombolo is the result of both wave refraction around the island converging at this location and longshore drift, which transports material around the island (Figures 13 and 14a,b). Its current geomorphology suggests that it is active only during conditions of greater than approximately 10-knot winds and 1-meter waves (pers. obsv.) with major storms being the most productive in re-working and re-organizing the tombolo. General composition of the tombolo is fine-coarse-grained clastics and shelly material. The erratic-rich locations, however, are probably the result of glacier-drift reworking and mantling along with human input. The island currently has electricity (run along the easterly side of the tombolo) and access to/from the island is commonly with vehicular traffic. As a result, concentrations of erratic boulders are likely accentuated due to reorganization for human purposes (such as the duck blinds on the west side of the island). Based on lake levels before the emplacement of dams along the St. Lawrence, the late-May battle date and historical accounts (e.g., Brown, 1827) the water level at the time of the assault was likely about knee-deep or "fordable depth" (Lossing, 1869)(Figures 14b).

STOP 4a – OIL-LOADING FACILITY EXPOSURE/WESTERN EDGE OF UK ADVANCE/CLIFF RETREAT AND JOINT EXPOSURES

N 43.946724°, W 76.132373°

Along this stretch of the lakeshore, advancing British troops were weaving through the dense underbrush of a wooded landscape. In addition, they were beginning to tackle the man-made defenses, *abatis* or an obstacle made of trees/sticks with sharpened end toward the enemy (Figure 5).

> **"The American artillerists toiling in Fort Tompkins repeatedly discharged the 32-pounder into the woods toward the oncoming British. A deluge of cannon balls, grapeshot, and bullets lopped off treetops and branches, which flew in every direction. One nearly killed Captain Jacques Adhimar [British Army]."** (Wilder, 1994)

The prominent structure at this location is the oil-loading mooring "dolphin," which was part of a Mobil Corporation petroleum bulk-storage facility that was emplaced during the 1920's (Figure 15). During WWII, tanks were added on the northern side of Ambrose Street expanding storage. Petroleum storage continued at this site until 1988 reaching 589Mbbl capacity with storage tanks being dismantled in 1989. Several environmental investigations have been completed since the 1980's evaluating the nature and extent of contamination; current results suggest that the site no longer contains any threat to human health or the environment (NYDEC, 2013).

STOP 4b – MEMORIAL CROSS VISTA/WESTERN EDGE OF UK ADVANCE/CLIFF RETREAT AND JOINT EXPOSURES AND LAKE "STACK"

N 43.947352°, W 76.131250°

Continuing north along the cliff face, the advancing British soldiers were under heavy fire from Fort Tompkins. In this approximate location, they were limited by the cliff and were mired in *abatis* or a man-felled brush-and-tree obstacle, but because the NYM were in retreat, much of this advance was unimpeded until they reached the cantonment clearing 100 meters or so farther north (Figure 5).

Geologically, this area shows pronounced weathering of the northwest-southeast joint sets, which are coincident with impinging wave fronts. The notched cliff face to the south (Horse Island way), begins to give way to a more vertical cliff that begins to show joint weathering deep into the cliff to reach the antithetic east-west joint sets. As a result, "lake stacks" are forming and collapsing from this point north to the harbor. From the cross location, you can see this transition from notched cliff face to sapped and retreating, vertical cliff face.

STOP 5 – FORT KENTUCKY (1814)/NYS MILITIA RETREAT/EARTHWORKS AND 32# CANNON

N 43.947241°, W 76.128554°

This 1960's reproduction 32# gun represents the firepower available atop Fort Tompkins. Just after the repulse of the British, Sackett's Harbour defenses were augmented with Forts Kentucky (palisaded earthwork), Chauncey (stone tower), Stark (earthworks) and a ring of earthworks connecting them to Forts Virginia and Volunteer (NAF, 2014). As the British advanced along the lakeshore, dealing with the woods and *abatis*, the NYM were making their way through the same along this path to the barracks, Fort Tompkins and Volunteer.

Figure 15. View from the memorial-cross location looking southward to Horse Island. Notice the notched lakeshore due to weathering of joint sets.

STOP 6 – BARRACKS/IN-LINE ENGAGEMENT

N 43.948224°, W 76.126645°

This is the approximate location of the Smith (Basswood) Cantonment (palisaded barracks complex with four blockhouses) where the soldiers were garrisoned (officers were quatered in village homes). At this point, the Americans were in line and prepared for the mired British advance. When the first "red jacket" was visible, the Americans fired from the line. Sending a staggering blow to the advancing British, the well-trained British responded in kind and were able to overcome the Americans with rapid and precise fire and advance, pushing the Americans back to the protection of the cantonment (Figures 5 and 6).

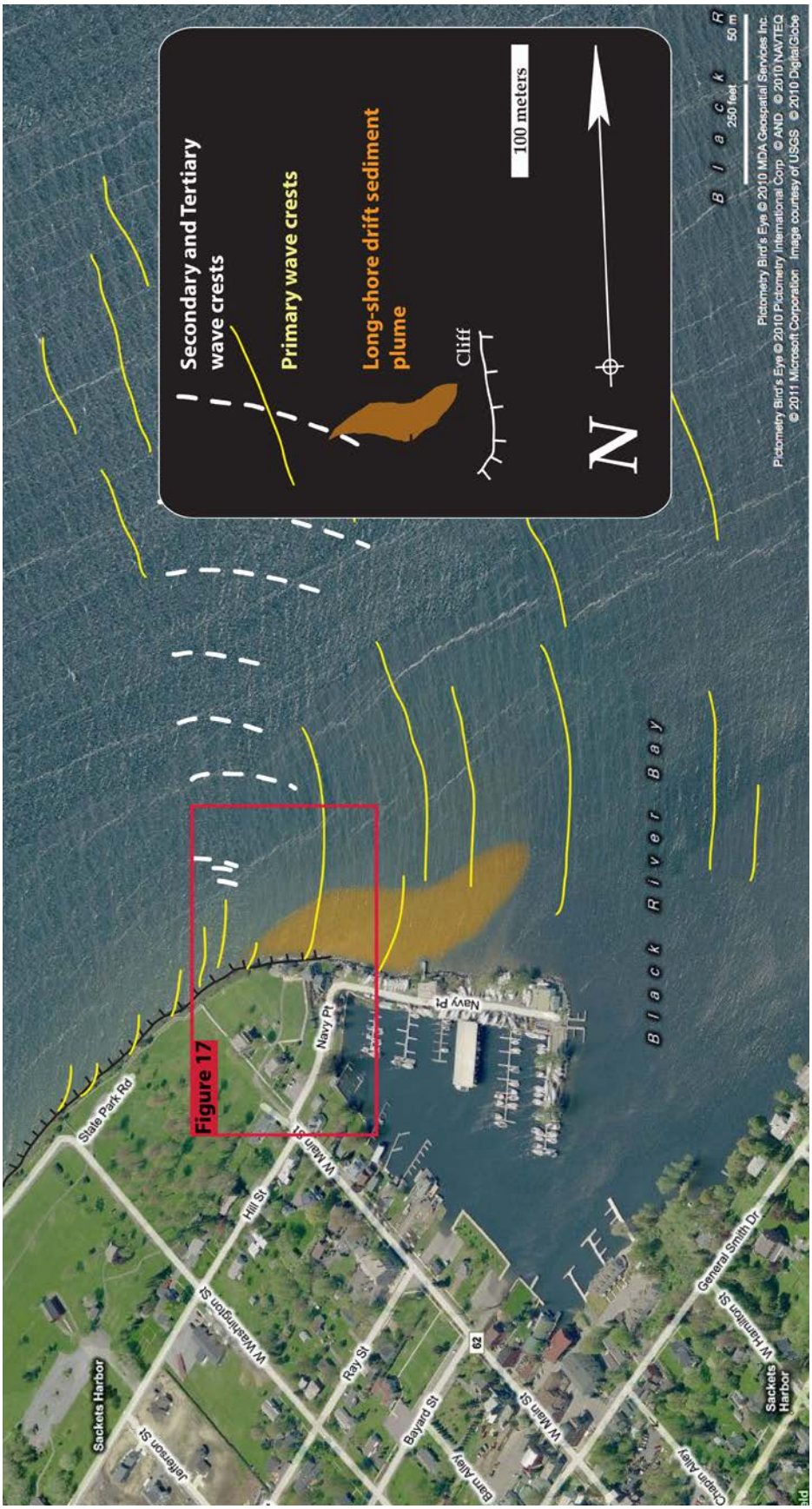

Figure 16. Satellite view of Navy Point and Sackets Harbor showing primary and secondary wave crests and long-shore drift sediment plume. The divergence between the current, low-energy sediment plume location and the actual Navy Point spit, shown in this image, is lessened during storm events. Stormy conditions increase the competence of longshore drift and wave refraction leading to preservation of the Navy Point.

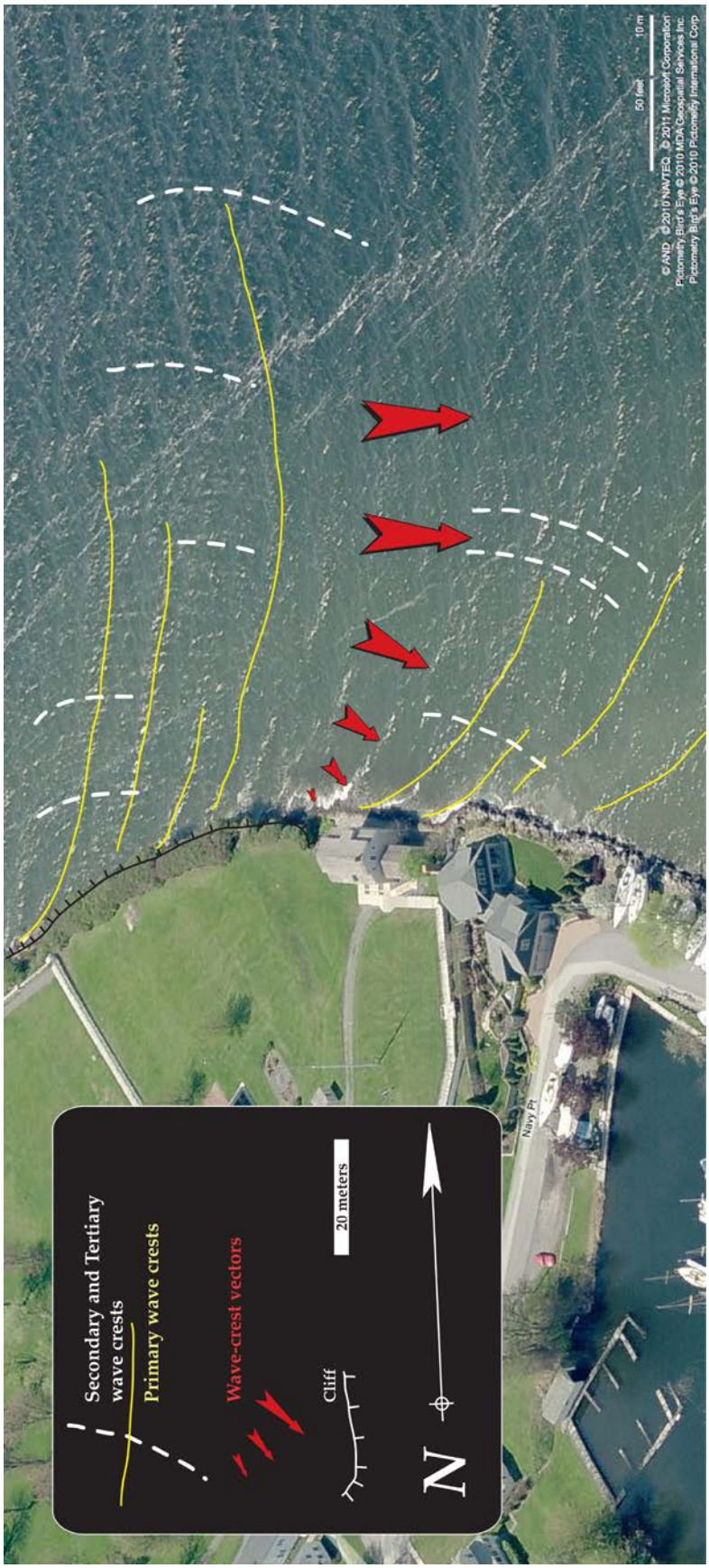

Figure 17. Close up of wave refraction into Navy Point (spit).

STOP 7 – NAVY POINT AND SACKETT'S HARBOUR/DRY-DOCKED USS *GENERAL PIKE* AND FORT PIKE/HARBOR AND STORM-DEPOSITED SPIT

N 43.950032°, W 76.123795°

From this location, the "Navy Point" spit is visible (Figures 16 and 17). In this relatively deep-water harbor (3-4m) the recently "laid down" USS *General Pike*, a 28-gun (24# each) corvette, named for the recently killed explorer/general Zebulon Pike (of Pike's Peak fame) was being constructed. This was the strategic key to the battle–completion of the USS *General Pike* would promise lake superiority to the US before the end of the sailing season, leading to control of Lake Ontario. This, however, was not the case, during the melee a signal was confused and sailors began setting the stores on Navy Point and the USS *General Pike* ablaze (Figures 6 and 7). Luckily, such hasty creations during wartime were made of green wood and the damage was limited, yet significant enough to guarantee British control of Lake Ontario until the following sailing season (1814).

Geologically, Navy Point is a storm-deposted spit resulting from the longshore transport of sediments from the southwest between here and Horse Island. At the time of the battle, this spit was likely a relatively fine-grained mass that would be altered during significantly stormy periods. With increased human intervention, the spit has become mantled and a more-or-less permanent structure for the protection of the harbor. Contemporaneous maps of the harbor (e.g., Wilkinson, 1816) show the "recurve" or waning wave-refracted, longshore drift appendage at the terminal end of the spit. This portion of the landform, too, has been mantled and has been turned into a docking structure.

STOP 8 – FORT TOMPKINS/PRIMARY HARBOR DEFENSE/JOINT-CONTROLLED MASS-WASTING BLOCK

N 43.950280°, W 76.125050°

This location was the center of the primary, blockhouse fortification for Sackett's Harbour. Mounted with a 32# cannon (like the replica at Fort Kentucky, Stop #5), it was the deciding factor in the success of the Americans and their downfall! Well-aimed shots from this gun kept the British at bay; however, because of confusion and lack of communication, overshots from the British Naval ships landing in/around Navy Point, were interpreted as enemy-controlled Fort Tompkins (Figure 6). Regardless, Fort Tompkins remained in American hands and was key to defending the harbor.

In this approximate location there is a block of harbor cliff that is in a medial state of mass-wasting failure. This intermediate failure is recognized by the joint-controlled gradient changes in the lawn adjacent the boathouse. These gradient changes (or escarpments) are coincident with the overall joint sets in the area (Figure 10). This portion of the cliff face is significantly larger than the other recently failed cliff sections (seen from Stops #4a,b) and, as a result, was "too large" to fully fail.

STOP 9 – LAKE ONTARIO SHORELINE/DEFENSIVE CLIFF FACE/SHOREHAM INTERVAL EXPOSURE AND WAVE-CUT CLIFF

N 43.950313°, W 76.125742°

Naval support of the British invasion at Sackett's Harbour was nil. Primarily, religated to an amphibious support role, the calm winds rendered their support useless. Of the ships near Horse Island, only one was equipped with "sweeps," or long oars, the HMS *Beresford*, which was able to slowly maneuver itself into a supporting role. This supporting role, however, was hampered by the incessant pounding of the the 32-pound Fort Tompkins gun and the inadvertant, yet careful placement of the Fort. The 7-meter cliff face below the Fort was a serendipitous protector (Figure 18). Because of the cliff and the placement of the Fort, at ranges naval firing ranges of 500 meters or so, accurate fire required an approximately 0.4-degree-boresight elevation

precision to place a shot through an approximately 25m^2 window of "opportunity." Although the British seamen were excellent shots and well trained the task proved too difficult.

> **"Most of the enemy's shot fell against the rocks [cliff] below the battery. One of these (a thirty-two-pound ball) came over the bluff, struck the earth not far from Sackett's mansion (then occupied by Vaughan's family), and plowed a deep furrow into the door-yard."** (Lossing, 1868)

Geologically, this cliff represents about seven meters of Trenton Group, "Shoreham" interval limestones of the Sugar River Formation (Table 2). From this location toward Horse Island, the overall topography of the land dips approximately 8m/km along the strike of the lakeshore (Wallach and Rheault, 2010), which is due to the Lake Ontario Homocline (Kay, 1942). This homoclinal structure is likely the result of Adirondack mountain orogenesis to the east with relatively recent glacial isostatic rebound. Along the lakeshore, from this location, there are excellent opportunities for fossil collection and observation of mass-wasting processes due to shoreline weathering and erosion.

Table 2: Formational descripton of the Navy Point cliff.

Formational description	Thickness (m) of unit	Thickness (m) to base of section
TRENTON GROUP		
Sugar River Formation		
Limestone and shale (90/10); limestone, medium-light gray (N6) to dark gray (N4), calcisiltite to fine-grained calcarenite; relatively homogenous……..	1.5	6.3
Limestone; light gray (N7) to dark gray (N4), calcarenite to calcisiltite with shaley partings and occassional shelly, coquina-type calcarenites; generally nodular bedding; occasional bioturbation; bryozoans, *Paucicrura, Sowerbyella, Flexicalymene, Cryptolithus* and *Prasopora*...	3	4.8
Limestone and shale (70/30); light gray (N7) to medium-light gray (N6), calcisiltite to calcarenite; laterally continuous centimeter-scale limestone beds with occassional thicker, 10-20cm, medium-grained calcarenite beds; bryozoans, *Paucicrura, Sowerbyella, Flexicalymene, Cryptolithus* and *Prasopora*……..	1.5	1.8
Limestone; medium-light gray (N6), calcirudite to very-coarse-grained calcarenite (shelly coquina); homogenous bed with rippled surface; *Oniella* and *Paucirura*…….	0.3	0.3

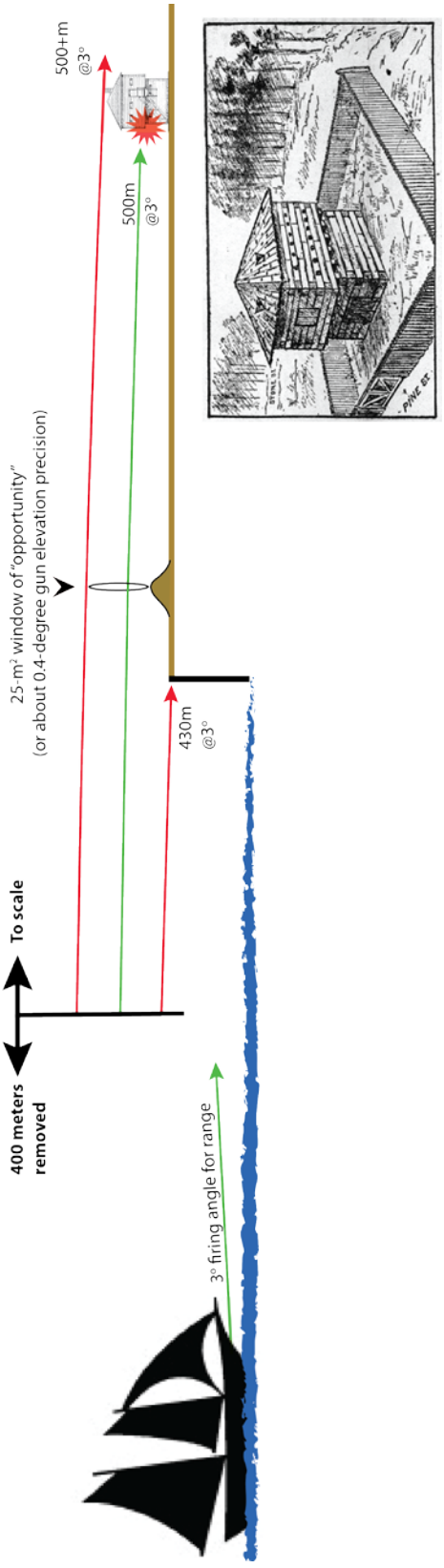

Figure 18. Scale reconstruction of the exemplarily-placed Fort Tompkins. Naval fire from the HMS Beresford (or other naval vessel) would be proximally limited to the harbor and the fort by a) fire from Fort Tompkins and b) unknown bathymetry of the lake. As a result, typical shots from the ship would be in the 100's meter range (here shown from 430 to 500 meters). In order to make a hit on Fort Tompkins, sailors would need to "hit" a 25-square-meter "window" of opportunity, which would only be successful if they were able to fine-tune their traverse (left-right) and elevation (up-down, 0.4-degree range at 500 meters). Although British sailors were excellent shots, winds, waves and return fire prevented them from successfully defending their advancing infantry.

ACKNOWLEDGMENTS

We thank Mrs. Diane Cozad and her father, Carl B. Martin, Jr. for granting us access to Horse Island on several occasions. Special thanks to Mrs. Cozad for her interest in the island, its lighthouse and for providing a tour for this group. Thanks also to Dr. Jennifer Gifford, Ms. Saddie Serviss, Ms. Catherine Heinrich and Ms. Erika Rodbell for field assistance. Many thanks to the staff of the Sackets Harbor Battlefield State Historic Site for their help and insight. Thanks to St. Lawrence University's Department of Geology for travel support.

REFERENCES

Brown, J., 1827. Original Memoirs of Distinguished Foreign Officers. The Naval and Military Magazine, v.1, p.59-87.

Guth, P.L., 1998. Military geology in war and peace: An introduction, *in* Underwood, J.R., Jr., and Guth, P.L., eds., Military Geology in War and Peace. Geol. Soc. of Am. Reviews in Engineering Geology, v.XIII, p.1-4.

Hannay, J., 1903, The War of 1812. Canadian Magazine, v.21, p.49-55.

Katchen, P. and Fosten, B., 1990. The American War, 1812-1814. Osprey Press: Men-at-Arms Series #226, London, 48p.

Kay, G.M., 1942. Ottawa-Bonnechere graben and Lake Ontario homocline. Geol. Soc. Am. Bull., v.53, n.4, p.585-646.

Kiersch, G.A. and Underwood, J.R., Jr., 1998. Geology and military operations, 1800-1960: An overview, *in* Underwood, J.R., Jr., and Guth, P.L., eds., Military Geology in War and Peace. Geological Society of America Reviews in Engineering Geology, v.XIII, p.5-27.

Latimer, J., 2010. 1812: War with America. Belknap Press, London, 656p.

Lighthousefriends (LHF), 2014. Horse Island (Sackets Harbor), NY. http://www.lighthousefriends.com/light.asp?ID=312 accessed (July, 2014).

Lossing, B. J., 1868. The Pictorial Field-Book of the War of 1812. New York, Harper Brothers, 1084p.

NAF, 2014. Sackets Harbor Forts, http://www.northamericanforts.com/East/New_York/Sackets_Harbor/Sackets_Harbor.html accessed (July, 2014).

NYDEC, 2013. Former AFMC Facility Record of Decision. Division of Environmental Remediation, NYDEC, http://www.dec.ny.gov/docs/remediation_hudson_pdf/e623014ou2rod.pdf accessed (July, 2014).

Rodgers, F. D., 1897. Folk-Stories of the Northern Border. Clayton NY, Thousand Islands Publish., p.110-111.

Stewart, A. K., 2014. U.S. Army Agriculture Development Teams: A Grassroots Effort in Afghanistan Supporting Development and Tackling Insurgency. Science and Diplomacy, v.3, n.1, p.70-87.

Wallach, J.L. and Rheault, M., 2010. Uplift of the Tug Hill Plateau in Northern New York State. Canadian Journal of Earth Sciences, v.47, p.1055-1077.

Wilder, P.A., 1994. The Battle of Sackett's Harbour. Nautical and Aviation Publishing Company of America, Baltimore, 162p.

Wilkinson, J., 1816. Memoirs of My Own Times (Vols. 1-3). Abraham Small Publisher, Philadelphia. 960p., https://archive.org/details/memoirsofmyownti01wilk accessed (July, 2014).

GEOCHEMISTRY OF TOURMALINE FROM SOME ADIRONDACKS LOCATIONS: INDICATOR OF THE HOST ENVIRONMENT

MARIAN V. LUPULESCU
Research and Collections, New York State Museum, Albany NY

JEFFREY R. CHIARENZELLI
Department of Geology, St. Lawrence University, Canton NY

"*With its plethora of chemical constituents, its wide range of stability from conditions near the Earth's surface to the pressures and temperatures of the upper mantle, and its extremely low rates of volume diffusion, tourmaline can acquire a chemical signature from the rock in which it develops and can retain that signature through geologic time*." (Dutrow and Henry 2011)

INTRODUCTION

Tourmaline is a complex borosilicate and it can record the chemistry of its host environment and the chemical changes in the composition of the generating fluids or associated minerals.

Tourmaline-supergroup minerals are found as a primary accessory phase in granites and pegmatites, breccia, and hydrothermal quartz veins (London and Manning 1995), metamorphic rocks ranging from zeolite to granulite facies (Henry and Dutrow 1992; Ertl et al. 2010), volcanogenic massive sulfide deposits (Slack et al. 1996), and authigenic overgrowths in sedimentary rocks (Henry et al. 1994; Lupulescu et al. 2010). Variation in the chemical composition of tourmaline species allows them to form in a wide range of environments. This feature makes them an excellent indicator of the environmental conditions of their host and is further enhanced by their very low rate of diffusion at high temperature and resistance to weathering (Hinsberg et al. 2011).

Due to its hardness and lack of cleavage, the tourmaline in sedimentary rocks can be used as a provenance indicator (Henry and Guidotti 1985; Henry and Dutrow 1992; Morton et al. 2005; Marschall et al. 2008) and the varied colors contribute to make it a desired gemstone (Pezzota and Laurs 2011). It also has pyroelectric, piezoelectric, and optical (polarizing light) properties. The ability to polarize light adds credibility to the legend of the "Viking Sunstone", but it was used in the modern times to make polarizers for petrographic microscopes.

The goal of this trip is to visit and discuss the significance of the chemical, major and trace elements, of tourmaline from different locations and environments within the Adirondack Lowlands, such as tourmalinites, talc-tremolite schists, quartz veins, simple pegmatites, Balmat SEDEX-type deposits, and authigenic tourmaline. In addition, some new geochronological information is present to help put the tourmaline occurrences in geologic context. The quantity and variability of tourmaline occurrences in the Adirondack Lowlands is still poorly understood and this trip hopes to bring attention to their diversity.

THEORETICAL BACKGROUND

Tourmaline generalized structural formula is: $XY_3Z_6(T_8O_{18})(BO_3)_3V_3W$ where:
X = Na^{+}, Ca^{2+}, K^{+};
Y = Fe^{2+}, Mg^{2+}, Mn^{2+}, Al^{3+}, Li^{+}, Fe^{3+}, Cr^{3+};
Z = Al^{3+}, Fe^{3+}, Mg^{2+}, Cr^{3+};
T = Si^{4+}, Al^{3+};
V = OH^{-}, O^{2-};
W = OH^{-}, F^{-}, O^{2-}

Table 1. Simplified classification of tourmaline species recognized by International Mineralogical Association (Henry et al. 2011 – modified)

Alkali group
Dravite - $NaMg_3Al_6Si_6O_{18}(BO_3)_3(OH)_3(OH)$
Schorl – $NaFe^{2+}{}_3Al_6(Si_6O_{18})\ (BO_3)_3(OH)_3(OH)$
Chromium-dravite – $NaMg_3Cr_6(Si_6O_{18})(BO_3)_3(OH)_3(OH)$
Vanadium-dravite – $NaMg_3V_6(Si_6O_{18})(BO_3)_3(OH)_3(OH)$
Fluor-dravite - $NaMg_3Al_6(Si_6O_{18})(BO_3)_3(OH)_3F$
Fluor-schorl - $NaFe^{2+}{}_3Al_6(Si_6O_{18})\ (BO_3)_3(OH)_3F$
Tsilaisite - $NaMn_3Al_6(Si_6O_{18})(BO_3)_3(OH)_3OH$
Elbaite - $Na(Li,Al)_3Al_6(Si_6O_{18})(BO_3)_3(OH)_3(OH)$
Fluor-elbaite – $Na(Li_{1.5}Al_{1.5})Al_6(Si_6O_{18})(BO_3)_3(OH)_3F$
Povondraite – $NaFe3+_3(Fe^{3+}{}_4Mg_2)_6(Si_6O_{18})(BO_3)_3(OH)_3O$
Chromo-alumino-povondraite – $NaCr_3(Al_4Mg_2)_6(Si_6O_{18})(BO_3)_3(OH)_3O$
Oxy-schorl – $Na(Fe^{2+}{}_2Al)Al_6Si_6O_{18}(BO_3)_3(OH)_3O$
Oxy-vanadium-dravite – $NaV_3(V_4Mg_2)(Si_6O_{18})(BO_3)_3(OH)_3O$
Vanadio-oxy-chromium-dravite – $NaV_3(Cr_4Mg_2)(Si_6O_{18})(BO_3)_3(OH)_3O$
Oxy-chromium-dravite – $NaCr_3(Cr_4Mg_2)(Si_6O_{18})(BO_3)_3(OH)_3O$
Oxy-dravite – $Na(Al_2Mg)(Al_5Mg)(Si_6O_{18})(BO_3)_3(OH)_3O$
Vanadio-oxy-dravite – $NaV_3(Al_4Mg_2)(Si_6O_{18})(BO_3)_3(OH)_3O$
Darrellhenryite – $Na(LiAl_2)Al_6\ (Si_6O_{18})(BO_3)_3(OH)_3O$
Fluor-buergerite – $NaFe^{3+}{}_3Al_6(Si_6O_{18})\ (BO_3)_3O_3F$
Olenite – $NaAl_3Al_6(Si_6O_{18})(BO_3)_3O_3(OH)$
Calcic-group
Fluor-uvite - $CaMg_3(Al_5Mg)(Si_6O_{18})(BO_3)_3(OH)_3F$
Feruvite – $CaFe^{2+}{}_3(MgAl_5)_6(Si_6O_{18})(BO_3)_3(OH)_3(OH)$
Uvite - $Ca(Mg,Fe^{2+})_3Al_5Mg(Si_6O_{18})(BO_3)_3(OH)_3(OH)$
Fluor-liddicoatite – $Ca(Li_2Al)_3Al_6(Si_6O_{18}(BO_3)_3(OH)_3F$
Vacant-group
Foitite - $?(Fe^{2+}{}_2Al)Al_6(Si_6O_{18})(BO_3)_3(OH)_3(OH)$
Magnesio-foitite - $?(Mg_2(Al)Al_6(Si_6O_{18})(BO_3)_3(OH)_3(OH)$
Rossmanite - $?(LiAl_2)Al_6(Si_6O_{18})(BO_3)_3(OH)_3(OH)$

TOURMALINES OF NEW YORK

The tourmaline-supergroup minerals are commonly found in the rocks of the Grenville Province in New York State. Although, most specimens are not of gem quality, the tourmaline minerals from New York are scientifically interesting. They are well documented and represented in the literature by: (a) occurrence; (b) composition; (c) mode of formation; (d) crystal structure; and (e) the potential for discovery of new species (Dunn et al. 1977; Ayuso and Brown 1984; Cotkin 1989; Grice and Ercit 1993; Dyar et al. 1998; Dalton 2003; Lupulescu, Bailey, and Pyle 2005; Lupulescu and Pyle 2006; Lupulescu 2007; 2008; Chamberlain, Lupulescu, and Rowe 2008; Lupulescu and Rakovan 2008; Lupulescu et al. 2010; Lupulescu and Rowe 2011).

Herein the trace element composition of the tourmaline-group minerals from New York State is examined in relationship to their local geological environment.

GENERAL FEATURES, HOST ENVIRONMENT, AND CLASSIFICATION OF THE NEW YORK TOURMALNE SPECIES

General features. The main features of the tourmaline species found in New York are:

(a) In polarizing light some crystals display weak zoning, however, the difference in the chemical composition between zones is not significant. An interesting exception occurs at Bigelow, St. Lawrence County, where diagenetic uvite is overgrown by dravite (Lupulescu et al. 2010);

(b) Alteration is not common, attesting to the recalcitrant nature of tourmaline. Only one specimen was found extensively altered to a glassy, yellow-green, sheet silicate along fractures and crystal faces;

(c) The chemical composition of New York tourmalines shows extensive substitutions of Na^{+} and K^{+} for Ca^{2+} in the X-site; and

(d) There is significant replacement of $(OH)^{-}$ and O^{2-} by F^{-} in the W-site. Fluorine-dominant species are predominant in marbles.

We studied the variation in major components in two of the zoned (in plane-polarized light) tourmaline crystals, one from Edwards and the other from the Rt. 58 pegmatite. Sodium, Ca, Mn, and F do not display significant variation while Al, Ti, Mg, and Fe show variation along the "c" axis of the crystals. This variation may cause the zonation observed optically in thin-section.

Host environment. The geological distribution of the tourmaline species shows their preference for a specific host. This indicates both the source of their chemical components and their mineral-forming reactions.

(a) Schorl and some dravite specimens generally occur in pegmatites and uvite, fluor-uvite, dravite, and fluor-dravite are found in marbles;

(b) Mn-rich uvite and Mn-rich dravite are specifically associated with talc-tremolite schists in the upper marble unit in the Adirondack Lowlands;

(c) The unusual occurrence of Al-rich, chromium-dravite in pods in talc-tremolite schists (Lupulescu and Rowe 2011) in the upper marble is related to the local geologic setting.

There is a remarkable occurrence of rossmanite in Newcomb, Essex County. This locality is significant because: (a) it is the first occurrence of rossmanite in New York; (b) rossmanite is extremely rare in the USA; (c) it occurs in marble rather than in its more typical setting within granitic pegmatites; and (d) this is a new occurrence of tourmaline with boron in tetrahedral coordination (Lupulescu and Rakovan 2008).

Classification. The chemical composition of tourmaline species was determined using JEOL 733 Superprobe or CAMECA SX 100 at the Department of Earth and Environmental Sciences, Rensselaer Polytechnic Institute, Troy, N.Y.. The operating conditions were 15 kV accelerating voltage, 15 nA beam current, and 5-μm beam diameter. Standards used were: kyanite (Si, Al), synthetic forsterite (Mg), synthetic fayalite (Fe), synthetic diopside (Ca), jadeite (Na), rutile (Ti), synthetic tephroite (Mn), orthoclase (K), chromite (Cr), synthetic V_2O_3, and topaz (F).

The dominant compositional groups of New York tourmalines, based on electron microprobe data and cation assignment to crystallographic sites (Henry et. al 2011), are: (a) alkali group - schorl, dravite, fluor-dravite, and Al-rich-chromium-dravite; (b) vacant group – rossmanite, and (c) calcic group (uvite, fluor-uvite, and feruvite) tourmalines.

In this article we present the revised classification of the tourmalines of New York utilizing modern nomenclature (Table 2 at end of manuscript). All the specimens mentioned in the table are from the New York State Museum mineral collection and were investigated by optics and SEM-EDS and quantitatively analyzed by electron microprobe as part of our ongoing research of New York's mineralogy. The tourmaline species are named according to the latest nomenclature (Henry et al. 2011). This data allows the establishment of 'standard' specimens from a specific site in order to help others label their tourmaline species more accurately.

Trace elements. Trace element analysis was carried out on polished thin-sections of tourmaline crystals using laser ablation – inductively coupled plasma- mass spectrometry (LA-ICP-MS). Laser ablation was carried out with a detachable Photon Machines, Inc. Analyte.193 ultra-short pulse, excimer laser ablation workstation. A Bruker 820-MS inductively coupled plasma mass spectrometer was used for major elements.

We analyzed tourmaline crystals from: (a) talc-tremolite schists (Arnold Pit, St. Lawrence County); (b) quartz-tourmaline vein cutting a metamorphosed ultramafic body (Warrensburg, Warren County); (c) paleokarst filling sandstone in marble (Bigelow, St. Lawrence County); (d) graphitic schists (Columbia graphite mine, Essex County); (e) quartz-tourmaline veins in calc-silicate schists (Bower Powers farm, St. Lawrence County); (f) pod of tourmaline in marble (Balmat, St. Lawrence County); (g) tourmalinite (Rock Island and Richville, St. Lawrence County); (h) danburite-diopside rock (Russell, St. Lawrence County); (i) pegmatoid separation with quartz, feldspar, and halite (Balmat, St. Lawrence County); (j) simple pegmatite vein in gneiss (Rt. 58, St. Lawrence County; and (k) rossmanite with dravite and scapolite in marble (Newcomb, Essex County). The concentrations of the trace elements in the tourmalines noted above are listed in Table 3.

Table 3. Trace elements in tourmaline specimens analyzed in this study.

Element (ppm)	AP	W	BG	CG	BP	B	RI	RUS	RICH	BP	RT58	N
Li	37.72	15.17	47.02	26.15	11.50	41.33	11.48	20.06	8.10	158.07	12.23	2825.5
Sc	2.76	7.88	3.40	0.54	61.28	34.33	87.62	2.17	78.66	0.52	31.48	nd
Ni	27.35	130.82	2.86	1.78	4.47	3.08	37.28	2.29	18.56	0.87	52.3	0.45
Cu	4.28	0.28	0	0.62	0.89	3.36	0.67	2.21	18.56	0.87	0	nd
Zn	7.57	89.16	33.6	82	60.72	55.06	11.82	148.74	10.30	726.4	38.75	nd
Rb	0.01	0.04	0.04	0.02	0.01	0	0	0	0.03	3.69	0.03	nd
Sr	509.63	203.4	533.6	196.68	1018.4	700.8	160.96	856.6	125.8	1213	51.2	51.78
Y	0.39	0.52	0.01	0.10	0.02	0.06	0.21	0.04	0.31	0.04	0.26	0.01
Zr	2.60	1.69	0.23	0.28	0.49	1.86	136.02	0.60	2.84	1.33	0.53	0.014
Nb	0.80	1.49	0.03	0.67	0.33	0.09	0.30	1.82	0.03	12.16	0.39	nd
Ag	0.03	0.03	0.02	0.02	0	0	0.01	0.01	0.01	0.02	0	nd
Ba	57.50	2.93	2.93	0.67	6.01	12.09	1.24	3.13	1.77	3.28	0.50	0.04
La	7.95	21.27	0.06	5.14	22.88	1.48	20.99	8.96	6.78	4.01	6.98	0.02
Ce	6.97	35.42	0.06	6.40	24.08	2.56	18.39	9.73	11.23	5.19	14.16	0.01
Pr	0.59	3.17	0.01	0.43	1.42	0.24	0.92	0.55	0.95	0.30	1.33	nd
Nd	1.27	9.26	0.09	0.91	3.07	0.88	1.76	0.94	2.91	0.56	3.71	nd
Sm	0.10	1.01	0.02	0.05	0.14	0.09	0.09	0.02	0.32	0.04	0.52	nd
Eu	0.03	0.58	0.03	0.31	0.26	1.24	0.19	0.12	0.50	0	0.40	nd
Gd	0.09	0.53	0.10	0.02	0.12	0.08	0.07	0.02	0.13	0.02	0.32	nd
Tb	0.01	0.04	0.01	0.01	0	0	0	0	0.01	0	0.03	nd
Dy	0.06	0.17	0.02	0.03	0	0.02	0.01	0.01	0.08	0.05	0.11	nd
Ho	0.02	0.03	0.01	0.01	0.01	0	0.01	0	0.01	0	0.02	nd
Er	0.04	0.05	0	0.01	0	0	0.03	0	0.05	0	0.04	nd
Tm	0.01	0.01	0.01	0.01	0	0	0.01	0	0.01	0	0	nd
Yb	0.06	0.12	0.04	0.06	0.02	0.01	0.12	0	0.12	0	0.03	0.06
Lu	0.01	0.05	0.01	0.02	0.01	0	0.02	0	0.03	0.01	0	nd
Hf	0.22	0.29	0.04	0.09	0.07	0.11	3.31	0.11	0.12	0.09	0.08	nd
Ta	0.25	0.54	0	0.21	0.06	0.01	0	0.12	0	0.14	0.10	nd
W	0.03	0.05	0.04	0.07	0.01	0.03	0.07	0.01	0	0.30	0.09	nd
Pb	15.93	19.36	0.42	7.30	0.73	2.03	0.22	1.04	0.41	53.98	2.45	0.07
Th	0	0	0	0.2	0	0.21	0.32	0.25	0.06	0.06	0	nd
U	0	0	0.02	0.03	0	0.03	0.25	0.02	0.05	0.06	0.12	0.01

Abbreviations: AP Arnold Pit; W Warrensburg; BG Bigelow; CG Columbia graphite mine; B Balmat; RI Rock Island; RUS Russell; RICH Richville; BP Balmat pegmatite; Rt 58 Route 58; N Newcomb; nd not-determined

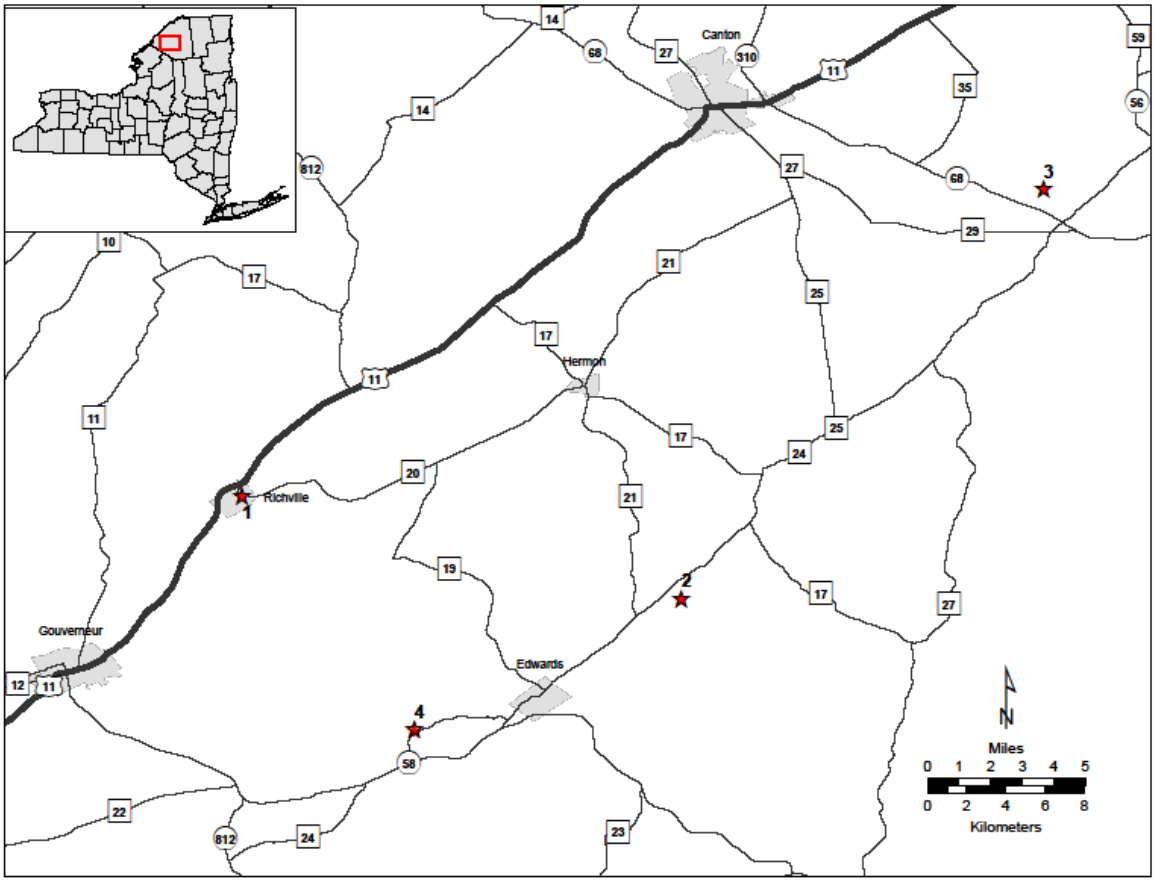

Figure 1. Map showing the tourmaline locations to be visited during this trip. Stop 1- Richville; 2. Stop 2 – Danburite location at Russell; 3. Stop 3 – Bower Powers Farm; 4. Stop 4 – Talcville.

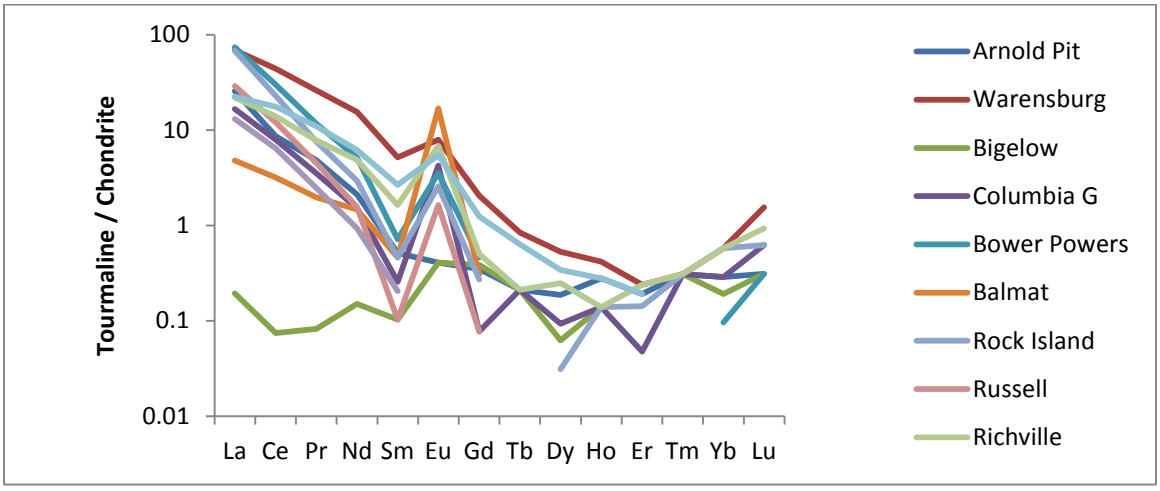

Figure 2. Rare earth elements in tourmaline normalized to chondritic values.

During this trip we will visit several interesting tourmaline occurrences in St. Lawrence County (Figure 1). Tourmaline species that formed in different environments show a wide rnage of trace element concentrations. The Bigelow tourmaline, formed as authigenic mineral in the paleo karst filling sandstones, is strongly depleted in trace elements. The Newcomb tourmaline contains the highest amount of lithium (2825.5 ppm) followed by the dravite associated with quartz, feldspar, and halite from Balmat (158.07). Strontium varies from 51.2 ppm (Rt. 58) to 1213 ppm (BP). Zirconium displays enrichment (136.02 ppm) in the Rock Island tourmaline. The REEs are at very low concentrations in all the tourmaline species analyzed; often below chondritic values for the mid-heavy REEs. Almost all of the tourmaline species display a high Eu* (Figure 2).

Divalent europium stability is predicted in aqueous solutions at high temperature and is consistent with large positive europium anomalies in some hydrothermal and metamorphic barite (Sverjensky 1984). The peak temperature of metamorphism in the Lowlands is estimated at 650º to 700ºC (Edwards and Essene 1988) and is consistent the presence of the Europium anomalies observed in Figure 2. Ratios of La_N/Yb_N, La_N/Sm_N, and Gd_N/Yb_N are a reflection of the enrichment of light REEs in the analyzed tourmalines.

FIELD TRIP STOP LOCATIONS

Stop 1.

TOURMALINE BEARING GNEISSES AT RICHVILLE (RT. 11)
N 44° 25' 21"N, W 75° 23' 19"
Outcrop on north side of busy State Highway 11, exercise extreme caution

Exposed in this outcrop is a layered sequence of quarztofeldspathic gneisses containing up to 50%, or more, black tourmaline as small equant grains (Figure 3). These tourmaline-rich rocks and tourmalinites can be traced for 50 kilometers or more north of Route 11 in the Lowlands. They occur as a northeast-trending belt of northwest-dipping tourmaline-bearing metasedimentary rocks in the lower marble and were originally studied by Brown and Ayuso (1984). Spectacular breccias comprised of angular blocks of these rocks help define the trace of a large Paleozoic wrench fault north of Goveurneur (Selleck, 2005).

Well defined layering within the outcrop is suggestive of a detrital origin for the rocks. Despite deformation and upper Amphibolite facies metamorphism layers are defined by changes in grain-size, layer thickness, color and staining, and modal mineralogy, including variations in quartz, k-spar, tourmaline, and pyrite. Note the iron staining related to sulfide-rich areas in the outcrop. A metasedimentary origin is also indicated by detrital zircon studies which are summarized below.

The meter-scale layer quartzose layer dipping slightly across the face of the outcrop to the west was sampled for U-Pb zircon analysis (Figure 4). The rock is a feldspathic quartzite with abundant detrital? tourmaline grains. Approximately one kilogram of rock was collected and a small number of zircons, ranging in size from 25-150 microns were separated by standard techniques at the Arizona Laserchron Center at the University of Arizona in Tucson. The zircons separated were imaged by scanning electron microscope including both back scattered electron (BSE) and cathodoluminscence (CL) modes (Figure 5).

While zoning and other internal features were common, metamorphic rims are restricted to 1-2 micron euhedral overgrowths on a small population of the zircon present prohibiting their analysis. The shape of grains ranges considerably from nearly perfect rounded grains in two dimensional cross-sections to a wide variety of euhedral and suhedral to subrounded shapes. The grains have substantially difference BSE and CL signatures suggestive of a wide variation in trace element chemistry and multiple sources.

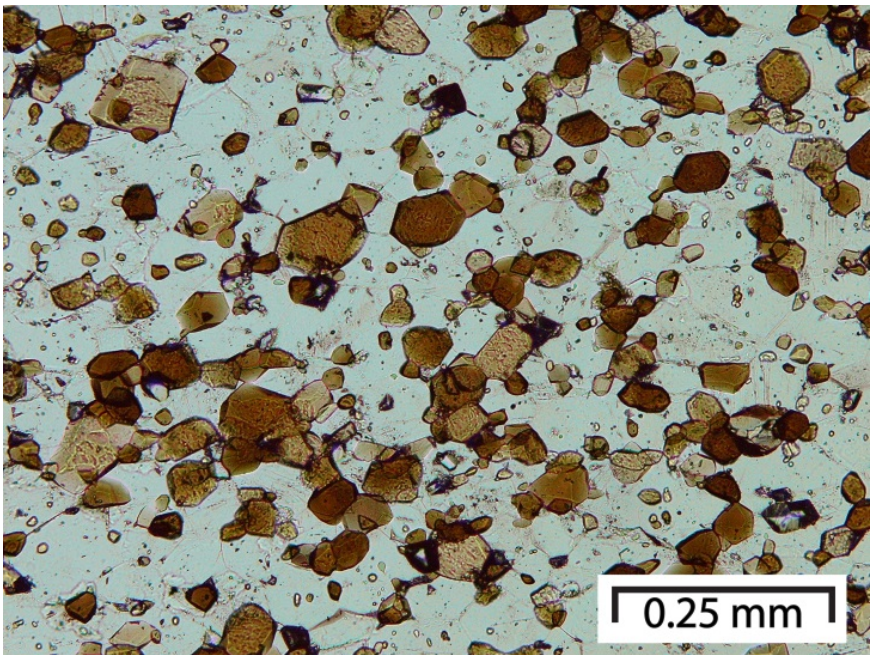

Figure 3. Polygonal to hexagonal, nearly equant grains of tourmaline in the tourmalinite layers from Richville.

Zircons from the quartzite layer have a complex age distribution (Figure 6). Most grains appear to have been derived from Proterozoic terranes to the west, yielding ages corresponding to the Mid-continent Granite-rhyolite province and Mazatzal, Yavapai, and Penokean orogens, rather than a more limited source to the north in the Grenville Province. Particularly telling are the lack of ca. 2.65-2.75 Ga zircons from the adjacent Southern Superior Province and the relative abundance of 1.80-2.00 Ga zircons compatible with Penokean or Trans-Hudson sourcing. A possible southern source is ruled out by the presence of Early Proterozoic and Archean components and the scarcity of 1.30-1.40 Ga detrital zircons indicative of the Southern Adirondack tonalitic rocks.

Figure 4. The layer sampled for detrital zircon analysis at Richville is just above Roselyne Laboso.

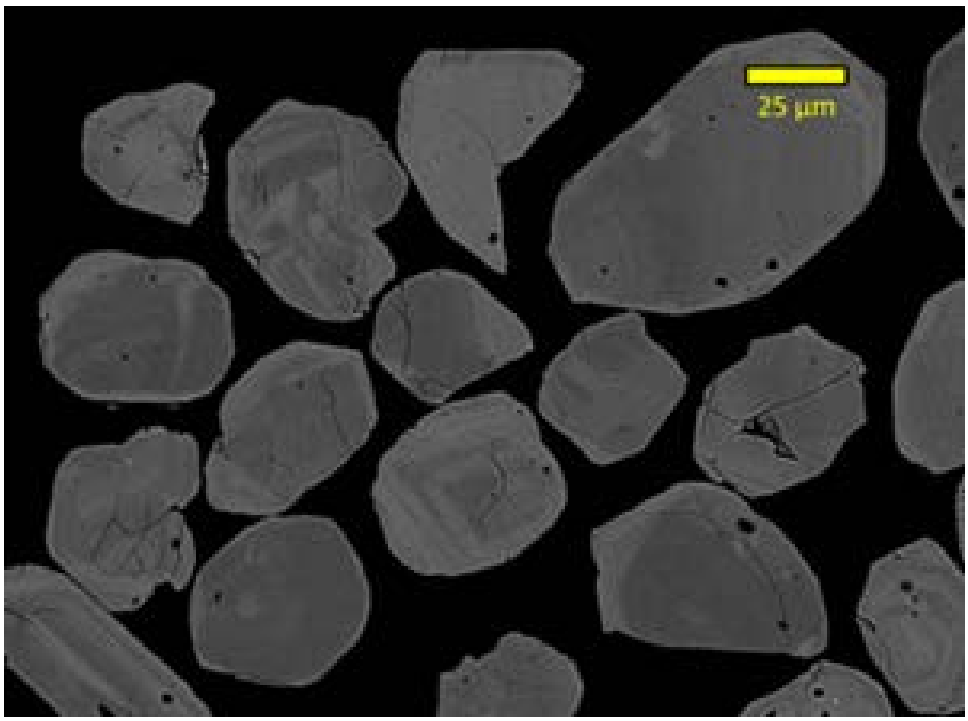

Figure 5. Back scattered electron image of detrital zircons from the Richville feldspathic quartzite.

The youngest zircons in the rock yield an age of 1257.6±16 Ma. This age yields maximum age of deposition for the Lower Marble between ca. 1241-1273 Ma and establishes its deposition prior to the Elzevirian Orogeny. This result is consistent with the Lu-Hf dating of apatite in the Lower Marble (1274+/-9 Ma; Barfod et al., 2005) and the presence of large isoclinal folds in the Lower Marble crosscut by the Antwerp-Rossie granitoids (1203±13.6 Ma; Chiarenzelli et al., 2010).

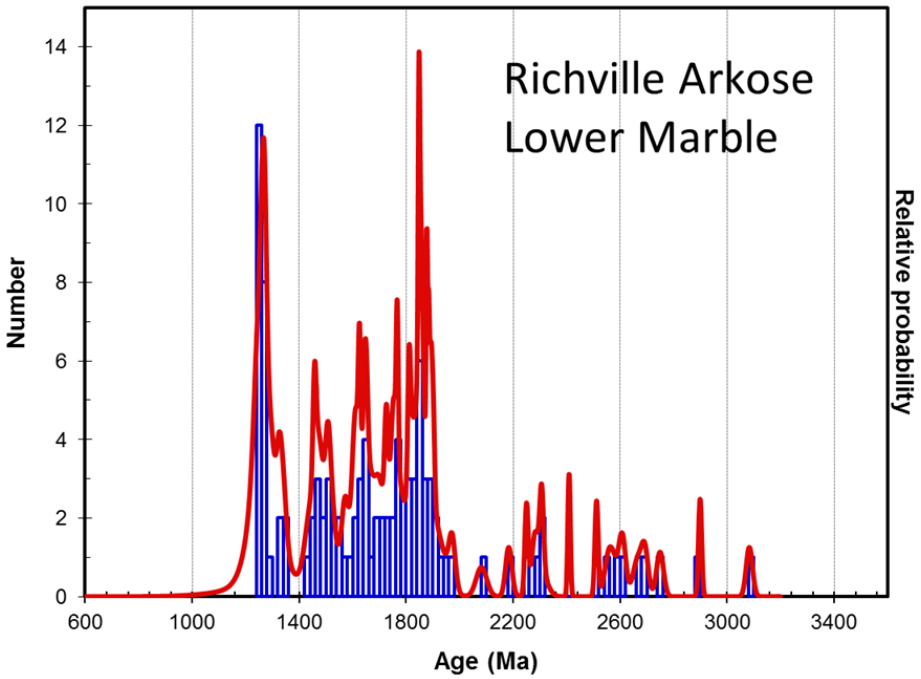

Figure 6. Detrital zircon (n = 100) age spectrum of the Richville feldspathic quartzite.

While the ultimate origin of these tourmaline-bearing gneisses is still equivocal; here they are undisputedly a reflection of a sedimentary environment yielding copious amounts of tourmaline. This environment punctuated the carbonate dominated shelf sedimentation of the Lower Marble. Here we interpret the rocks as arkosic to mud-rich playa deposits deposited within isolated fault blocks and rift basins during the opening of the Trans-Adirondack Back-arc Basin (Chiarenzelli et al. 2011).

Stop 2.

DANBURITE LOCATION AT RUSSELL (THE OLD VAN BUSKIRK FARM).
N 44° 22' 09", W 75° 11' 13"
Private property, please ask permission from the landowners to visit and collect. $5/person collection fee.

At Russell, danburite is found as compact masses, alternating layers of danburite and diopside and vugs with terminated prismatic crystals in a diopside-rich rock. It is associated with diopside, very rare datolite, dravite, phlogopite, quartz, pyrite, calcite (rare), fluorapatite, marialite, microcline, rare chalcopyrite and bornite, titanite, and tremolite.
Danburite formed as a prograde mineral in the assemblage danburite – diopside – microcline – quartz – scapolite. Dravite developed as a late mineral, probably at the expense of danburite. The metamorphic peak for the area seems to be T 650ºC to 700ºC and P 6 to 7 kbars (Edwards and Essene 1988). Grew (2002) considered that the layered danburite-diopside assemblage probably represents the highest-temperature danburite association ever reported. Danburite veins, cutting the host rock, formed after the metamorphic peak at lower temperature.

Stop 3.

BOWER POWERS FARM, PIERREPONT, NEW YORK
N 44º33’28”; W 75º01’14”
Private property, please ask permission from the landowners to visit and collect. $5/person collection fee.

The quartz-tourmaline veins from the Bower Powers Farm location occur cross-cutting metasedimentary rocks of Grenville-age. The main minerals found in different trenches and pits in this area are uvite-dravite, quartz, calcite, tremolite, diopside, fluorapatite, phlogopite. A very detailed mineral composition of the veins can be found in Chamberlain and Robinson (2013).

Fluid inclusion microthermometry on quartz from the quartz-tourmaline vein yielded a temperature of 438º – 500ºC and P 3.1 to 3.5 kbars (Kelson et al. 2013). A sample of coarse-grained tourmaline-quartz-calcite pegmatite yielded a substantial number of zoned euhedral zircon crystals (Figure 7) that gave an U-Pb zircon age of 1158.3±3 Ma Figure 8). This age is interpreted as the timing of intrusion of pegmatitic veins cross-cutting the country rock as can observed in the trenches along the stream. Given the lack of fabric in the pegmatites, this result suggests intrusion after, or during, the waning stages of the Shawinigan Orogeny.

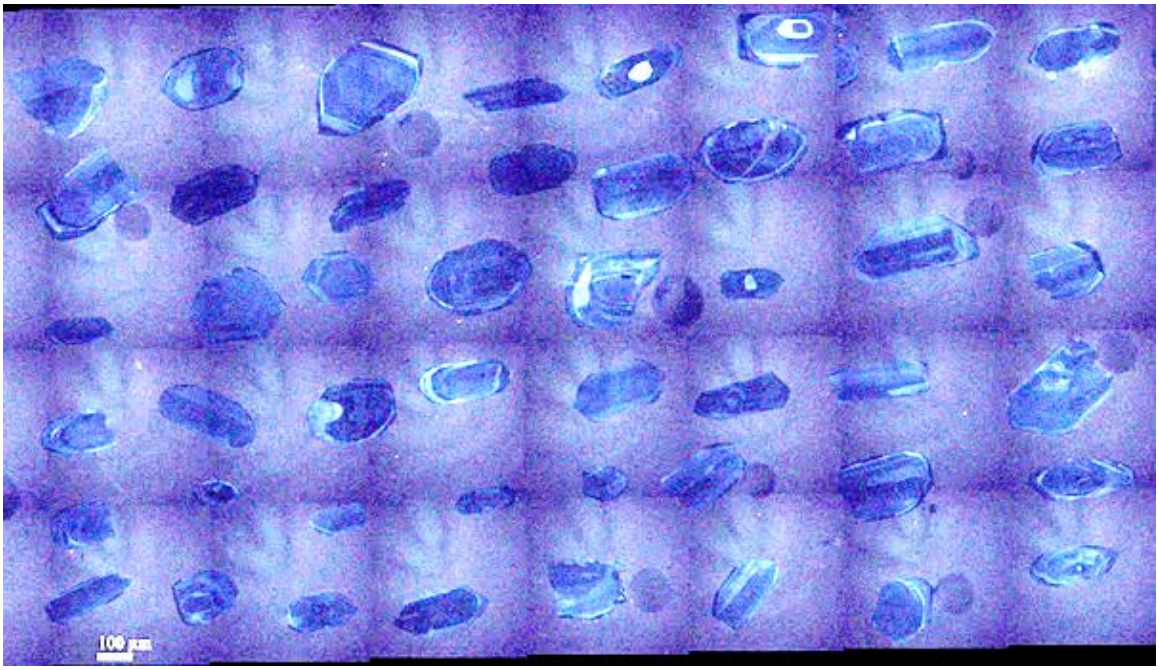

Figure 7. Cathodoluminscence photograph of zircons from Powers Farm tourmaline-bearing pegmatite.

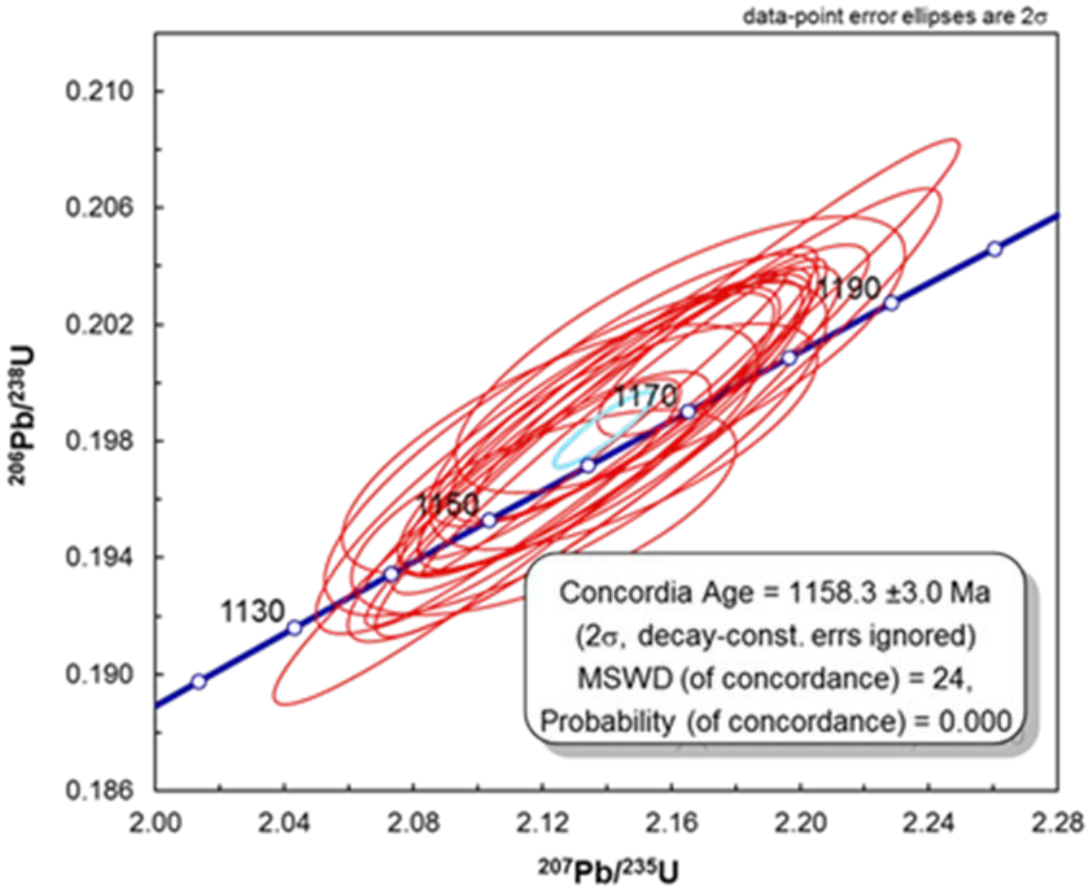

Figure 8. Concordia diagram of zircons separated from the tourmaline-bearing pegmatite at Bower Powers Farm.

Tourmaline crystals (some up to tens of cm in diameter) are black and shortened on the "c" axis. A few comments on the composition of some species and how this relates to the species name could be easily exemplified by the tourmaline from the Bower Powers Farm in Pierrepont. This is a well-known location and the name of the species varied in time from one author to another – uvite (Dunn et al. 1977) or dravite (Grice and Ercit 1993; Dyar et al. 1998; Lupulescu 2008). Some of our recent analyses (unpublished data) indicate~~s~~ dravite is present. The crystals from this location are large and zoned. Our analyses show very little difference between Na^{+} and Ca^{2+} in terms of their atoms per formula units at the *X*-site; some analyses have more Ca^{2+}, others with more Na^{+}. It is very difficult to assign the name uvite or dravite to the tourmaline from this location and would require multiple analyses on different parts of the large crystals from thorough the mineralized area. We feel that for the moment the best choice is not to use the species name, but to utilize the solid solution name uvite-dravite.

Stop 4.

WINTERGREEN MINE WASTE ROCK PILE, TALCVILLE
N 44º18'32.5"; W 75º18'34.2"

Our goal at this locality is to take a look at some mineral associations that are similar with those occurring in the Arnold Pit in Balmat. The Arnold Pit is no longer available for study and we will focus our observations and discussions on the rocks found on the dump of the Wintergreen mine. This location is part of the Balmat-Edwards talc belt, a metasedimentary sequence of rocks containing mainly talc and tremolite, mangancummingtonite, and serpentine. Locally, in the talc-tremolite sequences, some Mn-bearing minerals occur. The Mn-bearing-dravite or -uvite are common and in places they form centimeter wide layers containing more than 50 % tourmaline.

From the tailings dump along the Oswegatchie River one can collect pink to purple tremolite (hexagonite), brown, acicular crystals of mangancummingtonite, talc, and Mn-bearing tourmaline. Talc often shows a dark green to bluish color which gave the mine its name. Tourmaline from this location is dravite and contains up to 3 % MnO. An uvite crystal collected from the Arnold Pit (Ayuso and Brown 1984) contained 5% MnO.

REFERENCES

Ayuso, R. A. and C. E. Brown. 1984. Manganese-rich tourmaline from the Fowler talc belt, New York. *The Canadian Mineralogist*, V. 22, p. 327-331.

Barfod, G.H., Krogstad, E.J., Frei, R., and Albarede, F., 2005, Lu/Hf and PbSL geochronology of apatites from Proterozoic terranes; a first look at Lu/Hf isotopic closure in metamorphic apatite: Geochimica et Cosmochimica Acta, v. 69, no. 7, p. 1847-1859.

Brown C.E., Ayuso R.A. (1984) Significance of tourmaline-rich rocks in the Grenville complex of St. Lawrence County, New York. US Geological Survey Bull. 1626-C

Cotkin, S. J. 1989. Manganiferous dravite-uvite tourmaline, fluorine distribution, and talc formation, northwest Adirondacks, U.S.A. *Neues Jahrbuch fur Mineralogie Monatshefte*, H. 5, p.201-211.

Chamberlain, S. C., M. Lupulescu and R. Rowe. 2008. Discovery of fluorine-dominant dravite near Gouverneur, St. Lawrence County, New York. *Rocks & Minerals*, 83: 320-326.

Chamberlain, S. C. and Robinson, G. W. (2013) *The Collector's Guide to the Minerals of New York State*. Schiffer Books. 96 p.

Chiarenzelli, J., Lupulescu, M., Cousens, B., Thern, E., Coffin, L., and Regan, S., 2010. Enriched Grenvillian lithospheric mantle as a consequence of long-lived subduction beneath Laurentia: Geology, v. 38, p. 151-154.

Dalton, C. T. 2003. Geochemical characterization and petrologic implications of Grenville-aged tourmalines from the Adirondack Lowlands, St. Lawrence County, New York. *Master of Science thesis*, University of Akron, Ohio, 54 p.

Dunn, P. J., D. Appleman, J. A. Nelen and J. Norberg. 1977. Uvite, a new (old) common member of the tourmaline group and its implications for collectors. *The Mineralogical Record*, V. 8, p.100-108.

Dutrow, B. L., Henry D. J. 2011. Tourmaline: a geologic DVD. *Elements* 7:5, 301-306.

Dyar, M. D., M. E. Taylor, T. M. Lutz, C. A. Francis, C. V. Guidotti and M. Wise.1998. Inclusive chemical characterization of tourmaline: Mossbauer study of Fe valence and site occupancy. *American Mineralogist* 83:848-864.

Ertl, A., Marshall, H., Giester, G., Henry, D. J., Schert, H-P., Ntaflos, T., Luvizotto, G. L., Nasdala, L., Tillmans, E. 2010. Metamorphic ultrahigh-pressure tourmaline: structure, chemistry, and correlations to P-T conditions. *American Mineralogist* 95: 1-10.

Grice, J. D. and T. S. Ercit. 1993. Ordering of Fe and Mg in the tourmaline crystal structure: the correct formula. *Neues Jahrbuch fur Mineralogie Abhandlungen* 165:245-266.

Henry, D. J., Guidotti, C. V. 1985. Tourmaline as a petrogenetic indicator mineral: an example from the staurolite-grade metapelites of NW Maine. *American Mineralogist* 70: 1.15.

Henry, D. J., Lu, G., McCabe, C. 1994. Epigenetic tourmaline in sedimentary red-beds: an example from the Silurian Rose Hill Formation, Virginia. *The Canadian Mineralogist* 32: 599-605.

Henry, D. J., Dutrow, B. L. 1992. Tourmaline in a low-grade clastic metasedimentary rock: an example of the petrogenetic potential of tourmaline. *Contributions to Mineralogy and Petrology* 112: 203-218.

Henry, D. J., Novak, M., Hawthorne, f. C., Ertl, A., Dutrow, B. L., Uher, P. and Pezzota, F. 2011. Nomenclature of the tourmaline-supergroup minerals. *American Mineralogist* 96: 895-913.

Kelson, C. R., Coffey, C. V., Nigel, J. F. 2013. Mineralogical, geochemical, and isotopic characterization of the Powers Farm tourmaline occurrence, St. Lawrence County, New York. *NEGSA Abstracts with Programs* 45:1, 58.

London, D., Manning, D. A. C. 1995. Compositional variation and significance of tourmaline from southwest England. *Economic Geology* 90: 495-519.

Lupulescu, M., D. Bailey, and J. Pyle (2005) - Tourmaline-group minerals from New York. *Proceedings of the 32nd Rochester Mineralogical Symposium,* p 21-22.

Lupulescu, M. and J. Pyle. 2006. Three unusual tourmaline-group minerals from St. Lawrence Co., New York. *Proceedings of the 33rd Rochester Mineralogical Symposium,* p 15-16.

Lupulescu, M. 2007. Tourmaline-group minerals in the Grenville rocks from New York: relationship between composition and the geological setting. *NE GSA Abstracts with Programs*, Durham, New Hampshire, p.41.

Lupulescu, M. (2008) Tourmaline-group minerals from New York State. *Rocks & Minerals* 83: 202-208.

Lupulescu, M. and J. Rakovan. 2008. A new occurrence of tourmaline with tetrahedrally coordinated boron: rossmanite and associated minerals from Newcomb, Essex County, NY. *Proceedings of the 35th Rochester Mineralogical Symposium, p.10.*

Lupulescu, M., S. C. Chamberlain, M. Walter, and S. Wallace. 2010. Diagenetic uvite with overgrown dravite at Bigelow, St. Lawrence County, New York. *Rocks & Minerals, 85,* 250-259.

Lupulescu, M. Rowe, R. 2011. Al-rich chromium-dravite from the #1 mine, Balmat, St. Lawrence County, New York. *The Canadian Mineralogist,* 49, 1189-1198.

Marshall, H. R., Altherr, R., Kalt, A., Ludwig, T. 2008. Detrital, metamorphic and metasomatic tourmaline in high-pressure metasediments from Syros (Greece): intra-grain boron isotope patterns determined by secondary-ion mass spectrometry. *Contributions to Mineralogy and Petrology* 155: 703-717.

Morton, A. C., Whitham, A. G., Fanning C. M. 2005. Provenance of Late Cretaceous to Paleocene submarine fan sandstone in the Norwegian Sea: integration of heavy mineral, mineral chemical and zircon age data. *Sedimentary Geology* 182: 3-28.

Selleck, B.W. 2005. Exploring the root zone of an ancient fault-driven hydrothermal system in the Adirondack Lowlands, New York; *NYSGA Fieldtrip Guidebook,* 77th annual meeting, pp. 12-31

Sverjensky, D. A. 1984. Europium redox equilibria in aqueous solutions. *Earth and Planetary Science Letters*, 67:1, 70-78

Pezzota, F., Laurs, B. M. 2011. Tourmaline: the kaleidoscopic gemstone. *Elements* 7:5, 333-338.

van Hinsberg, V.J., Henry D. J., Dutrow, B. L. 2011. Tourmaline as a petrologic forensic mineral: a unique recorder of its geologic past. *Elements* 7:5, 327-332.

Table 2. The tourmaline species of New York held in the State Museum.

TOURMALINE FROM NEW YORK

NYSM #	Location	Species
2048	Crown Point (Essex Co.)	Schorl
426.61	Crown Point (Essex Co.)	Schorl
20560	Russell (St. Lawrence Co.)	Feruvite
1987	Edenville (Orange Co.)	Dravite
426.57	Roe Spar Bed (Essex Co.)	Schorl
2957-8	Macomb (St. Lawrence Co.)	Fluor-uvite
15295(A)	Pierces Corners (St. Lawrence Co.)	Schorl
15295(B)	Pierces Corners (St. Lawrence Co.)	Fluor-uvite
15658	Broadway (New York Co.)	Uvite
15927	Chestertown (Warren Co.)	Schorl
13855	Chestertown (Warren Co.)	Dravite
51.4.6.0-45	Brant Lake (Warren Co.)	Fluor-uvite
15768	Brown Site? (St. Lawrence Co.)	Fluor-uvite
19245	Dale Bush Farm (St. Lawrence Co.)	Fluor-uvite
18935	Bigelow (St. Lawrence Co.)	Fluor-uvite
17900	Rustley Road (St. Lawrence Co.)	Fluor-uvite
19007	Jefferson Co.?	Dravite
13794	St. Joe Lead Mine (St. Lawrence Co.)	Fluor-uvite
14143	Beaver Creek (St. Lawrence Co.)	Fluor-uvite
12925	Wight Mine (St. Lawrence Co.)	Dravite (Mn)*
10373	Parishville (St. Lawrence Co.)	Fluor-uvite
19739	Selleck Road (St. Lawrence Co.)	Fluor-uvite
10357	Brant Lake (Warren Co.)	Fluor-uvite
2003	Edenville (Orange Co.)	Fluor-uvite
20838	Seven Springs (St. Lawrence Co.)	Dravite
12702	Newcomb (Essex Co.)	Fluor-uvite
20244	Port Henry (Essex Co.)	Uvite
12583	Newcomb (Essex Co.)	Fluor-uvite
22534	Long Lake (Hamilton Co.)	Fluor-uvite
22547	Talcville st. Lawrence Co.)	Uvite
426.21	Newcomb (St. Lawrence Co.)	Rossmanite
	Cream of Valley (St. Lawrence Co.)	Fluor-dravite
15248	Wight Mine (St. Lawrence Co.)	Uvite (Mn)*
	Columbia Graphite Mine (Essex Co.)	Dravite
	Balmat (with halite)-St. Lawrence Co.	Dravite
	Rock Island (St. Lawrence Co.)	Schorl
	Talcville (St. Lawrence Co.)	Dravite (Mn)*
	Sugar Hill (Essex Co.)	Uvite
	Warrensburg (B minerals outcrop)-Warren Co.	Dravite
21435 (brown core)	Fowler (St. Lawrence Co.)	Fluor-uvite
21435 (green rim)	Fowler (St. Lawrence Co.)	Fluor-uvite
20902	Alexandria Bay (Jefferson Co.)	Uvite
21489 (yellow)	Balmat (St. Lawrence Co.)	Dravite
21489 (green)	Balmat (St. Lawrence Co.)	F-uvite
20149	Newcomb (Essex Co.)	Feruvite
21008	Dana Hill (St. Lawrence Co.)	Dravite
15909	Emery Quarry (Westchester Co.)	Dravite
2980-1	Macomb (St. Lawrence Co.)	Fluor-uvite
21300	Macomb (St. Lawrence Co.)	Fluor-uvite

12337	Tilly Foster (Putnam Co.)	Dravite
51.4.6.0-35	Rossie (St. Lawrence Co.)	Fluor-uvite
12333	Tilly Foster (Putnam Co.)	Dravite
51.4.6.0-46	Hague (Warren Co.)	Dravite
18091	Atlas Quarry (Saratoga Co.)	Fluor-uvite
1991	Cedar Lake (St. Lawrence Co.)	Uvite
17781	Trout Lake (St. Lawrence Co.)	Schorl
12701	Newcomb (Essex Co.)	Fluor-dravite, dravite (yellow), elbaite (green and dark green)
	Balmat, # 1 American Mine (St. Lawrence Co.)	Al-rich chromium dravite
51.4.6.0-47	Overlook Quarry (Saratoga Co.)	Schorl
23575	Benson Mines (St. Lawrence Co.)	Schorl
22933	Peekskill (Westchester Co.)	Dravite
13581	Balmat (St. Lawrence Co.)	Dravite
51.4.6.0-27	DeKalb (St. Lawrence Co.)	Fluor-uvite
1654	Wight Mine (St. Lawrence Co.)	Dravite (Mn) (listed under tremolite -hexagonite). Newland specimen.*
426.39	DeKalb (St. Lawrence Co.)	Fluor-uvite
2064	New York Co?	Dravite
1863	Monroe (Orange Co.)	Fluor-uvite
20592	Oxbow (Jefferson Co.)	Fluor-uvite
10242	North Creek (Warren Co.)	Uvite
19390	Arnold Pit (St. Lawrence Co.)	Schorl
10353	Horicon?	Fluor-uvite
18336	Pottersville (Warren Co.)	Uvite
21064	Bower Powers Farm (St. Lawrence Co.)	Dravite
2000	Edenville (Orange Co.)	Fluor-uvite
1989	Bedford (Westchester Co.)	Schorl
16919	Manhattan (New York co.)	Dravite
21430	Glenn Mills Road (St. Lawrence Co.)	Dravite
2064	New York (no precise location)	Dravite
18592	Ellis farm (St. Lawrence Co.)	Dravite

MESOPROTEROZOIC MAGMATISM OF THE ADIRONDACK LOWLANDS: THE RESULT OF CLOSURE OF THE TRANS-ADIRONDACK BACKARC BASIN

SEAN P. REGAN
Department of Geosciences, University of Massachusetts, Amherst, MA 01003-9297

W. H. PECK, B. W. SELLECK, and M. S. WONG
Department of Geology, Colgate University, Hamilton, NY 13346

J. R. CHIARENZELLI
Department of Geology, St. Lawrence University, Canton NY 13617

INTRODUCTION AND REGIONAL BACKGROUND

The Mesoproterozoic Grenville orogenic belt is one of the world's largest preserved Precambrian convergent margins, with a North American extent from Labrador to Texas. It records several tectonic, magmatic, and accretionary pulses typically referred to as the Grenville orogenic cycle (Ca. 1.30 – 1.0 Ga; Rivers, 2008). This sequence of punctuated crustal growth is thought to have culminated during a ca. 1.08 Ga terminal collision, which resulted in the final assembly of the supercontinent Rodinia (McLelland et al., 2001). The Adirondack Mountains in New York are a domical uplift forming the southern extension of the Canadian Shield into New York, and expose rocks that formed and evolved during this orogenic cycle. The Adirondack Highlands and Adirondack Lowlands are separated by the Carthage-Colton shear zone (Fig. 1; Selleck et al., 2005). The Adirondacks record sedimentation, plutonism, high-grade metamorphism and deformation during the Elzevirian and Shawinigan orogenies of the Grenville orogenic cycle, and are variably affected by terminal, Ottawan, deformation (Fig. 1b; McLelland et al., 1992; Chiarenzelli et al., 2011c;).

The Adirondack Lowlands are dominated by supracrustal, amphibolite-facies metasedimentary rocks arrayed in NE-SW striking belts (Wong et al., 2011; Baird and Shrady, 2012). The Lowlands contain relatively subordinate, variably deformed igneous intrusives (Carl and deLorraine, 1997; Wasteneys et al., 1999; Peck et al., 2013). In contrast, the Adirondack Highlands are dominated by granulite facies metaigneous rocks, with minor supracrustal rocks (McLelland et al., 2004). Published data suggest that unlike the Highlands, the Adirondack Lowlands did not experience penetrative Ottawan deformation, and that the rocks of the Lowlands were likely at a higher crustal position during the Ottawan (McLelland et al., 1992; Selleck et al., 2005; Heumann et al., 2006). Thus, the Adirondack Lowlands are an ideal location to study earlier phases of Grenvillian orogenesis because of a lack of pervasive overprinting, such as is seen in the Highlands.

This field trip focuses on the major igneous rock suites that were emplaced into the metasedimentary units of the Adirondack Lowlands. Recent work on these rocks is presented in several contributions (Chiarenzelli et al., 2010b; Wong et al., 2011; Peck et al., 2013), which grew from a Keck Geology Consortium Project led by Colgate University during the summer of 2008. This project produced a new igneous whole rock geochemical dataset from many of the major intrusive suites exposed in the Lowlands. Accompanying these data, Sm-Nd isotopic analyses were acquired along with SHRIMP-RG U-Th-Pb analyses of zircon and titanite (Chiarenzelli et al., 2010b; Wong et al., 2011; Peck et al., 2013). This trip will visit localities where igneous bodies are in contact with surrounding metasediments, providing an opportunity to address the deformation history of the metasedimentary rocks. However, the central goal is to document how magmatism evolved during Shawinigan orogenesis, and the relationships between igneous rock geochemistry and regional tectonic history of the Grenville Province.

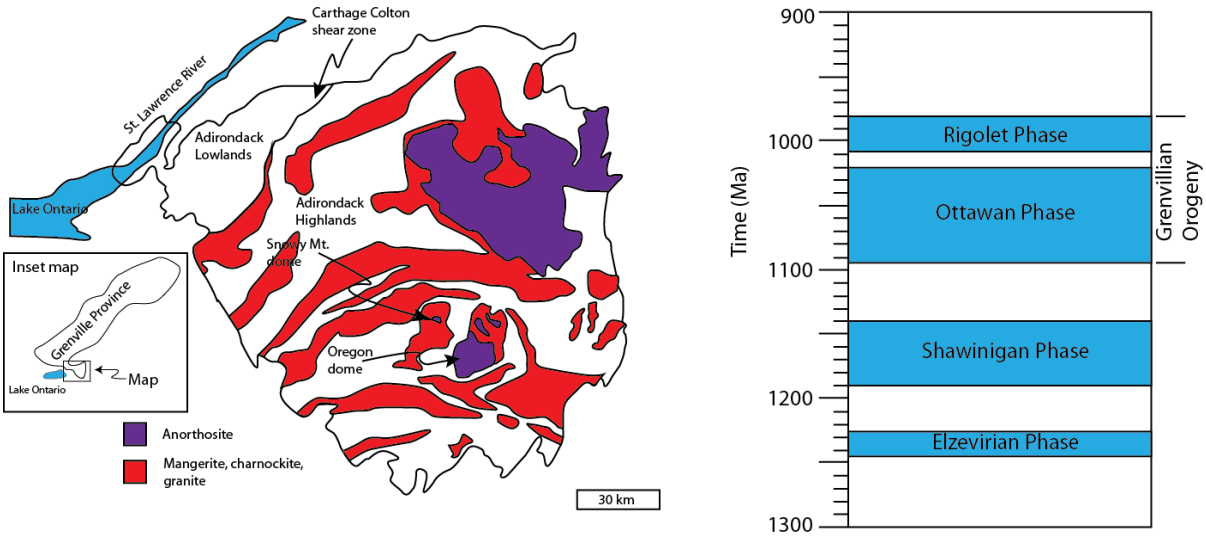

Figure 1. Left: A simplified map of the Adirondacks divided into the northwestern lowlands and southeastern highlands. The map displays the distribution of the ca. 1155-1165 Ma AMCG suite (modified from McLelland et al., 2004). Right: A schematic diagram displaying the traditional orogenic phases of the Grenville Province (after Rivers, 2008).

The Adirondack Lowlands of northern New York are primarily composed of amphibolite facies metasedimentary rocks that can be grouped into three lithotectonic units. These may represent an originally coherent stratigraphic sequence, consisting of, from bottom to top: 1) lower marble, 2) the Popple Hill Gneiss, and 3) upper marble (Carl et al., 1990). Subsequent to the deposition of this sequence, several intrusive suites were emplaced into the metasedimentary rocks (Carl et al., 1990; Wasteneys et al., 1999). Four distinct and variably deformed intrusive suites are recognized within the Adirondack Lowlands, from oldest to youngest: 1) the 1203 Ma Antwerp-Rossie Suite (Wasteneys et al., 1999; Chiarenzelli et al., 2010b), 2) the 1182 Ma Hermon granite gneiss (Heumann et al., 2006), 3) the 1172 Ma Hyde School Gneiss and Rockport Granite (McLelland et al., 1992), and 4) relatively undeformed ca. 1150 Ma syenite to monzonites (Peck et al., 2013).

Recent geochemistry, geochronology, and structural work in area of the Black Lake shear zone (BLsz) was undertaken to determine its regional significance, and to test the hypothesis that it is a fundamental boundary between the Adirondack Lowlands and the Frontenac terrane to the northwest (Chiarenzelli et al., 2010b; Wong et al., 2011; Peck et al., 2013). The Black Lake shear zone is a belt of intensely deformed rocks oriented parallel to the NE-SW structural grain variably developed throughout the Adirondack Lowlands. In addition to differences in Shawinigan metamorphic ages and grade across the boundary, it delineates a major discontinuity in igneous activity between the terranes, with Lowlands igneous suites older than ca. 1180 Ma only occurring to the south and 1170 Ma magmatism stitching the boundary (Wong et al., 2011; Peck et al., 2013).

A recently discovered ophiolite and newly recognized oceanic crust (Pyrites ultramafic complex; Chiarenzelli et al., 2011b; Pyrites Field Trip B-2) in the Adirondack Lowlands has led to further evidence for major differences across the BLsz. These observations suggest that metasediments in the Lowlands were deposited proximal to oceanic crust, but no fragments of ophiolite or oceanic crust have been identified in the Frontenac terrane north of the BLsz. Furthermore, the geochemical character of the ophiolite suggests a suprasubduction origin (Chiarenzelli et al., 2010a), and it has been interpreted as having developed in a back arc basin (Chiarenzelli et al., 2010b, 2011b).

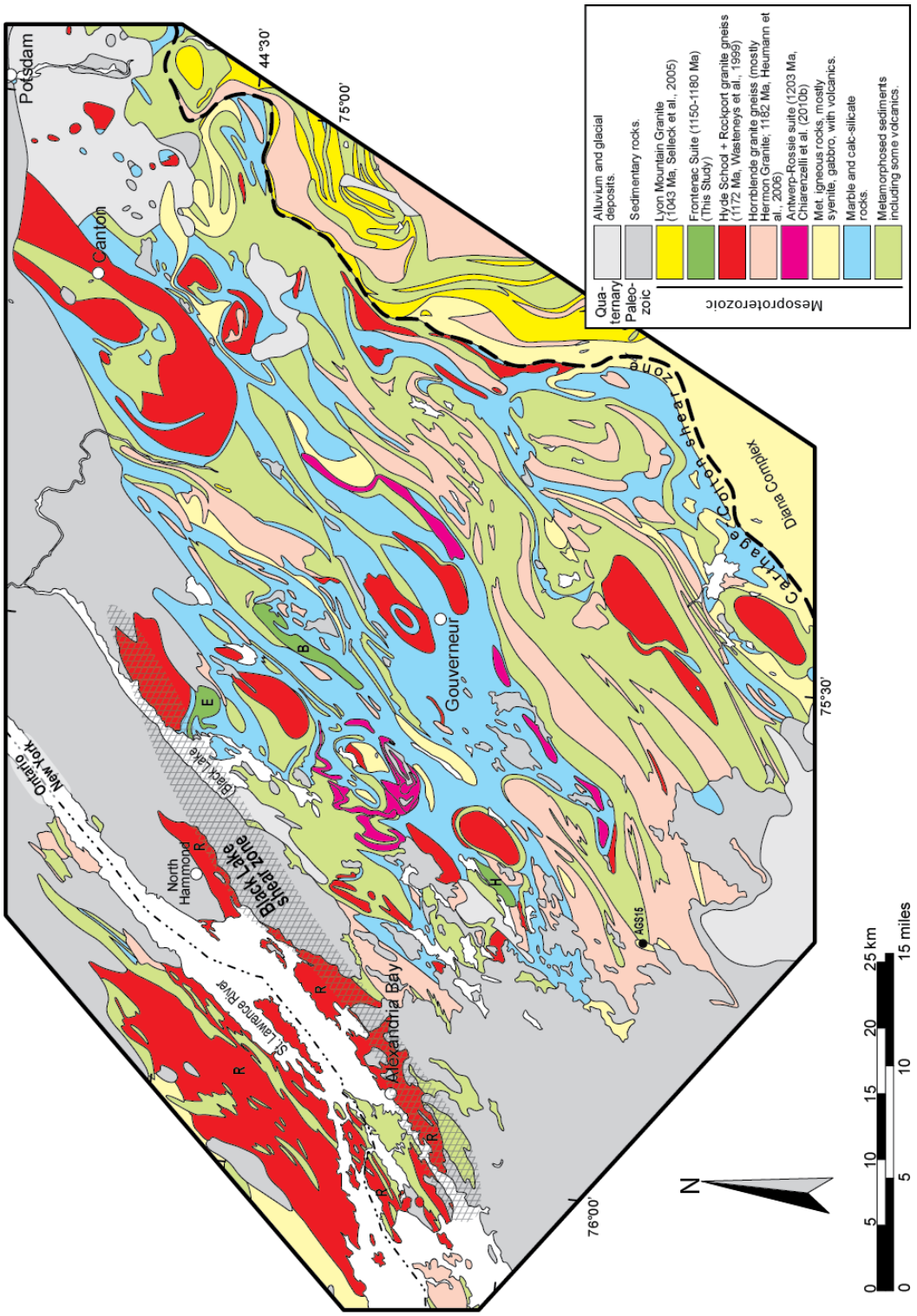

Figure 2. Geology of the Adirondack Lowlands complied from Fisher et al. (1970), Carl et al. (1990), Wasteneys et al., (1999), Selleck et al. (2005), and Wong et al. (2011). E – Edwardsville pluton, R – Rockport Granite, H – Honey Hill pluton, B – Beaver Creek pluton (from Peck et al., 2013).

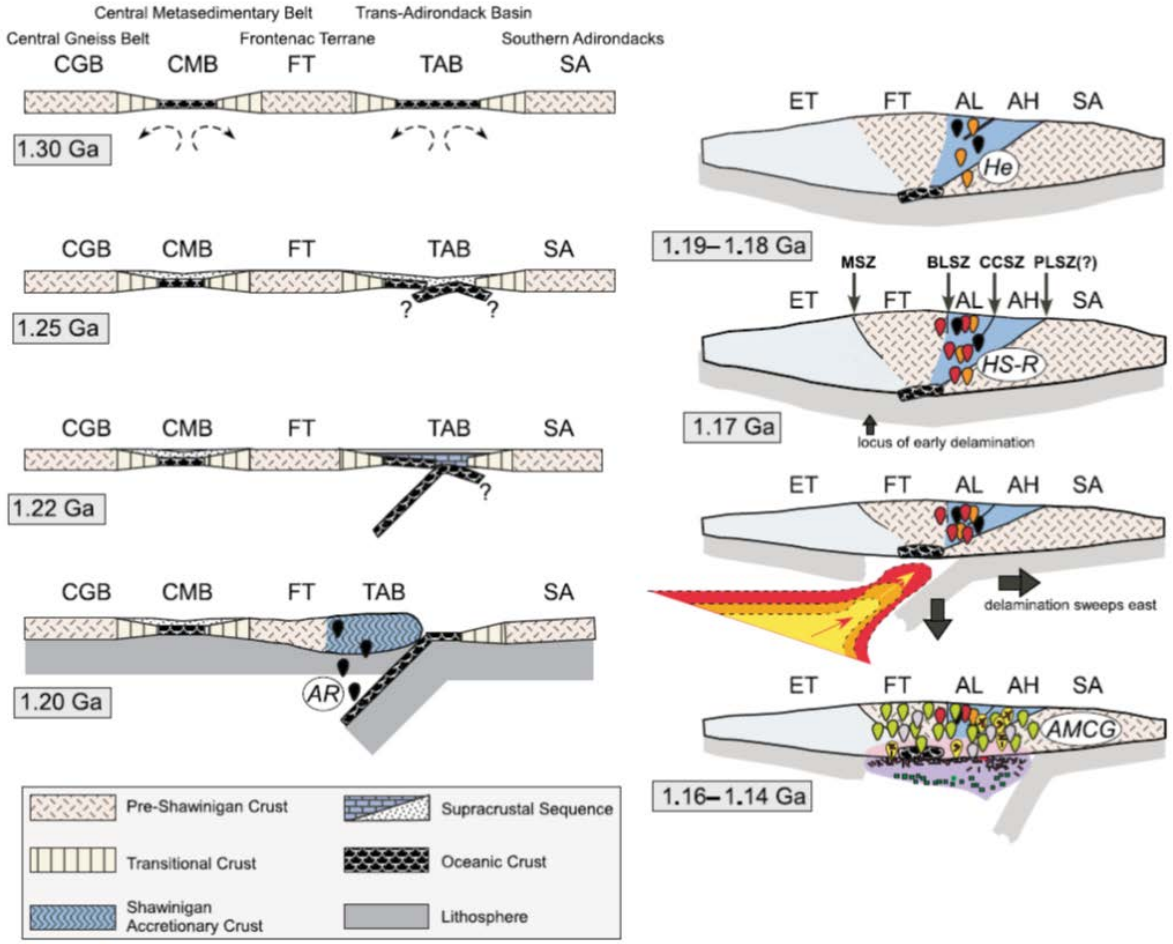

Figure 3. Tectonic model for the evolution of the Trans-Adirondack back arc basin and subsequent closure during Shawinigan orogenesis after Chiarenzelli et al. (2010b), Regan et al. (2011), and Peck et al. (2013). Subduction and other details of the ca. 1.19–1.14 Ga Shawinigan orogeny are not specified in the Central Metasedimentary Belt (CMB.) CGB—Central Gneiss Belt, ET—Elzevir terrane, FT—Frontenac terrane, TAB—Trans-Adirondack basin, SA—Southern Adirondacks, AH—Adirondack Highlands, AL—Adirondack Lowlands, MSZ—Maberly shear zone, BLSZ—Black Lake shear zone, CCSZ—Carthage-Colton shear zone, PLSZ—Piseco Lake shear zone, AR—Antwerp-Rossie suite (black plutons), He—Hermon granite gneiss (orange plutons), HS-R—Hyde School gneiss and Rockport granite (red plutons), AMCG—anorthosite-mangerite-charnockite-granite (and gabbro) plutons, including the Frontenac suite (anorthosites are yellow, granitoids are green, and gabbros are purple). Dark purple is underplating mafic magma, and dark pink is melted lower crust. In panels after 1.20 Ga (right), light blue is undifferentiated crust in the Elzevir terrane and dark blue shows the amalgamated Trans-Adirondack basin (Adirondack Lowlands and Adirondack Highlands). For these panels, the nature of the pre-Ottawan lower crust is necessarily schematic.

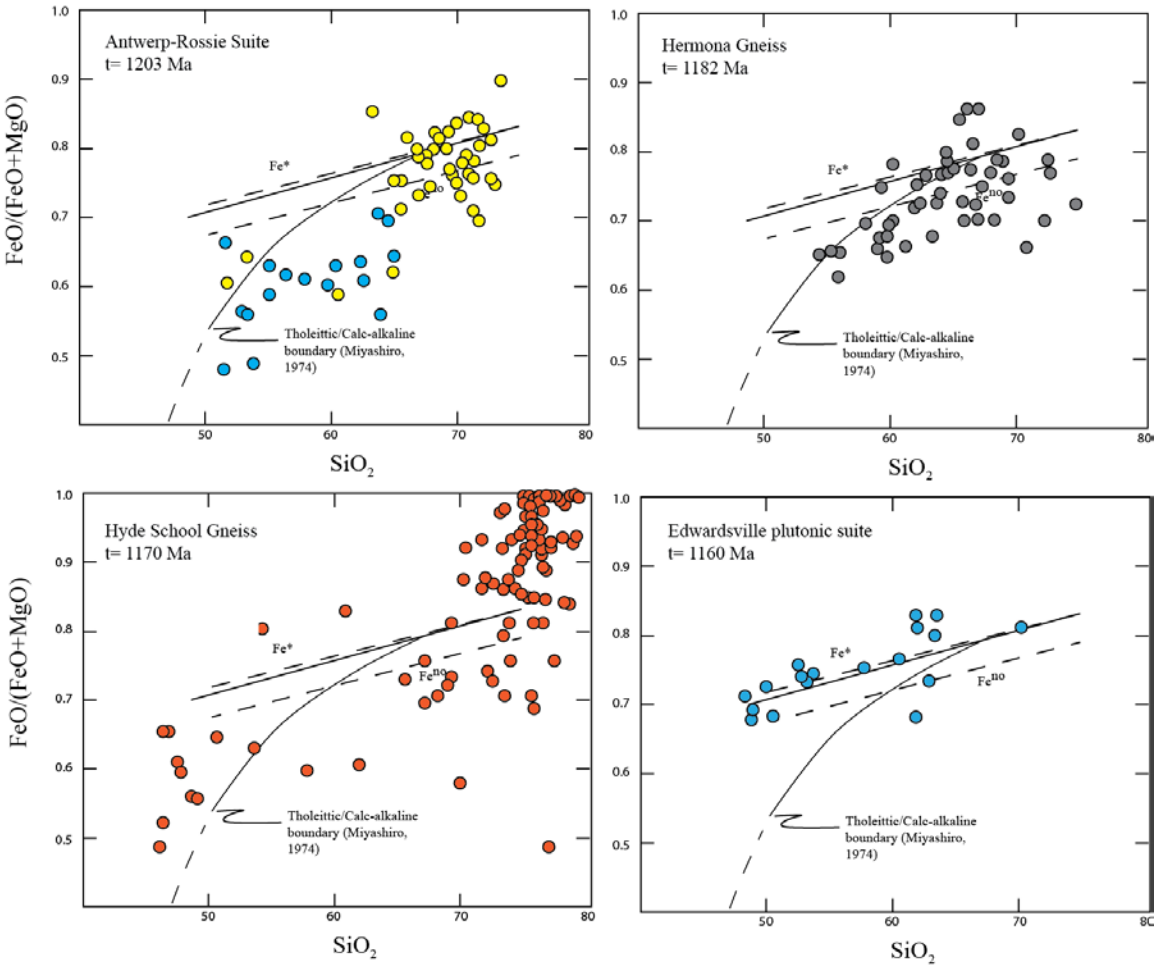

Figure 4. Fe index vs. SiO_2 after Frost and Frost (2008) of major igneous suites within the Adirondack Lowlands. Fe-index (FeO/(MgO+FeO) differentiates rocks categorized as ferroan or magnesian. Magnesian rocks are generally interpreted as being sourced from a hydrous protolith (oxidizing) and ferroan rocks are interpreted as being sourced from an anhydrous protolith (reducing magma). The oldest igneous events within the Adirondack Lowlands have a magnesian trend (Antwerp-Rossie suite and the Hermon Granite) whereas subsequent intrusions appear to be more ferroan (Hyde School Gneiss and Edwardsville plutonic suite). These are believed to be original magmatic characteristics imparted by their respective source(s).

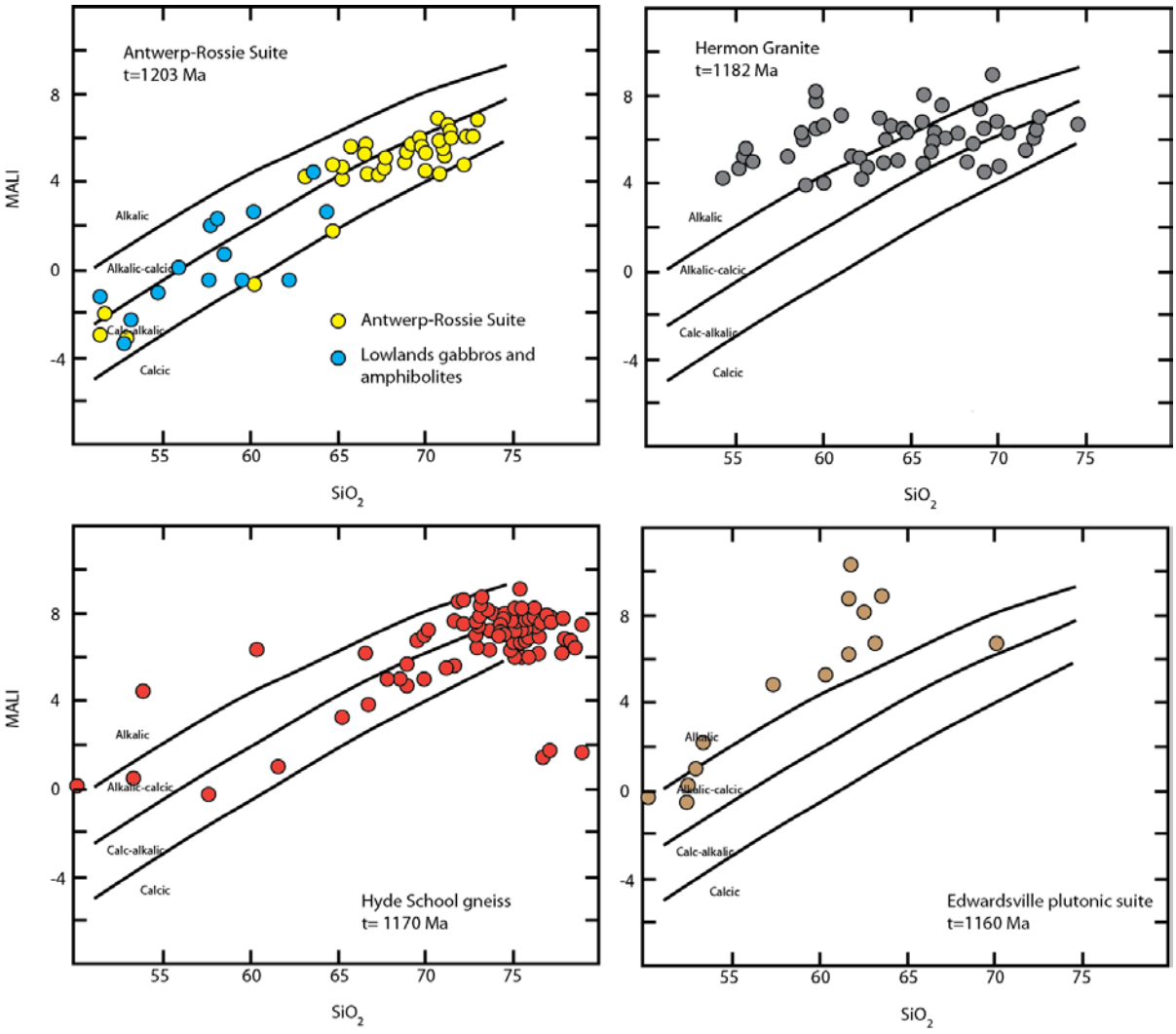

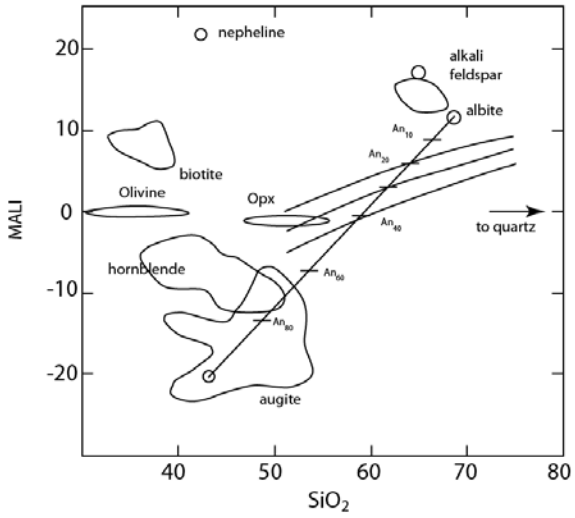

Figure 5. Modified alkali-lime index plot (MALI; Na_2O+K_2O-CaO) of all major igneous events in the Adirondack Lowlands. Left: redrawn figure from Frost and Frost (2008) displaying the location of many rock-forming minerals on the MALI projection. The Antwerp-Rossie Suite shows a strong calc-alkaline trend which weakens through time to the more alkalic Edwardsville pluton (Peck et al. 2013).

The Black Lake shear zone represents a major lithotectonic boundary within the Mesoproterozoic basement of New York and Ontario marking the NE extent of ca. 1180 – 1200 Ma subduction and the >1250 Ma ophiolite in the Lowlands (Chiarenzelli et al., 2010b; 2011a; Wong et al., 2011; Peck et al., 2013). This shear zone has recently been interpreted to represent magmatism and the approximate location of the rifted margin of Laurentia prior to Shawinigan orogenesis (Fig. 3; Chiarenzelli et al., 2010b). This interpretation suggests that stratigraphic correlations across the shear zone are possible, and would predict shallower facies assemblages (ie quartzites, psammites) consisting of clastic material to the northwest, grading into carbonate (limestone) and pelitic (mud) assemblages to the southeast. The gross stratigraphy preserved within the Adirondack Lowlands is interpreted to record a period of protracted opening and subsequent basin closure and restriction consistent with a back arc model (Carl et al., 1990; Chiarenzelli et al., 2010b; 2011b)

A maximum age on rifting is not well constrained, despite well understood stratigraphic and spatial relationships. Detrital zircon analyses from quartzites in the Frontenac terrane yield a maximum deposition age of 1306 Ma (Sager-Kinsman and Parrish, 1993). Detrital zircon geochronology three samples from the metasedimentary sequence indicates deposit prior to ca. 1250 Ma (Chiarenzelli et al., 2013), and likely represents silicilastic deposition during basin evolution from opening to closure. Deposition of carbonate and evaporitic rocks of the upper Marble likely occurred in isolated remnants of the collapsing basin restricted from the open ocean immediately prior to Elzevirian orogeneisis. Cessation of extension likely occurred during the onset of the Elzevirian orogeny within the Central Metasedimentary Belt to the NW (ca. 1220-1240 Ma) and stepped to the southeast into the Adirondack Lowlands (Chiarenzelli et al., 2011b).

MAJOR IGNEOUS EVENTS

The Antwerp-Rossie Suite (data from Chiarenzelli et al., 2010b; Peck et al., 2011; and Carl and deLorraine, 1997; Carl, 2000)

The ca. 1200 Ma Antwerp-Rossie suite (ARS) is the oldest recognized plutonic suite within the Adirondack Lowlands (Wasteneys et al., 1999; Chiarenzelli et al., 2010b). Rocks of the ARS outcrop only southeast of the Black Lake shear zone (Fig. 2), and are exposed near the villages of Antwerp and Rossie, NY. This suite intrudes lower marble unit, is equigranular, and lacks a well-defined and/or regionally extensive tectonic fabric despite experiencing amphibolite facies metamorphism. The ARS includes rocks ranging from diorite to granite in composition. These rocks are plagioclase, quartz, K-spar, and hornblende-bearing, with rare clinopyroxene in more mafic members of the suite. Apatite, monazite, and zircon are common accessory phases. Compositions span relatively broad spectrum of SiO_2, ranging from 46.8 to 78.8 wt% SiO_2, with a noticeable gap between 52.5-62.5 wt% SiO_2. However, some analyzed mafic bodies (Carl, 2000) have been thought to be correlative to the Antwerp-Rossie suite and span some of that compositional gap (Peck et al., 2013). Data form linear trends on Harker-type variation diagrams, and plot in the magnesian field on Fe index vs. SiO_2 diagrams (Fig. 4; Frost and Frost, 2008). On modified alkali-lime index plots (Fig. 5; after Frost and Frost, 2008), the ARS displays a linear trend, defining a shallow slope of increasing SiO_2 with increasing MALI, plotting largely in the calc-alkalic field (Fig. 5). The ARS exhibits relatively high-K chemical trends, mildly calc-alkaline compositions, and plot in the volcanic arc granite field on tectonic discrimination diagrams (Pearce et al., 1984). When normalized to primitive mantle (Fig. 7; Sun and Mcdonough, 1981), the suite shows strong enrichment in LILE and Pb, and depletion in HFSE. Furthermore, the ARS contains REE that display LREE enrichment and HREE depletions, typical of a garnet-bearing source.

Sm-Nd isotopic systematics have been used extensively to fingerprint magmatic processes, and have been quite successful at differentiating juvenile vs. evolved sources (Fraure and Mensing, 2005). Twelve ARS samples were analyzed for Sm-Nd isotopes, with sampling focused on spatial and compositional representation (Fig. 6; Chiarenzelli et al., 2010b). The ARS contains $\varepsilon_{Nd(t)}$ (t=1200 Ma) values, ranging from 1.5 – 5.4, plotting

between contemporaneous depleted mantle and CHUR. These values show no discernable correlation with SiO_2, suggesting minimal, if any, continental contamination. Furthermore, the majority of samples have T_{DM} (depleted mantle model age) values <1400 Ma, consistent with a juvenile source region. However, there is a geographic pattern with the lowest $\varepsilon_{Nd(t)}$ values corresponding to samples located along the eastern margin of the BLsz. These three samples also yield the three oldest T_{DM} ages (>1600 Ma). This excursion is interpreted to represent an increase in continental influence, and may be the expression of more evolved crust along the BLsz as suggested by the tectonic model above where the BLsz marks the southeastern rifted margin of Laurentia prior to Shawinigan orogenisis.

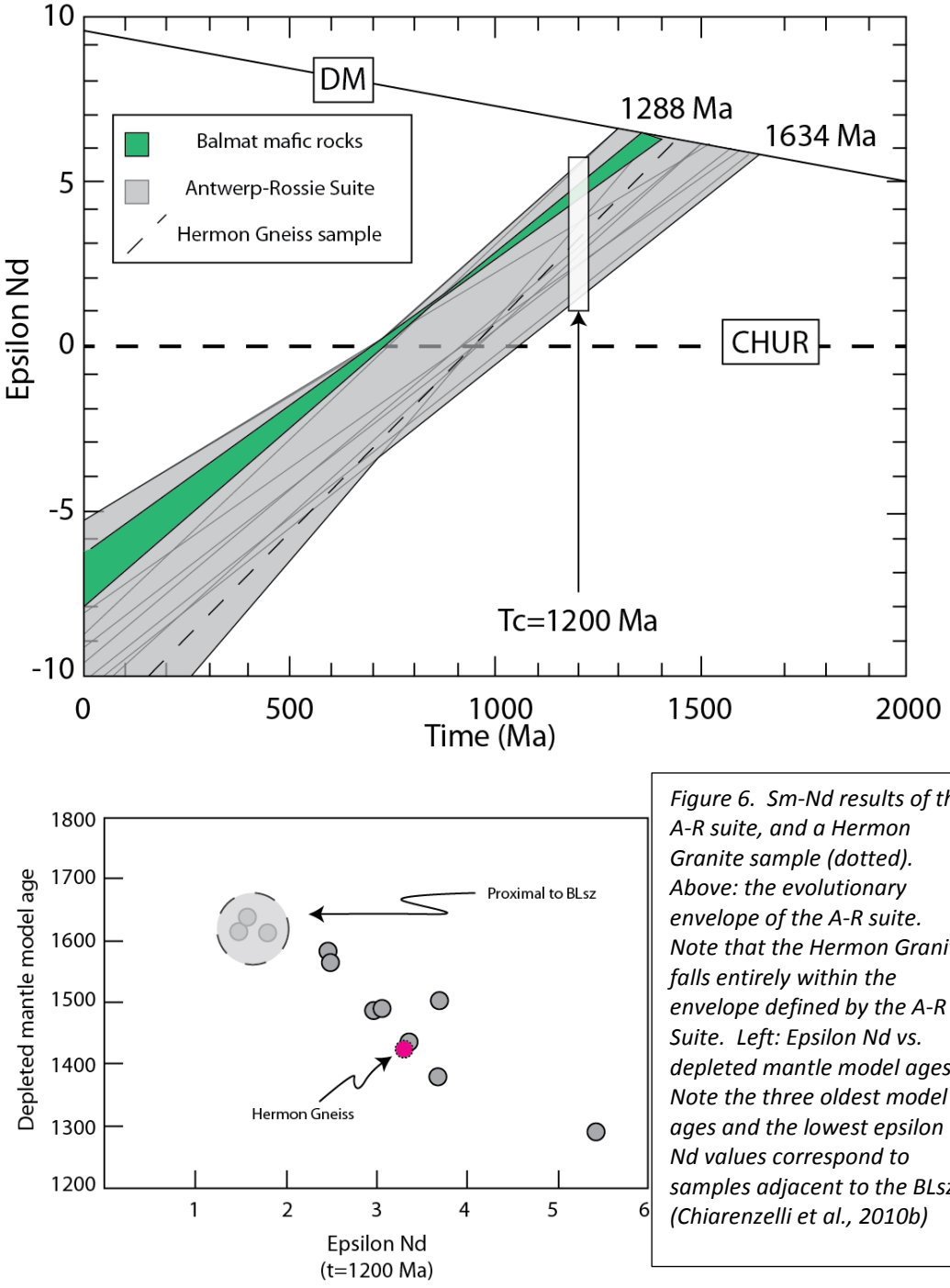

Figure 6. Sm-Nd results of the A-R suite, and a Hermon Granite sample (dotted). Above: the evolutionary envelope of the A-R suite. Note that the Hermon Granite falls entirely within the envelope defined by the A-R Suite. Left: Epsilon Nd vs. depleted mantle model ages. Note the three oldest model ages and the lowest epsilon Nd values correspond to samples adjacent to the BLsz (Chiarenzelli et al., 2010b)

Hermon Granite (data from Peck et al., 2014; Carl and DeLorraine, 1997)

The Hermon granite is a megacrystic, K-feldspar hornblende granite that occurs southeast of the Black Lake shear zone (Fig.2). Despite its geographic overlap with the ARS, the Hermon granite is slightly younger, yielding a U-Pb zircon age of 1182 +/- 7 Ma (Heumann et al., 2006). It is often observed intruding the Popple Hill Gneiss, unlike the ARS, which is commonly in contact with marble. The Hermon Granite Gneiss suite has a broad compositional range, from 54.5 to 74.6 wt % SiO_2, and plots from calc-alkalic to alkalic on MALI diagrams (Fig. 5), with no systematic variation despite a broad range in SiO_2 contents. Like the ARS, the Hermon lithologies are predominately magnesian with regard to their Fe-index (Fig. 4; Frost and Frost, 2008).

On tectonic discrimination diagrams, the Hermon granite plots as a volcanic arc granite, but forms a broad field which straddles the within-plate granite field (Pearce et al., 1984). When normalized to primitive mantle (after Sun and McDonough, 1989), the Hermon granite shares similar geochemical attributes as the preceding ARS, but lacks the distinctive Pb anomaly. The Hermon granite has similar Sm-Nd isotopic systematics (Chiarenzelli et al., 2010b).

1172 Ma Hyde School Gneiss (data from Fischer, 1995; Carl and deLorraine, 1997; Carl, 2000; Peck et al., 2013)

The Hyde School Gneiss (HSG) forms domical bodies initially interpreted as rootless intrusions, or phacoliths (Buddington, 1929). These bodies range from alkali granite to tonalite in composition and have been interpreted as intrusive igneous rocks (McLelland et al., 1992) or ash flow tuffs (Carl and deLorraine, 1997). On the map scale, the Hyde School gneiss forms large (>10 km) domes with apparently concordant lenses of amphibolite, and have a composite igneous/metamorphic fabric that parallels the margin of individual bodies (Carl et al., 1990). The HSG contains variable enrichments with respect to its LILE and minor depletions in its HFSE when normalized to primitive mantle (Sun and McDonough, 1989), with the majority of samples sharing many of the trace element characteristics of the ARS. They plot from alkali-calcic to calc-alkalic with nearly constant MALI with increasing SiO_2 (Peck et al., 2013). Both multi-grain TIMS and single grain SHRIMP U-Pb analyses of zircon yield igneous age of ca. 1170 Ma (McLelland et al., 1992; Wasteneys et al., 1999). The zircon ages of the Hyde School Gneiss require that it was emplaced as a series of plutons within the Adirondack Lowlands. Deformation and associated gneissic layering developed during or subsequent to emplacement, consistent with monazite and garnet ages from leucosomes in the Popple Hill Gneiss (Heumann et al., 2006).

The Hyde School Gneiss intrusive ages overlap with zircon ages of the Rockport Granite, which outcrops immediately northwest of the BLsz.

1160-1150 Ma Edwardsville Pluton (and other members of the Frontenac Suite) Post Shawinigan Ferroanmagmatism (data from Peck et al., 2013)

The youngest igneous suite within the Adirondack Lowlands, and, importantly, the adjacent Frontenac Terrane, is a series of ferroan rocks referred to as the Frontenac Suite, represented in the area of this trip by the Edwardsville Pluton (the Pope Mills mass of Buddington, 1929). Ranging from syenitic to subordinate gabbro, the Edwardsville pluton is texturally and compositionally heterogeneous. Recent single grain SHRIMP analyses (Peck et al., 2013) have corroborated older multi-grain TIMS work (1164 Ma; McLelland et al., 1993), which yield an age of 1149 +/- 22 and 1161+/- 16 Ma from a monzonitic member of the Edwardsville plutonic suite and a granite from the Honey Hill syenite, respectively (Peck et al., 2013). These ages correspond to anorthosite-mangerite-charnockite-granite (AMCG) magmatism within the Adirondack Highlands (McLelland et al., 2004; Hamilton et al., 2004) and the similarly ferroan Frontenac Suite in the Frontenac terrane to the northwest (1180-1160 Ma).

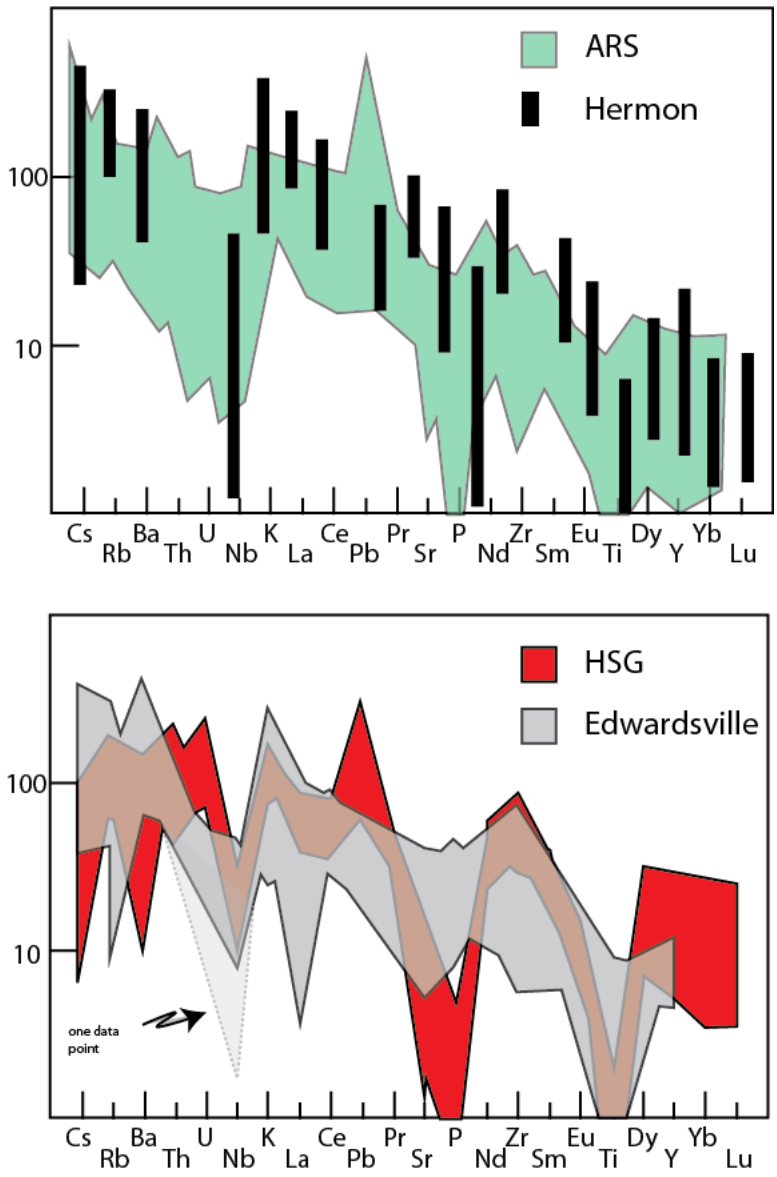

Figure 7. Incompatible element plots normalized to primitive mantle (Sun and McDonough, 1989) of the four major igneous suites. Note the strong enrichment in LILE and depletion in HSFE, characteristic of a metasomatized source (Chiarenzelli et al., 2010).

Unlike the older igneous suites in the Lowlands, this late intrusive suite plots as strongly ferroan and alkali-rich on geochemical diagrams. These data suggest that the influence of a metasomatized lithospheric mantle/lower crust was completely gone by this time and that anhydrous, lower crustal sources were likely dominant. This is consistent with post-orogenic delamination of the lithospheric mantle as presented in several other contributions (McLelland et al., 2004; Regan et al., 2011; Peck et al., 2013). This was likely due to upwelling of asthenospheric mantle, and melting of the lower crust (McLelland et al., 2010a,b; Regan et al., 2011; Peck et al, 2013), processes that extended across the Adirondack Lowlands and adjacent Frontenac Terrane as Shawiningan plutonism was ending. These relationships establish that the Lowlands and Frontenac terranes were a coherent tectonic unit by ca 1160 Ma, representing complete closure of the earlier, pre-Shawinigan sedimentary basin. The high-strain features observed within the BLsz are a manifestation of this collisional boundary.

CONCLUSIONS

The Adirondack Lowlands record several geochemically distinct, plutonic suites which were emplaced into an older metasedimentary sequence. The earliest pulse of magmatism, the Antwerp-Rossie, has a wide range in SiO_2 content and has a strong arc signature with mild calc-alkaline character. Despite its pre-Shawinigan age (ca. 1203 Ma), it appears to cross-cut tectonic fabrics within the surrounding metasedimentary units (stop 1), suggesting that an earlier (accretionary phase?) of deformation preceded the Shawinigan orogeny. Sm-Nd isotopic analyses suggest a juvenile source for the ARS, but with a strong continental influence immediately adjacent to the BLsz, where ε_{Nd} values decrease drastically and yield T_{DM} ages >1600 Ma. Following this phase of magmatism, the 1182 Ma (Heumann et al., 2006), megacrystic Hermon gneiss was emplaced, which shares many of the same geochemical attributes as the ARS. Circa 1172 Ma magmatism (McLelland et al., 1992; Wasteneys et al., 1998) is represented by the domical Hyde School Gneiss bodies southeast of the BLsz, and the voluminous Rockport granite to the northwest. Although sharing some of the incompatible element trends present within earlier magmatic suites, the HSG and Rockport granite are more ferroan and aluminous. The last magmatic event, the Frontenac suite (ca. 1180-1150 Ma; McLelland et al., 1991; Peck et al., 2014), represented by the Edwardsville pluton in New York, has recently been interpreted as the southern extension of ferroan magmatism in the Frontenac terrane (Peck et al., 2013). Furthermore, this event is interpreted to represent the mid-crustal expression of AMCG plutonism present in the Adirondack Highlands (Peck et al., 2013). Therefore, these suites contain a record of the evolving tectonic environment during the final closure of the Trans-Adirondack back arc basin from subduction to post collisional delamination.

STOPS AND TRIP LOG

Meeting Location: Price Chopper parking lot (east of I-81; last exit before bridge if headed north)

Address: 43615 New York 12, Alexandria Bay, NY 13607

Secondary meeting location: outcrop at 8:45 am

Meeting time: 8 AM; Depart Price Chopper by 8:15 AM
Drive I-81 S, take exit 49….. 9.7 Miles
Turn Left onto NY-411 E….. 3.1 Miles
Continue on NY 26 S….. 1.7 Miles
Turn Left onto Commercial St…… 0.2 miles
Continue onto NY 26-S/Mill Street….. 6.1 miles
Turn left onto US-11 N….. 6.4 miles
27.2 Miles, 30 minutes
Pull over on southeast side of road (Right side – large shoulder). Cross carefully! Heavy traffic.
Arrive: 8:45 AM

Stop 1: Route 11 east of Antwerp, NY

Coordinates: N 44°14,184' W 075°35.950'

This outcrop is one of many exposures of the Antwerp-Rossie suite, and surrounding marble, exposed along this section of US-11. Interestingly, the granitoid appears to cross -cut an isoclinal, recumbant fold in the marble, and contains quartzite xenoliths. However, Shawinigan deformation is generally accepted to postdate 1200 Ma. An important question to consider at this outcrop is the origin of this layering. Is the folding related to deformation around the more competent granitoid, or does the granitoid cross cut an earlier phase of deformation?

Depart 9:30 AM
Head North on US-11….. 11.3 Miles
Turn right on NY-812/58/William Street….. 2.9 Miles
14.2 Miles, 17 minutes
Pull over on east shoulder of road, outcrop immediately adjacent to road.
Arrive: 9:47 AM

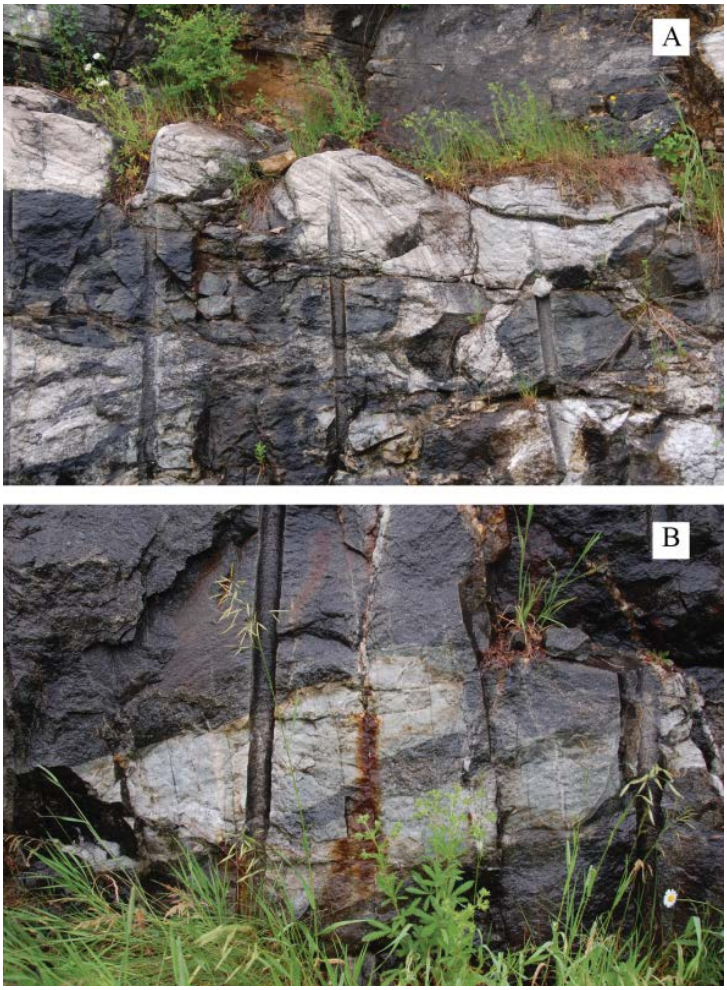

Figure 8. Photographs from Stop 1. A) intrusive contact between the Antwerp-Rossie suite and the lower marble; note isoclinal fold.. B) quartzite xenoliths in granodiorite of the Antwerp-Rossie suite.

Stop 2: The Steers Head locality

Coordinates: N 44°18,723' W 075°27.289'

The steers head locality is one of the many classic field trip localities in the Adirondack Lowlands. The marble contains graphite-rich layers and dismembered calc-silicate gneisses with well-developed reaction rims along their margins. The reaction rims contain tremolite, diopside, phlogopite, quartz, and calcite, among others. Do you see any other minerals in the reaction rims? Also, try to find the folded tourmaline vein on the north end of the outcrop within the marble.

It is important to note that the ARS has a wide range of SiO_2 contents. The rocks seen at Stop 1 and 2 are representative of the more felsic members of the ARS. Samples from this belt have relatively juvenile Sm-Nd systematics with no systematic relationship between ε_{Nd} with SiO_2, suggesting a minimal, if any, signal of crustal contamination.

This outcrop was host to an important stable isotope study by Cartwright and Valley (1991). Stable isotope ratios were measured in both metaigneous and metasedimentary country rocks across the intrusive contact to assess the importance of metamorphic fluid flow; essentially looking for a hydrologic 'breakthrough curve' caused by the difference in $\delta^{18}O$ between these lithologies. No breakthrough curve is present, and the gradient in $\delta^{18}O$ between lithologies contains an inflection point at the contact, with a several meter equilibration gradient from high $\delta^{18}O$ values in the marble, to lower $\delta^{18}O$ values in the granite. The preservation of these steep isotopic gradients and lack of offset of the inflection point suggest that minimal fluid flow occurred during regional metamorphism (Cartwright and Valley, 1991).

Figure 9. The classic "steers head" locality. Notice the large marble block entrained in the surrounding granodioritic Antwerp-Rossie Suite rocks.

Depart 10:30 AM
Head Northeast on NY812/58 towards Main Street….. 2.9 Miles
Turn right onto NY-812/US-11/East Main Street….. 11.4 Miles
Turn left onto NY-812 N….. 2.6 Miles
Turn left onto County Road 17/86….. 0.6 Miles
17.9 Miles, 24 minutes
Please pull over onto right (east) shoulder.
Arrive: 10:54 AM

Stop 3: County Road 17 north of De Kalb Junction

Coordinates: N 44°30.369' W 075°21.405'
The megacrystic Hermon Granite gneiss is a distinctive rock unit throughout the Adirondacks, with coarse K-spar augen. Here, the Hermon gneiss was emplaced into marble. With an age of 1182 Ma (Heumann et al., 2006), all deformation within the Hermon Granite gneiss is likely associated with Shawinigan tectonism. As noted above, this suite of rock shares many similarities to the ARS, but lacks a major Pb anomaly when normalized to primitive mantle and typically plots on field boundaries on tectonic discrimination diagrams (Pearce et al., 1984). Note the strong fabric development at this outcrop. Do the different minerals show varying amounts of deformation or recrystallization? What is the strike and dip of the gneissic layering?

Depart: 10:40 AM
Continue on County Road 17/86/7….. 2.7 Miles
Park at intersection with Child's Road
3.2 Miles, 5 minutes
Arrive: 10:45 AM

Figure 10. A concordant layer of Hermon granite in pelitic gneiss, containing xenoliths of the host rock along its margin.

Stop 4: South of Beaver Creek, County Route 7. Park on Childs Road. BE CAREFUL!!! SMALL SHOULDER!

Coordinates: N 44°31.517' W 075°24.001'

This outcop contains meter to submeter concordant layers of the Hermon granite gneiss (HGG) within a fine grained sulfidic, pelitic gneiss. Both contain a well-developed, upright foliation, and a moderately plunging stretching lineation. Near the margin of the Hermon granite gneiss, there are sub-meter scale pelitic xenoliths aligned with the tectonic fabric (Figure 10). What is the strike and dip of the major fabric in the metapelite? The granitic gneiss? The foliation is fairly representative of the major structural fabrics throughout the Adirondack Lowlands and is well developed within the Hermon granite gneiss, suggesting that the NE-SW structural grain, predominate throughout the Adirondack Lowlands occurred after the emplacement of the Hermon granite gneiss.

Similarly to the ARS, the Sm-Nd systematics for the HGG form a fairly steep evolutionary curve. They plot between CHUR and contemporaneous depleted mantle at time of crystallization suggesting a juvenile source. The sample analyzed plots entirely within the evolutionary envelope for the ARS.

Depart: 11:45 AM
Head North on County Road 17/86/De Kalb DePeyster Road….. 1.3 Miles
Turn Right onto County Rd 11/45….. 1.8 Miles
Turn Right on County Road 10….. 1.1 Miles
Take first left onto Plimpton Road….. 1.4 Miles
Continue onto Lake and Kokomo Road….. 0.1 Miles
Turn left onto NY-184 W….. 7.9 Miles
Sharp left onto County Road 7/95….. 1.5 Miles
Total: 15.2 Miles, 28 Minutes
Park on right shoulder (east side of road), and cross road carefully.
Arrive 12:13 PM Bring Lunch

Stop 5: County Road 76, north of Cooper Rd, south of Turner Rd. BEWARE ANTS

Coordinates: N 44°27.568' W 075°33.354'

This outcrop is representative of the Hyde School Gneiss (HSG). The HSG has been interpreted alternatively as having an intrusive, or an extrusive (ash flow) protolith. However, substantial work has confirmed its plutonic origin (McLelland et al., 1992; Wasteneys et al., 1999). This outcrop displays rhythmic layering characteristic of the HSG, with amphibolite lenses to continuous layers that are relatively thin here. On a larger scale, the HSG forms km-scale domical lenses within surrounding metasedimentary packages, and contains a composite igneous/metamorphic fabric that parallels its margin. Medium grained in this locality, the HSG ranges from coarse leucogranite to tonalite, to finer grained aplitic layers. Geochemically, it shares many of the same characteristics as the older magmatic suites. It contains minor enrichments with respect to its LILEs and minor depletions in its HFSE when normalized to primitive mantle (Sun and McDonough, 1989), and plots from alkali-calcic to calc-alkalic with constant MALI with increasing SiO_2. Furthermore, unlike the ARS and Hermon Gneiss, the HSG samples plot as largely ferroan with regard to their Fe-index, with a subset plotting in the magnesian field (Peck et al., 2013; Frost and Frost, 2008).

Depart: 1:00 PM

Head north on County Road 7/95….. 1.8 Miles
Continue onto NY-184W….. 0.6 Miles
Contine straight onto NY-58 N….. 0.3 Miles
Total: 2.5 Miles, 7 minutes
Park on right shoulder just north of Pope Mills town center
Arrive: 1:07 PM

Stop 6: Route 58 north of junction with Acres Road outside Pope Mills, NY.

Coordinates: N 44°29.282' W 075°34.880'

The youngest igneous suite within the Adirondack Lowlands is a series of ferroan rocks collectively referred to as the Edwardsville pluton (Buddington, 1929). Ranging from syenitic to subordinate gabbro, this suite of rocks is both texturally and compositionally heterogeneous. Recent single grain SHRIMP analysis (Peck et al., 2013) has corroborated older multi-grain TIMS work (1164 Ma; McLelland et al., 1993), which yield an age of 1149 +/- 22 and 1161+/- 16 Ma from a monzonitic member of the Edwardsville pluton and a granite from the Honey Hill syenite, respectively (Peck et al., 2013). These ages correspond to anorthosite-mangerite-charnockite-granite (AMCG) magmatism within the Adirondack Highlands (McLelland et al., 2004; Hamilton et al., 2004), and the similarly ferroan magmatic event in the Frontenac terrane to the northwest (1180-1160 Ma).

Although texturally similar to the Hermon Gneiss, can you see a mineralogical difference? Is there a strong tectonic fabric? Lastly, is this outcrop homogeneous, or are there texturally distinct rocks types, and, if so, what is the relationship between them?

Depart: 1:50 PM
Head north on NY-58 toward Brown Road….. 2.6 Miles
Turn left on County Route 6….. 6.8 Miles
Continue onto Lake street….. 0.5 Miles
Turn left onto NY-37 W/South Main street….. 0.9 Miles
Take 3rd left onto County Road 3/31….. 1.7 Miles
Turn right onto Split Rock Road….. 2.3 Miles
Total: 14.8 Miles, 23 minutes
Park on right shoulder. Please park as far right as possible. This is a narrow road.
Arrive: 2:13 PM

Stop 7: Rossie Diorite, Split Rock Road. Very close to private property, please be courteous!

Coordinates: N 44°23.598' W 075°41.807'

The Rossie diorite represents a more mafic component of the ARS suite. It is important to note that we are very close to the Black Lake shear zone, an important structural and lithologic discontinuity separating the Adirondack Lowlands from the Frontenac Terrane (Wong et al., 2011). Although slightly more mafic than its southern counterparts, the Rossie diorite displays similar geochemical signatures. However, despite these similarities, the belt of dioritic rocks exposed along the eastern margin of the Black Lake shear zone contain the lowest $\varepsilon_{Nd(T)}$ values, and yield the oldest T_{DM} ages, approximately as much as 400 My older than ARS samples

analyzed further south. These data suggest a major source of contamination by, or interaction with, older more evolved continental lithosphere (n=3 samples along the northwestern extent of the ARS).

Depart: 2:50 PM
Head South on Split Rock Road….. 1.2 Miles
Take 1st right onto South Hammond Road….. 3.1 Miles
Turn left onto NY-37 W….. 0.1 Miles
Take 1st right onto Webster Road….. 1.6 Miles
Continue onto Calaboga Road….. 1.7 Miles
Turn left onto NY-12 S….. 3.0 Miles
Total: 10.7 Miles, 22 minutes
Park on right (north) shoulder. Large shoulder, but abundant and very fast traffic on road. Please do not cross Rt. 12
Arrive 3:12 PM

Stop 8: Rockport Granite; US 12.
Coordinates: N 44°24.182' W 075°47.984

These exposures are on the NW side of the Black Lake shear zone (Wong et al., 2011). We are now in the Frontenac Terrane. This outcrop exposes the voluminous Rockport granite (ca. 1170 Ma; Wasteneys et al., 1998), which extends across the Thousand Islands region and into Ontario, Canada. Here, the Rockport Granite is in contact with strongly deformed calc-silicate (metasedimentary) gneisses. There is a faint, near-vertical gneissic layering within the Rockport Granite that is shared by the adjacent calc-silicate gneisses. This suite of granitic rocks is time equivalent to the domical Hyde School gneisses in the Adirondack Lowlands. However, the Rockport Granite has a much different intrusive style, and is hosted most commonly by quartzite and quartzite-calc-silicate country rock. The Rockport granite is generally slightly to moderately deformed, and doesn't occur as strongly deformed domical bodies like its Hyde School gneiss counterpart. Furthermore, no exposures of ARS or Hermon Granite gneiss have been identified on this side of the Black Lake shear zone.

Discussion: 4:15 PM
Depart 5:00 PM

Figure 11. Intrusive contact between ca. 1170 Ma Rockport granite and calc-silicate gneisses NW of the BLsz.

ACKNOWLEDGEMENTS

We thank all the participants of the 2008 Adirondack Lowlands Keck Geology Consortium project lead by Colgate University: Joseph Catalano, Isis Fukai, Steven Hochman, Josh Maurer, Robert Nowak, Ashley Russell, Andrew Stocker, and Celina Will. Their hard work and participation is reason that the abundant data presented above exists. Amanda Van Lankvelt is acknowledged for revisions on an earlier version of this guide. The majority of data presented in this field trip can be found in the compilation papers: Peck et al. (2014) and Chiarenzelli et al. (2010b; ARS), which both were products of the Keck project. Lastly, we would like to thank all of the trip attendees!

REFERENCES CITED

Baird, G.B., and Shrady, C.H., 2011, Timing and kinematics of deformation in the northwest Adirondack Lowlands, New York State: Implications for terrane relationships in the southern Grenville Province: Geosphere, v. 7, p. 1303–1323, doi:10.1130/GES00689.1.

Buddington, A.F., 1929, Granite Phacoliths and Their Contact Zones in Northwest Adirondacks: New York State Museum Bulletin, v. 281, 51-107.

Buddington, A.F., 1934, Geology and mineral resources of the Hammond, Antwerp, and Lowville quadrangles: New York State Museum Bulletin, v. 296.

Buddington, A.F., 1939, Adirondack igneous rocks and their metamorphism: Geological Society of America Memoir,v. 7, 354 p.

Carl, J.D., 2000, A geochemical study of amphibolite layers and other mafic rocks in the NW Adirondack Lowlands, New York: Northeastern Geology and Environmental Sciences, v. 22, 142-166.

Carl, J.D., deLorraine, W.F., 1997, Geochemical and field characteristics of metamorphosed granitic rocks, NW Adirondack Lowlands, New York: Northeastern Geology and Environmental Science, v. 19, p. 276-301.

Carl, J.D., deLorraine, W.F., Mose, D.G., Shieh, Y.N., 1990, Geochemical evidence for a revised Precambrian sequence in the Northwest Adirondacks, New York: Geological Society of America Bulletin,v. 102, 182-192.

Chiarenzelli, J., Kratzmann, D., Selleck, B., Christoffersen, P., and Durham, A., 2013, Constraining the depositional history and evolution of the Trans-Adirondack Back-Arc Basin using detrital zircon geochronology: Geological Society of America Abstracts with Programs, Vol. 45, No. 7, p.739.

Chiarenzelli, J., Lupulescu, M., Cousens, B., Thern, E., Coffin, L., Regan, S., 2010a, Enriched Grenvillian lithospheric mantle as a consequence of long-lived subduction beneath Laurentia: Geology, v. 38, p. 151-154.

Chiarenzelli, J., Regan, S., Peck, W.H., Selleck, B.W., Cousens, B., Baird, G.B., Shrady, C.H., 2010b,Shawinigan Arc Magmatism in the Adirondack Lowlands as a Consequence of Closure of the Trans-Adirondack Back-Arc Basin: Geosphere, v. 6, p. 900-916.

Chiarenzelli, J., Hudson, M., Dahl, P., and deLorraine,W.D., 2011a, Constraints on deposition in the Trans-Adirondack Basin, northern New York: Compositionand origin of the Popple Hill Gneiss: Precambrian Research, v. 214–215, p. 154–171, doi:10.1016/j.precamres.2011.10.024.

Chiarenzelli, J., Lupulescu, M., Thern, E., and Cousens,B., 2011b, Tectonic implications of the discovery of a Shawinigan ophiolite (Pyrites Complex) in theAdirondack Lowlands: Geosphere, v. 7, p. 333–356, doi:10.1130/GES00608.1.

Fisher, D.W., Isachsen, Y.W., Rickard, L.V., 1970, Geologic Map of New York: New York State Museum and Science Service, Map and Chart Series, 15, 1:250,000, 5 sheets.

Fraure, G., Mensing, T.M., 2005, Isotopes: Principles and applications, Third edition, John Wiley and Sons.

Frost, B.R. and Frost, C.D., 2008, Geochemical classification for feldspathic igneous rocks: Journal of Petrology, v. 49, p 1955-1969.

Heumann, M.J., Bickford, M., Hill, B.M., McLelland, J.M., Selleck, B.W., Jercinovic, M.J., 2006, Timing of anatexis in metapelites from the Adirondack Lowlands and southern Highlands: A manifestation of the Shawinigan orogeny and subsequent anorthosite-mangerite-charnockite-granite magmatism: Geological Society of America Bulletin, v. 118, p. 1283–1298.

McLelland, J., Chiarenzelli, J., and Perham, A., 1991, Age, field, and petrological relationships of the Hyde School Gneiss, Adirondack Lowlands, New York: Criteria for an intrusive origin: Journal of Geology, v. 100, p. 69-90.

McLelland, J.M., Hamilton, M., Selleck, B.W., McLelland, J., Walker, D., and Orrell, S., 2001, Zircon U-Pb geochronology of the Ottawan Orogeny, Adirondack Highlands, New York: Regional and tectonic implications: Precambrian Research, v. 109, p. 39–72, doi: 10.1016/S0301-9268(01)00141-3.

McLelland, J., Daly, J. S., Chiarenzelli, J., 1993, Sm-Nd and U-Pb isotopic evidence for Juvenile crust in the Adirondack Lowlands and implications for the evolution of the Adirondack Mts: Journal of Geology, v. 101, p. 97-105.

McLelland, J.M., Daly, J.S., McLelland, J.M., 1996, The Grenville orogenic cycle (ca. 1350-1000 Ma); an Adirondack perspective: Tectonophysics, v. 265, p. 1-28.

McLelland, J.M., Selleck, B.W. Bickford, M.E., 2010a, Review of the Proterozoic evolution of the Grenville Province, its Adirondack outlier, and the Mesoproterozoic inliers of the Appalachians, *in*: Tollo, R.P., Bartholomew, M.J., Hibbard, J.P., and Karabinos, P.M., (Eds.), From Rodinia to Pangea: The Lithotectonic Record of the Appalachian Region: Geological Society of America Memoir, v. 206, p. 1–29.

McLelland, J.M., Selleck, B.W., Hamilton, M.A., and Bickford, M.E., 2010b, Late-to post-tectonic setting of some major Proterozoic anorthosite–mangerite–charnockite–granite (AMCG) suites: Canadian Mineralogist, v. 48, p. 729-750.

McLelland, J.M., Bickford, M.E., Hill, B.M., Clechenko, C.C., Valley, J.W., and Hamilton, M.A., 2004, Direct dating of Adirondack massif anorthosite by U-Pb SHRIMP analysis of igneous zircon: Implications for AMCG complexes: Geological Society of America Bulletin, v. 116, p. 1299-1317.

Pearce, J.A., Harris, N.B.W, and Tindle, A.G., 1984, Trace element discrimination diagrams for tectonic interpretations of granitic rocks: Journal of Petrology, v. 25, p. 956-983.

Peck, W. H., Selleck, B.W., Wong, M. S., Chiarenzelli, J.R., Harpp, K. S., Hollocher, K., Lackey, J.S., Catalano, J., Regan, S.P., and Stocker, A., 2013, Orogenic to postorogenic (1.20-1.15 Ga) magmatism in the Adirondack Lowlands and Frontenac terrane, southern Grenville Province, USA and Canada: Geosphere, v. 9, n. 6, p. 1637-1663.

Peck, W.H., Selleck, B.W., and Wong, M.S., 2011, Geology of The Black Lake Shear Zone and Northwestern Adirondack Lowlands, Grenville Province, New York: Friends of the Grenville Annual Field Trip, September 10-11, 2011, Alexandria Bay, N.Y., 63 p.

Rivers, T., 2008, Assembly and preservation of lower, mid, and upper orogenic crust in the Grenville Province—Implications for the evolution of large hot long-duration orogens: Precambrian Research, v. 167, p. 237–259, doi: 10.1016/j.precamres.2008.08.005.

Sager-Kinsman, A.E., Parrish, R.R., 1993. Geochronology of detrital zircons from the Elzevir and Frontenac terranes, Central Metasedimentary Belt, Grenville Province, Ontario: Canadian Journal of Earth Sciences, v. 30, p. 465–473.

Selleck, B.W., McLelland, J.M., Bickford, M.E., 2005, Granite emplacement during tectonic exhumation; the Adirondack example: Geology, v. 33, p. 781-784.

Sun, S.S. and McDonough, W.F., 1989, Chemical and isotopic systematics of oceanic basalts; implications for mantle composition and processes: Magmatism in the ocean basins. Saunders, A.D. and Norry, M.J. (Editors), Geological Society of London, v. 42, p. 313-345.

Wasteneys, H., McLelland, J., Lumbers, S, 1999. Precise zircon geochronology in theAdirondack Lowlands and implications for revising plate tectonic models of theCentral Metasedimentary Belt and Adirondack Mountains, Grenville Province, Ontario and New York: Canadian Journal of Earth Sciences v. 36, p. 967-984.

Wong, M.S., Peck, W.H., Selleck, B.W., Catalano, J.P., Hochman, S.D., and Maurer, J.T., 2011, The Black Lake Shear Zone: A boundary between terranes in the Adirondack Lowlands, Grenville Province: Precambrian Research, v. 188, p. 57-72.

GEOLOGY OF THE BALMAT ZINC REGION

WILLIAM deLORRAINE

St. Lawrence Zinc Co. LLC, 408 Sylvia Lake Rd., Gouverneur, NY 13642

The Balmat-Edwards district zinc orebodies are located in the northwest Adirondack Lowlands of northern New York State (Fig. 1). The Adirondacks are an extension of the Canadian Shield into New York State via the Frontenac Axis/ Thousand Islands region located along the St. Lawrence River and are underlain by poly-deformed rocks metamorphosed to a high grade during the Grenvillian orogeny about 1.1 bya. Zinc orebodies of the Balmat district occur in an eight mile long strip of rocks comprised of dolomitic marbles and calc-silicate rocks referred to as the Balmat-Edwards marble belt. The Balmat-Edwards marble belt cores a nappe-scale, doubly plunging, recumbent fold referred to as the Sylvia Lake syncline (Fig. 1). Lithologically similar silicated dolomitic marble host rocks, sulfide ore, and structure reappear 28 miles/45 km to the northeast of Balmat at Pierrepont, NY (Fig.1).

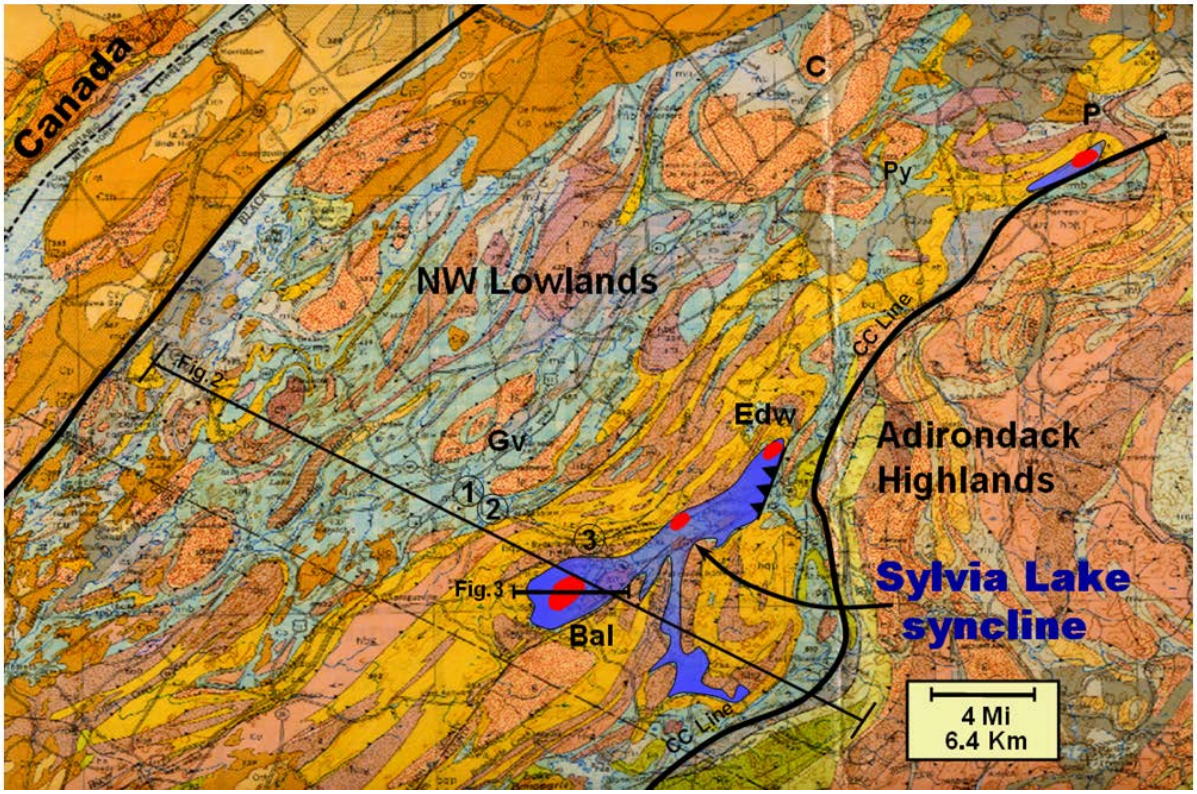

Figure 1. NYS geologic map (Adirondack Sheet of Isachsen and Fisher, 1970) of the NW Adirondack Lowlands. Locations of Zinc deposits shown in red at Balmat (Bal), Hyatt (Hy), Edwards (Edw), and Pierrepont (P). Zinc deposits in upper marble, darker shaded blue areas. Village of Gouverneur labeled "Gv", Village of Canton labeled "C".

On this field trip we will make a NW-SE transect across the Lowlands beginning in Gouverneur and ending at Balmat, NY. We will examine, in a general sense, the structural architecture and tectono-stratigraphic setting of what has been referred to as the "Trans Adirondack Back-Arc Basin" (TABB) comprising the NW Adirondack Lowlands between the Highlands and the Black Lake region (deLorraine and Carl, 1993; Chiarenzelli et al., 2012). As we progress from Stop 1 to Stops 2 and 3 we'll gradually move up section.

Stops 1 and 2 in calcitic lower marble record rift and drift phase chemogenic sedimentation in the (TABB) whereas up section at Stop 3 Popple Hill gneiss records basin fill turbididic sedimentation initiated by convergence (Chiarenzelli et al., 2012). Stop 4 takes us to dolomitic upper marble at the top of the section. Host rocks record cyclic dolomitized and silicified algal mat carbonate and evaporite deposition in shallow restricted marine seas during the final stages of backarc basin fill. Overall objective will be to take a look at the different high grade metamorphic rock types and mineral assemblages, styles of folding, relate minor folds to major folds, and to gain an appreciation for why the tectono-stratigraphic setting of the NW Adirondack Lowlands as a back-arc basin might be the ideal setting for the formation of SEDEX ore deposits such as the Balmat-Edwards-Pierrepont deposits

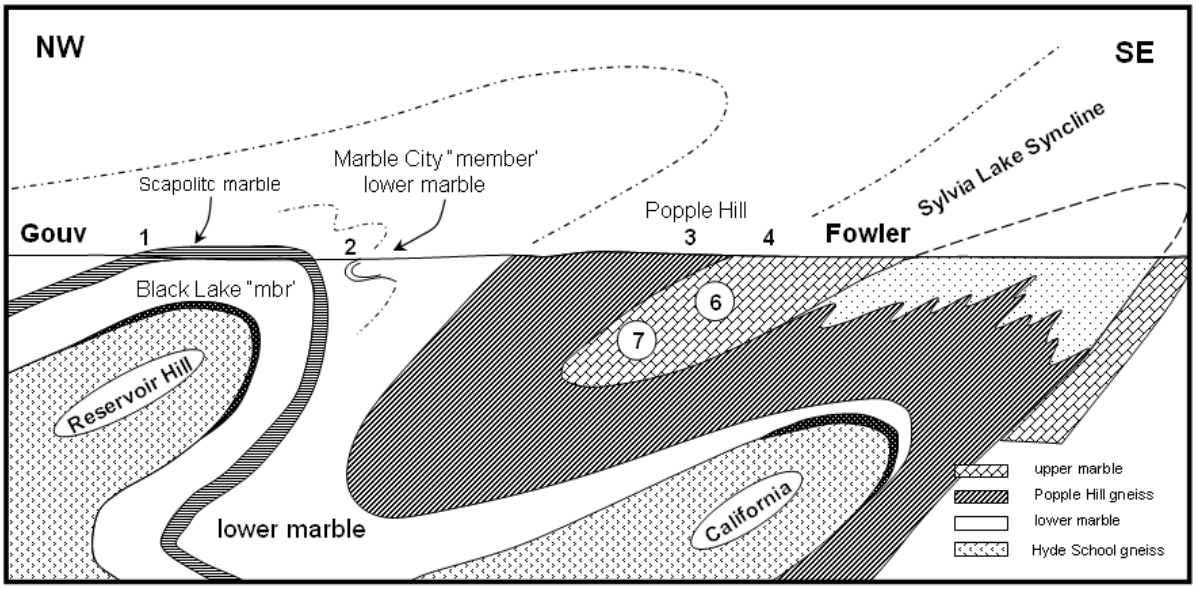

Figure 2. Vertical NW-SE section along Rt. 58/812, Gouverneur to Fowler, NY. Numbers refer to stops. Section line shown on Fig. 1.

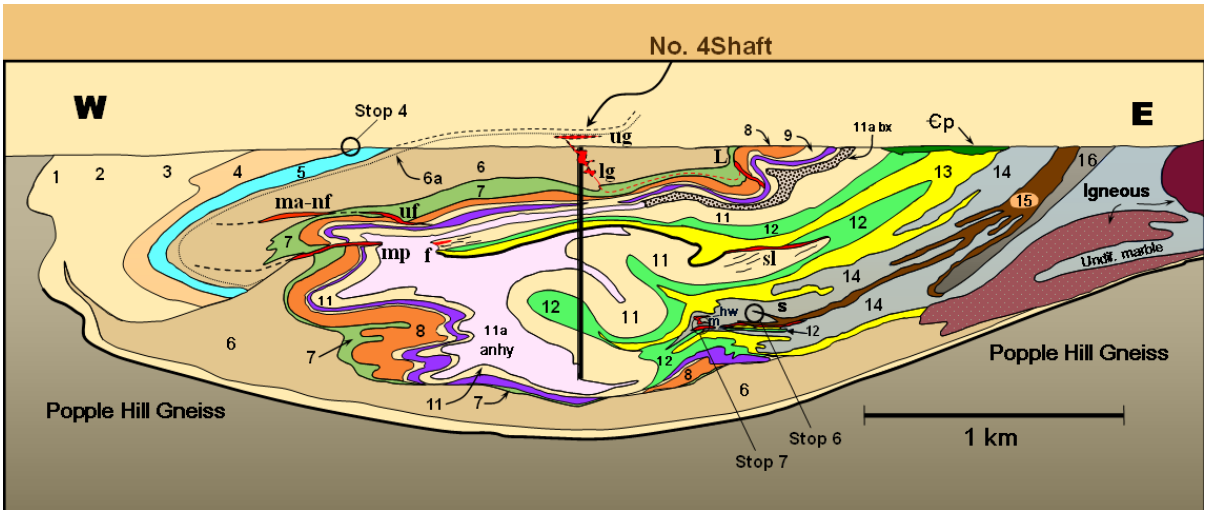

Figure 3. W-E vertical section through the Sylvia Lake Syncline. Section line shown on Fig. 1. Relative structural position of stops shown on section.

Zinc orebodies are believed to have originated as Mesoproterozoic seafloor exhalations that accumulated as conformable sedimentary massive sulfide lenses and layers deposited some 1.25 bya in the TABB within a sequence of dolostones, thinly layered stromatolitic cherty dolostones, and evaporites (Fig. 4). Sphalerite and pyrite accompanied by very minor galena are the principal sulfide minerals. Host rocks and orebodies attained burial depths of 20 km or more during Grenvillian orogenesis when they underwent polyphase deformation. Upper Amphibolite grade peak metamorphic conditions generated migmatites and anatectic melts in surrounding rocks and mobilized significant sulfide fractions within and away from the orebodies. In a few places, sheet-like, aerially extensive, nearly pure sphalerite "dikes" segregated from their parent lenses and intruded macrofracture surfaces where these large cracks intersected parent sulfide masses. Macrofractures evolved into thrust faults at a high metamorphic grade during deep-seated regional ductile shearing. Sheetlike "daughter" orebodies thus formed are found on three major ductile fault surfaces that are refolded by the Sylvia Lake syncline. Most of the intruded sphalerite segregated along the fault surfaces into tabular lozenges elongated in the direction of associated fold hinges. A typical daughter orebody "footprint" is several hundred feet wide by 6000 ft/1800 m long by perhaps 1.8-2.5 m thick on average. Tonnages average up to 6 million.

Daughter orebodies are inherently lower grade and finer grained because of their locations on fault surfaces making them inherently more susceptible to recurrent deformational strains. Ductile faulting abraded and rounded admixed adjacent wall rock inclusions in the ore thereby imparting their signature deformational texture referred to as "Durchbewegung" texture. "Parent" ore lenses from which the daughter orebodies are derived can be 1500 ft/450 m or more in length, 450ft/150 m wide, and up to 80ft/25 m or more thick. Parent ore is coarse grained and twice the tenor of daughter ore. Presently there are several daughter orebodies in production or have been drilled whose predicted source bed or parent massive body awaits discovery.

Parent orebodies originally deposited in more ductile carbonate lithologies that flowed rather than faulted during deformation did not necessarily give rise to daughter offshoots. Rather, those stratabound sulfides remobilized within and parallel to fold hinges associated with the Sylvia Lake syncline. The largest of these orebodies, the Main and Hanging Wall, are located at No. 2 mine within the core of the Sylvia Lake syncline in Unit 14 (Fig. 3).

Individual orebodies exhibit good continuity and are quite predictable in the down-plunge dimension, though the details of host structure change and evolve from section to section in the mine. This leads to a variety of dips of ore shoots from flattish to vertical hence requiring an array of different mining methods, from inclined room and pillar to long-hole extraction.

Multiple lines of evidence suggest differentiation of sphalerite from stratiform massive sulfide ore lenses occurred during the Upper Amphibolite grade Shawinigan (Grenville) Orogeny (ca. 1.20-1.15 Ga) prior to development of the host Sylvia Lake Syncline. Syntectonic macrofractures impinged upon massive lenticular, polymetallic stratiform orebodies forming subsidiary ores as sheet-like radial dikes. Several of the monomineralic sphalerite daughter orebodies remain linked to parents by thin, refolded, "durchbewegt" ore sheets that cross-cut stratigraphy and metamorphic fabrics (Fig. 3, daughter orebodies L and lg linked to UG near No. 4 mine). Long after intrusion of daughter sphalerite dikes, admixed xenolithic fragments of wall rock contained within the initially massive, coarse-grained, sphalerite became rounded by tectonic milling resulting from recurrent strains partitioned along macrofracture surfaces. Daughter orebodies thereby acquired distinctive durchbewegung textures while nearly doubling their thicknesses but halving their tenors as macrofractures evolved into tectonic slides -- some with km-scale displacements.

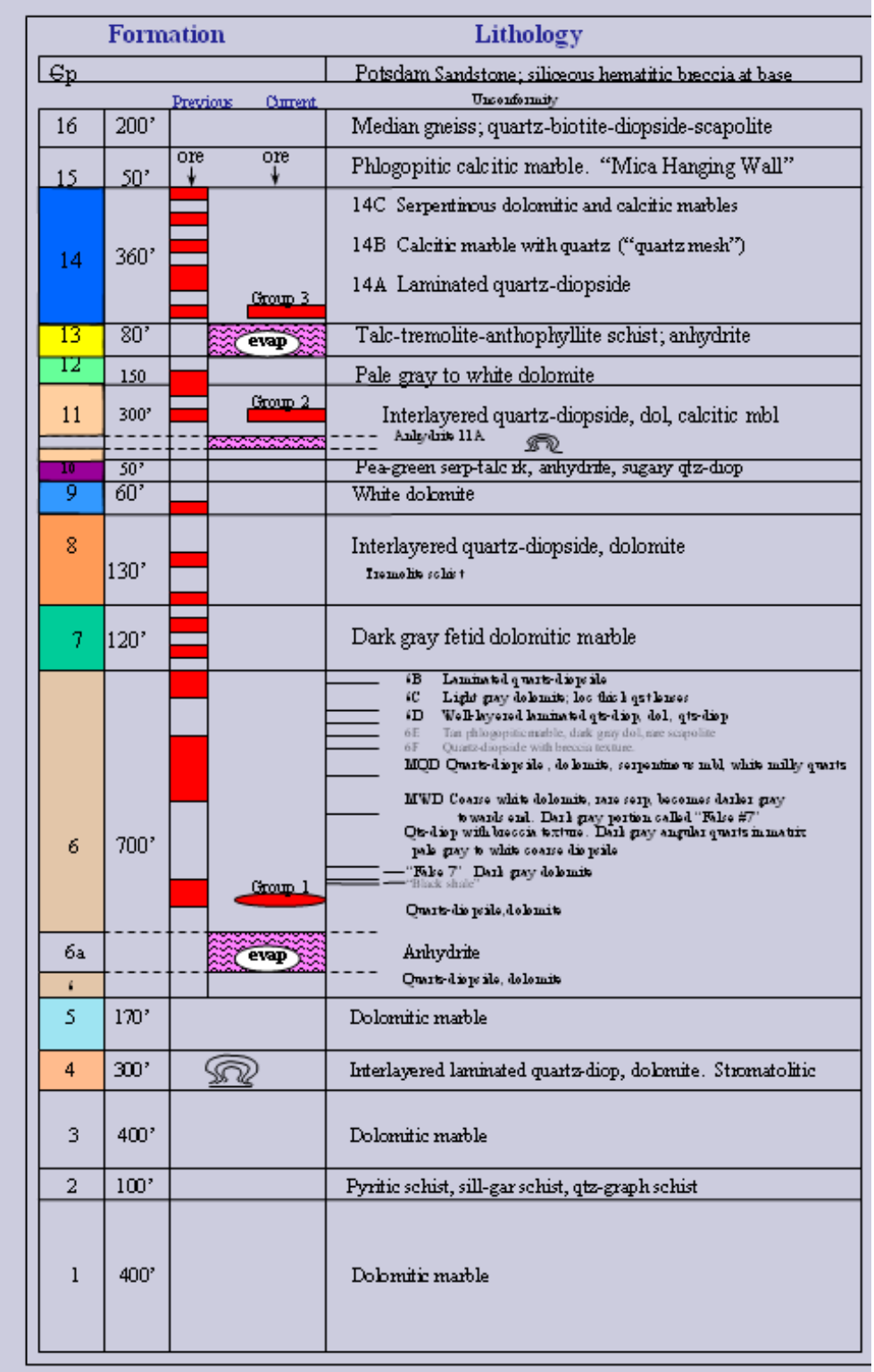

Figure 4. Stratigraphic Column through the Balmat District. Black bars represent stratigraphic horizons at which zinc mineralization has been found. Column marked "Previous" shows locations of sulfide ore formerly interpreted as (Fig.4 cont'd) conformable, stratabound occurrences but known to occur along cross-cutting metamorphic faults therefore have no stratigraphic significance. Column marked "Current" shows confromable, stratiform sulfide ore horizons (after deLorraine (2001); deLorraine and Sangster (1997).

Polyphase deformation culminated with superposition of the nappe-scale Sylvia Lake syncline accompanied by refolding and inversion of parent-daughter ore complexes on its upper limb. This complex fold displays elements of both passive flow and concentric geometries due to extremes of ductility contrast induced by intercalation of marble, exceedingly ductile anhydrite strata, and competent quartz-diopside-rich units. Long thought to have been the driving force or "tectonic engine" responsible for large scale sulfide mobilization to dilatent sites within its major and minor fold hinges, the Sylvia Lake syncline is now known to refold durchbewegt "daughter" ore sheets and thus is a late stage feature in the evolution of orebodies of the district. Mobilization of originally disseminated sulfides from throughout the Upper Marble section to dilatent structural sites either within fold hinges or along syn-kinematic faults via metahydrothermal fluid phases is precluded by direct linkage of daughter ore to parent source beds. As well, the emplacement of daughter mineralization along synmetamorphic faults that transgress metamorphic foliations and recrystallized bedding suggests emplacement after cessation of major devolitization reactions under "dry" ambient metamorphic conditions.

Geochemical groupings of orebodies are consistent with three "SEDEX" horizons (Fig. 4). Significantly, three major epochs of evaporite deposition in that interval coincide with the three epochs of stratabound sulfide deposition such that anhydrite sedimentation shortly precedes sulfide deposition in each case. Resulting from this are three "evaporite—ore" couplets within units 6, 11, and 14 (Fig. 4). Stratiform massive sulfide source bed lenses or layers specifically occur in those units. The association of evaporites and ore is an indirect, but important one that is common to other important sulfide deposits.

Deciphering the origin of the Balmat zinc deposits is made somewhat problematic by the effects of high grade metamorphism, polydeformation, and post-metamorphic annealing recrystallization. Nevertheless, the following scenario can be pieced together from petrological, geochemical and isotopic data, underground mapping and photographs, deposit-wide and regional structural geology, and deposit and regional stratigraphy. Orebodies fall into three geochemical groupings, each of which appears in the section not long after major evaporative epochs. Orebodies lowest in section are highest in Hg and vice versa, consistent with the interpretation that earliest SEDEX orebodies precipitated from saline brines that stripped most of the available Hg from the volcano-sedimentary pile in the Back-Arc basin repository during the first SEDEX cycle. In so doing less and less Hg was left for successive ore-forming cycles. This interpretation places evaporites immediately available to SEDEX ore fluids as a source of saline brines capable of leaching metals and presumes depletion of halide reservoirs after each SEDEX depositional epoch. Consequently SEDEX ore deposition is precluded until after the end of the next evaporative sedimentation epoch pending restoration of anhydrite and halite reservoirs.

An interpretation consistent with available data is that Balmat Zn deposits are ultimately of late Proterozoic, vent-distal, carbonate-hosted, SEDEX origin and that metamorphogenic "Daughter" orebodies spawned from massive "Parent" orebodies during Upper Amphibolite grade metamorphism as differentiated offshoots in the form of sheetlike sphalerite "dikes". Local preservation of flow banding, sulfur isotope gradients, color gradations in sphalerite and mineralogic differentiation ZnS+Py>ZnS>PbS in the direction of transport suggests that plastic flow or fluid-aided plastic flow was the dominant mechanism of mass transfer. Distances of migration are truly epic with readily demonstrable, km-scale, cross-stratal flow.

REFERENCES

Chiarenzelli, J.R., Hudson, M.R., Dahl, P.S., and deLorraine, W.D., 2012, Constraints on deposition in the Trans-Adirondack Basin, northern New York; composition and origin of the Popple Hill Gneiss: Precambrian Research, v. 214-215, p. 154-171.

Chiarenzelli, J., Lupulescu, M., Thern, E., and Cousens, B., 2011a. Tectonic implications of the discovery of a Shawinigan ophiolite (Pyrites Complex) in the Adirondack Lowlands: Geosphere, v. 7, no. 2; 2, p. 333-356.

deLorraine, W.F., 2001, Metamorphism, polydeformation, and extensive remobilization of the Balmat zinc orebodies, northwest Adirondacks, New York: Guidebook Series [Society of Economic Geologists [U.S.], v. 35, p. 25-54.

deLorraine, W.F., and Carl, J.D., 1993, Precambrian geology of the Northwest Adirondack Lowlands; a stratigraphic viewpoint: Guidebook - New York State Geological Association, Meeting, v. 65, p. 1-51.

deLorraine, W.F., and Sangster, A.L., 1997, Geology of the Balmat Mine, New York: Field Trip A5, Geological Association of Canada and Mineralogical Association of Canada Joint Annual Meeting, Ottawa, 43 p.

Isachsen, Y.W.,and Fisher, D.W., 1970, Geologic map of New York: Adirondack Sheet: New York State Museum, Map and Chart Series 15, scale 1:250,000.

ROAD LOG FIELD TRIP A-5: GEOLOGY OF THE BALMAT ZINC REGION

Start location: Aubuchon Hardware parking lot, 32 Clinton Street, Gouverneur, NY, just down the street from Jumbo's restaurant, across the street from Kinney Drugs at the intersection of Rt. 11 and Rt. 58N.

0.00 mi. Aubuchon parking lot exit: turn left on 58 S toward Edwards. (At traffic light route becomes 58/812 S). Proceed straight through light.

0.91 mi. Stop 1 Scapolite marble roadcut, lower marble. Dips to south at end of Reservoir Hill leucogneiss dome. Note black, N60ºE trending, late dike. Near the base of the lower marble section. Scapolite may be evidence for early evaporative chemogenic sedimentation in the Trans-Adirondack Back-Arc Basin (TABB).

1.58 mi. Stop 2 "Train Wreck" road cut, lower marble. "Graph-phlogo-cal" marble with brown tourmaline. Stratigraphically overlies the scapolitic marble. "Rift and Drift" phase of development of the TABB. Large blocks represent dismembered mafic dike fragments rotated and "strewn" about in the marble like a derailed train. This is the marble quarried extensively in the late 1800's to early 1900's making Gouverneur famous as "Marble City". It is a prominent local building stone which is a major component of churches, post offices, and other buildings in the region. 1274 +/- 9 Lu-Hf .

5.16 mi. Stop 3 Popple Hill migmatite gneiss road cut. Plag-qtz-biot gneiss; ca 1220. Migmatite-agmatite roadcut. Look for refolded migmatitic leucosomes, ptygmatic folds, folds with "S" asymmetric sense appropriate for structural position on upper limb of the Sylvia Lake Syncline and many that aren't... ? Basin Fill stage metasediments; here a poly-deformed migmatite-agmatite exposure. 1180-1160ma anatectic zircons. Local sill-gar-biot gneiss layers; rare carbonate seams. Currently nterpreted as immature turbiditic sediments, plag-rich wackes, qtz-arenites to Al-rich shales fining upward toward contact with upper marble as the back arc basin evolved into a foreland basin. Sourced from the Southern Adirondack terrane (Chiarenzelli et al, 2012).

6.15 mi. Rt. turn on 812 S towards Balmat at caution light.

6.40 mi. Rt. turn onto Sylvia Lake Road

7.48 mi. Arrive at front gate, St. Lawrence Zinc Co. No. 4 Mine. Do a "U" turn, park well off on the right-hand side of Sylvia Lake Road.

7.48 mi. Stop 4 . Units 4/5 Contact, No. 4 Mine. Upper marble Ca. 1210 ma. Upper limb of the Sylvia Lake syncline. Contact between silicated Unit 4 and overlying dolomitic marble, Unit 5. Unit 4 is stromatolitic. How are they identified? Look for laminated qtz-diopside rocks locally retrograded to serp-talcose-diop. What is stratigraphic "tops"? How do you think stroms formed and what might be their mode of preservation? How did theysurvive Upper Amphibolite grade metamorphism and polydeformation? "Footprint" of one inverted strom slightly elongated N10º W parallel to major and minor fold hinges.

8.57 mi. Intersection of Sylvia Lake Road and 812 S. Turn right on 812 toward Balmat.

10.40 mi. Balmat. Turn right at 4 corners on CR 24 (Russell Turnpike Road).

11.25 mi. Stop 5. Langevin Lane (private drive). Turn right, drive up paved driveway to top of hill.

11.44 mi. Private residence. Permission required. South end of Sylvia Lake, viewing N. Sweeping northerly vista of the lake with Balmat No. 4 mine headframe in right background. Topographic expression of the lake is a reflection of the geometry of the hourglass-shaped core of the Sylvia Lake syncline. Filled with Unit 11A anhydrite, the core of the fold was easily eroded so that the shape and great depth of the lake of over 150 feet in places is attributable to this unusual lithology.

11.62 mi. Return to CR 24, turn left and return to Balmat.

12.46 mi. Balmat. Turn left onto Rte. 812 N toward Fowler.

12.78 mi. Stop 6. Turn left onto short, dead-end paved road segment leading downhill toward abandoned open pit mine. Permission Required. Gouverneur Minerals Co. (formerly referred to as Gouverneur Talc Co); Vanderbilt Corp. Exposed in the east sidewall of the pit facing Rte. 812 is a spectacular isoclinal fold hinge in Unit 15 "Mica Hanging Wall" in the core of the Sylvia Lake syncline. Look for axial planar schistosity and transposed bedding in this tightlyappressed hinge. Good examples of boudinage. Are the long axes of the boudins parallel to the fold axes?

Turn around, return to 812, turn left onto 812 N.

13.21 mi. Turn left onto Pumphouse Road, entrance to Gouverneur Minerals Co.

13.38 mi. Drive past "Dead End" sign; Gouverneur Minerals Co. office and mill complex on right.

13.58 mi. RR tracks. Cross tracks, take immediate left-hand turn onto narrow paved lane.

13.72 mi. Stop 7. Gate to No. 2 mine. (Gate is locked, access by appointment only St. Lawrence Zinc Co.). We'll proceed into the No. 2 mine grounds, past the inclined shaft and hoist house, to the No. 2 open pit. The shaft and hoist are kept in good running condition on a stand-by basis serving as a second way out, escape route for the No. 4 mine. High tenor zinc ore is exposed in the pit along with numerous examples of high temperature cross-cutting relationships with host rocks. Numerous minor folds, examples of surficial oxidation of the massive sulfide ore resulting in "gossan", examples of bird's eye alteration texture, numerous different rock types and mineral parageneses. A suite of high grade carbonate metamorphic minerals for the student mineralogist and retrograde assemblages as well.

Return to intersection of Pumphouse Road and 812 N.

~14.21 mi. Turn left onto 812 N.

15.36 mi. Left turn onto Sylvia Lake Road

16.44 mi. Stop 8. St. Lawrence Zinc Co., No. 4 Mine entrance. Turn left into parking lot. Stop to view mine models, maps, core logging facilities, diamond drill core displayed on core racks, ore specimens, recap trip and discuss genetic models.

End of Trip

THREE AND A HALF SKARNS

GEORGE W. ROBINSON
Research Associate, Department of Geology, St. Lawrence University, Canton, NY 13617

STEVEN C. CHAMBERLAIN
Center for Mineralogy, 3140 CEC, New York State Museum, Albany, NY 12230

INTRODUCTION

The Central Metasedimentary Belt (CMB) of the Precambrian Grenville series rocks of St. Lawrence, Jefferson and Lewis Counties, New York has been the source of a wide range of high-quality mineral specimens for over 150 years. Most of these localities occur in the Grenville Marble and associated calc-silicate rocks, as well as in skarns or skarn-like assemblages, with or without an obvious intrusive igneous source that supplied the heat, pressure and fluids required to make the skarn. Some of the latter have been called "vein-dikes," and their origin is not well understood. Recent research suggests their calcite cores have both a mantle-derived carbonatitic component as well as a crustal derived marble component (Sinaei-Esfahani, 2013). This trip will visit sites hosting both types, and includes four stops:

Stop 1 – Bradley Farr property, Natural Bridge, Lewis Co.
Stop 2 – Gouverneur Minerals' open pit wollastonite mine, Lake Bonaparte, Lewis Co.
Stop 3 – Rose Road Skarn (Purple Diopside Mound) adjacent to Rose Road skarn
Stop 4 – Rose Road Skarn (Mulvaney property) near Pitcairn, St. Lawrence Co.

Stops 1, 3 and 4 are best known to mineral collectors for having produced high-quality specimens of titanite, diopside, scapolite, zircon, albite, microcline, and other minerals. Wollastonite is present at three of the four sites, and is commercially mined at Stop 2. At stops 1 and 4 wollastonite occurs as euhedral crystals, some of which have been replaced by quartz, calcite and pyroxene, resulting in sharp pseudomorphs. Descriptions of these sites, their collecting histories, and major minerals of interest are summarized below and treated in greater detailed by Chamberlain et al. (1987, 1999, and 2013).

ROAD LOG AND STOP DESCRIPTIONS FOR TRIP A-6

Meet at 9:30 a.m. opposite the small church at the intersection of Route 3 and Richter Drive at the east end of the village of Natural Bridge. Allow at least an hour and 15 minutes to drive from Alexandria Bay to our rendezvous point.

NOTE 1. Stop 2 is at a working open pit mine and will require participants to sign a liability release waiver. Participants will also be required to provide their own hardhats, safety goggles and boots in order to gain access to the property.

NOTE 2. All stops are on private property and permission to visit them should be obtained in advance.

NOTE 3. Field Trip A-6 will end around 2:30 p.m., near the village of Pitcairn.

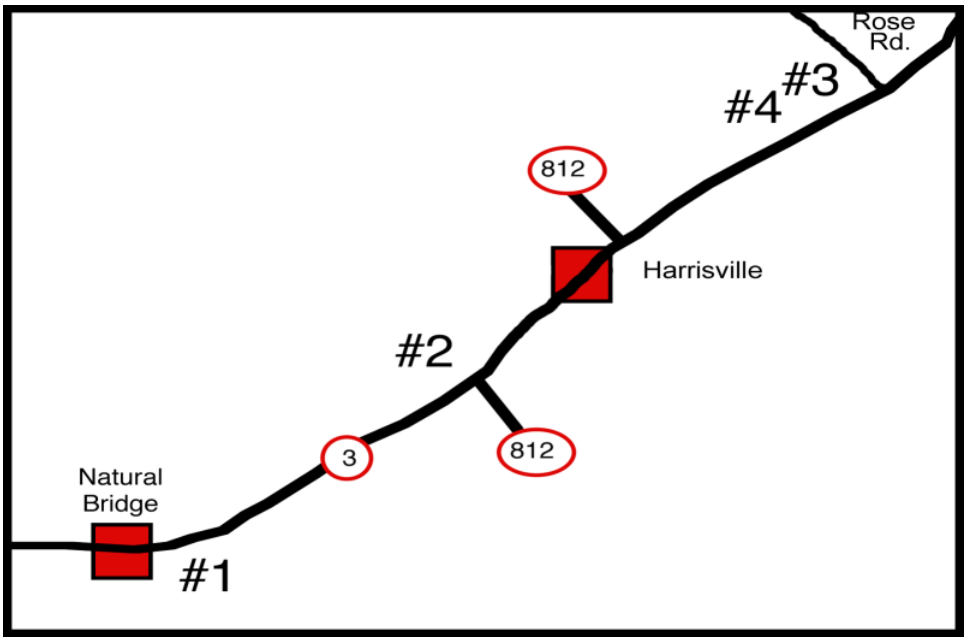

Figure 1. Field trip stop locations. See road log below for detailed directions.

Cumulative Mileage

0.0 From the church at Route 3 and Richter Dr. in Natural Bridge, take Route 3 east toward Harrisville for 1.1 miles. Just past the old K.O.A. Campground on the left (north) side of highway, you will come to a narrow, gated, gravel road on the right side of the highway. Park here. Walk south along the gravel road approximately 100 feet and enter the wooded area on the right (west). Walk approximately 75 -100 feet into the woods to the several old, hand-dug trenches that comprise the site.

1.1 **Stop 1**. Classic Dana mineral locality for wollastonite, titanite, scapolite, diopside, etc.

7.1 Continue east on Route 3 for 6.0 miles to Hermitage Road; turn left (north) onto Hermitage Road and proceed downhill ~ 0.1 mile to the mine entrance on your left.

7.2 **Stop 2**. Gouverneur Minerals No. 4 (Valentine) wollastonite mine.

17.7 Return to Route 3 and continue east 10.4 miles to Rose Road. Turn left (north) onto Rose Road.

17.9 At approximately 0.2 miles on Rose Road, you will come to a gravel road on your left. Take this road to the second house on the right, the LaPlatney residence, where permission to visit the site(s) should be obtained. (note: a small collecting fee is normally charged). Continue on the gravel road to mile 18.2. Stop 3 is approximately 50 feet into the wooded area to your left.

18.2 **Stop 3:** Purple Diopside Mound

Continue on the gravel road for approximately another 0.1 mile to Stop 4, which should be visible high on the hillside to your left about 100 feet into the woods.

18.3 **Stop 4:** classic Dana locality for wollastonite, diopside, titanite and albite at Pitcairn.

END of TRIP

STOP DESCRIPTIONS

Stop 1: Bradley Farr Property, Natural Bridge, NY

INTRODUCTION

This stop is famous for its well-formed crystals of wollastonite that occur in calcite-filled veins in syenite, associated with crystals of titanite, meionite, microcline, diopside and zircon. Known prior to 1840, it is among the earliest of American mineral localities, and has been referred to as the Cleveland, Ashmore, or Whitestone farm, depending on when reference is made. It is also commonly referred to as simply Natural Bridge, Diana, Lewis County, NY, and is the type locality for the two now discredited species *lederite* (= titanite) and *nuttallite* (= meionite).

GEOLOGY

The two principal rock types present at the locality are Grenville Marble and a gneissic pyroxene syenite of the Diana Complex. Previous investigators all conclude that the observed skarn assemblage formed when the syenite intruded the marble (Smyth and Buddington, 1926; Agar, 1923). However, what first appears to be a simple contact metamorphic skarn, upon closer examination also shows characteristics of calcite vein-dikes (Mills, 2014; Moyd, 1990). There can be little doubt that mineralogically, the observed assemblage is typical of a skarn, but if it formed by the syenite intruding the marble, then one should expect to see additional skarn development at the syenite – marble contacts in the immediate area, rather than being confined solely to the "veins." The syenite in contact with the skarn assemblage developed on the walls of the veins shows a marked cataclastic texture that would have provided a preferential pathway for the mineralizing fluids to enter and form the minerals observed. Similar skarn-like deposits occur throughout the CMB of the Grenville in Canada, and have recently been interpreted as having formed from a mixed crustal and mantle-derived fluid based on carbon and oxygen isotope studies (Sinaei-Esfahani, 2013). Preliminary carbon – oxygen isotope analyses of the calcite from the Natural Bridge locality yield similar results ($\delta^{13}C_{pdb}$ = -1.1 ‰, $\delta^{18}O_{smow}$ = +16‰), but additional isotopic and trace element analyses, as well as radiometric age determinations of both the skarn and syenite will be required to resolve which (if either) model is correct. Unfortunately, detailed mapping of the area is greatly hampered by copious glacial overburden and vegetation.

MINERALS

The brief descriptions that follow are for the more important species only. For more complete information on these as well as additional minerals present, see Chamberlain et al. (1987).

Diopside occurs as dark green to black prismatic crystals to 10 cm associated with white microcline, titanite, wollastonite and meionite. While sometimes referred to as "augite" microprobe analyses show the dark pyroxene crystals are a diopside – hedenbergite solid solution series with approximately $Di_{75\%}$ - $Hd_{25\%}$.

Meionite forms equant gray-white crystals to 5 cm associated with diopside and microcline. Sometimes the meionite has a distinctive gray-blue surface coating of a K-Al-silicate (probably microcline) that was originally described as the now discredited "species" *nuttallite*.

Microcline is perhaps the most abundant of the well-crystallized minerals in the skarn assemblage, and occurs as blocky, somewhat rounded, white crystals several cm across.

Titanite occurs in sharp, dark brown, wedge-shaped crystals to 7 cm, though most are much smaller. One of the crystal habits of titanite from this locality was originally described as the species *lederite* (Shepard, 1840), but has since been shown to be titanite.

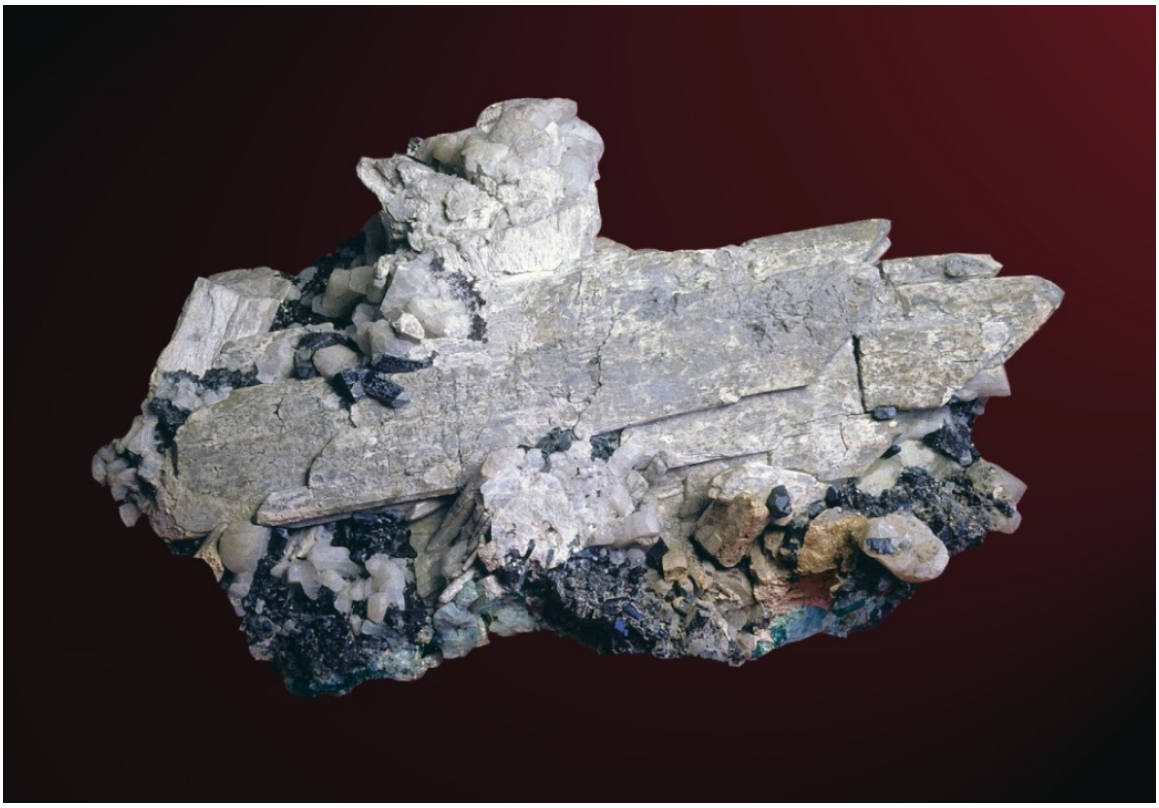

Figure 2. A 30-cm long wollastonite crystal with microcline and diopside from Natural Bridge, NY. Hamilton College collection, New York State Museum. S. Chamberlain photo.

Figure 3. Titanite, 7-cm crystal from Natural Bridge, NY. Harvard University specimen, S. Chamberlain photo.

Wollastonite forms elongated, pinacoidal, cream-white crystals to nearly 30 cm in length, making them among the largest and best examples of the species known.

Zircon forms small, pink, prismatic crystals seldom exceeding 2 cm in length. They are not common.

Retrograde minerals. Several of the species described above show evidence of partial to nearly complete replacement by other minerals, resulting in a variety of pseudomorphs. These are thought to have formed as a result of retrograde metamorphism, and include diopside coated by ferroactinolite, titanite by rutile and amorphous Ti-oxide, and wollastonite by quartz, calcite, diopside and hedenbergite.

Figure 4. Zircon, 3-cm crystal with calcite and meionite from Natural Bridge, NY. New York State Museum specimen and photo.

Stop 2: Gouverneur Minerals No. 4 Wollastonite Mine

INTRODUCTION

Originally known as the Valentine property, this active wollastonite mine commenced operations in 1977, and is today operated by the Gouverneur Minerals Division of Vanderbilt Minerals, LLC, producing commercial grade wollastonite which is used primarily in the ceramics and plastics industries. In addition to the wollastonite, other minerals of interest include abundant blue calcite, graphite, prehnite, quartz, and the rare species orientite and brewsterite-Ba, the latter for which it is the type locality.

GEOLOGY

The main orebody at the mine consists of a wollastonite skarn developed along the contact of Grenville Marble with a metasyenite of the Diana complex. The wollastonite occurs as coarse interlocking creamy white crystals 1- 6 inches long, locally cut by veinlets of fine-grained, fibrous wollastonite and veins or pods of massive, pale yellow prehnite. It is thought that the skarn resulted from silica-rich hyrothermal solutions reacting with the silica-poor marble under relatively low pressure, forming wollastonite ($CaSiO_3$). Subsequent retrograde alteration is responsible for epidote and quartz replacing the metasyenite and wollastonite, the prehnite and secondary wollastonite veins noted above, and calcite veins cutting the metasyenite and marble. Open cavities in some of the prehnite and quartz veins host a variety of crystallized minerals, the more interesting of which are described below. For an in-depth discussion of the geology of this deposit, as well as a more detailed coverage of the 30 some mineral species that have been found here, the reader is referred to Chamberlain et al. (1999), Gerdes (1991), Petersen and Totten (1993) and Gerdes and Valley (1994).

MINERALS FOUND IN THE MARBLE

Calcite. Ton quantities of pale-to-dark blue intergrown cleavages of calcite constitute much of the marble, particularly along the eastern edge of the skarn. The blue color is thought to be due to the development of radiation-induced lattice defects in sheared calcite.

Graphite is found throughout the marble units, where it occurs in a variety of habits varying from small euhedral hexagonal plates to unusual spherical aggregates several millimeters across. The hexagonal crystal plates occasionally show remarkable spiral growth features on their {0001} pinacoids.

Wollastonite is uncommon as a "secondary" mineral, yet it has been found here clearly as a late-stage species in dense, fine-grained fibrous veinlets in the earlier-formed wollastonite and marble skarn. This material may resemble a fine-grained quartzite in hand specimens, and fluoresces a powder blue color with an intense, and long-lived phosphorescence (afterglow) in longwave UV light.

Figure 5. Blue calcite from the Grenville Marble, Gouverneur Minerals No. 4 mine, 6 cm, G. Robinson photo.

Figure 6. Typical wollastonite ore. Gouverneur Minerals No. 4 mine, 10 x 12 cm, G. Robinson photo

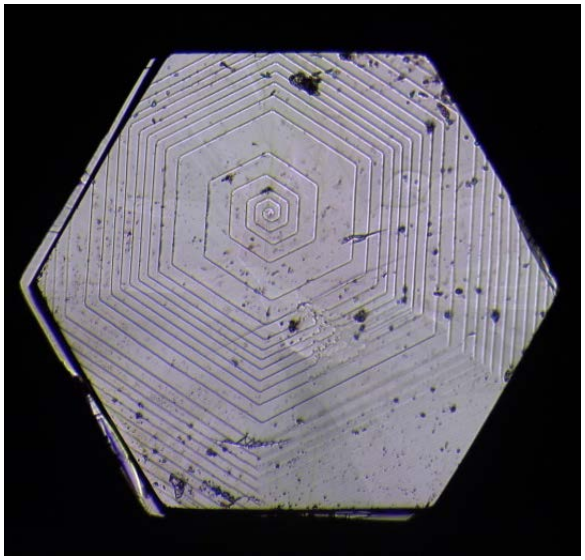

Figure 7. A 1-mm crystal of graphite showing well-developed spiral growth features. John Jaszczak specimen and photo.

Figure 8. A 4-mm rosette of graphite in calcite. A. E. Seaman Mineral Museum specimen, John Jaszczak photo .

MINERALS FOUND IN CAVITIES IN MASSIVE PREHNITE

Apophyllite group minerals occur as chalky white tapered pyramidal crystals generally less than 2 mm in length. Electron microprobe scans show they are compositionally zoned with respect to fluorine, and both fluorapophyllite and hydroxyapophylite may be present within a single small crystal. Rarely fluorapophyllite cleavages up to 2 cm across have been found.

Brewsterite-Ba is a rare member of the zeolite group that was first noted here in the late 1980s, but not formally described until 1993 (Robinson and Grice, 1993). At the same time the mineral was also found and described from Italy (Cabella, et al. 1993). Both occurrences have been referred to as "type localities." At the No. 4 mine it occurs sparingly in some cavities in the massive prehnite as aggregates of colorless, tabular crystals 1-3 mm across. It is easily found using a shortwave UV lamp, since it fluoresces yellow-green.

Datolite is an uncommon mineral in some of the prehnite veins, but has been found in glassy, yellow-green crystals to 1 cm.

Hedenbergite is relatively common in some of the prehnite veins, where it forms elongated dark green prismatic crystals1-2 mm long. Diopside is also present, but tends to be much paler in color.

Microcline is a common accessory mineral in the prehnite cavities. It's most common habit is small, white, adularia-habit crystals, often with serrated edges.

Orientite is a rare species, and is included here solely because of that fact. It is known from only six other localities, worldwide. At the No. 4 quarry it forms brush-like aggregates of acicular brown crystals to 1 mm as well as smaller, granular, rounded red-brown coating prehnite and babingtonite. To date, only two specimens are known (see Chamberlain et al., (1999) for a more complete description).

Pectolite occurs as micro tufts of white acicular crystals, which are practically indistinguishable from the more common wollastonite without X-ray or chemical data.

Prehnite crystals 1-5 mm across occur as pseudo-octahedral, dipyramidal, pale yellow-green crystals lining cavities in the massive prehnite.

Figure 9 (above). A 0.2-mm crystal of Brewsterite-Ba. New York State Museum specimen, S. Chamberlain photo.

Figure 10 (below). A 6-cm group of hematite-stained quartz crystals. S. Chamberlain collection and photo.

Figure 11. A 9-cm group of hematite-stained quartz crystals. S. Chamberlain collection and photo.

MINERALS OF THE NORTHWEST ALTERATION ZONE

Albite. In June, 1995, a large brecciated quartz vein was encountered while building a ramp along the northwest boundary of the skarn. While quartz was the predominant mineral present (q.v.), there were others worthy of mention, among them albite, which occurred as twinned, white, crystals to 1 cm associated with acicular microcline and reddish brown, botryoidal andradite on quartz.

Andradite occurs as coatings of red-brown microcrystals on quartz.

Calcite occurs as gray scalenohedral crystals up to 2 inches long, frequently with red and black inclusions of hematite and goethite, making interesting and attractive specimens.

Epidote crystals form aggregates up to a foot across in some of the larger pockets encountered.

Quartz is the mineral of primary interest in the northwest alteration zone, where it forms colorless to milky prismatic crystals several inches in length, and crystal groups several times that size. Some of the crystals have a dusting of hematite, giving them a pinkish hue, while others have a wide variety of hematite and goethite inclusions, resulting in an equally wide variety of appearance. Amethyst is also present, but less common.

Stop 3: Rose Road - Purple Diopside Mound near Pitcairn, NY.

INTRODUCTION

Although the mineralization at this stop was only recently discovered, an interesting variety of specimens has been recovered in the past two years. Despite being a few hundred yards from the classic wollastonite skarn, the purple diopside mound has a very distinctive suite of minerals of different age and origin from the skarn. Large quantities of well-crystallized scapolite, fine-grained masses and crystals of purple diopside, black titanite, and transparent phlogopite are noteworthy. The discovery of lesser amounts of pink corundum and pink spinel, secondary natrolite and prehnite, and still unidentified “gieseckite” pseudomorphs, have all added interest.

GEOLOGY

Excavations have revealed an occurrence of calcite-filled “vein dikes” typical of regional metamorphism in the Grenville Central Metasedimentary Belt. The zircon age of the vein-dike mineralization is 1170 Ma (Chamberlain et al., 2014), making it slightly older than the nearby wollastonite skarn. The principal veins are lined with scapolite crystals facing into a coarse calcite center. At places black titanite is an accessory mineral. Locally significant masses of acicular natrolite crystals coat the scapolite. Other parts of the mound have silicate-marble contacts with purple diopside crystals and “gieseckite” crystals developed at the contact. Phlogopite crystals are developed in the marble near the silicate-marble contacts. Spinel occurs as a rare accessory with the phlogopite in marble. Pink corundum occurs as anhedral masses in scapolite several centimeters away from the scapolite crystals developed facing into the vein. The association of corundum with fluorescent scapolite is noteworthy and appears paragenetically similar to the recently discovered gem sapphire occurrences in the Kimmirut area, Baffin Island, Nunavut, Canada (Cade et al., 2005; Lepage and Rohtert, 2006).

MINERALS

Since no detailed description of the minerals identified from this occurrence has yet been published, a summary of the complete list follows.

Albite occurs as white euhedral crystals to 1 cm and as white masses in purple diopside.

Corundum occurs as bright purplish-pink, anhedral masses to 25 mm in meionite on the margins of the scapolite vein dike.

Diopside occurs as grayish purple prismatic crystals to several cm and as fine-grained masses. The composition includes about 1 wt % FeO and 1 wt % TiO_2, which may account for its unusual color. The dark green diopside crystals, the yellow acicular diopside formed as an alteration of wollastonite, and the dark blue-green actinolite overgrowths at the adjacent wollastonite skarn all contain significantly more iron and no detectable titanium (by SEM/EDS).

Fluorapatite forms bright blue-green transparent prisms to 8 cm in the marble.

"***Gieseckite***" occurs as sharp euhedral pseudomorphs to several cm associated with graphite rosettes. These pseudomorphs have a complex internal replacement texture and variable composition. Some have zones of fine-grained plagioclase (labradorite). The original mineral has not been found nor inferred.

Graphite occurs as sharply developed crystals and rosettes to several mm, most often associated with "gieseckite".

Natrolite is present as radial aggregates of coarse, white, crystals to 5 cm and also as masses of acicular crystals in localized portions of the scapolite vein. This is a sodium zeolite with little detectable calcium that appears to have formed from the breakdown of scapolite, similar to other zeolite minerals found in similar "skarn" assemblages in the Grenville CMB (VanVelthuizen, et al., 2006).

Phlogopite occurs as honey-brown, transparent crystals to 1 cm and as masses of 20 cm or more in marble. Rarely, pseudomorphs of phlogopite after scapolite occur in the scapolite vein.

Prehnite occurs sparingly as brown botryoidal masses to 4 cm on a matrix of calcite, graphite, and pyrite. Like natrolite, it probably formed from the breakdown of scapolite.

Pyrite occurs as modified cubes to 5 mm, and as minute crystals often altered to goethite in "gieseckite", prehnite and scapolite. It also forms oriented arrays of acicular crystals embedded in meionite.

Scapolite occurs as sharp crystals to 20 cm on the walls of the scapolite vein. These crystals have intermediate compositions close to the middle of the meionite (calcium-rich)-marialite (sodium-rich) isomorphous series. Generally glassy gray scapolite is slightly enriched in calcium and is meionite. Sometimes a rind of white, translucent scapolite coats the crystals and is slightly enriched in sodium (marialite). Most of the volume of scapolite is meionite.

Spinel occurs as pink octahedral crystals to 1 mm in marble associated with phlogopite.

Titanite occurs as tabular, almost black crystals to 5 cm associated with scapolite and also as minute crystals of complex morphology embedded in albite.

Zircon occurs as minute euhedral crystals embedded in meionite.

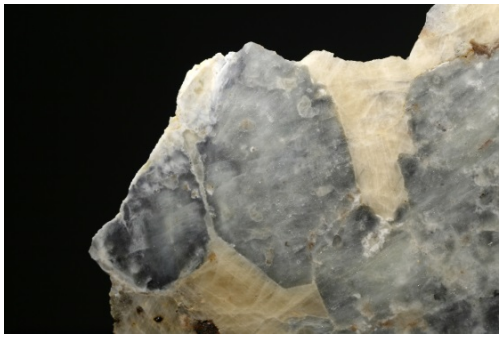

Figure 12a. A 5 cm gray meionite crystal in calcite, in ordinary white light. G. Robinson photo.

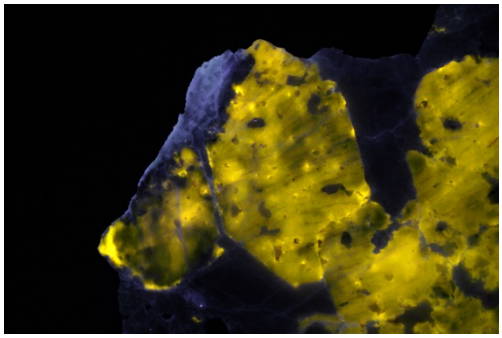

Figure 12b. Same specimen at left illuminated by LW ultraviolet light. G. Robinson photo.

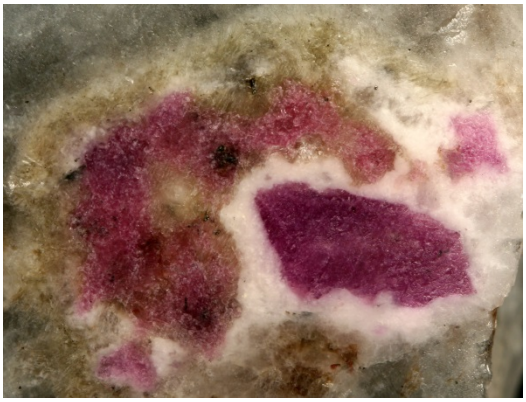

Figure 13. Pink corundum from the purple diopside mound; 3 cm field of view. St. Lawrence Univ. specimen, G. Robinson photo.

Figure 14. Purple diopside with calcite, 5 x 5 cm. S. Chamberlain collection and photo.

Figure 15. A 2.5 cm "gieseckite" crystal from the purple diopside mound. M. Walter specimen and photo.

Figure 16. A 16.5 cm group of scapolite crystals from the purple diopside mound. M, Walter specimen and photo.

Stop 4: Rose Road - Wollastonite Skarn near Pitcairn, NY.

INTRODUCTION

This classic locality (also known as the Mulvaney sugar bush) has been a source for well-formed crystals of wollastonite, titanite, diopside and albite for about 125 years. Williams (1885), Luquer (1893), and Ries (1893-94, 1895) all published reports on various aspects of the mineralogy of this site. All of the various species reported from this site (Chamberlain and Robinson, 2013) are still collectible today

GEOLOGY

The locality is a wollastonite skarn formed by the emplacement of the Diana Complex (estimated at ~ 1164 +/- 11 Ma (Hamilton et al. 2001)). It is a secondary skarn in the sense that it was apparently formed by solutions from the Diana Complex invading fractures along a contact between the Grenville Marble and a metamorphic albite-diopside rock. The age relationships between the skarn formation and the regional metamorphism of the Adirondack Lowlands are somewhat confusing, given the zircon age we report for the nearby vein dikes at Stop 3. Significant alteration of the wollastonite and minor uralitization of the diopside have occurred subsequent to the original mineralization.

Minerals

A summary description of the minerals is provided below. For more details see Walter et al. (2009) and Chamberlain and Robinson (2013).

Actinolite occurs relatively rarely as a blue-green coating on diopside crystals. It contains 7.5 wt % FeO which is significantly more iron than is found in the diopside.

Albite occurs as equant or elongated white blocky crystals to 8 cm. Both Carlsbad and Manebach twins have been found (Chamberlain, 1985; Walter, 2009; Chamberlain and Robinson, 2013). The perthitic texture is due to minor exsolution lamellae of microcline making this an antiperthite.

Diopside is perhaps the best known species from this locality, and forms lustrous dark green prismatic crystals to 20 cm. It contains about 2.5 wt % FeO. Diopside also occurs as a granular replacement of wollastonite.

Fluorapatite occurs as prismatic crystals to 8 cm in colors ranging from dark blue to bright blue to blue-green.

Goethite usually replaces pyrite, forms brown stains on the adjacent albite and occasionally forms small clusters of microscopic needles.

Graphite rarely forms small tabular crystals to 2 mm. It is more common as gray inclusions in albite.

Pyrite occurs as microscopic crystals on albite. Most have completely altered to goethite.

Quartz occurs as granular masses and white to colorless rounded crystals to 1 cm replacing wollastonite.

Titanite occurs as tabular, clove-brown crystals to 12 cm. Some of the finest titanite crystals found in New York have come from this skarn. Most of the larger crystals have somewhat rounded faces and prominent parting.

Wollastonite occurs as white well-developed, euhedral crystals to 35 cm. These are almost always altered, at least on the surface. Pale brown alteration consists of acicular yellow diopside crystals containing 5 wt % FeO intermixed with calcite formed from the breakdown of wollastonite. Greenish, granular alteration is mostly diopside. White granular alteration is quartz. Green and white patchy altered wollastonite crystals are typical (Chamberlain et al. 2009).

Figure 17. A 4.5-cm titanite crystal in calcite-wollastonite from the Rose Road wollastonite skarn. S. Chamberlain specimen and photo.

Figure 18: A 7-cm specimen of wollastonite from the Rose Road wollastonite skarn. S. Chamberlain specimen and photo.

Figure 19. An 8-cm specimen of fluorapatite in calcite from the Rose Road wollastonite skarn. S. Chamberlain specimen and photo.

Figure 20. A 7-cm specimen of diopside and titanite on albite from the Rose Road wollastonite skarn. S. Chamberlain specimen and photo.

REFERENCES CITED

Agar, W. M. (1923) Contact metamorphism in the western Adirondacks. *Proceedings of the American Philosophical Society*, Vol. 62, 95-174.

Cabella, R., G. Lucchetti, A. Palenzona,S. Quartieri, and B. Vezzalini (1993) First occurrence of a Ba-dominant brewsterite, *European Journal of Mineralogy*, Vol. 5, 353-360.

Cade, A. M., G. M. Dipple and L. A. Groat (2005) Geochemical study of the Kimmirut sapphire occurrence, Baffin Island, Canada. *Goldschmidt Conference Abstracts, Geochemistry of Gem Deposits*.

Chamberlain, S. C. (1985) New occurrences of twinned crystals in St. Lawrence and Lewis Counties, New York. *Rocks and Minerals*, Vol. 60, 285-286.

Chamberlain, S. C., G. W. Robinson and C. A. Smith (1987) The occurrence of wollastonite and titanite, Natural Bridge, Lewis County, New York. *Rocks and Minerals*, Vol. 62, No. 2, 78-89.

Chamberlain, S. C., V. T. King, D. Cooke, G. W. Robinson and W. Holt (1999) Minerals of the Gouverneur Talc Company No. 4 quarry (Valentine deposit) Town of Diana, Lewis County, New York. *Rocks and Minerals*, Vol. 74, No. 4, 237-249.

Chamberlain, S., M. R. Walter, R. Rowe and D. Bailey (2009) Investigations of wollastonite from the Rose Road wollastonite deposit, Pitcairn, St. Lawrence County, New York. *Rocks and Minerals*, Vol. 84, 167-168.

Chamberlain, S. C. and G. W. Robinson (2013) *The collector's guide to the minerals of New York State*. Schiffer Publishing, Ltd., Atglen, PA, 96p.

Chamberlain, S., M. R. Walter, D. G. Bailey, J. Chiarenzelli and G. Robinson (2014) A new collecting site at the Rose Road locality, Pitcairn, St. Lawrence Co., New York. *Proceedings of the 41st RochesterAcademy of Science Mineralogical Symposium*, Rochester, New York, April, 2014, p.11.

Gerdes, M. L. (1991) A petrographic and stable isotopic study of fluid flow and mass transport at the Valentine wollastonite mine, northwest Adirondack mountains, New York. Unpublished thesis, University of Wisconsin.

Gerdes, M. L. and J. W. Valley (1994) Fluid flow and mass transport at the Valentine wollastonite deposit, Adirondack mountains, New York State. *Journal of Metamorphic geology*, Vol. 12, 589-608.

Hamilton, M.A., J. McLelland, and B. Selleck (2004) SHRIMP U-Pb geochronology of the anorthosite-mangerite-charnockite-granite (AMCG) suite, Adirondack Mountains, New York: Ages of emplacement and metamorphism, *in* Tollo, R.P., et al., eds., Proterozoic tectonic evolution of the Grenville orogen in North America: *Geological Society of America Memoir 197*, 337–356.

Lepage, L. and Rohtert, W. (2006) Ultraviolet mineral prospecting for sapphire on Baffin Island, Nunavut, Canada. *Gems and Gemology*, Vol. 42, No. 3, 155.

Luquer, L. MCI (1893) Mineralogical Notes: Microcline from Pitcairn, N. Y. *School of Mines Quarterly*, Vol. 14, 328-329.

Mills, J. (2014) Metamorphic Geology in Bancroft, Canada, http://www.depauw.edu/academics/departments-programs/geosciences/research/jim-mills-research/

Moyd, L. (1990) Davis Hill near Bancroft, Ontario: an occurrence of large nepheline, biotite, and albite - antiperthite crystals in calcite-cored vein-dikes. *Mineralogical Record*, Vol. 21, No. 3, 235-248.

Petersen, E. U. and R. Totten (1993) Wollastonite ores at the valentine mine, NY. In *Selected mineral deposits of Vermont and the Adirondack Mountains, New York: Part 1. Mineral Deposits of the Adirondack Mountains.* Ed. by E. U. Petersen, *Society of Economic geologists, Guidebook Series 17,* 65 -73.

Ries, H. (1893-1894) On some new forms of wollastonite from New York State. *Transactions of the Academy of Science of New York*. Vol. 13, 146-147.

Ries, H. (1893-1894) Additional note of wollastonite from New York State. *Transactions of the Academy of Science of New York*. Vol. 13, 207-208.

Ries, H. (1896) Monoclinic pyroxenes of New York State. *New York Academy of Science Annals*, Vol. 9, 124.

Robinson, G. W. and J. D. Grice (1993) The barium analog of brewsterite from Harrisville, New York. *Canadian Mineralogist*, Vol. 31, 687-690.

Sinaei-Esfahani, F. (2013) Localized metasomatism of Grenvillian marble leading to melting, Autoroute 5 near Old Chelsea, Quebec. MSc thesis, McGill University, Montreal, 133 p.

Smyth, C. H., Jr. and A. F. Buddington (1926) Geology of the Lake Bonaparte quadrangle. *New York State Museum Bulletin 269*.

Van Velthuizen, J., R. A. Gault, G. W. Robinson and J. Scovil (2006) Zeolite occurrences in the central metasedimentary belt of the Grenville Province, Ontario, Quebec and New York State. *Mineralogical Record*, Vol. 37, 283-296.

Walter, M. R., S. C. Chamberlain, R. Rowe and D. Bailey (2009) The minerals of the Rose Road wollastonite deposit, Pitcairn, St. Lawrence County, New York. *Rocks and Minerals*, Vol. 84, 454-455.

Williams, G. H. (1885) Cause of the apparently perfect cleavage in American sphene (titanite). *American Journal of Science, Series 3*, Vol.29, 486-490.

BLACK RIVER AND TRENTON GROUPS, NORTHWESTERN NEW YORK STATE

BRUCE W. SELLECK
Department of Geology, Colgate University, Hamilton, NY 13346

INTRODUCTION

Black River and Trenton Group strata in eastern North America record the last phases of deposition on the "Great American Bank" (Sloss, 1963), the long-lived Cambrian through late Ordovician cratonic-passive margin carbonate depositional system. Carbonate deposition ended with tectonically-driven foreland basin deepening, coupled with the influx of terrigenous clastics from Taconic Orogenic source lands to the current east of the continental interior. The change from carbonates to clastics was diachronous across the basin in the New York State region, with Utica Formation muds derived from the orogenic hinterlands progressively flooding the platform from east to west. This facies transition, and the structural framework of basin development linked to collisional mountain-building, were critical to the plate tectonic model elucidated by Bird and Dewey (1970), which was among the very first studies to document the link between plate collision and basin development on ancient continental margins.

The Black River and Trenton Groups have also been central in the historical development of our understanding of the relationships of stratigraphic patterns such as lateral facies changes, stratal continuity and chronostratigraphic correlation, and abrupt vertical contacts, to basin dynamics, including tectonic, eustatic and climate forcing factors. Following the early descriptive work of Vanuxem (1838, 1842) and Hall (1847), subsequent paleontological (Young 1943a, b) and stratigraphic analyses (Kay, 1939, 1960; Fisher, 1962, 1977, for example) documented large-scale facies relationships, biostratigraphic correlations, and established a workable stratigraphic nomenclature. Sedimentological analyses and actualistic facies models were also developed, including, for example, the work of Winder (1960), Textoris (1968), and Walker (1973). Integrated paleoecological-stratigraphic studies (Cameron and Mangion, 1977; Titus and Cameron, 1976; Brookfield, 1988; Brookfield and Brett, 1988), and continued refinement of graptolite and bentonite-based regional correlations (e.g. Mitchell, et al, 1994, 2004) provided important new understandings of the Black River-Trenton-Utica system. Within the last 20 years, revision of the global time scale has resulted in assignment of the Black River-Trenton-Utica sequence to the Upper Ordovician, whereas in older literature, these rocks were considered Middle Ordovician. This sequence is placed within the Caradoc Stage, with deposition spanning the interval 457- 449 million years ago.

In the last two decades, the framework established formed the basis of studies that further documented regional temporal and spatial depositional patterns, and placed these within a modern depositional systems framework. In a series of excellent papers published by Carleton Brett and Gordon Baird, and co-workers (e.g. Baird, et al, 1992; Brett and Baird, 2002, Baird and Brett, 2002; Brett et al, 2004), a modern depositional systems model for the Black River-Trenton-Utica system was developed. Additionally, the fine work of Cornell (2001, 2008, Cornell, et al 2005) deserves special mention, as much of the information in this guidebook article is derived from those studies.

The Black River-Trenton-Utica interval has also received attention as an economic resource system. Important natural gas reservoirs hosted by Black River/Trenton carbonates – so-called hydrothermal dolomite (HTD) reservoirs – were developed in the southern Finger Lakes region of New York State. The origin of these high-permeability systems is linked to burial diagenetic processes, with saline, higher-temperature fluids derived from underlying rocks, associated with basement faulting (Smith, 2006). Some of these reservoirs host exceptionally productive wells; however, there have been few new discoveries in the New York HTD play in the last decade. Application of horizontal well and hydraulic fracturing technology has promoted development of gas and gas-condensate extraction in the Trenton-Utica interval in western Pennsylvania, Ohio, and West Virginia. The Point Pleasant Formation, for example, is age-equivalent to the upper Trenton Group in New York, and has seen significant recent hydrocarbon production in Ohio (Wickstrom, et al, 2012). Organic carbon content and thermal maturation play key roles in determining the production potential for these unconventional resource intervals.

This field guide focuses on the Black River Group and basal Trenton Group exposed in northwestern New York State, in the area south of the St. Lawrence River, and east of Lake Ontario, extending south to the Black River Valley. This guide provides only a brief overview of these units. Interested readers are referred to the bibliography, and the extensive resources available online at http://www.mcz.harvard.edu/Departments/InvertPaleo/Trenton/Intro/trentonintro.htm

GEOLOGIC OVERVIEW

The Black River and Trenton Groups are exposed, in the area of this field trip, in a broad outcrop belt north of the Tug Hill Plateau region, extending to the Lake Ontario Plain and southwestern St. Lawrence Valley. In that area, basal Black River strata rest disconformably on the Lower Ordovician Theresa Formation. To the south-southeast, in the Black River Valley, the outcrop belt narrows, and the Black River Group directly overlies Proterozoic rocks of the Adirondack Massif. Locally, outcrops are found in watercourses and lake shorelines, and in portions of the area where glacial cover is limited. Outcrops tend to form linear terraces that interrupt topography, and road cuts through these terraces provide fresh exposures.

The Upper Ordovician units in the region are generally flat-lying, although localized folding and faulting is present. These structures may be linked to basement faults which were active during and after foreland basin development related to Taconic orogenesis, a pattern which has been well-documented in the Mohawk Valley (Jacobi, et al, 2000; Jacobi and Mitchell, 2002). Importantly, some of these faults are mineralized, and localized dolomitization and vein development associated with faults and minor folds are likely related to fluid movement, perhaps analogous, on a small scale, to the hydrothermal dolomitization seen in the subsurface in southern New York State. Regional joint patterns in the Trenton-Utica interval responded to stress patterns during later stages of the Taconic Orogeny, with later overprinting by Acadian (Devonian) and Alleghanian (Carboniferous-Permian) (Garrand, et al, 2011). Locally, joint patterns reflect stress systems related to basement faults.

PALEOGEOGRAPHIC AND TECTONIC SETTING

The Late Ordovician Black River and Trenton Group carbonate system, and adjacent Utica Formation basin formed a platform-to-foredeep setting on the southern margin of Laurentia during the collision of island arc system(s) that characterized the Taconic Orogeny (Figure 1). At this time, the margin faced south, with New York State at approximately 30^{o} south latitude. The interior of the craton to the north of this area was of generally of very low relief; however there were likely areas where Proterozoic basement and overlying Cambrian-Middle Ordovician sedimentary rocks were exposed in uplifted horsts, and broad upwarps, to the current west and northwest, were also present. During lowstands, terrigenous clastic debris would have been supplied to the platform from these land areas, perhaps by aeolian processes.

A likely modern analogue for this Late Ordovician setting is the north Australia lithospheric plate collision with the Timor Arc (Cornell, 2008). In this scenario, the broad carbonate and mixed-siliciclastic platform offshore of northern Australia represents the ‘Great American Bank’ of the Laurentian continent. Timor is the analogue of the arc system that was actively colliding with the Laurentian margin during the Late Ordovician. The foredeep of the Timor Trough is the analogue to the Utica mud basin that progressively deepened east to west as the collisional margin migrated westward, depressing the continental crust. This basin development (the ‘seafloor inversion’ of Bird and Dewey, 1970) continued as older passive margin sediment and accretionary prism material was overthrust onto the margin, further loading the crust, and providing uplifted source regions for terrigenous clastic sediments. These terrigenous muds and sands eventually prograded across the foreland basin, ending carbonate-dominated deposition, and progressively infilling the basin by the end of Ordovician time.

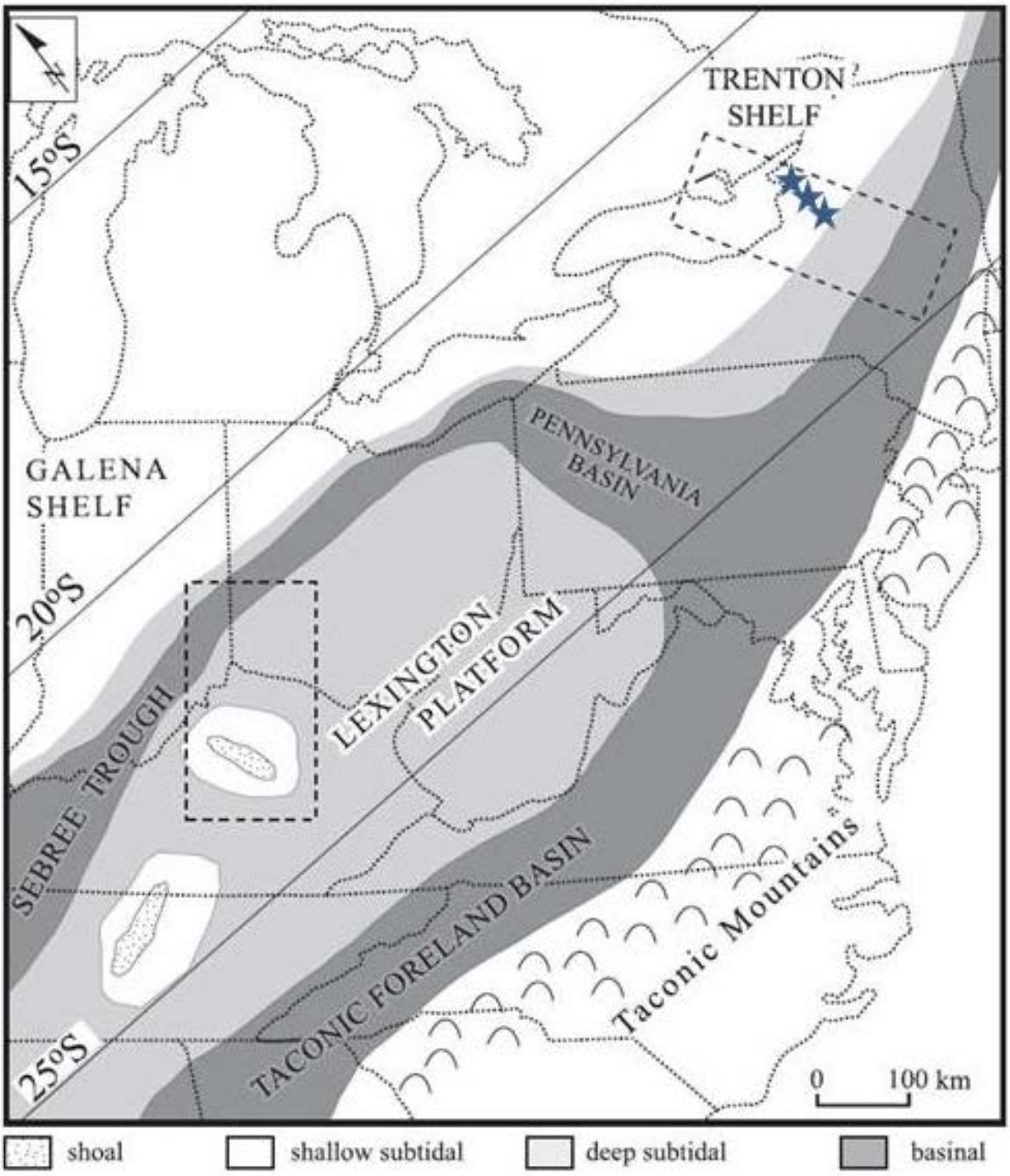

Figure 1. Schematic regional map showing location of the Trenton carbonate shelf relative to the Taconic Foreland Basin. Stars indicate approximate location of sites seen on this field trip. (from Brett, et al, 2004).

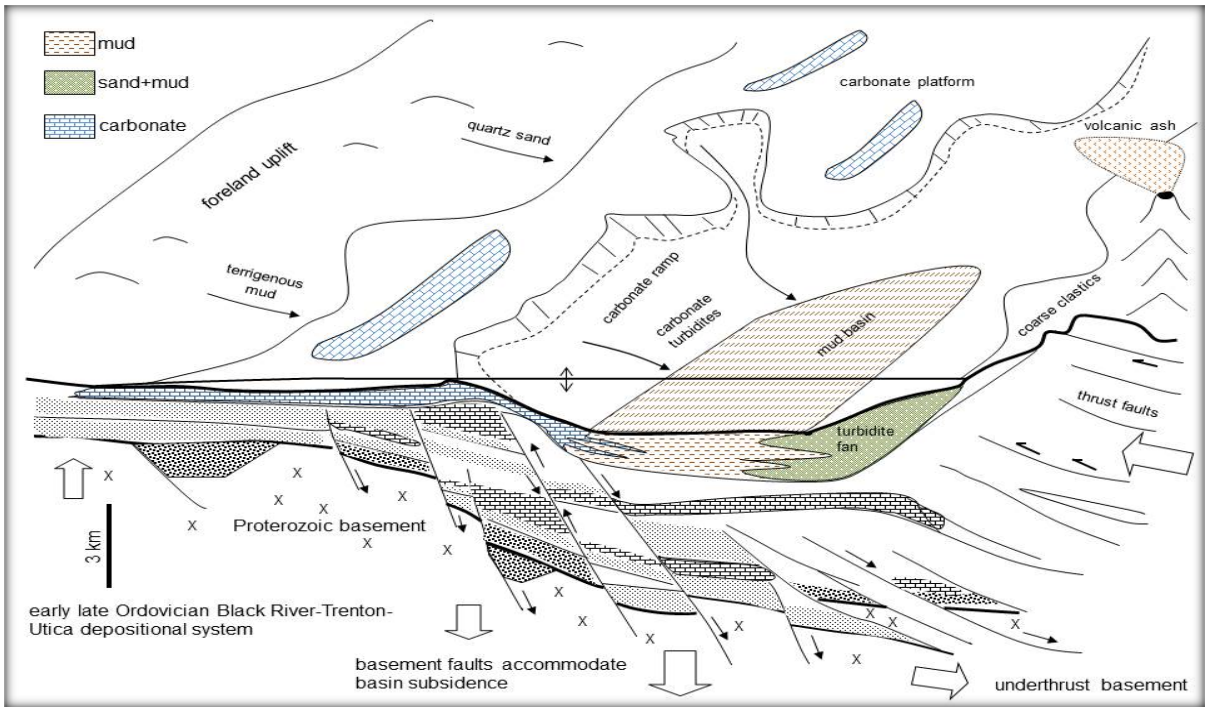

Figure 2. Schematic diagram illustrating facies relationships, collisional tectonics and basin development during the Late Ordovician of eastern Laurentia. Note that minor sea level changes would have significant impact on location of facies belts on the carbonate platform. Overall, basin deepening, and transition from carbonate to terrigenous clastic deposition progressively from east to west (current geography) across the basin. Note that basin subsidence was accommodated by basement faulting, as well as crustal flexure. These normal faults were active during deposition.

BLACK RIVER GROUP STRATIGRAPHY

Pamelia Formation: The Black River Group in the area of this field trip is traditionally divided into three formations. The basal Pamelia Formation, which reaches about 45 meters in thickness in northwestern New York, includes terrigenous sandy and muddy carbonates with purer grey lime mudstones and dolostones. The Pamelia Formation thins to the south in the Black River Valley, and is absent south of Boonville, NY, where basal Lowville Formation beds rest directly on Proterozoic basement.

Lowville Formation: The uppermost Pamelia Formation is overlain by the lower unnamed member of the Lowville Formation. The contact is marked by a widespread unit, the Pittsburgh Quarry Bed, which documents a lowstand event characterized by increased terrigenous clastic input, succeeded by transgressive to highstand facies deposited in intertidal to shallow subtidal settings (Cornell, 2008). The lower Lowville consists of grey lime mudstones and wackestones, plus shaley to massive dolostones and contains a sparse marine fauna, dominated by ostracods and gastropods. The lower member of the Lowville (10-13 meters thick in the area north of the Tug Hill Plateau) is overlain by the House Creek Member, consisting of generally more fossiliferous mudstones, wackestones and packstones. Typical House Creek fossils include the tubular coral *Tetradium*, gastropods, bryozoans, brachiopods, tabulate corals, stromatoporoids and trilobites. Some beds are dominated by in place thickets of colonial *Tetradium* set in fine-grained lime mudstone. The uppermost House Creek Member consists of shaley, dolomitic mudstone with mudcracks and algal structures, termed the Weaver Road Beds (Cornell, 2008) documenting a regressive interval.

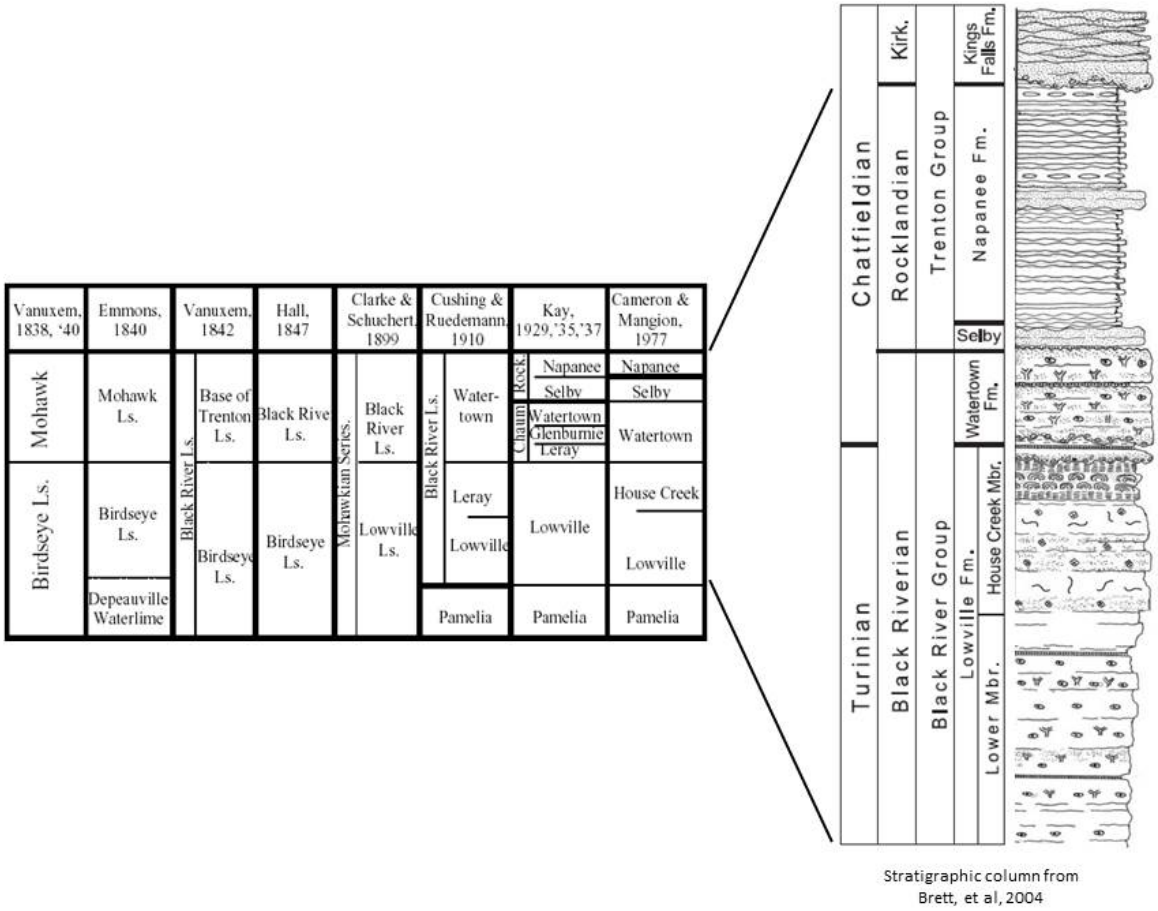

Figure 3. Stratigraphic nomenclature. Table on left from Cornell, et al (2005). Note the various nomenclature used for the upper Lowville-Chaumont-Watertown interval. In this report, Chaumont Formation is used for the uppermost formation in the Black River Group; it is subdivided into the LeRay, Glenburnie and Watertown Members. The LeRay and Glenburnie Members are well developed only in the northern Black River Valley area, and to the north in southern Ontario. The Black River-Trenton Group contact is the base of the Selby Formation, atop the Watertown Member of the Chaumont Formation.

Chaumont Formation: In the northern Black River Valley, the upper contact of the House Creek Member of the Lowville Formation with the basal Chaumont Formation is marked by ~1 meter of bioclastic grainstone containing crinoids and bryozoans (LeRay Member) overlain by ~1 meter of shaley, nodular limestone (Glenburnie Member). The overlying Watertown Member consists of 2-3 meters of thick bedded to massive bioclastic grainstone/packstone with large tabulate corals, rugose corals, crinoids, stromatoporoids and other typical open marine fauna. The LeRay and Glenburnie are progressively truncated to the east and south of the northern Black River Valley (Cornell, 2008). South of Lowville, NY, the massive Watertown is directly underlain by the House Creek Member of the Lowville Formation. The term Watertown Formation is sometimes used to represent the Chaumont Formation interval in regions where the LeRay and Glenburnie Members are absent. The Watertown Member also thins to the south and east in the southern Black River Valley, and becomes less fossiliferous, changing to muddy peritidal facies with more Lowville-like aspect (Cornell, et al 2005).

TRENTON GROUP STRATIGRAPHY

Selby Formation: In the northern Black River Valley and adjacent southern Ontario, the upper Watertown Member of the Chaumont Formation is overlain by 1-3 meters of dark, irregularly bedded bioclastic packstone to grainstone known as the Selby Formation. This base of the Selby Formation interval is marked by a prominent bentonite in the Lowville, NY area, where the Selby is thinned to 20-50 centimeters. The Selby Formation appears to represent a period of limited sediment accumulation on a marine subtidal platform. Large gastropods and orthocone cephalopods are sometimes found in the Selby.

Napanee Formation: Overlying the Selby Formation is the Napanee Formation, which consists of thin to medium bedded silt-grade lime mudstones with abundant brachiopods and bryozoans. Thin terrigenous mud interbeds are characteristic of the Napanee Formation, and some beds are relatively organic rich and slightly cherty. The Napanee Formation records a major deepening event, with the establishment of deeper shelf to carbonate ramp depositional environments.

Kings Falls Formation: The Napanee Formation is sharply overlain by relatively coarse, medium to thick bedded bioclastic grainstones of the Kings Falls Formation. The basal Kings Falls beds occupy erosional channels cut into the top of the underlying Napanee, with some truncation of upper Napanee strata. Typical Kings Falls Formation structures include large wave rippled beds, coquinas of well-sorted brachiopod and crinoid debris, and laterally lensing grainstone beds. Thin, very dark shale interbeds separate the coarse bioclastic strata. These coarser, wave-dominated facies fine upward into darker, shaley, more organic rich lime mudstones, to be succeeded by coarser bioclastic intervals. A number of these higher order deepening-shallowing intervals are present in the Kings Falls (Cornell, et al 2005).

Upper Trenton Group: The remaining stratigraphic units in the Trenton Group, (Sugar River, Denley, Rust, Steuben and Hillier Formations) will not be seen on this trip. These units comprise a sequence documenting shallowing and deepening intervals on a subtidal carbonate shelf, coupled with variations in terrigenous clastic input. The Hillier Formation is abruptly overlain by the Indian Castle Member of the Utica Formation in the northern Tug Hill Plateau region. Interested readers are referred to the field guide article by Cornell, et al (2005) for additional information and field localities for the upper Trenton Group units.

BURIAL DIAGENESIS

The burial diagenetic history of the Black River-Trenton-Utica sequence has received considerable study in the last two decades, spurred by the interest in hydrocarbon potential of the sequence. Localized hydrothermal dolomitization, related spatially to basement faults and fluid flow, is recognized as the origin of important Trenton-Black River gas reservoirs in the subsurface of southern New York State (Smith, 2006). While early (pre-stylolite) dolomitization of carbonate appears to have been a common process in the Pamelia and Lowville Formations, as we will discuss at Stop 1 today, this process did not lead to significant porosity enhancement. In the Chaumont Formation, and generally in the overlying Trenton Group facies, minor amounts of dolomite are present, and widespread, but rarely form discrete beds. Coarsely ferroan crystalline dolomite is associated with vertical fractures that appear to post-date stylolites, and, as seen at Stop 2, coarse dolomite is often localized in areas of inferred faulting and folding. Horizontal veins of calcite and dolomite, as seen at Stop 5, document fluid-related mineralization developed during layer-parallel thrusting, or during episodes of elevated fluid pressure related to hydrocarbon maturation.

Chert is common in the Watertown Member of the Chaumont Formation, as seen at Stop 3. Chert nodules often contain poorly-preserved sponge spicules, suggesting that biogenic opaline silica from sponges may have served as a source of dissolved silica. Sparse to common certification of carbonate bioclasts is present in most Trenton lithologies, with more abundant chert associated with deeper-water facies. Petrographic studies show that echinoderm bioclasts are most likely to show chert replacement. Chert replacement involved initial precipitation of watery opal-CT, followed by recrystallization to quartz. This recrystallization causes a reduction of solid volume (related to dewatering of opal-CT), and often the chert is finely fractured as a result. In the Trenton Group, hydrocarbon staining often follows the microfractures in chert, suggesting that fluid hydrocarbons were generated during the chert recrystallization.

In the area of this field trip, thermal maturity indicators (vitrinite reflectance, conodont alteration index) and fluid inclusion studies of horizontal veins suggest that the Trenton Group strata reached burial temperatures in excess of 145°C. These rocks are thus overmature in terms of petroleum hydrocarbons, but would like be gas-bearing in the subsurface. Trenton Group strata served as gas reservoirs for small fields in the central and southern Tug Hill region.

ROAD LOG AND STOP DESCRIPTIONS FOR TRIP B-1
(UTM locations in NAD 83, Zone 18T)

Cumulative miles	Miles from last point	Depart from Bonnie Castle Resort Parking Area; follow Holland Street to Church Street, turn left (S) onto Church Street)
0.8	0.8	Intersection with NYS Route 12. Turn right (SW). Continue SW on Route 12 to Clayton, NY, crossing I81
13.1	11.3	Intersection of Rt. 12 and James Street. Turn left (S) on Rt. 12. Continue S on Route 12.
20.1	7.0	Depauville, NY. Roadcuts on Route 12 expose upper Pamelia Formation and lower Lowville Formation. Parking here is difficult and somewhat dangerous. Continue S on Route 12.
26.6	6.5	Stop 1 – Park on right shoulder adjacent to road cut approximately 300 meters SSE of Perch River WMU. Road cuts on both side of road; proceed cautiously to outcrop on E side of Route 12. Be very watchful of traffic.

STOP 1. LOWVILLE FORMATION AT PERCH RIVER GAME MANAGEMENT AREA (UTM 422131 m E, 4881179 m N)

The basal ~2 meters of the outcrop on the NE side of Rt. 12 exposes the contact interval between the uppermost Pamelia Formation and lower Lowville Formation of the Black River Group. This unit, known as the Pittsburgh Quarry Bed (Cornell, et al 2005: Cornell, 2008) is now considered to form the base of the Lowville Formation. It consist of weak-weathering dolomitic mudstone, overlain by thick laminated and occasionally cross-laminated, relatively massive brown to yellow weathering quartz sandy dolostone. Angular to subrounded polycrystalline quartz grains in the massive dolostone approach 4 mm in diameter, and must have been derived from exposed Proterozoic basement nearby. Overlying the Pittsburgh Quarry Bed, shaley dolostones and medium to thick bedded lime mudstones comprise the lower (unnamed) member of Lowville Formation.

Key sedimentary features to observe are cryptalgal/microbial laminations, bentonite (volcanic ash) beds, mudcracks, evaporite (gypsum/anhydrite) mineral casts, and storm event beds represented by mud rip-ups clasts, intraclast breccias, stylolites and solution voids. Grey limestone beds contain vertical "*Phytopsis*" burrows that are backfilled with grainy sediment or occasionally filled with calcite spare cement. Body fossils are relatively rare, but some beds contain abundance ostracodes; scattered gastropod and trilobite debris is present in some beds. The SE end of the outcrop is capped by a massive, tan-weathering laminated dolostone with abundant large mineralized voids. Immediately beneath the dolostone, beds of grey limestone are arrayed in a low amplitude fold with an axial trend approximately N80W, parallel to the highway. The basal beds of the overlying House Creek Member of the Lowville Formation are poorly exposed and partially hidden by brush at the summit of the exposure on the west side of the highway.

Thin (mm-cm thick) dolomite+calcite+pyrite+barite veins trending N70E are present in the limestone, and cm-scale calcite spar-filled voids are common in the dolostone and some limestone beds. The mineralized fractures

here are small-scale hydrothermal features that may be related to the dolomitization and related mineralization. Note also that some of the larger voids have dark, hydrocarbon-stained calcite as the void fill.

Examine the limestone - dolostone contact and see if you can trace mineralized fractures into the dolostone. Is the dolomitization here 'early' (preburial – related to Mg-rich brines derived from seawater that had precipitated gypsum) or is the dolomitization related to the later mineralized fractures? What is the relationship between dolomitization and stylolitization? Why is some rock dolomitized whereas other rock remains nearly pure calcite limestone? Was there significant porosity in this rock at any time during its diagenetic history?

Is the folding related to the minor mineralization or a later phenomenon? When during the burial history were hydrocarbons generated?

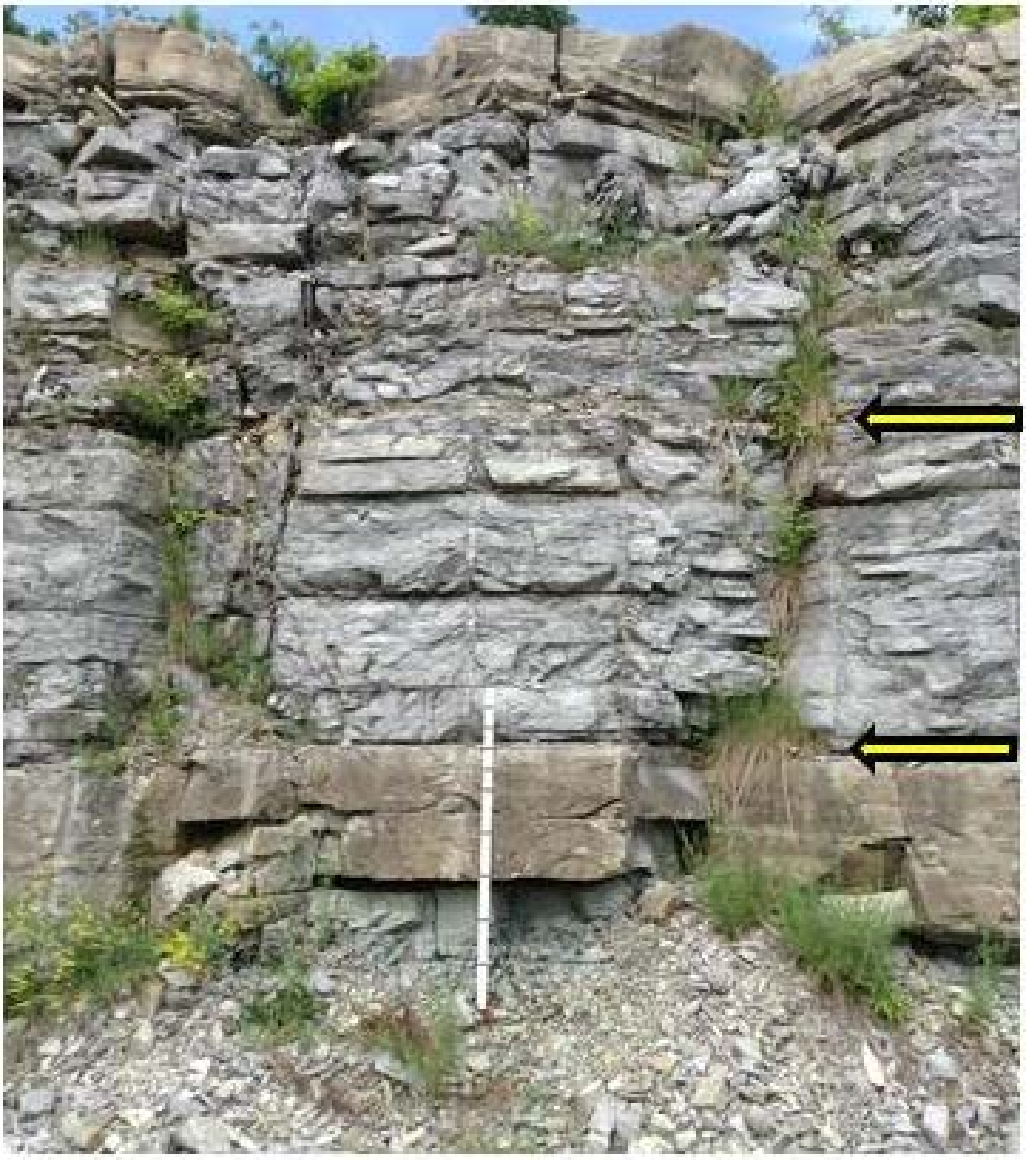

Figure 4. Lower unnamed member of the Lowville Formation at Stop 1. Rod is 1.5 meters, and rests on the Pittsburgh Quarry Bed and overlying lime mudstone. Note the prominent rentrants marking bentonite horizons (arrows). Additional thin shaley partings may represent other ash horizons.

Figure 5. Stop 1. Upper left. Tilted strata in east-dipping limb of minor fold. Upper right. Mm-scale evaporite crystal molds. Tip of hammer gives scale. Lower left. Calcite/hydrocarbon void fill. Lower right. Stylolite with stylocumulate dolomite.

26.9	0.5	Continue SSE on Rt. 12 to intersection with Star Schoolhouse Road. Turn right (SW) onto Star Schoolhouse Road; continue SW
29.8	2.9	Intersection of Star Schoolhouse Road and County Route 54 (Perch River Road). Turn left (S) onto Route 54; continue S.
33.2	3.4	Intersection of County Route 54 and NYS Route 12E in Village of Brownville (East Main Street). Turn left (E) onto Route 12E. Continue E on 12E to Glen Park
34.9	1.7	Stop 2 – Glen Park entrance to parking area for hydroelectric fishing access. Walk to gate entrance, crossing canal. Follow signs to fishing access site, descending path to river level. Watch for poison ivy along path. Be aware that warning sirens provide only 5 minutes before river level rises due to water releases. Be cautious – rocks are slippery.

STOP 2. UPPER LOWVILLE FORMATION AND CHAUMONT FORMATION AT BLACK RIVER GORGE, GLEN PARK, NY. (UTM 423767 m E, 4872115 m N)

The Black River Gorge from Great Bend to Brownville, NY exposes Black River and Trenton Group strata in a series of spectacular narrow river channel walls, waterfalls, and challenging rapids favored by rafters and kayakers. The river has been partially diverted and dammed for hydropower, and here at Glen Park the control structures provide access to riverside exposures along a foot path which descends to the natural channel south of the diversion canal. The strata exposed in the river gorge in the immediate vicinity of the access area include the upper portion of the House Creek Member of the Lowville Formation, including the Weaver Road Beds, the entire Watertown Formation, and the overlying Selby and Nappanee Formations of the basal Trenton Group.

At the river bank where the access trail ends, the outcrops consist of massive to thick-bedded bioclastic packstone/grainstone of the Watertown Member of the Chaumont Formation. The gorge wall across the channel exposes the Weaver Road Beds (House Creek Member of the Lowville Formation), and LeRay and Glenburnie Members of the Chaumont Formation, succeed by the massive Watertown. The Selby and Nappanee Formations of the Trenton Group overlie the Watertown. Looking west, downstream, it appears that the strata are downdropped to the north, although the perspective here is somewhat problematic. This could represent a tight monoclinal fold or high-angle fault. The course of the river here may be in part controlled by this structure. Coarsely crystalline ferroan dolomite in the Watertown here suggests hydrothermal fluids were active, perhaps related to the faulting/folding.

Figure 6. View downstream from fishing access site at Glen Park (Stop 2). The massive bed (upper arrow) is the Watertown Limestone Member of the Chaumont Formation. Note the apparent offset of the Watertown and underlying strata (Glenburnie, LeRay Members, Weaver Road Beds of House Creek Member of the Lowville Formation).

Figure 6. Close-up of Watertown Member bioclastic grainstone/packstone with large voids filled with ferroan dolomite. The proximity to the inferred fault may indicate that hydrothermal fluids were responsible for leaching of carbonate and subsequent precipitation of void-filling dolomite. U.S. quarter provides scale.

		Return to vehicles, exit parking area, turn right (E) on Route 12E, continue E.
35.8	0.9	Intersection of Route 12E with County Route 281 (Teal Drive). Turn left onto Route 281
36.5	0.7	Intersection of Route 281 with NYS Route 12. Turn left (N) onto Route 12. Continue N.
38.4	1.9	Intersection of Route 12 with NYS Route 342. Turn right (E) onto Route 342. Continue E.
45.2	6.8	Intersection of Route 342 with NYS Route 283 in Calcium, NY. Turn right (W) onto Route 283.
45.4	0.2	Stop 3 - Park on shoulder next to road cut on right (N) side of road.

STOP 3. HOUSE CREEK MEMBER OF LOWVILLE FORMATION OVERLAIN BY CHAUMONT FORMATION ON NYS ROUTE 283 NEAR CALCIUM, NY. (UTM 434297 m E, 4874691 m N)

The massive Watertown Member of the Chaumont Formation forms the resistant upper ledge at this road cutting. A prominent reentrant at the base of the Watertown is likely a bentonite horizon, with the underlying House Creek Member of the Lowville Formation forming the base of the exposure. Notably, the LeRay and Glenburnie Members of the Chaumont do not appear to be represented here (compare with Stop 2).

The House Creek Member beds here include typical *Tetradium*-rich wackestone with scattered, poorly-preserved ostracodes, gastropod and trilobite fragments. The moderately weathered faces of the overlying Watertown Member provide a good opportunity to examine this facies in some detail. Good examples of colonial tabulate corals ('Hexagonaria") and the small solitary rugose coral *Lambeophyllum* are relatively common. Brachiopods, crinoid plates, bryozoans and rare trilobites are also present. This fauna signals fully open marine conditions with normal salinity and well-oxygenated water.

Typical of the Watertown Member, chert nodules and certified bioclastic material is common in this outcrop. Nodular cherts are generally arrayed in laterally discontinuous horizons, perhaps related to the abundance of original siliceous skeletal material (sponge spicules, radiolarian) or possibly volcanic ash. Biogenic silica and volcanic ash are chemically unstable in seawater, and would provide dissolved silica for certification.

Are some fossil types here more likely to be chert-replaced than others? Use a hand lens to examine the void filling minerals in the tabulate coral fossils. What diagenetic minerals are present?

Figure 7. Stop 3. Massive bedded Watertown Member of the Chaumont Formation overlying ~60 centimeters of upper House Creek Member of Lowville Formation. Note the prominent reentrant (possible bentonite) at the base of the Watertown.

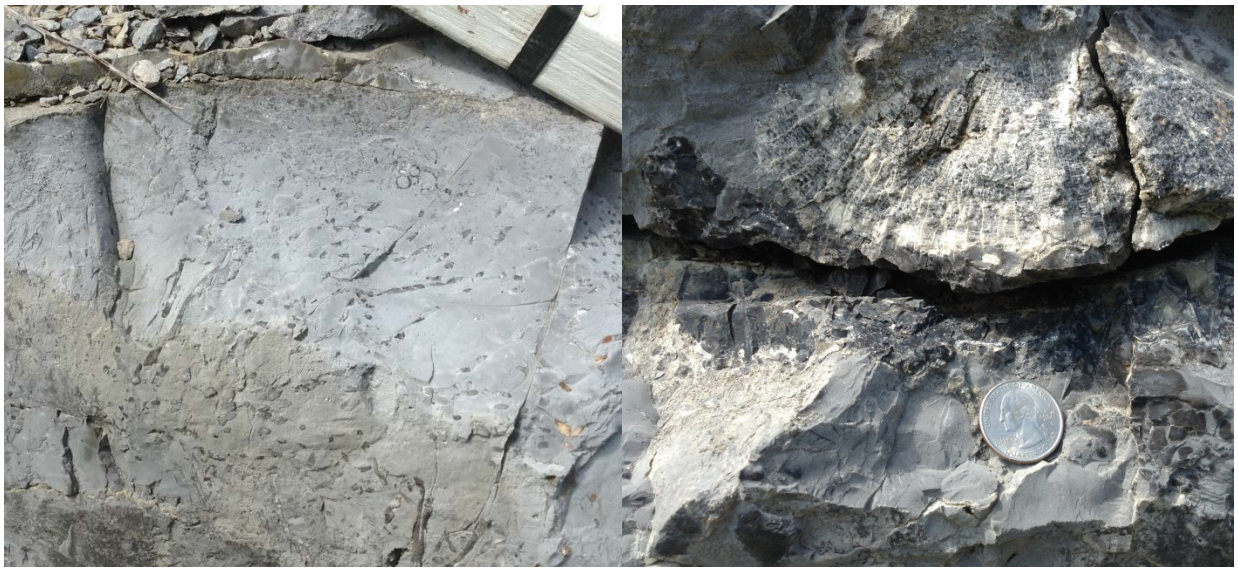

Figure 8. Stop 3. Left. Tetradium wackestone of the upper House Creek Member. Right. Overturned colonial tabulate coral head, partially chert-replaced.

45.7	0.3	Continue W on Route 283 to intersection with Five Corners Road (on right). Turn right (NE). Continue NE on Five Corners Road
46.1	0.4	Intersection with Route 342. Turn right (SE). Continue SE on Route 342
48.0	1.9	Intersection with NYS Route 3. Turn left (E). Continue E on Route 3.
53.3	5.3	Intersection with NYS Route 26 in Great Bend, NY. Turn right (SE) on Route 26. Continue SE on Route 26.
58.6	6.8	West Carthage, NY. Continue SE on Route 26.
72.8	14.2	Intersection with NYS Route 12 in Lowville, NY. Continue SE on Routes 12 and 26.
73.4	0.6	Routes 12 and 26 diverge. Bear left (SE) on Route 12. Continue SE on Route 12.
74.3	0.9	Stop 4 - Road cut on right (W) side of highway. Park on right shoulder adjacent to outcrop.

STOP 4. HOUSE CREEK MEMBER OF LOWVILLE FORMATION ON NYS ROUTE 12 NEAR LOWVILLE, NY. (UTM 462063 m E, 4846699 m N

The road cut on the west side of NYS Route 12 is developed in the House Creek Member of the Lowville. Only the uppermost House Creek Member was seen at Stop 3, and here a fuller range of lithologies is exposed. The subtidal facies in this exposure are typical of the House Creek, with grey-weathering *Tetradium* wackestones forming the basal portion of the interval, succeeded by a series of thick beds of bioclastic and intraclastic packstones and grainstones. There are relatively few large whole shell fossils in these units, but abundant fragmental ostracode, trilobite, bryozoan and coral material is present.

Note the wispy dolomite developed in the upper beds. Is the dolomite fabric-selective, that is selectively replacing a particular primary carbonate material, or are these wisps of stylocumulate origin? Carefully examine the intraclastic packstone bed. Is the fabric indicative of simple rip-up clasts, the result of bioturbation, or are these algal 'clots'?

Figure 9. Stop 4. House Creek Member of Lowville Formation at Stop 4. Note the thick bedded character, generally lower terrigenous clastic content (less shaley), compared to the Lower Lowville seen at Stop 1.

Figure 10. Stop 4. Tetradium wackestone. Note wisps of dolomite.

		Continue SE on Route 12.
86.9	12.6	Village of Lyons Falls. Continue SE on Route 12.
93.7	6.8	Stop 5 - Road cut on right (W) side of Route 12. Park on shoulder (caution – broad road shoulder to right may be muddy).
		End of Trip.

STOP 5. KINGS FALLS AND NAPANEE FORMATIONS AT SUGAR RIVER ON NYS ROUTE 12. (UTM - 473796 m E, 4819529 m N)

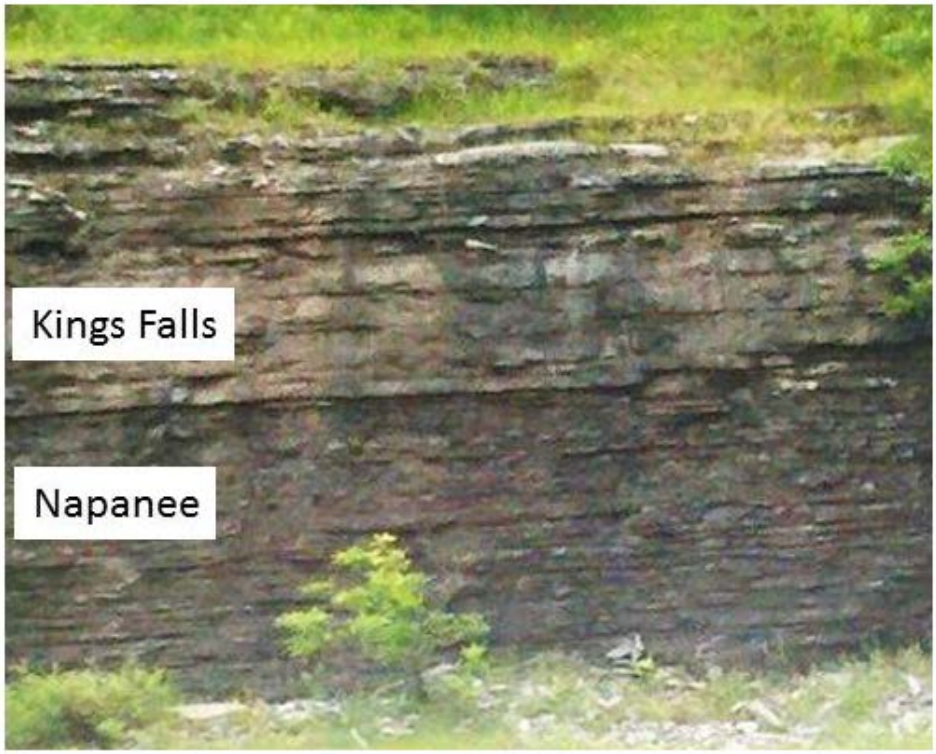

Figure 11. Stop 5. Note the very sharp (erosional?) contact between deeper shelf Napanee Formation and wave-dominated grainstones of the basal Kings Falls Formation.

The road cuts on Route 12 and adjacent stream sections in the Sugar River at this locality allow observation of more or less continuous exposures of the lower and middle Trenton units. The Barrett Corporation quarry on the west side of Route 12 is developed in the upper Black River Group (upper Lowville and Chaumont Formations). On this trip we will limit our observations to the section exposed north of the Sugar River on the west side of Route 12.

Medium to thin bedded lime mudstones and silty shales of the Napanee Formation are overlain sharply by thick bedded, coarse bioclastic grainstones with thin interbedded shales of the basal Kings Falls Formation. The Napanee mudstones and shales are relatively organic-rich, and represent highstand facies. The succeeding wave and storm-dominated Kings Falls facies overlie a sharp, possibly erosional contact with the Napanee. Coarse , coquina-like brachiopod and crinoid grainstones are characteristic of the Kings Falls Formation. Many bedding surfaces show very fine preservation of brachiopods, crinoids, bryozoans and rare trilobites. Horizontal veins within shale horizons in the Napanee Formation document bed-parallel thrusting, perhaps related to high fluid pressure during burial diagenesis. Fluid inclusion temperatures in vein carbonate suggest burial heating to >145^{o}C.

REFERENCES CITED

BAIRD, G.C., & BRETT, C.E., 2002, Utica Shale: Late synorogenic siliciclastic succession in an evolving Middle/Late Ordovician foreland basin, eastern New York, Physics and Chemistry of the Earth, vol. 27, pp. 203– 230.

BAIRD, G.C., BRETT, C.E., and LEHMANN, D., 1992, The Trenton – Utica problem revisited: new observations and ideas regarding Middle – Late Ordovician stratigraphy and depositional environments in central New York: In Goldstein, A., ed., New York State Geological Association, 64th Annual Meeting Guidebook, p. 1-40.

BRETT C.E., & Baird, G.G., 2002, Revised stratigraphy of the Trenton Group in the type area, central New York State: Sedimentology, and tectonics of a Middle Ordovician shelf-to-basin succession, Physics and Chemistry of the Earth, vol. 27, pp. 231– 263.

BIRD, J.M. AND DEWEY, J.F., 1970. Lithosphere plate-continental margin tectonics and the evolution of the Appalachian orogen: Geol. Soc. Amer. Bull., 81, 103-136

BRETT, C.E., MCLAUGHLIN, P.I., CORNELL, S.R., & BAIRD, G.C., 2004, Comparative sequence stratigraphy of two classic Upper Ordovician successions, Trenton Shelf (New York–Ontario) and Lexington latform (Kentucky–Ohio): implications for eustasy and local tectonism in eastern Laurentia, Palaeogeography, Palaeoclimatology, Palaeoecology, vol. 210, pp. 295-329.

BROOKFIELD, M.E., & BRETT, C.E., 1988, Paleoenvironments of the Mid-Ordovician (Upper Caradocian) Trenton limestones of southern Ontario, Canada: storm sedimentation on a shoal-basin shelf model: Sedimentary Geology, vol. 57, p. 185-198.

BROOKFIELD, M.E., 1988, A mid-Ordovician temperate carbonate shelf – the Black River and Trenton limestone groups of southern Ontario, Canada: Sedimentary Geology, vol. 60, p. 137-153.

CAMERON, B., & MANGION, S., 1977, Depositional environments and revised stratigraphy along the Black River – Trenton boundary in New York and Ontario: American Journal of Science, vol. 277, p. 486-502.

CONKIN, J.E., & CONKIN, B., 1991, Middle Ordovician (Mohawkian) paracontinuous stratigraphy and metabentonites of eastern North America: University of Louisville Studies in Paleontology and Stratigraphy, vol. 18, 81 p.

CORNELL, S.R., 2001, Sequence Stratigraphy and Event Correlations of upper Black River and lower Trenton Group Carbonates of northern New York State and southern Ontario, Canada, unpub. M.S. Thesis, University of Cincinnati, Cincinnati, OH.

CORNELL, S.R., 2005, Stratigraphy of the Upper Ordovician Black River and Trenton Group Boundary Interval in the Mohawk and Black River Valleys, Geological Society of American Northeast Section Field Trip Guidebook, Saratoga Springs, New York, pp. C1-C23.

CORNELL, S. R. 2008 The Last Stand of the Great American Carbonate Bank: Tectonic Activation of the Upper Ordovician Passive Margin in Eastern North America; unpub. PHD Thesis, University of Cincinnati, Cincinnati, OH.

FISHER, D.W., 1962, Correlation of Ordovician rocks in New York State: New York State Museum and Science Service, Geological Survey Map and Chart Series # 3.

FISHER, D.W., 1965, Mohawk Valley strata and structure, Saratoga to Canajoharie, New York State Geological Association, Field Trip Guidebook, Schenectady area meeting, 58 p.
FISHER, D.W., 1977, Correlation of the Hadrynian, Cambrian, and Ordovician rocks in New York State:

New York State Museum Map and Chart Series # 25, 75 p.

GARRAND, K., VALENTINO, B. AND VALENTINO, D. (2012) Joint analysis across the Trenton-Utica boundary in the Mohawk River headwaters region, New York; Geological Society of America *Abstracts with Programs*, Vol. 44, No. 2, p. 96

GOLDMAN, D., MITCHELL, C.E., BERGSTRÖM, S.M., DELANO, J.W., & TICE, S., 1994, K-bentonite and graptolite biostratigraphy in the Middle Ordovician of New York State and Quebec: A new chronostratigraphic model: Palaios, vol. 9, p. 124-143.

HALL, J., 1847, Paleontology of New York, Vol. I, containing descriptions of the organic remains of the lower division of the New York system (equivalent of the Lower Silurian rocks of Europe), 318 p.

JACOBI, R. D., AND C. E. MITCHELL, 2002. Geodynamical interpretation of a major unconformity in the Taconic Foredeep; slide scar or onlap unconformity? p. 169-201. *In* C. E. Mitchell and R. Jacobi (eds.), Taconic Convergence: Orogen, Foreland Basin and Craton, Physics and Chemistry of the Earth, 27

JACOBI, R.D., S. LOEWENSTEIN, J. P. MARTIN, AND G. SMITH. 2000. Magnetic, gravity, and Landsat lineaments in the Appalachian Basin, New York State: groundtruth, faults, and traps. American Association of Petroleum Geologists Bulletin, 84(9):1387

KAY, G.M., 1931, Stratigraphy of the Ordovician Hounsfield Metabentonite, Journal of Geology, vol. , p. 361-376.

KAY, G.M., 1935, Distribution of Ordovician altered volcanic materials and related clays: Geological Society of America Bulletin, vol. 46, p. 225-244.

KAY, G.M., 1937, Stratigraphy of the Trenton Group: Geological Society of America Bulletin, vol. 48, p. 232-302.

KAY, G.M., 1960, Classification of the Ordovician System in North America: 21st International Geological Congress, Copenhagen, Denmark, part VII 7, p. 28-33.

MITCHELL, C.E., GOLDMAN, D., DELANO, J.W., SAMSON, S.D., & BERGSTRÖM, S.M., 1994, Temporal and spatial distribution of biozones and facies relative to geochemically correlated K-bentonites in the Middle Ordovician Taconic foredeep: Geology, vol. 22, p. 715 – 717.

MITCHELL, C.E., ADHYA, S., BERGSTRÖM, S., JOY, M.P., DELANO, J.W., 2004, Discovery of the Ordovician Millbrig K-bentonite Bed in the Trenton Group of New York State: implications for regional correlation and sequence stratigraphy in eastern North America, Palaeogeography, Palaeoclimatology, Palaeoecology vol. 210, pp. 331-346.

SLOSS, L.L, 1963, Sequences in the cratonic interior of North America, Geological Society of America Bulletin, 74, pp. 93-114.

SMITH, L.(2006) Origin and reservoir characteristics of Upper Ordovician Trenton-Black River hydrothermal dolomite reservoirs in New York; AAPG Bulletin, v. 90, #11, p. 1691-1719

TEXTORIS, D.A., 1968, Petrology of supratidal, intertidal, and shallow subtidal carbonates, Black River Group, Middle Ordovician, New York, U.S.A.: 23rd International Geological Congress, Prague, part VIII, p. 227-248.

TITUS, R., & CAMERON, B., 1976, Fossil communities of the lower Trenton Group (Middle Ordovician) of central and northwestern New York State: Journal of Paleontology, vol. 50 # 6. p. 1209-1225.

VANUXEM, L., 1838, Second annual report of so much of the geological survey of the third district of the

State of New York as relates objects of immediate utility, New York Geological Survey, 255 p.

VANUXEM, L., 1842, Geology of New York, Part III, comprising the survey of the Third Geologic District, 306 p.

WALKER, K.R., 1973, Stratigraphy and environmental sedimentology of the Middle Ordovician Black River Group in the type area – New York State: New York State Museum and Science Service Bulletin # 419, 43 p.

WICKSTROM, L., PERRY, C., RILEY, R. AND ERENPRIESS, M. (2012) The Utica-Point Pleasant Play of Ohio; http://geosurvey.ohiodnr.gov/portals/geosurvey/energy/Utica-PointPleasant_presentation.pdf

WINDER, C.G., 1960, Paleoecological interpretations of Middle Ordovician stratigraphy in southern Ontario, Canada: International Geological Congress – Report of the 21st Session Norden, part VII: Ordovician and Silurian stratigraphy and correlations p. 18-27.

YOUNG, F.P., 1943a, Black River Stratigraphy and faunas: I, American Journal of Science, vol. 241, p. 141-166.

YOUNG, F.P., 1943b, Black River Stratigraphy and faunas: II, American Journal of Science, vol. 241, p. 209-240.

ULTRAMAFIC/MAFIC ROCKS OF THE PYRITES COMPLEX

JEFFREY CHIARENZELLI
Department of Geology, St. Lawrence University, Canton, New York 13676

MARIAN LUPULESCU
Research and Collections, New York State Museum, Cultural Education Center,
222 Madison Avenue, Albany, NY 12230

DAVID BAILEY
Department of Geosciences, Hamilton College, 198 College Hill Road, Clinton, NY 13323

INTRODUCTION

General overviews of the geology of the Adirondack Lowlands incorporating new results can be found in Chiarenzelli et al. (2010a; 2010b; 2011a; 2012), Lupulescu et al. (2010), Peck et al. (2013), and Wong et al. (2011), among others. The purpose of this trip is to provide additional insight into the tectonics of the Adirondack Lowlands by highlighting mafic and the ultramafic rocks exposed in the region. The trip will leave from Alexandria Bay and end at Pyrites, where ultramafic rocks of the Pyrites Complex occur (Figure 1).

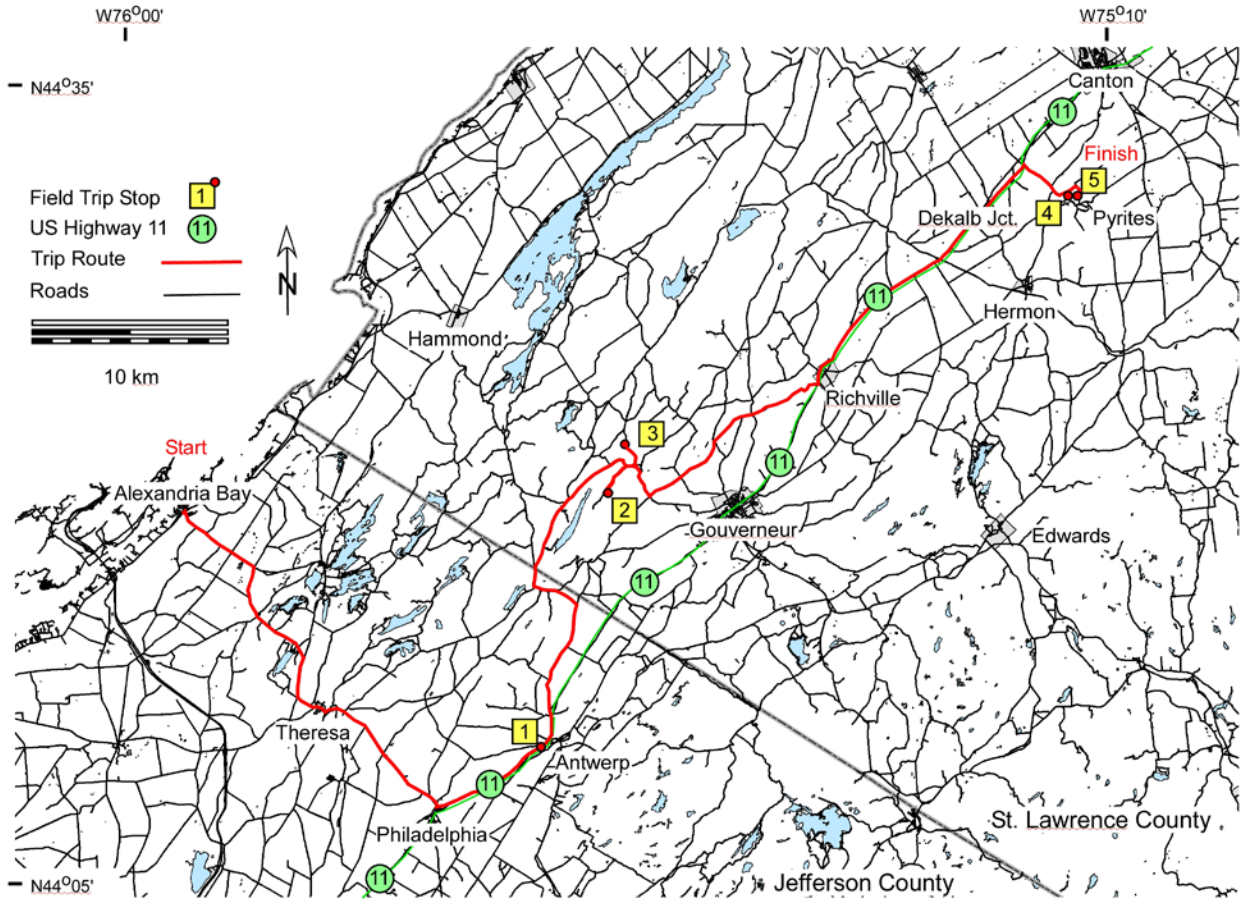

Figure 1. Route of trip B-2 showing location of roadways, field trip stop locations, larger lakes, villages, and other features.

The Adirondack Lowlands are a small part of the greater Grenville Province (Figure 2), a Mesoproterozoic orogenic belt of global proportions. The tectonic assembly and collisional orogenesis recorded here, and elsewhere, resulted in the formation of Rodinia, one of the Earth's Supercontinents. In fact, breakup of Rodinia set the stage for the deposition of the widespread blanket of Potsdam sandstone along the rifted margin of Laurentia, to our east in the Champlain Valley, and exposed nearby on the fringes of the Ottawa Embayment.

The Adirondack Lowlands are delineated from the Adirondack Highlands by a long-lived shear zone that displays evidence for both a ductile and brittle history (Figure 3). This structure, named the Carthage-Colton Shear Zone, marks a number of distinct geologic changes such as the proportion of metasedimentary to metaigneous lithologies, differences in metamorphic grade, variation in the timing of metamorphism, the orientation of structural grain, and a change in topographic relief and elevation. The Lowlands is composed mostly of metasedimentary rocks, predominantly marble, and was metamorphosed to Upper Amphibolite facies during the Shawinigan Orogeny (ca. 1150-1200 Ma), leading to widespread melting in some pelitic gneisses and the growth of metamorphic zircon at 1160-1180 Ma (Heumann et al., 2006). Its position higher in the crust has led to a lack of widespread (any?) effects of the Ottawan Orogeny (ca.1020-1090 Ma), in contrast to the Highlands where metamorphic zircon of this age and resetting of zircon is widespread (Chiarenzelli and McLelland, 1993; Chiarenzelli et al., 2011b).

The oldest known rocks in the Lowlands consist of metasedimentary rocks of Grenville Supergroup, first noted in the literature by Sir William Logan in 1863 to describe the sequence of metasedimentary rocks that occur across large areas of southern Ontario and adjacent parts of Quebec. In the Lowlands these rocks provide evidence of shallow water, marine deposition and include, among other lithologies, voluminous marbles, calc-silicate gneisses, tourmaline-rich quarztofeldspathic gneisses, the sedex sulfide exhalatives of the Balmat zinc mines, and metaevaporites. A tripartite stratigraphy and/or structural stratigraphy has been recognized and consists of the lower marble, Popple Hill Gneiss, and the upper marble, which has been further subdivided into 16 lithologic units (deLorraine, 2001; deLorraine and Sangster, 1997). In contrast to the proposed setting of the carbonate rocks, a deep water turbidite origin has been proposed for the Popple Hill pelitic and psammitic gneisses and equivalents (Chiarenzelli et al., 2012). However, all of these rocks may be allochthonous, as older basement rocks have yet to be identified. The maximum depositional age for the Grenville Supergroup in the Lowlands has recently been constrained between <1258 and <1284 Ma (Chiarenzelli et al., in review).

Recent investigation has revealed that ultramafic-mafic igneous rocks occur within northeast-trending linear belts (Figure 4) in the Lowlands and may be older or equivalent in age to the Grenville Supergroup. Named the Pyrites Complex for exposures along the Grasse River near Pyrites, New York, these rocks have required rethinking of the depositional environment of not only the Grenville Supergroup equivalents in the Adirondack Region but the origin of the Zn-Pb sedimentary exhalatives of the Balmat-West Pierrepont Belt. A model incorporating the discovery of ultramafic rocks suggests that the rocks of the Grenville Supergroup were deposited after 1300 Ma in a back-arc basin which closed at about 1240 Ma during the Elzevirian Orogeny (Chiarenzelli et al., 2011a; 2012). This back-arc basin has been named the Trans-Adirondack Back-arc Basin and is thought to be temporally equivalent to a similar basin in the Central Metasedimentary Belt of Ontario and Quebec (Dickin and McNutt, 2007). This implies that a broad region of the southeast margin of Laurentia underwent rifting and extension at this time.

During this trip we will see what is thought to be the remnants of a highly disrupted ophiolite complex and deep water sedimentary rocks including hydrothermal altered ultramafic rocks (Stops 4 and 5), amphibolite (Stop 1), and possible turbidites (Stop 4). We will observe a lamprophyre dike cutting the ultramafic rocks at Stop 5. In addition, two stops will be made to investigate candidates for inclusion in the the Pyrites Complex including a large block of serpentine (Stop 2) and a hornblendite unit (Stop 3), both which require further investigation. Isotopic and geochemical studies indicate widespread enrichment in incompatible elements suggests that the Pyrites ultramafic complex and associated rocks formed in a suprasubduction zone setting. Although the surface exposure of the ultramafic rocks is small, the largest gravity anomaly in the Lowlands extends from Pyrites to the southwest for over 10 km parallel to the trend of the Carthage-Colton Shear Zone, indicating substantial amounts of high density rocks at depth.

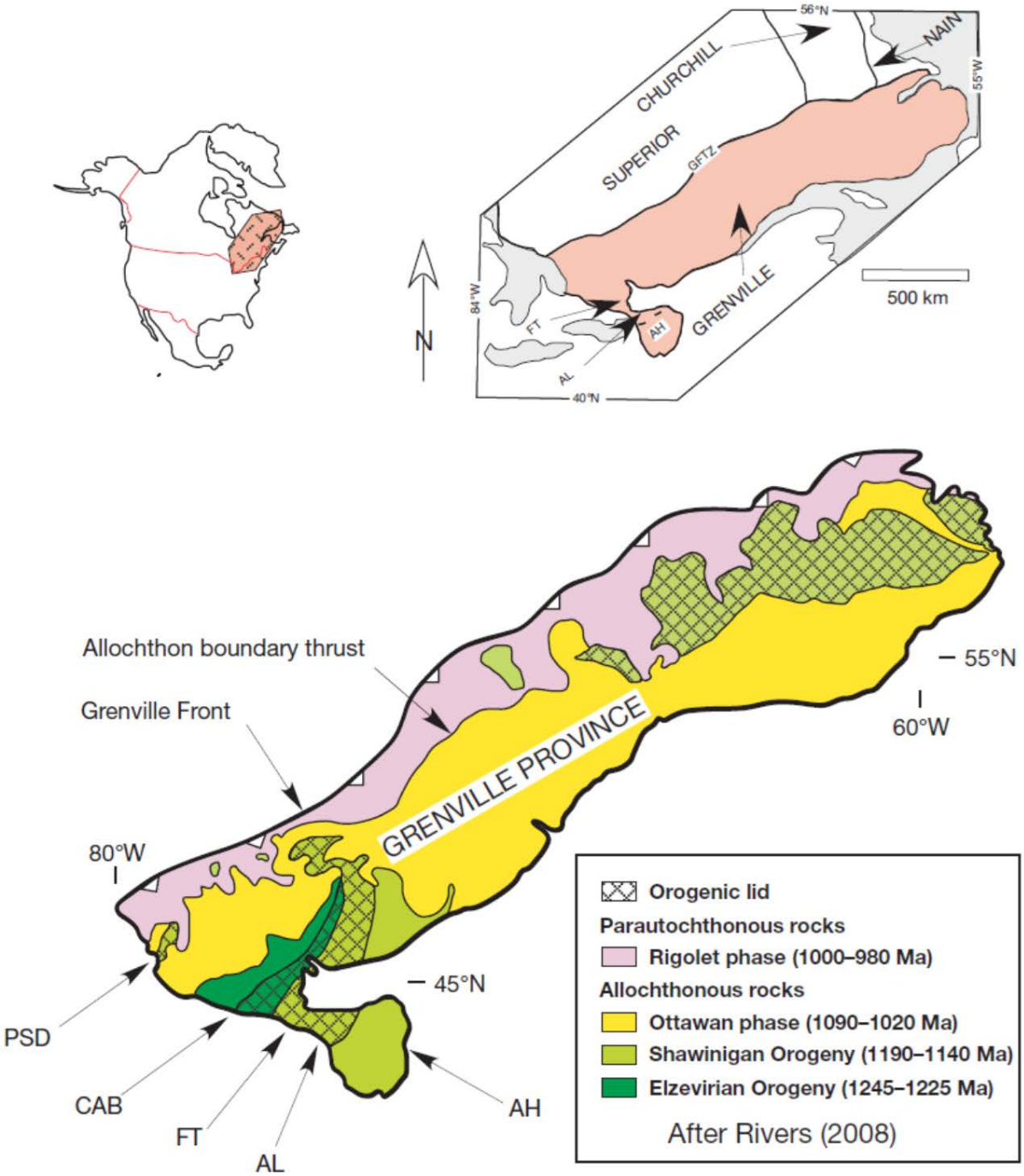

Figure 2. Figure showing the location of the Grenville Province within North America (upper left). Expanded polygon (upper right) shows the same region blown up to show surrounding provinces of the Canadian Shield. Abbreviations include: AH (Adirondack Highlands), AL (Adirondack Lowlands), FT (Frontenac Terrane), and GFTZ (Grenville Front Tectonic Zone). Lower figure shows the timing of recognized deformational events that make up the Grenville Orogenic Cycle (after Rivers, 2008). Additional abbreviations include: CAB (Central Arc Belt) and PSD (Parry Sound Domain). From Chiarenzelli et al. (2011a).

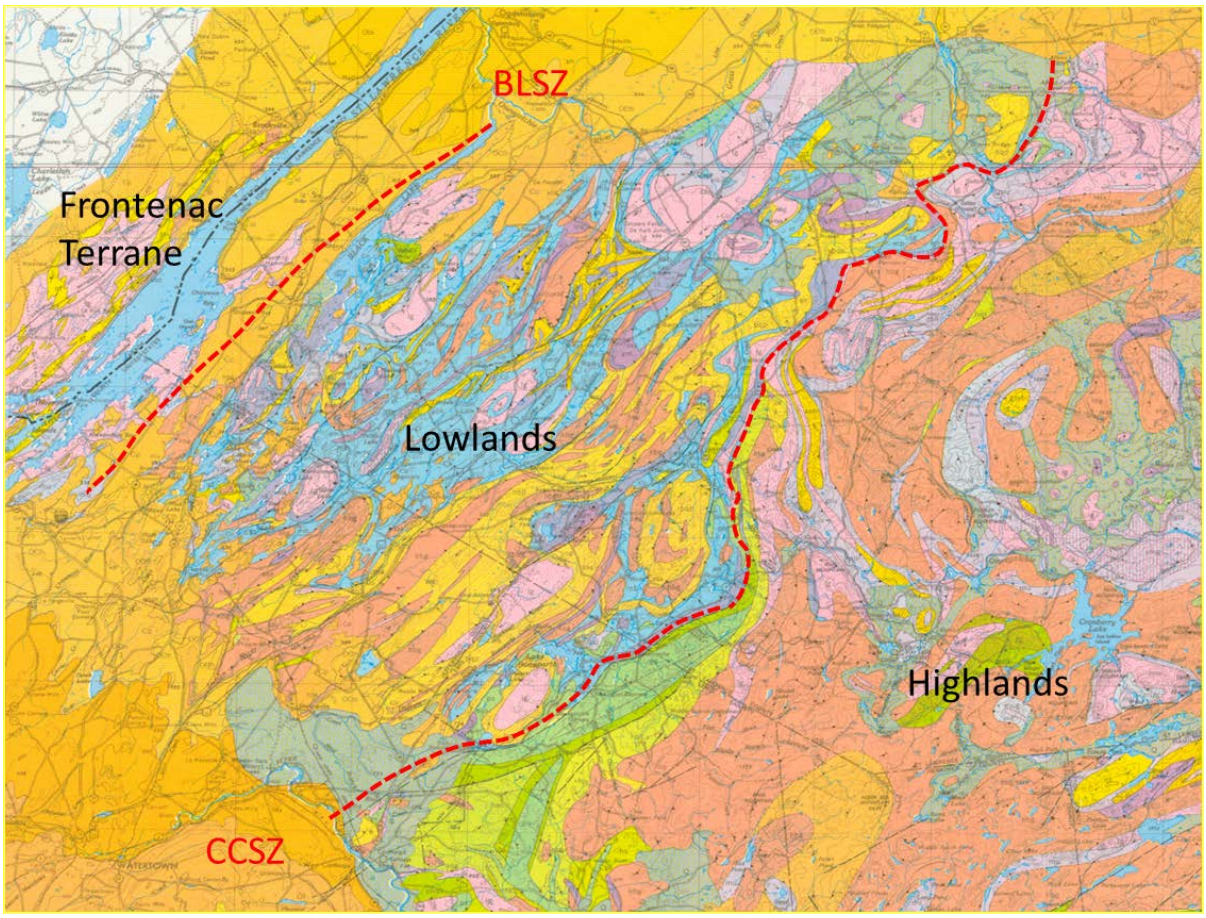

Figure 3. Geology of the Adirondack Lowlands and surrounding terranes from Isachsen and Fisher (1970). The Black Lake (BLSZ) and Carthage-Colton (CCSZ) shear zones define the boundaries of the Adirondack Lowlands. Flat-lying Paleozoic rocks (orange) overlie Grenville basement rocks much of the St. Lawrence River Valley and Tug Hill plateau to the southwest. Note the predominance of marble (blue) in the Lowlands and general lack thereof in bounding Frontenac Terrane and Adirondack Highlands.

Stop 1 Amphibolite and Pyritic Gneisses near Antwerp
<1 km southwest of Antwerp, along Rt. 11; Latitude 44°11'41.7", Longitude 75°37'28.8"

We have driven south from Alexandria Bay to the southern belt of pyritic gneisses, amphibolites, metagabbros, and ultramafic rocks exposed in the Lowlands. Here near Antwerp, New York we will see some of the amphibolites, associated pyrite-rich metasedimentary rocks, and igneous rocks which intrude them (Figure 4). This belt can be traced nearly 50 kilometers to Pyrites and beyond. The large outcrop in the foreground shows a sequence of rocks dipping shallowly to the northwest. The darker rocks are amphibolites with MORB-like geochemistry. Those with rusty staining are of metasedimentary origin and contain detrital zircons, in addition to pyrite. Unfortunately these zircons are metamict and discordant. However, similar rocks at Pyrites have yielded intriguing results that will be discussed later at Stop 4. Both of these rocks are cut by a variety of intrusive pegmatites which are correlative in age to the Antwerp-Rossie Suite (ca. 1200 Ma).

The intrusive age of the Antwerp-Rossie Suite provides a minimum age for rocks of the Grenville Supergroup and ultramafic mafic rocks of the Pyrites Complex. Further east along Route 11 large banded outcrops of marble, and isoclinal folds within it, are cut by rocks of the Antwerp-Rossie Suite (Figure 5) dated at ca. 1200 Ma. The Antwerp-Rossie Suite is calc-alkaline and the product of northward subduction which preceded the Shawinigan Orogeny.

Figure 4. Field photograph showing dark amphibolitic rocks along Route 11 in Antwerp, NY cut by light-colored pegmatite veins related to the Antwerp-Rossie plutonic suite (ca. 1200 Ma). Note the strongly layered rusty gneisses on either side of the geologist.

Figure 5. Outcrop of Grenville Supergroup lower marble along Route 11 showing a large recumbent isoclinal fold (just above the geologist's hand) cut by rocks of the Antwerp-Rossie Suite (ca. 1200 Ma).

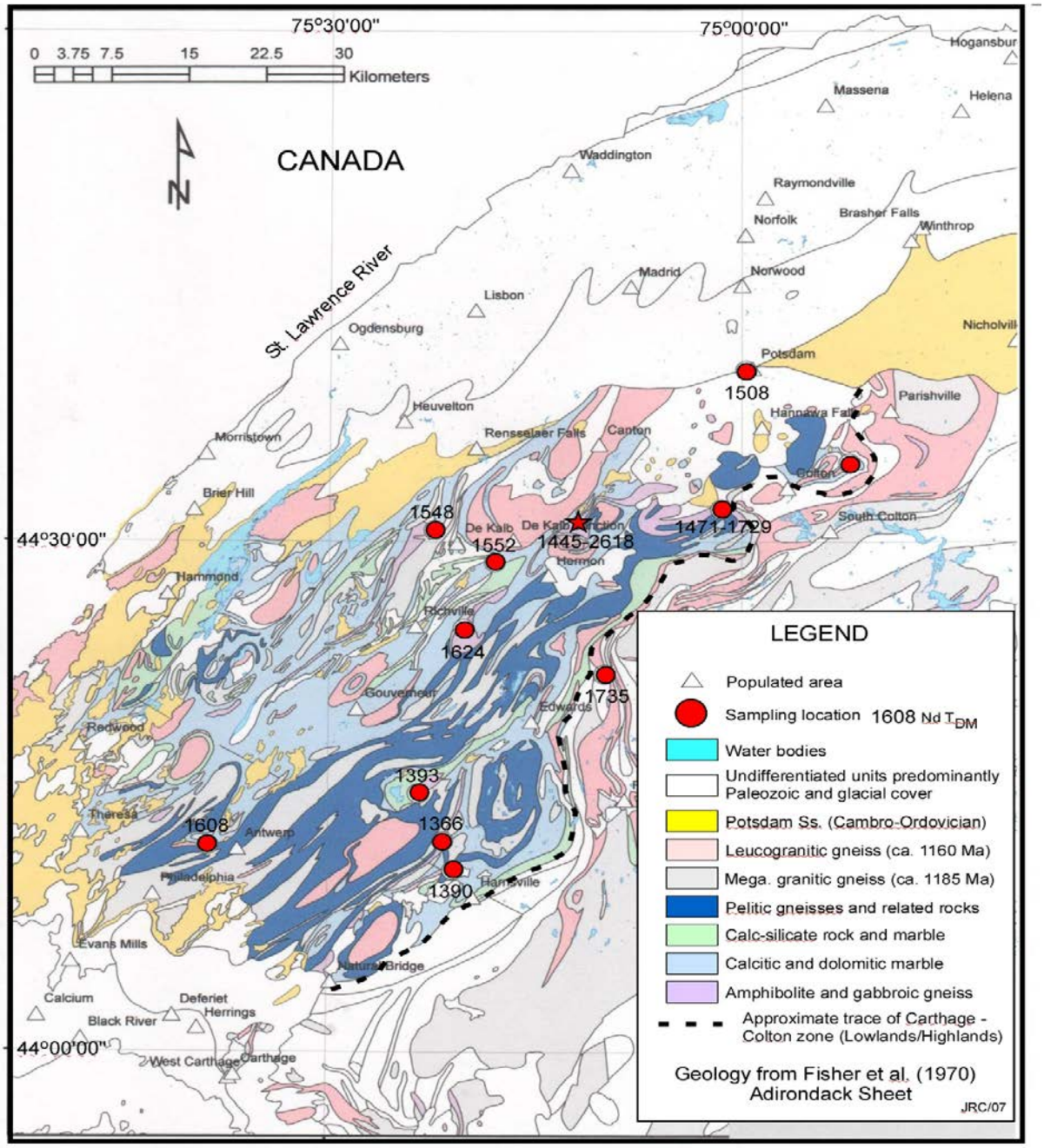

Figure 6. Generalized geologic map of the Adirondack Lowlands showing the locations of mafic and ultramafic rocks (in purple) analyzed for Nd isotopic systematics and corresponding Nd T_{DM} (red circles). The sample collected along Rt. 11 at Antwerp, which we will visit, yielded an unrealistically old model age of 1608 Ma). The red star denotes the cluster of samples collected at Pyrites where model ages varied between 1445-2618.

Orogeny (ca. 1150-1200 Ma). The deformation preserved in the marble must pre-date this subduction event and subsequent Shawinigan orogenesis (Figure 5). This implies that the Grenville Supergroup and Pyrites Complex where deformed during the Elzevirian Orogeny (ca. 1220-1245 Ma), consistent with the minimum age for the Grenville Supergroup in the region constrained by detrital zircons (Chiarenzelli et al., in review).

The amphibolite outcropping here has been characterized by geochemistry and Nd-systematics. The amphibolites and metagabbros of this belt yield unrealistically old NdT_{DM} ages of 1508-1624 Ma, as do

ultramafic rocks at Pyrites, which in some cases are even older (Figure 6). This suggests disturbance of the Sm-Nd isotopic system and the influence of a metasomatically altered mantle wedge in their origin. Elevated oxygen isotopic ratios have been found zircon in plutonic rocks extending across the Lowlands into the Frontenac Terrane by Peck et al. (2004). Peck et al. (2004) interpreted these elevated ratios as indicative of the influence of subducted hydrothermally altered oceanic crust and/or sedimentary material beneath the leading edge of Laurentia. As a group, rocks of the Pyrites Complex plot between the Nd isotopic arrays of Quebecia ca. 1570 Ma (Dickin and Higgins, 1992) and Ontario Juvenile Crust ca. 1277 Ma (Dickin and McNutt, 2007) indicating an age in excess of 1277 Ma (Figure 7) but younger than 1570 Ma.

An age greater than 1277 Ma for the Pyrites Complex is compatible with several lines of evidence. Barfod et al (2005) obtained a 1274±9 Ma Lu-Hf date on apatite from the lower marble and interpreted it as the time of diagenetic apatite growth in the marble. Sager-Kinsman and Parrish (1993) obtained a maximum depositional age of <1306±16 Ma from the youngest detrital zircon in a quartzite unit of the Grenville Supergroup on Wellesley Island. And as will be discussed below, Chiarenzelli et al. (in review) found a maximum age of 1284+/-7 on detrital zircons from turbiditic rocks overlying ultramafic rocks at Pyrites. A model for the generation of oceanic crust within a series of back-arc basins along the leading edge of Laurentia has been proposed by Chiarenzelli et al. (2011a). The opening of the Trans-Adirondack Back-arc Basin is believed to have been synchronous with the opening of a similar basin in the Central Metasedimentary Belt of Ontario and Quebec (Dickin and McNutt, 2007).

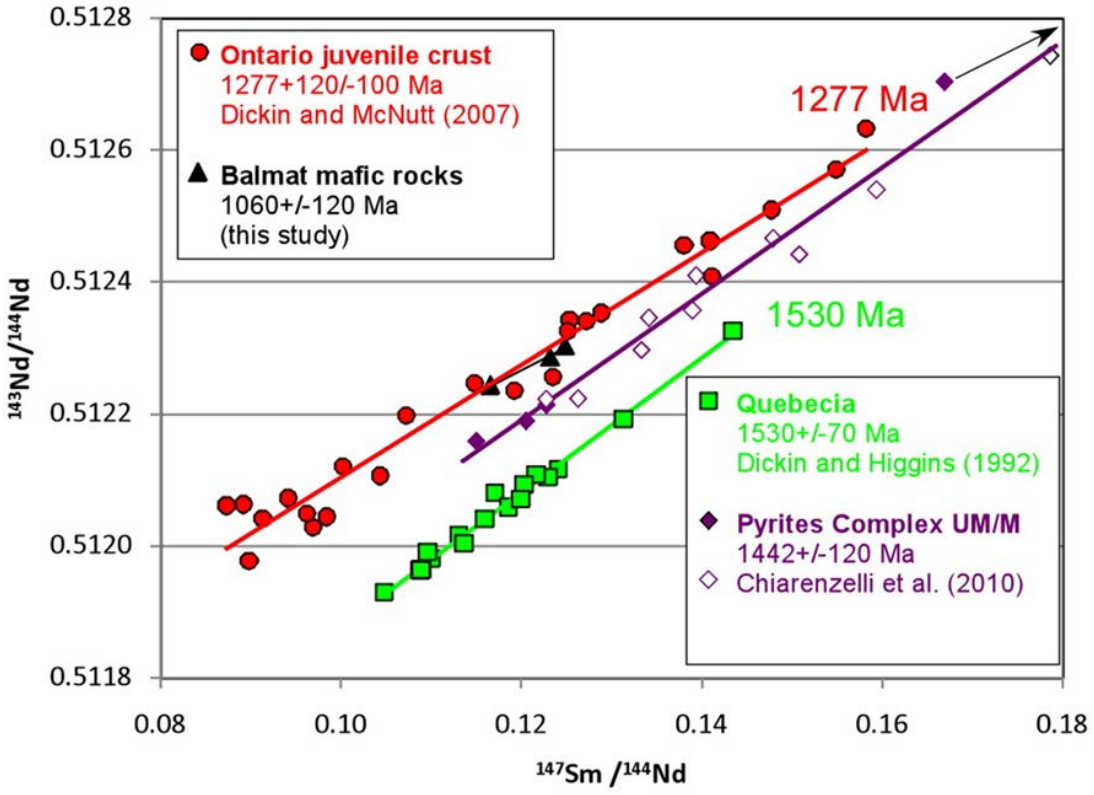

Figure 7. Neodymium evolution diagram showing the trend from mafic and ultramafic rocks of the Pyrites Complex and other Grenville rock suites from Dickin and McNutt (2007) and Dickin and Higgins (1992) used for comparative purposes.

Stop 2 Yellow Lake Serpentinite
~8.5 km west of Gouverneur, off of Campbell Rd between Yellow Lake and the Oswegatchie River; Latitude 44°20'14.3", Longitude 75°34'47.8"

This stop is on private land and permission was obtained for this field trip to visit the area. Please respect the landowner's wishes and do not revisit this location without permission. Respecting land owners rights insures that future geologists will have access to key scientific sites. If in doubt, ask first.

While serpentine is a common mineral throughout much of the Lowlands, massive serpentinite, like that exposed here, is unusual. While this exposure may be a large serpentinized block of metasedimentary rock, the location of this body puts it within a linear trend of mafic and ultramafic rocks approximately 10 kilometers north and west of the Pyrites belt which we will visit again in the near future. These and other linear belts may represent separate thrust sheets, or perhaps, opposing limbs of a major nappe-like structure. In any event, the uniqueness of this exposure makes it an excellent place to visit regardless of its origin.

The Yellow Lake serpentinite is an unusually large body (~100 m) of massive serpentine hosted within marble of the Adirondack Lowlands metasedimentary sequence. The only detailed geologic map of the area shows a thin band of lower marble surrounded by the "Hermon granite-amphibolite" unit (Buddington, 1934). On the Adirondack Sheet this unit is denoted as amg and consists of highly disrupted and intruded amphibolite and metagabbro engulfed within the Hermon granitic gneiss. While localized areas of disseminated serpentine within the marble were noted in the report and are particularly common in the upper marble which is found to the south, this large mass of serpentine was apparently not recognized or described. Intriguingly about 10 kilometers to the southwest near Theresa a small stream is named Soapstone Creek, suggesting more massive serpentinite or talc is yet to be rediscovered.

It appears that the Yellow Lake serpentinite first came to the attention of geologists in the mid-1980s when it was discovered by George Robinson and Michel Picard while on a St. Lawrence County mineral collecting excursion (G. Robinson, pers. comm.). Since that time, local mineral collectors have explored the outcrop and found nice sky blue apatite crystals and a few nicely formed pseudomorphs of serpentine after forsterite (S. Chamberlain, pers. comm.).

The outcrop is extensively fractured and incoherent, and because of this property, has been used locally as a source of rock aggregate and fill. Most of the exposure is composed of a dull yellow-green massive serpentine with abundant radiating dendrites of an unknown black oxide /hydroxide mineral coating fracture surfaces and disseminated throughout the massive serpentine (Figure 8). Small (2-20 cm wide) irregular veins of coarsely crystalline calcite cut through the unit, and it is within these veins that the blue apatite crystals (up to 3 cm long) are found. Pseudomorphs after forsterite occur along the sides of the veins (S. Chamberlain, pers. comm.). Pyrite, talc, and an unidentified Ca-Mg-silicate (possibly harkerite?) have also been found within these veins (Chamberlain and Bailey, unpub. data). Table 1 gives the composition of select mineral phases in the serpentinite, including Mn-rich dendritic growths and serpentine.

The occurrence of a relatively large body of ultramafic rock within the metasedimentary sequence of the Adirondack Lowlands is enigmatic; possible explanations for its origin include a localized accumulation of komatiitic ash, or an unusual clay-rich evaporite horizon within the carbonate sequence. Alternatively it may prove to be another block of highly altered ultramafic metaigneous rock such as that exposed at Pyrites. Additional field, mineralogical, and geochemical studies at this location and along this belt are needed to better understand this unusual ultramafic body and place it in its proper geologic context.

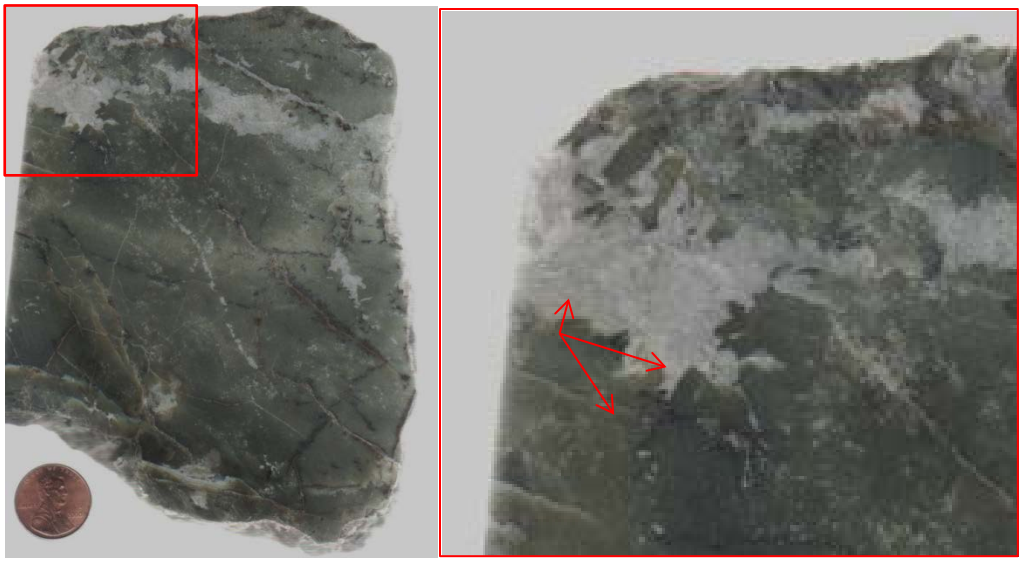

Figure 8. Cut slab of Yellow Lake serpentinite body showing dull green color, calcite pockets and veins, and massive nature. Note the irregular network of carbonate veins and black dendritic growths. The area in the red square has been enlarged in the right hand photograph to show the region where pseudomorphs after euhedral crystals, perhaps olivine, can be seen in the calcite pocket in the upper left of the left-hand figure.

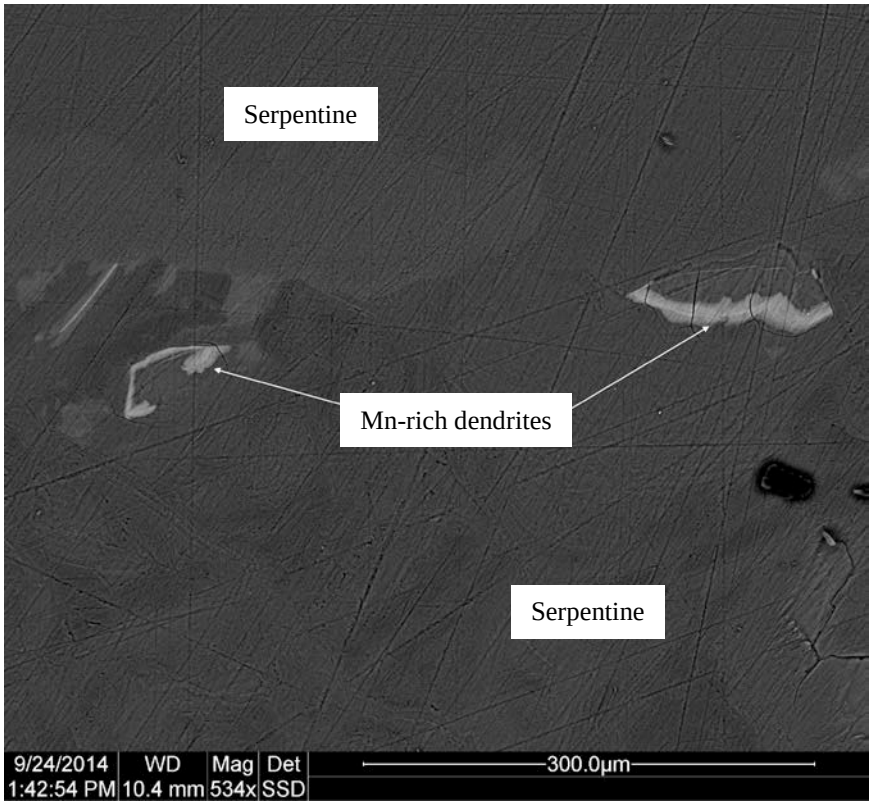

Figure 9. Scanning electron microscope back scatter image of the Yellow Lake serpentinite showing Mn-rich dendritic growths in a groundmass of serpentine.

Stop 3 Hornblendite near Elmdale
~1 mile north of Elmdale, right side of Rt. 58; Latitude 44°22'20", Longitude 75°33'14"

This outcrop consists largely of hornblendite whose age and origin is unknown. The rock falls along the general trend of serpentinite (last stop), and within a 40 kilometer linear, but highly disrupted, belt of amphibolite, pyritic gneisses, and metagabbro extending to the northeast from Yellow Lake to near Kendrew Corners, north of Dekalb. It is composed 1-2 centimeter blocky, equant black crystals of hornblende surrounded by k-feldspar, titanite, and apatite (Table 1 and Figures 10 and 11). The rock shows relatively little evidence of wholesale deformation but is cut by pegmatite, which is also undeformed.

Table 1. Composition (wt.%) of select mineral phases from Stops 2 and 3 (Analysis by David Bailey).

Sample	Serpentinite	Serpentinite	Hornblendite	Hornblendite	Hornblendite
Mineral	Serpentine	Mn-dendrites / serpentine	Epidote	Hornblende	K-Fsp
SiO2	51.93	39.17	38.32	42.73	64.95
TiO2				1.16	
Al2O3	0.08	0.52	20.12	13.57	19.84
FeO	1.64		12.46	17.50	
MnO		25.44			
MgO	46.35	30.27	0.80	10.10	
CaO		3.44	15.04	10.35	
BaO		1.15			1.56
Na2O				2.26	2.06
K2O				2.32	11.58
P2O5					
La2O3			4.21		
Ce2O3			8.15		
Sm2O3			0.91		
Total	100	100	100	100	100

Figure 10. Cut slab of the Elmdale hornblendite displaying large, equant hornblende crystals.

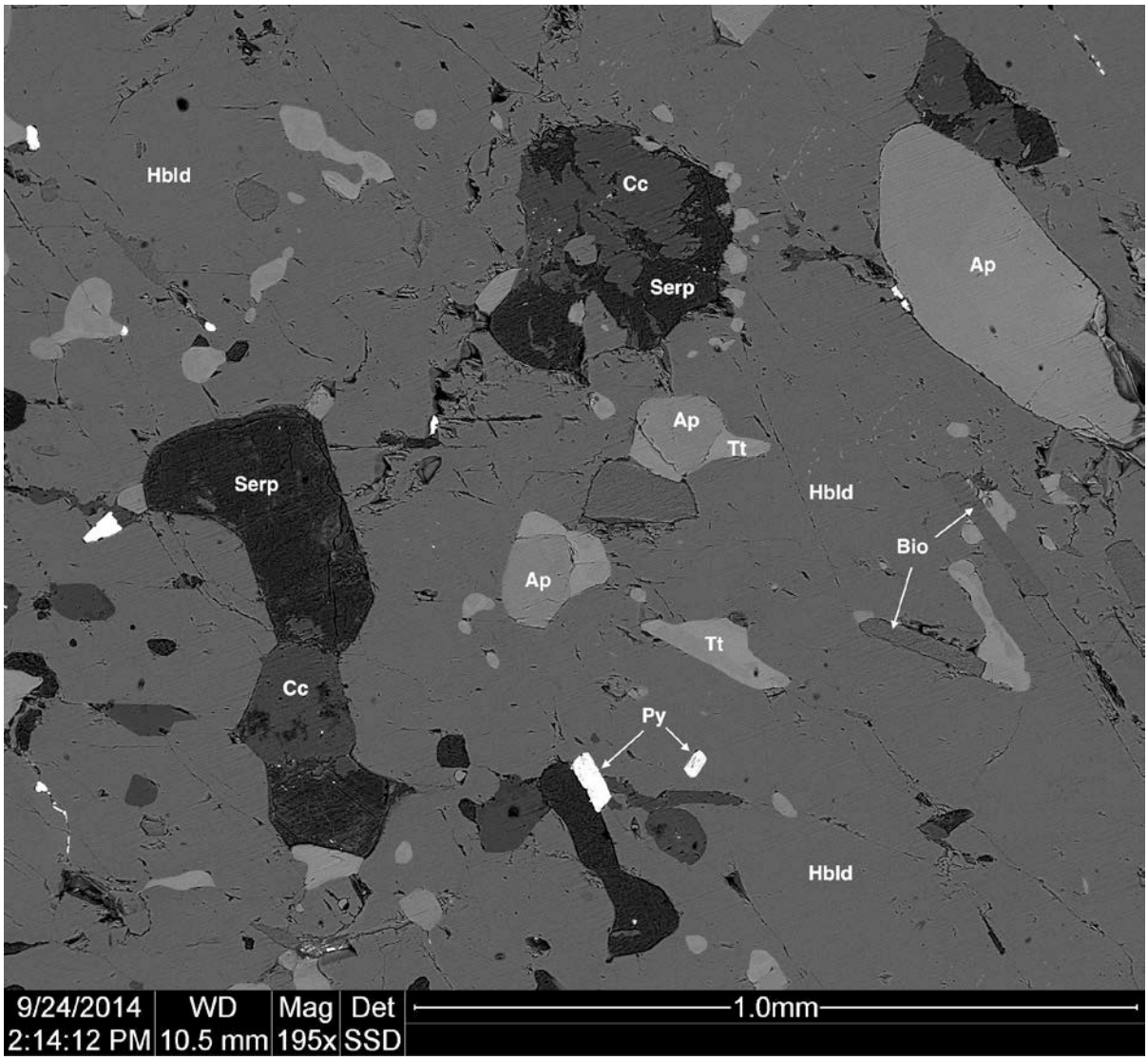

Figure 11. Scanning electron microscope back scatter image of the Elmdale hornblendite. Abbreviations: Ap-apatite; Bio-biotite; CC-calcite; Hbld-hornblende; K-spar-potassium feldspar; Py-pyrite; Serp-serpentine; Tt-titanite.

Hornblende-rich ultramafic rocks are relatively rare and can have a variety of origins. Detailed petrographic, geochemical, and geochronological study will hopefully provide further constraints on the origin of this rock. However, it may represent the one of the magmatic products of subduction in the Lowlands. Previous work has identified a strong subduction signature in many of the plutonic rocks exposed in the Lowlands (Figure 12; Chiarenzelli et al., 2010b). In particular, the lamprophyre dike we will see later in the day is indicative of this enriched mantle signature prevalent in mafic and ultramafic rocks of the Pyrites Complex as well.

Shawinigan plutonic suites in the Lowlands crosscut the fabric and isoclinal folds (Figure 5) in metasedimentary rocks of the Grenville Supergroup (Chiarenzelli et al., 2010a; Peck et al., 2013). The geochemistry and Nd signature of these plutonic suites (Antwerp-Rossie Suite, Hermon Granitic Gneiss, and Hyde School Gneiss), intruded between 1170-1200 Ma, mark the evolution of arc magmatism to granitic

magmatism of the Anorthosite-Mangerite-Charnockite-Granite suite prevalent in the Adirondack Highlands but also found in isolated plutons in the Lowlands (Peck et al., 2013). These rocks track the tectonic evolution of the region and underlying mantle dynamics.

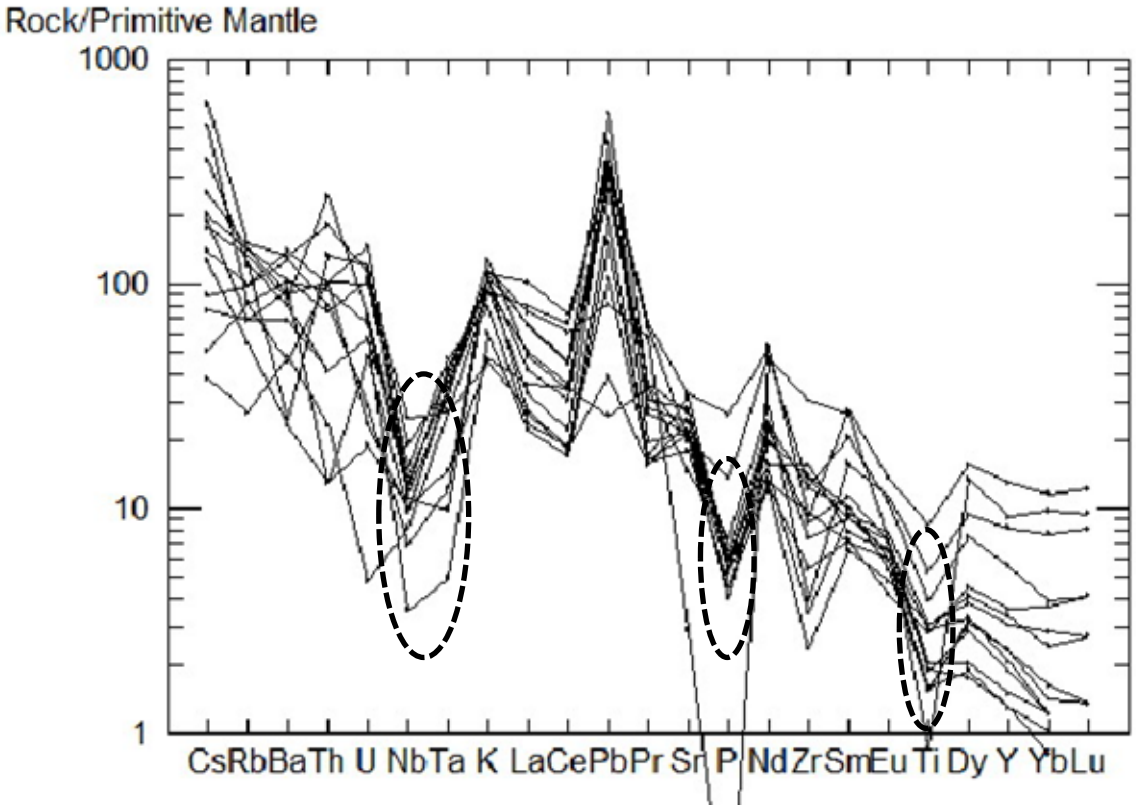

Figure 12. Incompatible element spidergram for the Antwerp-Rossie Suite. Note characteristic depletions in Nb, Ta, P, and Ti, typical of arc rocks. The hornblendite seen at this stop may be part of the suite.

Based on its state of deformation and geochemical affinities (alkali-rich), the hornblendite unit exposed here may be an ultramafic variant of the Antwerp-Rossie Suite. If this is verified, it would be the only ultramafic body yet recognized as part of the Antwerp-Rossie suite. Intrusive gabbros and diorites associated with the Antwerp-Rossie suite occur nearby at Pleasant Lake and Split Rock, and to the south near Balmat and Harrisville (see Carl, 2000; Chiarenzelli et al., 2011). If it is indeed part of the Antwerp-Rossie Suite, the hornblendite's occurrence along the linear trend of mafic and ultramafic rocks would be coincidental. However, like the serpentine body just investigated, the hornblendite occurs within a large belt of the Lower Marble. It may be an older tectonically emplaced block as will be demonstrated for the ultramafic rocks at Pyrites later in the trip. Regardless of its origin, this ultramafic rock is unique and has much to tell us about the geologic history of the Adirondack Highlands.

Stop 4 Contact between Pyritic gneiss and Ultramafic Rocks along the Grasse River
Dirt trail on right just after crossing the Grasse River on County Route 21 when headed east ; Latitude 44°31'24.7", Longitude 75°11'28.5"

The rocks at Pyrites lie with the triangular core zone of a large winged structure defined by amphibolite and gabbroic rocks that extends northeast from Stellaville (former site of the largest pyrite mine in St. Lawrence County) nearly 15 km to Crary Mills (red star, Figure 6 and Figure 13). The general shape of the structure

indicates it is folded and most of the amphibolitic rocks have a strong foliation and are highly disrupted by later magmatism. The belt of mafic and ultramafic rocks lies within marble. Although the actual surface exposure of the ultramafic rocks is modest (~ 1 km^2), the largest gravity anomaly in the region (Revetta and McDermott, 2003) extends from here southwest for about 10 kilometers (Figure 14). This suggests that it represents just a small part of the body and that a considerable mass of ultramafic rock, extending downward for some distance, lies parallel to the Carthage-Colton Shear Zone.

At this stop we will examine rocks associated with one of several pyrite mines that was in production between ca. 1880 to 1920 (Prucha, 1957) as a source of sulfur for industrial processes and sulfuric acid feedstock. Two adits can be seen on the side of the mustard-colored hill (Figure 15) as you approach the outcrop along the bank of the Grasse River. The adits intersect the steeply-dipping ore zone and the workings continued downward for as much as two hundred feet and extend underneath the river. On the bank, the rocks can be seen dipping steeply to the northwest and show differential weathering related to the variation in their mineral content and extent of weathering. Investigation at the top of the exposure shows the characteristic red coloration of pre-Potsdam weathering indicating that the unconformity was likely within a few feet of the current erosional level at the top of the hill.

The main ore zone consists of a ~2m thick planar layer of pyritic breccia. Examination of the rock at the outcrop, and in thin-section, indicates the ore is composed of rounded 1-2 cm fragments of breccia indicating enrichment of the ore during repeated fault movement. A black, rounded, 5 centimeter wide fragment composed of breccia within breccia can be seen at the foot of the hill within the primary ore zone. Carefully examination of the ore and surrounding rock reveals highly weathered lath-like crystals of sillimanite. Other minerals within the sequence include quartz, feldspar, mica, chlorite, sericite, garnet, graphite (Figures 16-18), and a host of trace minerals including pyrrhotite, rutile, sphalerite, chalcopyrite, molybdenite (Figure 17), and chromite (Tiedt and Kelson, 2008). Tiedt and Kelson (2008) suggest a possible biogenic origin for the pyrite on the basis of sulfur isotopes, in line with the presence of graphite. However, a hydrothermal volcanic influence is also possible based on the variety of metals found and association with mafic and ultramafic rocks.

In addition to a strong foliation and compositional layering, the sequence is cut by shallowly dipping veins which weather in positive relief. These veins are composed mostly of pyrite, minor pyrrhotite, and silica and represent a much later event in the history of the deposit. Early deformation is defined by compositional layering which is isoclinally folded. Thin seams of breccia less than a 1 cm wide can be seen cutting the foliation and/or folded layers in several areas in the exposure. Near the ore, within white feldspathic pods, relatively large, brown rutile crystals can be seen (Figure 18). Other non-sulfide minerals observed in the ore include chlorite, graphite, quartz, rutile, and monazite (Figure 18). Note the variation in resistance of the rocks to weathering, colors, and variation in layering as you walk upstream.

Towards the end of the accessible outcrop area along the river the rocks change in character and color to a massive, knobby weathering green ultramafic rock. The actual contact between the ultramafic rocks and metasedimentary sequence is well exposed in the wall of the river bank. Whether the contact is sedimentary or tectonic, or both, can be debated here. Regardless of the nature of the contact, the layered metasedimentary rocks become progressively greener in color and more Mg-rich towards the contact. Given the occurrence of chromite noted by Tiedt and Kelson (2008) in these rocks, proximity to ultramafic rocks during deposition is likely. Depositional along a transform fault is one possibility that could account for the juxtaposition of these two rock types and lend additional credibility to a deep water turbidity origin for the pyritic gneisses.

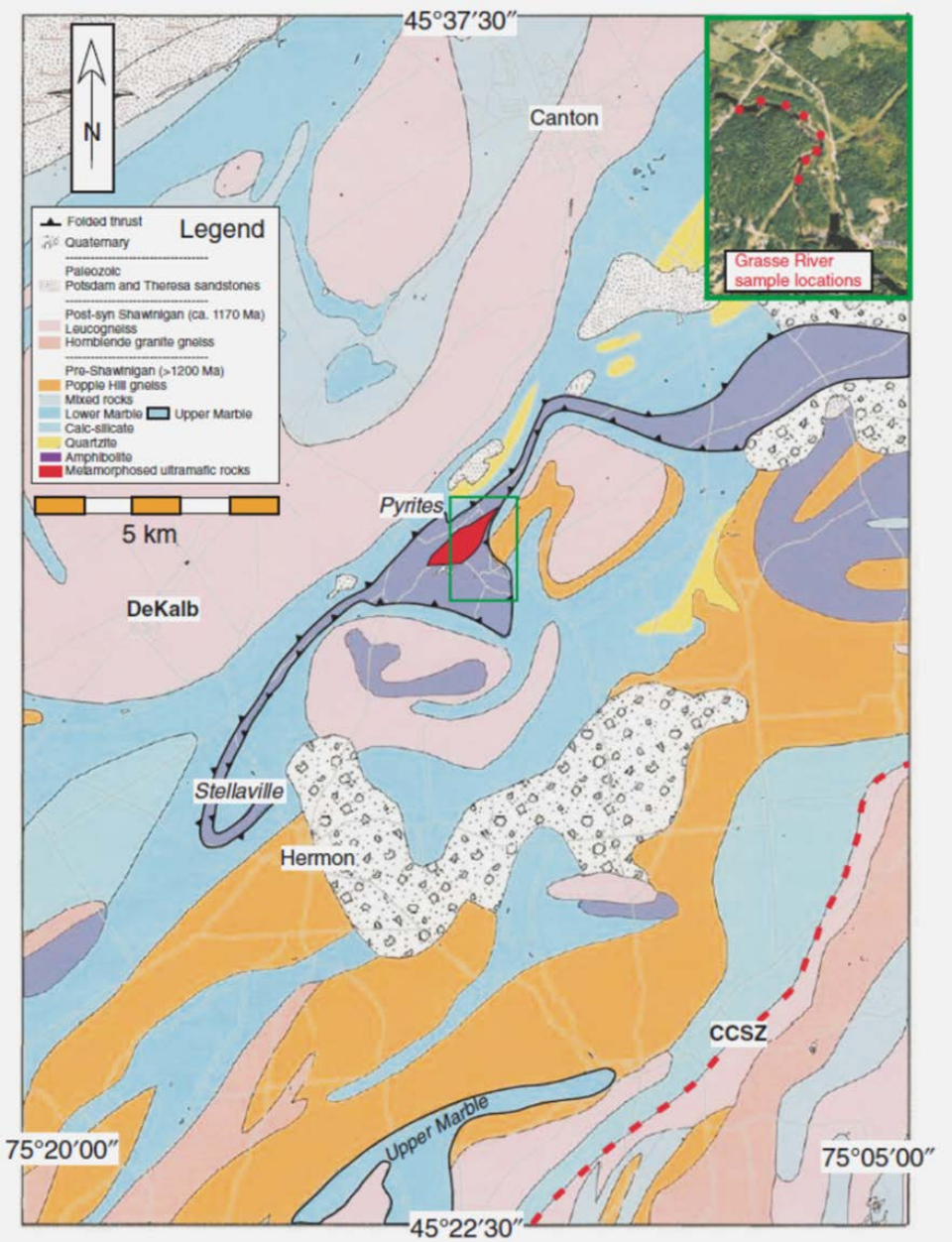

Figure 13. Geological map of the greater Pyrites area of the Adirondack Lowlands (geology modified from the Adirondack Sheet). Inset shows sample locations of ultramafic rocks plotted on a Google Earth image.

Several meters above the contact a large isoclinal fold can be seen. About the hinge of the fold, one can see both recessive and resistant cm-scale layering (Figure 19). The recessive layers consist of quartzofeldspathic gneiss with both sillimanite and garnet, whereas the more resistant layers consist of up to 85% or more quartz. This exposure provides insight into both the original nature of the layered metasedimentary rock and its metamorphic grade. Couplets of mud and sand are suggestive of a turbiditic sequence deposited in a relatively deep water setting. At some point, likely associated with the Shawinigan Orogeny (1150-1200 Ma), these rocks were intensely deformed and metamorphosed to Upper Amphibolite facies (garnet-sillimanite).

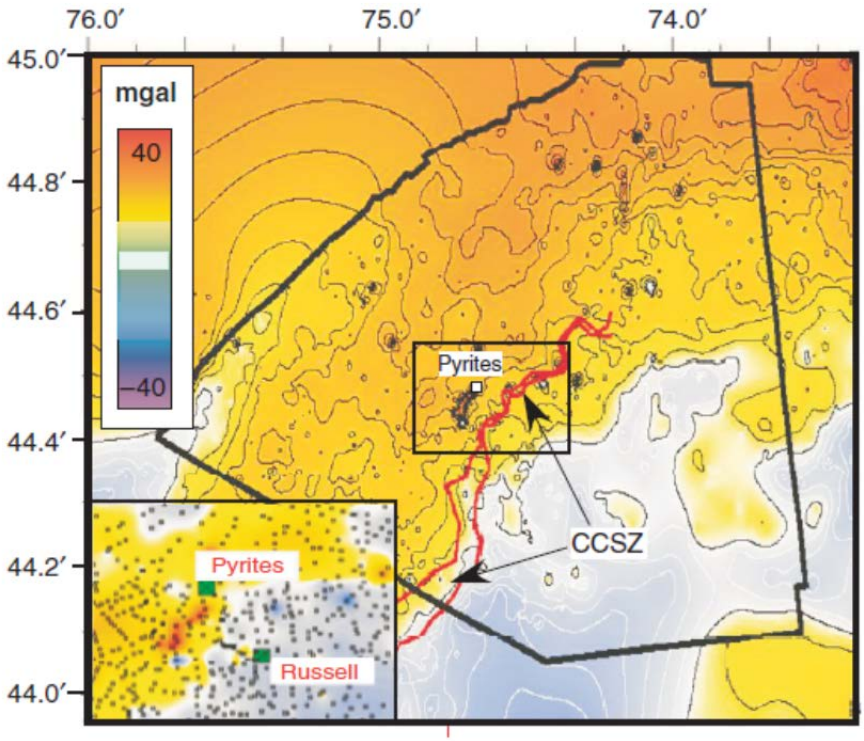

Figure 14. Gravity anomaly map of St. Lawrence County and surrounding environs. Inset shows the gravity anomaly associated with the exposure of ultramafic rocks at Pyrites and its extension to the southwest (after Revetta and McDermott, 2003).

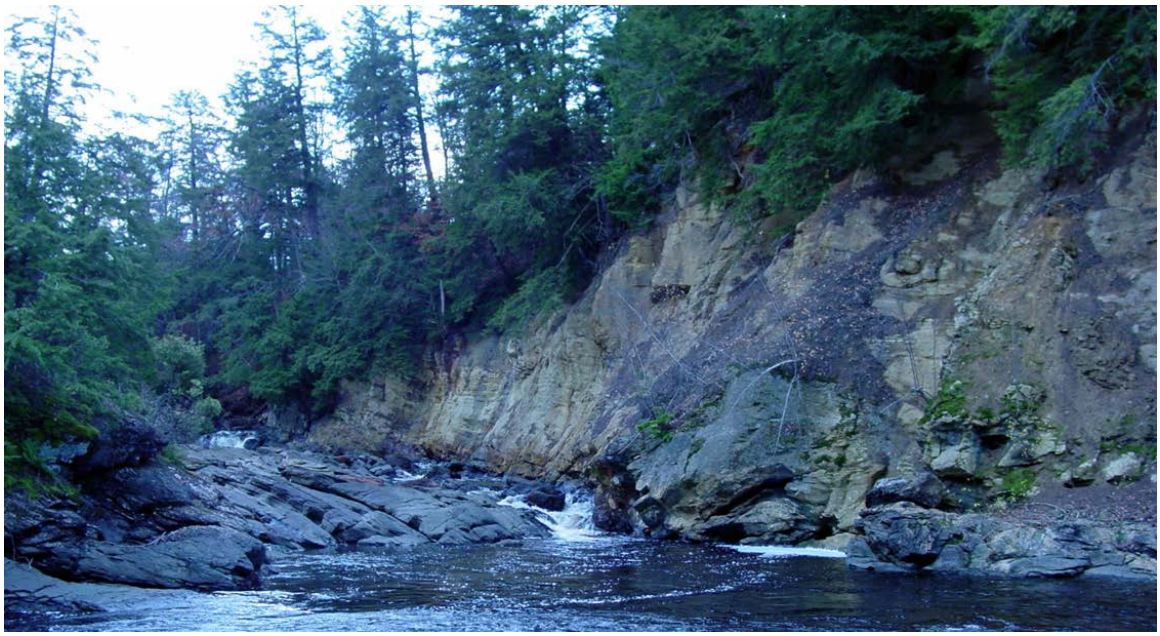

Figure 15. Field photograph showing the contact between the underlying mustard colored pyritic gneisses and underlying dark green ultramafic rocks along the Grasse River at Pyrites. The photograph was taken looking upstream from the Enel Hydropower Station.

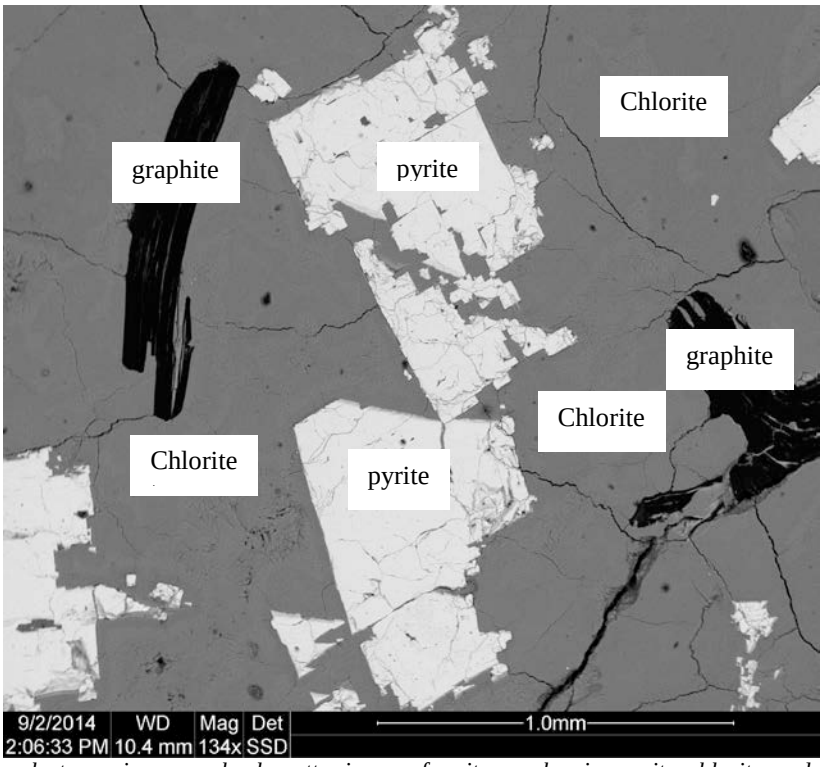

Figure 16. Scanning electron microscope back scatter image of pyrite ore showing pyrite, chlorite, and graphite characteristic of the ore.

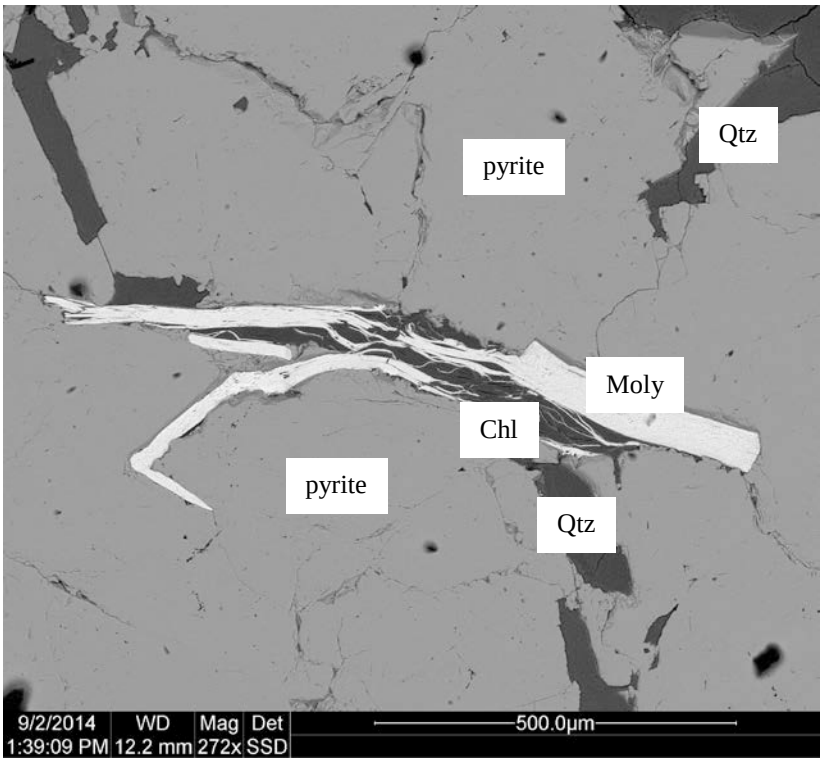

Figure 17. Scanning electron microscope back scatter image of pyrite ore showing pyrite, chlorite (Chl), quartz (Qtz), and molybdenite (Moly) characteristic of the ore.

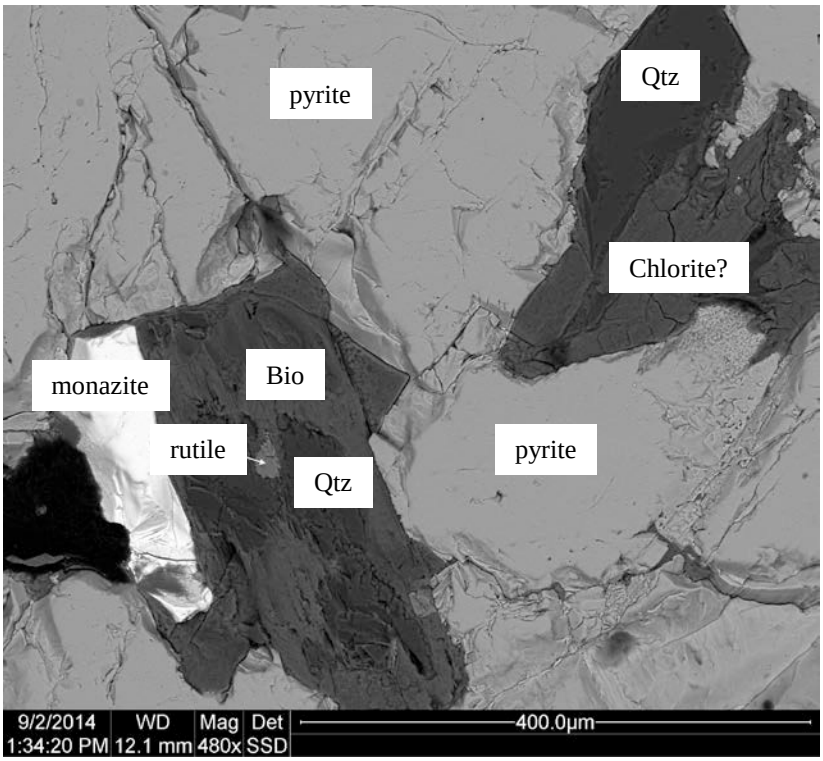

Figure 18 Scanning electron microscope back scatter image of pyrite ore showing pyrite, chlorite, quartz (Qtz), rutile, biotite,(Bio) and monazite.

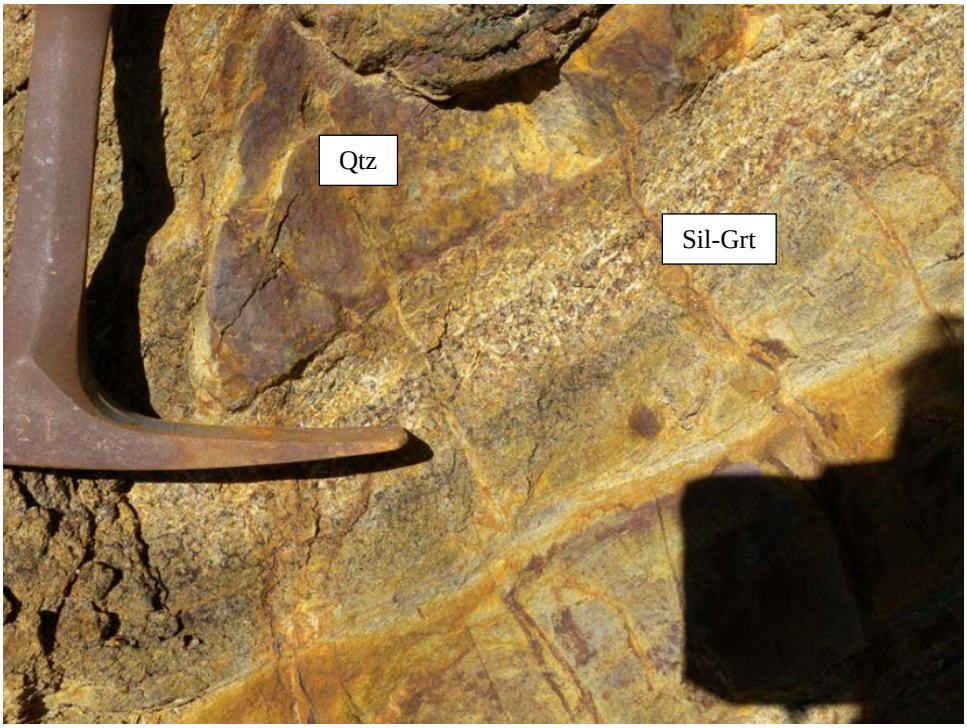

Figure 19. Nose of isoclinal fold showing resistant quartzite layers (Qtz) and recessive weathering garnet-sillimanite gneiss layers (Sil-Grt). Note gradual gradation in metamorphic mineral grain-size, indicative of original composition. Several of the thicker resistant layers were sampled for detrital zircon geochronology.

The thin, resistant, quartz-rich layers were sampled for detrital zircon geochronology and yield a sparse, but very homogeneous, population of detrital zircons. The zircons are between 25-100 microns in length, fairly euhedral, and zoned (inset Figure 20). Limited evidence of metamorphic rims or xenocrystic cores was found, despite BSE and CL imaging of cross-sectioned grains. The zircon yielded a near unimodal population of grains with a maximum depositional age of 1284+/-7 Ma (Figure 20). This result is compatible with a restricted source consisting of igneous zircon, perhaps derived from a sheet of rift-related volcanic rocks.

The massive green rock at the end of the outcrop is composed of a mass of hydrous secondary minerals including Mg-rich phases such as talc, tremolite, chlorite, serpentine, and phlogopite. While the vast majority of primary minerals are replaced, isolated core fragments of augite survive in addition to chromite. Consisting of ~40% SiO_2 and nearly 33% MgO, it also contains substantial amounts of Cr and Ni (Chiarenzelli et al., 2011). Its knobby texture likely represents the pseudomorphic replacement of large okiocrysts. Further upriver the ultramafic rock varies from peridotite to pyroxenite to layered ultramafic rocks (Figure 21) all highly altered and nearly completely pseudomorphically replaced (Figure 22). Nonetheless, original layering is frequently preserved and no indication of ductile deformation is found in stark contrast to the adjacent metasedimentary lithologies, which are isoclinally folded. Classification based on normative mineralogy determined by the CIPW method indicates that most ultramafic rocks are peridotites and a few pyroxenites, consistent with field observations (Figure 23).

The lower grade assemblage and undeformed nature of the ultramafic rocks appears to be at odds with the intensely folded garnet-sillimanite gneisses they are in contact with. This can be explained either juxtaposition of the rocks after peak metamorphic conditions or the competent and hydrous nature of the ultramafic rocks which contain as much as 10% H_2O.

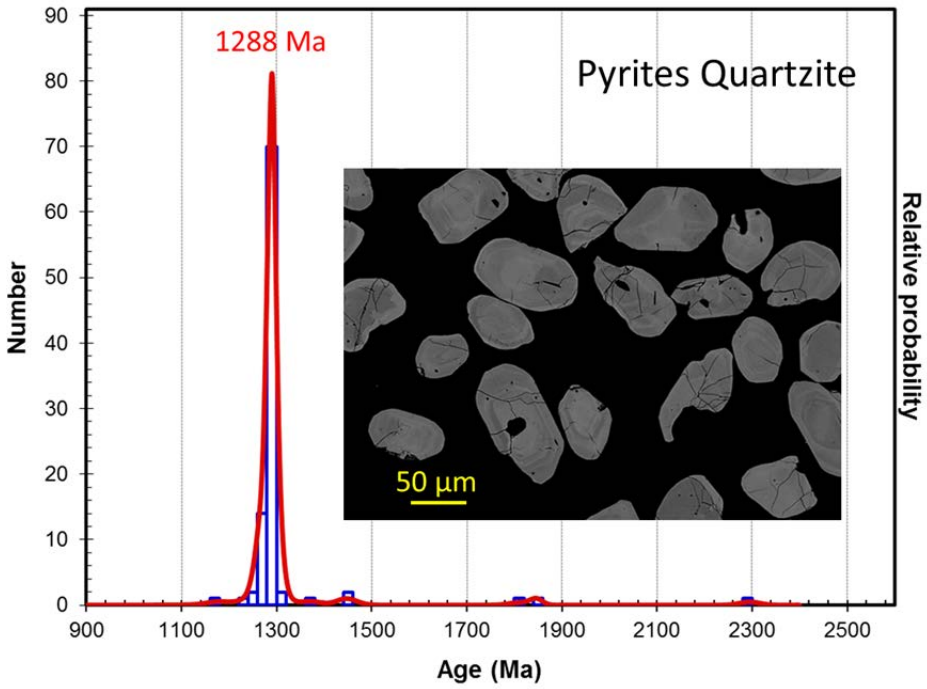

Figure 20. Analysis of ~100 detrital zircon grains yielded an essentially unimodal population with a peak at 1288 Ma. Statistical analysis indicates the rock was deposited at some point after 1284±7 Ma. Note the small size, zoning in BSE, and homogeneity in the zircon population shown in the insert.

Figure 21. Contact between knobby weathering pyroxenite (below) and overlying layered ultramafic rock (above).

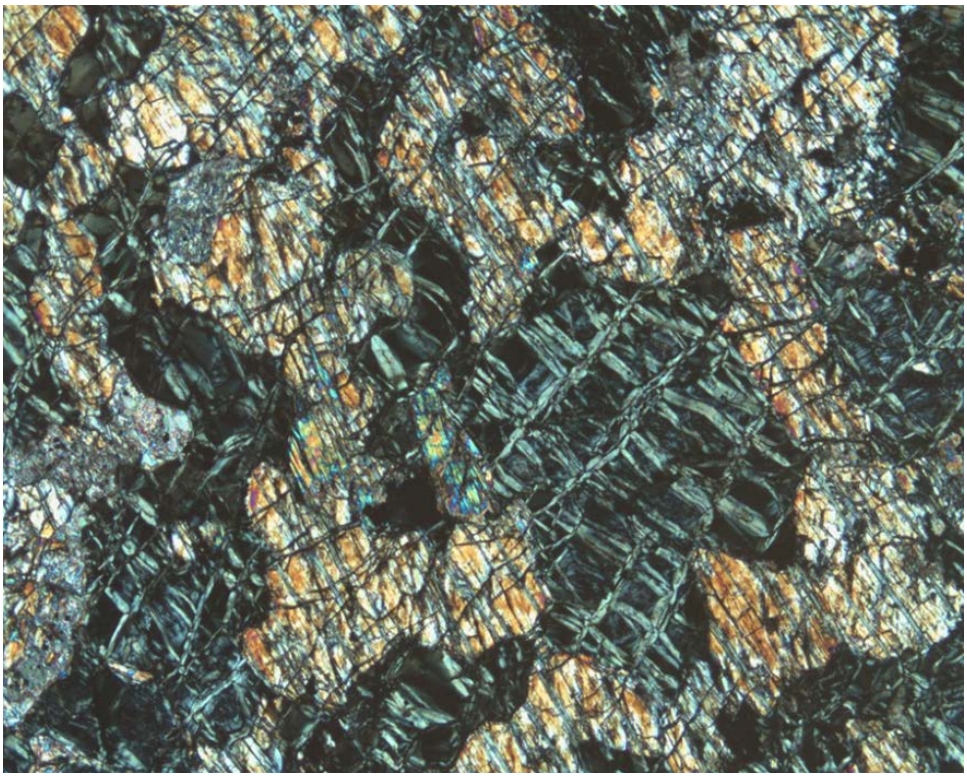

Figure 22. Photomicrograph showing pseudomorphic replacement of pyroxenite by a variety of hydrous secondary minerals including talc, chlorite, serpentine, and tremolite. The field of view is 4 mm and the photograph was taken with crossed polarizers.

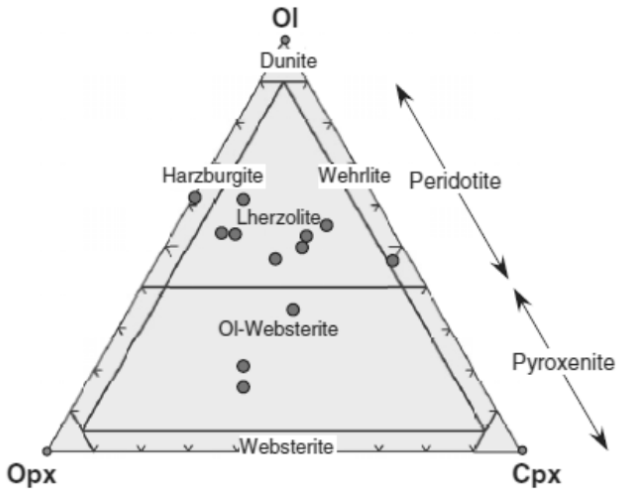

Figure 23. CIPW normative mineralogy classification of Pyrites ultramafic rocks.

Several attempts were made to directly determine the age of the ultramafic rocks. A range of rock types were analyzed for both Rb-Sr and Sm-Nd isotopes but unfortunately both systems appear to have undergone strong disturbance and provide isochron ages with large errors. Small zircons (~50-200 microns) were observed within thin mm-scale, calcite-rich veins in samples of both periodite and pyroxenite (Figure 24). Attempts to recover them were successful and isotopic analysis by laser ablation – inductively coupled plasma mass spectrometry (LA-ICP-MS) and Sensitive High Resolution Ion Microprobe (SHRIMP) were conducted.

Zircons from the peridotite were dated by SHRIMP in Perth, Australia and yielded an age of 1140±7 Ma with a few older grains yielding an age of 1202±20 Ma (Figure 25). Zircon from the pyroxenite were dated by LA-ICP-MS at the Arizona Laserchron Center and yielded and age of 1197±5 Ma (Figure 25). Given the unlikely occurrence of zircon as a magmatic product in silica-undersaturated rocks, these ages are thought to represent the timing of zircon growth during metamorphic events and thus provide only a minimum age for the ultramafic rocks. The ages correspond to the known effects of the Shawinigan Orogeny in the Lowlands from previous studies (Heumann et al., 2006).

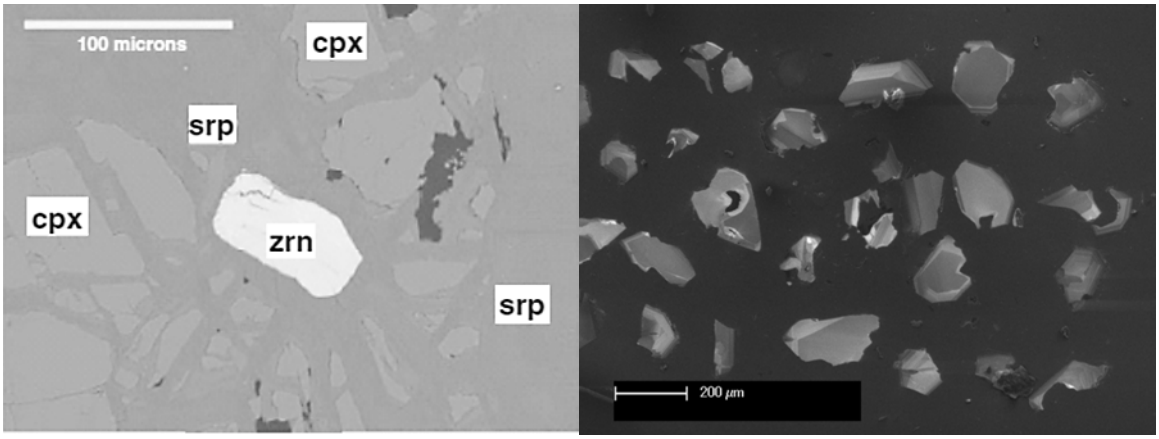

Figure 24. Left-hand side. Scanning electron microscope photograph in the back-scattered electron mode showing 80 micron long zircon (zrn) within secondary minerals including serpentine (srp). Augite (cpx) occurs as remnant cores which have undergone partial replacement. Right-hand side scanning electron microscope photograph in the cathodoluminscence mode showing zoning in zircons separated from pyroxenite.

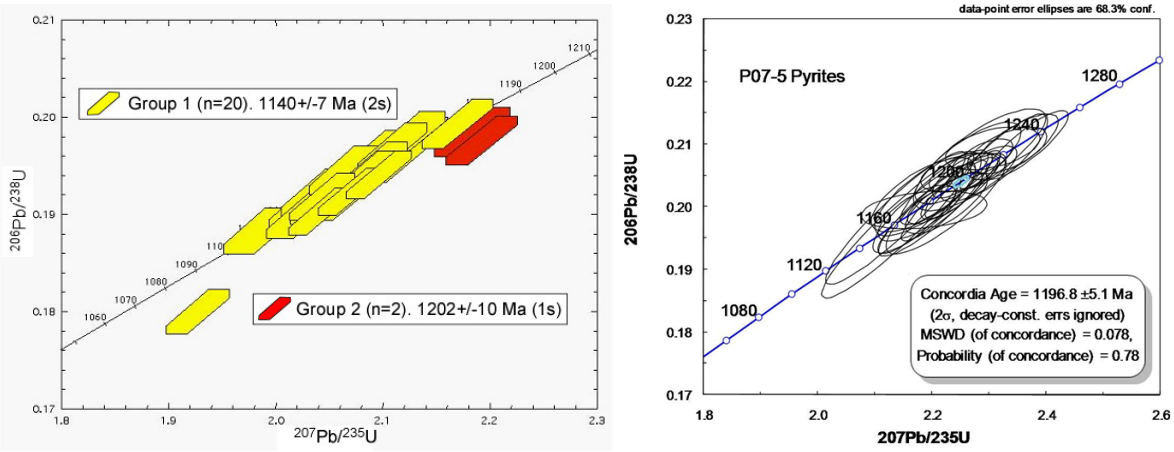

Figure 25. Left-hand side - Concordia diagram for zircons separated from peridotite and analyzed by SHRIMP at Curtin Technical University in Perth, Australia. Right-hand side - Concordia diagram from zircon separated from pyroxenite and analyzed by LA-MC-ICP-MS at the Arizona Laserchron Center.

Stop 5 Enel Hydropower Station on Grasse River at Pyrites
Entrance to Hydrostation is sharp right turn on to a dirt road which follows the penstock when headed south towards Pyrites on Churchill Street; Latitude 44°31'18.5", Longitude 75°11'17.1"

Our final stop will be just a few hundred meters upriver from the last stop at the Pyrites Enel Hydropower Station. This area is privately owned and off-limits to the public. Special arrangements have been made to bring our group here and the owners require prior submission of a liability waiver. If you wish to visit this site in the future please respect private property laws and get permission beforehand.

Along the back wall of the parking lot of the Enel Hydrostation a layered sequence of ultramafic rocks occurs. Here the layers dip steeply to the right. Obvious and widespread alteration can be seen and the rocks are composed of a variety of Mg-rich secondary minerals and are discolored by hematitic veins. Secondary minerals included substantial amounts of serpentine and few, if any, primary phases survive (Figure 26).

A number of layer perpendicular fractures occurs here (Figure 27) and appear to define columnar jointing, a typical cooling-related phenomena in some volcanic sequences. Preservation of columnar jointing seems unlikely, but the general appearance and alteration of these rocks is distinctly different than the mostly massive periodite and pyroxenite downriver. Here layering on the decimeter to meter scale is well developed. It is conceivable that the rocks are metamorphosed lavas, but, if so, they are ultramafic in composition!

Proceed carefully down from the parking lot to river. Here near the discharge from the Hydrostation, you can again see the contact between the pyritic gneisses and ultramafic rocks exposed in the far wall of the river bank. However, of special interest is a meter-wide lamprophyre dike consisting of large, cm-scale, phlogopite phenocrysts with a black serpentine-rich groundmass cutting the other ultramafic rocks (Figure 28). Again small areas of augite are preserved but little else. Large, euhedral apatite crystals, several millimeters in size are also abundant and likely a primary phase.

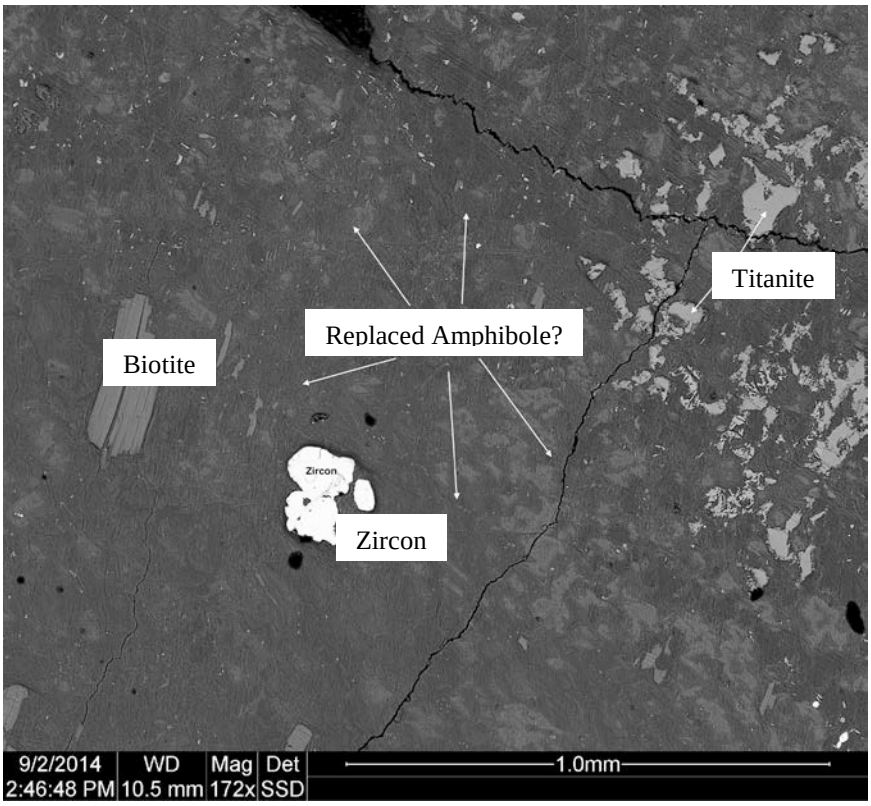

Figure 26. Strongly altered ultramafic rock composed almost exclusively of secondary hydrous magnesium silicates.

Figure 27 Dipping ultramafic rocks in parking lot of Enel Hydropower Station in Pyrites, New York. Note meter to decimeter-scale layering and set of fractures perpendicular to the layers. Field book for scale.

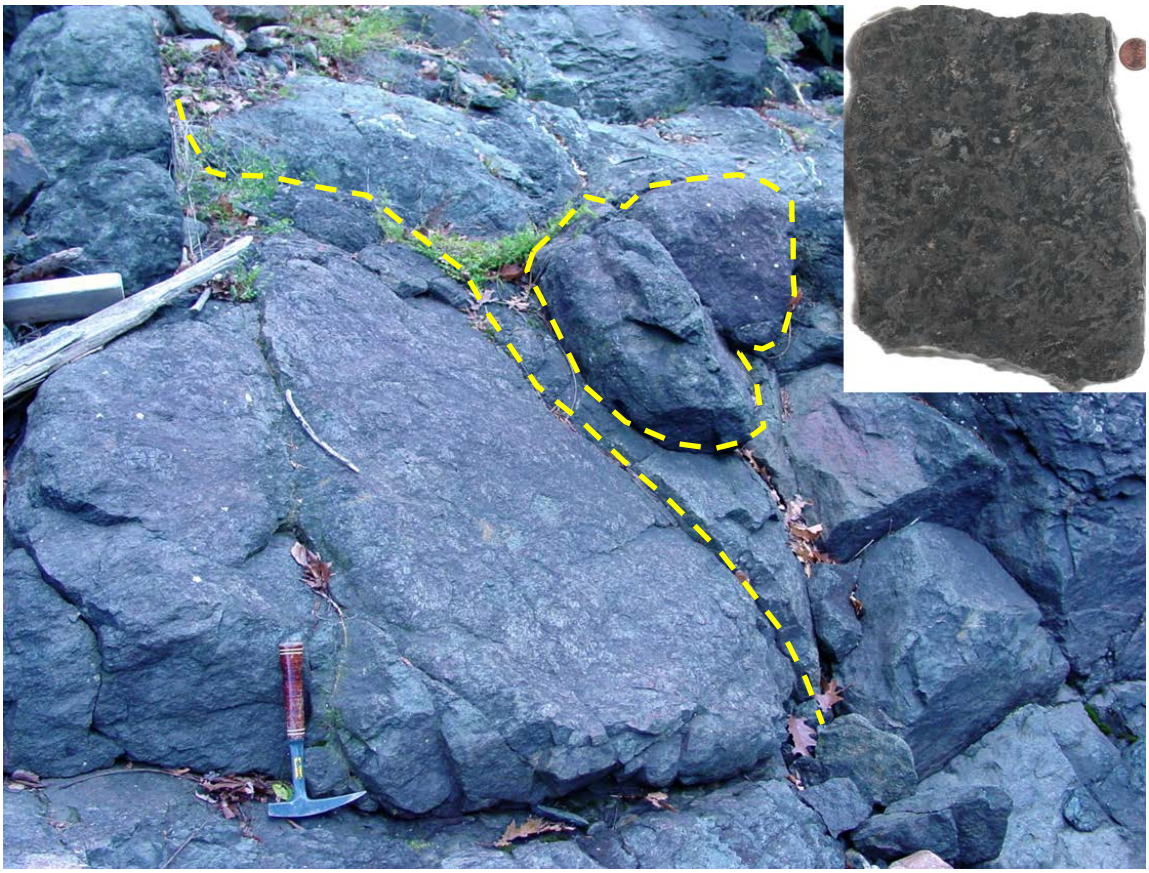

Figure 28. Field photograph of the lamprophyre dike (foreground) cross-cutting ultramafic rocks (background) at Pyrites, New York. Insert shows cut and polished slab of lamprophyre showing its texture and coarse grain-size. Dashed line shows approximately contact of dike with altered peridotite.

The geochemistry of this rock indicates substantial enrichment in incompatible elements and suggests derivation from metasomatized mantle. Despite having just 33% SiO_2 a population of zircons was separated from this rock. The zircons, nearly all concordant, gave an age of 1183±6 Ma with individual grains as old as 1213±16 Ma (Figure 29), again indicative of growth during Shawinigan metamorphism or conversely, intrusion at that time. If the zircons do indeed mark the time of intrusion they are likely related to arc magmatism associated the Antwerp-Rossie suite (ca. 1200 Ma).

Further upriver these rocks are in structural contact with a sequence of gabbroic rocks cut by finer-grained dikes. The gabbros appear exceptionally coarse-grained, baseball-sized (Figure 30), however, this appears to be the consequence of anastomosing, closely-spaced shear zones and the widespread growth of coarse phlogopite rather than the original grain-size. Some low strain domains between the sheared areas show a typical gabbroic texture. Samples of gabbro and a fine-grained dike rock cutting the gabbro share similar geochemical and isotope trends with the ultramafic rocks and are likely part of the same sequence. Given the occurrence of ultramafic rocks, gabbros, amphibolites, and sulfide deposits Chiarenzelli et al. (2011b) interpreted the Pyrites Complex as a highly dismembered and intruded ophiolitic complex. If so, it must be in thrust contact with shallow water metasedimentary marbles of the Grenville Supergroup it is often enveloped by.

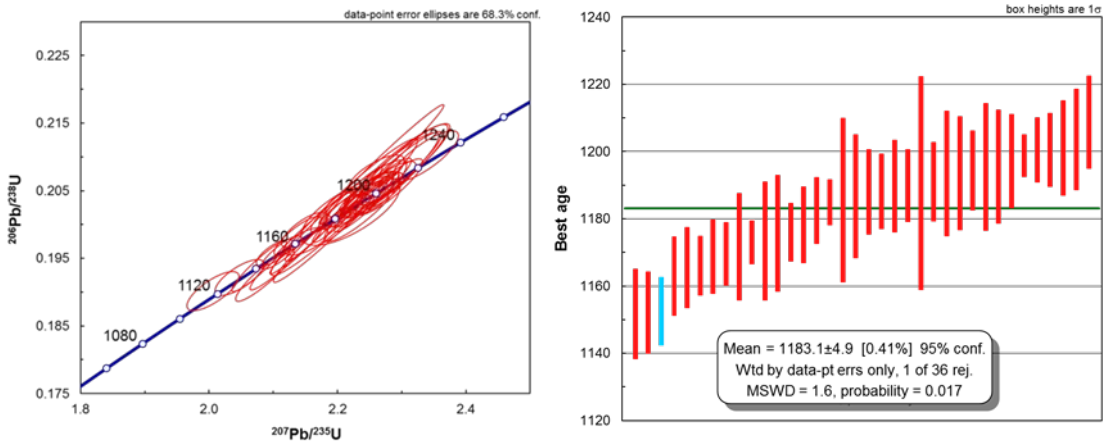

Figure 29. Left-hand side - Concordia diagram for zircon from the Pyrites lamprophyre dike showing spread of concordant data point. Right-hand side - Weighted mean age calculation for zircon separated from the pyrites lamprophyre. Note that concordant analyses yield a range of ages from ~1150-1210 Ma.

Figure 30. Gabbroic gneiss upriver of the Pyrites Enel Hydrostation. Note interesting fabric created by anastomosing shear zones of phlogopite.

ACKNOWLEDGMENTS

We would like to acknowledge the financial support of the James S. Street Fund at St. Lawrence University. Drs. Eric Thern (Curtin Technical University), Brian Cousins and Lyndsey Coffin (Carleton University), George Gehrels (Arizona Laserchron Center), and Sean Regan (UMass) are thanked for their help with geochronology and isotopic analysis. St. Lawrence students Peter Christoffersen, Ashley Durham, Hillary Hagen-Peter, and Thomas Lockwood participated in data collection. The authors have benefited from discussion with many of our colleagues including Larry Aspler, William deLorraine, J. Allan Donaldson, Yngvar Isachsen, James McLelland, William Peck, Bruce Selleck, Phil Whitney, and David Valentino. Chiarenzelli would like to thank his undergraduate mentors at St. Lawrence University, Drs. William Elberty, William Romey, and Char Mehrtens, for imparting a sense of wonder and insatiable curiosity for the study of the geology.

REFERENCES CITED

Barford, G. H., Krogstad, E. J., Frei, R., and Albarède, F., 2005, Lu-Hf and PbSL geochronology of apatites from Proterozoic terranes: A first look at Lu-Hf isotopic closure in metamorphic apatite: Geochimica et Cosmochimica Acta, v. 69, p. 1847-1859.

Buddington, A. F., 1934. Geology and mineral resources of the Hammond, Antwerp, and Lowville quadrangles. New York State Museum Bulletin No. 296, University of the State of New York, 251p.

Carl, J. D., 2000, A geochemical study of amphibolites layers and other mafic rocks in the NW Adirondack Lowlands, New York: Northeastern Geology and Environmental Sciences, v. 22, p. 142-166.

Chiarenzelli, J. and McLelland, J., 1993, Granulite facies metamorphism, paleoisotherms, and disturbance of the U-Pb systematics of zircon in anorogenic plutonic rocks from the Adirondack Highlands. Journal of Metamorphic Geology, v. 11, p. 59-70.

Chiarenzelli , J., Kratzman, D., Selleck B., and deLorraine, W., in review, Opening, spreading, and closing of a Mesoproterozoic back-arc basin: tectonic evolution tracked by detrital zircons in upper amphibolite facies rocks: Submitted to Geology, July 29th, 2014.

Chiarenzelli, J.R., Hudson, M.R., Dahl, P.S., and deLorraine, W.D., 2012, Constraints on deposition in the Trans-Adirondack Basin, northern New York; composition and origin of the Popple Hill Gneiss: Precambrian Research, v. 214-215, p. 154-171.

Chiarenzelli, J., Lupulescu, M., Thern, E., and Cousens, B., 2011a. Tectonic implications of the discovery of a Shawinigan ophiolite (Pyrites Complex) in the Adirondack Lowlands: Geosphere, v. 7, no. 2; 2, p. 333-356.

Chiarenzelli, J., Valentino, D., Lupulescu, M., Thern, E., and Johnston, S., 2011b, Differentiating Shawinigan and Ottawan Orogenesis in the Central Adirondacks: Geosphere, v. 7, p. 2-22.

Chiarenzelli, J., Regan, S., Peck, W.H., Selleck, B.W., Cousens, B., Baird, G.B., and Shrady, C.H., 2010a, Shawinigan arc magmatism in the Adirondack Lowlands as a consequence of closure of the Trans-Adirondack backarc basin: Geosphere, v. 6, no. 6; 6, p. 900-916.

Chiarenzelli, J., Lupulescu, M., Cousens, B., Thern, E., Coffin, L., and Regan, S., 2010b, Enriched Grenvillian lithospheric mantle as a consequence of long-lived subduction beneath Laurentia: Geology, v. 38, p. 151-154.

deLorraine, W.F., 2001, Metamorphism, polydeformation, and extensive remobilization of the Balmat zinc orebodies, northwest Adirondacks, New York: Guidebook Series [Society of Economic Geologists [U.S.], v. 35, p. 25-54.

de Lorraine, W. F. and Sangster, A. L., 1997, Geology of the Balmat Mine, New York: Field Trip A5, Geological Association of Canada/Mineralogical Association of Canada Joint Annual Meeting, Ottawa, 43p.

Dickin, A.P., and McNutt, R.H., 2007, The Central Metasedimentary Belt (Grenville Province) as a failed back-arc rift zone; Nd isotope evidence: Earth and Planetary Science Letters, v. 259, no. 1-2; 1-2, p. 97-106.

Dickin, A. P. and Higgins, M. D., 1992. Sm/Nd evidence for a major 1.5 Ga crust-forming event in the central Grenville province: Geology, v. 20, p. 137-140.

Heumann, M.J., Bickford, M.E., Hill, B.M., McLelland, J.M., Selleck, B.W., and Jercinovic, M.J., 2006, Timing of anatexis in metapelites from the Adirondack lowlands and southern highlands; a manifestation of the

Shawinigan Orogeny and subsequent anorthosite-mangerite-charnockite-granite magmatism: Geological Society of America Bulletin, v. 118, no. 11-12, p. 1283-1298.

Isachsen, Y.W., and Fisher, D.W., 1970, Geologic map of New York: Adirondack sheet: New York State Museum, Map and Chart Series 15, scale 1:250000.

Logan, W. E., 1863, Geology of Canada, Geol. Survey of Canada, Report of Progress from Commencement to 1863.

Lupulescu, M., Chiarenzelli, J., Pullen, A., and Price, J., 2011, Using pegmatite geochronology to constrain temporal events in the Adirondack Mountains: Geosphere, v.7, p. 23-39.

Peck, W., Selleck, B., Wong, M., Chiarenzelli, J., Harpp, K., Hollocher, K., Lackey, J., Catalano, J., Regan, S., and Stocker, A., 2013, Orogenic to postorogenic (1.20–1.15 Ga) magmatism in the Adirondack Lowlands and Frontenac terrane, southern Grenville Province, USA and Canada: Geosphere, v. 9, p. 1637-1663.

Peck, W.H., Valley, J.W., Corriveau, L., Davidson, A., McLelland, J., and Farber, D.A., 2004, Oxygen-isotope constraints on terrane boundaries and origin of 1.18–1.13 Ga granitoids in the southern Grenville Province: in: Tollo, RP, Corriveau, L, McLelland, J, and Bartholomew, MJ, (Eds.), Proterozoic tectonic evolution of the Grenville orogen in North America: Boulder, Colorado, Geological Society of America Memoir 197, p. 163-182.

Prucha, J., 1957. Pyrite deposits of St. Lawrence and Jefferson Counties, New York: New York State Museum Bulletin No. 357, The University of the State of New York, 87 p.

Revetta, F.A., and McDermott, A. M., 2003, The compilation and preparation of high resolution gravity data for petroleum exploration in New York State and adjoining regions: New York State Energy Research Development Authority (NYSERDA) PON #715-02

Rivers, T., 2008. Assembly and preservation of lower, mid, and upper orogenic crust in the Grenville Province – Implications for the evolution of large hot long-duration orogens: Precambrian Research, v. 167, p. 237-259.

Sager-Kinsman, A. E. and Parrish, R. R., 1993, Geochronology of detrital zircons from the Elzevir and Frontenac terranes, Central Metasedimentary Belt, Grenville Province, Ontario, Can. J. Earth Sci. , v. 30, p. 465–473.

Tiedt, K. and Kelson, C., 2008, Geochemical and mineralogical characterization of ore from the Pyrites and Stella pyrite deposits, St. Lawrence County, NY.: Geol. Soc. Am., Abstr. Program v. 40, p. 6.

Wong, M.S., Peck, W.H., Selleck, B.W., Catalano, J.P., Hochman, S.D., and Maurer, J.T., 2011. The Black Lake Shear Zone: A boundary between terranes in the Adirondack Lowlands, Grenville Province: Precambrian Research, v. 188, p. 57-72.

Trip B-2 Mileage and Road Log								
Distance	Cumulative			Latitude	Longitude			
0.0	0.0	Big M Parking lot Alexandria Bay, SH 12		N 44° 19' 38"	W 75° 55' 09"			
0.4	0.4	Turn right on to Church Street/SH 26		N 44° 19' 55"	W 75° 54' 52"			0.41
3.7	4.1	Turn right at Browns Corners and stay on SH 26 pass		N 44° 17' 56"	W 75° 51' 23"			3.66
		through Plessis						
4.7	8.7	Right hand turn on to SH 37		N 44° 14' 47"	W 75° 48' 59"			4.66
1.7	10.4	Left hand turn on to CR 193/SH 26 at Coopers Corners		N 44° 13' 22"	W 75° 49' 18"			1.68
0.8	11.2	Turn left on to Main Street/SH26		N 44° 13' 01"	W 75° 48' 28"			0.78
0.6	11.7	Turn left on to Commerical Street/SH 26 downtown Theresa		N 44° 12' 55"	W 75° 47' 51"			0.55
0.5	12.2	Turn right on to Miller Street /SH 26		N 44° 13' 01"	W 75° 47' 18"			0.50
5.8	18.0	Turn left at traffic light in Philadelphia on to SH 11		N 44° 09' 32"	W 75° 42' 23"			5.80
4.9	22.9	Park on right, outcrop on left hand (north) side of SH 11		N 44° 11' 42"	W 75° 37' 28"			4.90
		just west of Antwerp						
Stop 1: Antwerp Amphibolite (Please exercise extreme caution crossing SH 11)								
0.4	23.4	Continue on SH 11 then turn left on to CR 24		N 44° 12' 46"	W 75° 36' 54"			0.44
5.9	29.3	Turn left on to CR 25 pass through Oxbow		N 44° 17' 13"	W 75° 36' 43"			5.89
1.7	31.0	Bear right and continue on CR 10		N 44° 18' 01"	W 75° 37' 43"			1.72
3.2	34.2	Turn right on to Liscom/Hall/Yellow Lake Road		N 44° 20' 29"	W 75° 36' 07"			3.20
3.1	37.3	Turn right on to Campbell Road		N 44° 21' 37"	W 75° 33' 22"			3.10
1.9	39.2	Park, outcrop on left hand (south) side of Campbell Road		N 44° 20' 19"	W 75° 34' 46"			1.94
Stop 2: Yellow Lake Serpentinite (Private property, permission required)								
1.9	41.2	Reverse direction and return on Campbell Road,		N 44° 21' 37"	W 75° 33' 22"			1.94
		turn right on Yellow Lake Road						
1.0	42.2	Turn left on to SH 58, travel 1 mile north		N 44° 21' 41"	W 75° 32' 52"			1.00
0.9	43.1	Park, outcrop on right (east side) of road		N 44° 22' 20"	W 75° 33' 14"			0.88
Stop 3: Yellow Lake Hornblendite (Please exercise extreme caution crossing SH 58)								
2.4	45.5	**Carefully** reverse direction onto SH 58 head south until		N 44°20'34"	W 75° 32'7.5"			2.44
		Gravel-Beaman-Seavey-Welsh Road turn left towards						
		Richville, pass dolomite quarry on right						
12.5	57.9	Continue on SH 58, through Dekalb Jct. and turn right on		N 44° 32' 16"	W 75° 13' 58"			12.45
		Eddy-Pyrites Road, cross Harrision Creek						
2.4	60.3	Turn left on to CR 21		N 44° 31' 20"	W 75° 11' 41"			2.40
0.2	60.5	Cross Bridge over Grass River, park on right and follow		N 44° 31' 25"	W 75° 11' 32"			0.17
		dirt path to outcrop along east bank of the river						
Stop 4: Pyrites Complex and overlying Metasedimentary Rocks								
0.2	60.7	Continue on CR 21 turn right on Churchill Street towards		N 44° 31' 33"	W 75° 11' 21"			0.19
		Pyrites Village						
0.4	61.0	Sharp right hand turn on to dirt road following pensotck		N 44° 31' 13"	W 75° 11' 12"			0.38
		(big green pipe) to Enel Hydropower Station						
Stop 5: Pyrites Complex and Lamprophyre Dike (Private property permission required)								
End of Trip (Return from whence you came)								

Stop 1 Amphibolite and Pyritic Gneisses near Antwerp

<1 km southwest of Antwerp, along Rt. 11; Latitude 44°11'41.7", Longitude 75°37'28.8"

Stop 2 Yellow Lake Serpentinite
~8.5 km west of Gouverneur, off of Campbell Rd between Yellow Lake and the Oswegatchie River; Latitude 44°20’14.3”, Longitude 75°34’47.8

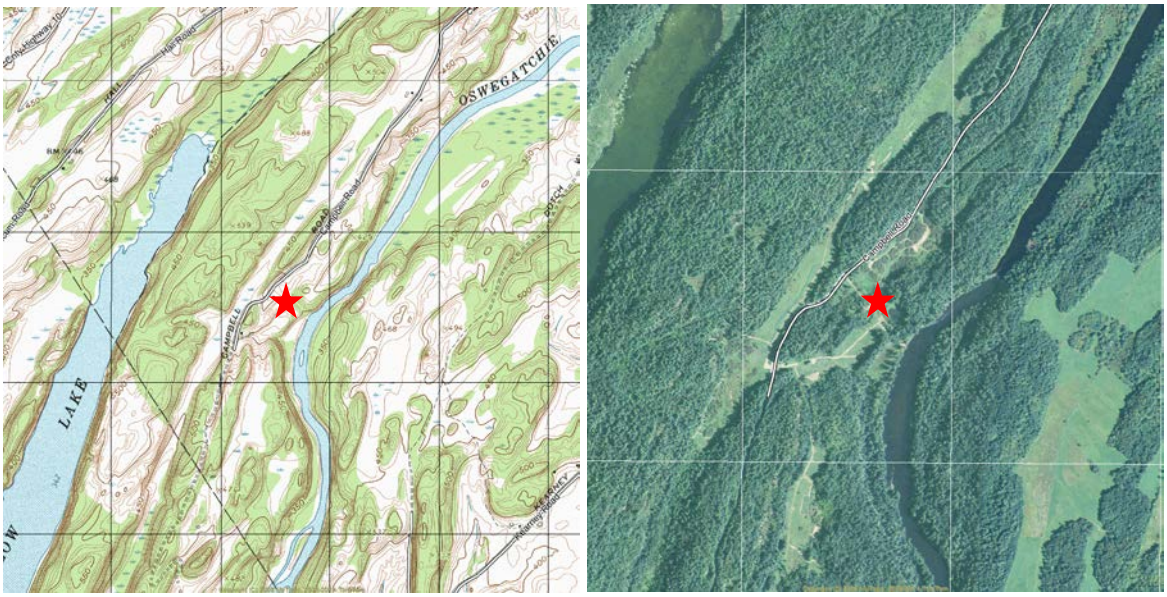

Stop 3 Hornblendite near Elmdale
~1 km north of Elmdale, along Rt. 58; Latitude 44°22'19.5", Longitude 75°33'14.02"

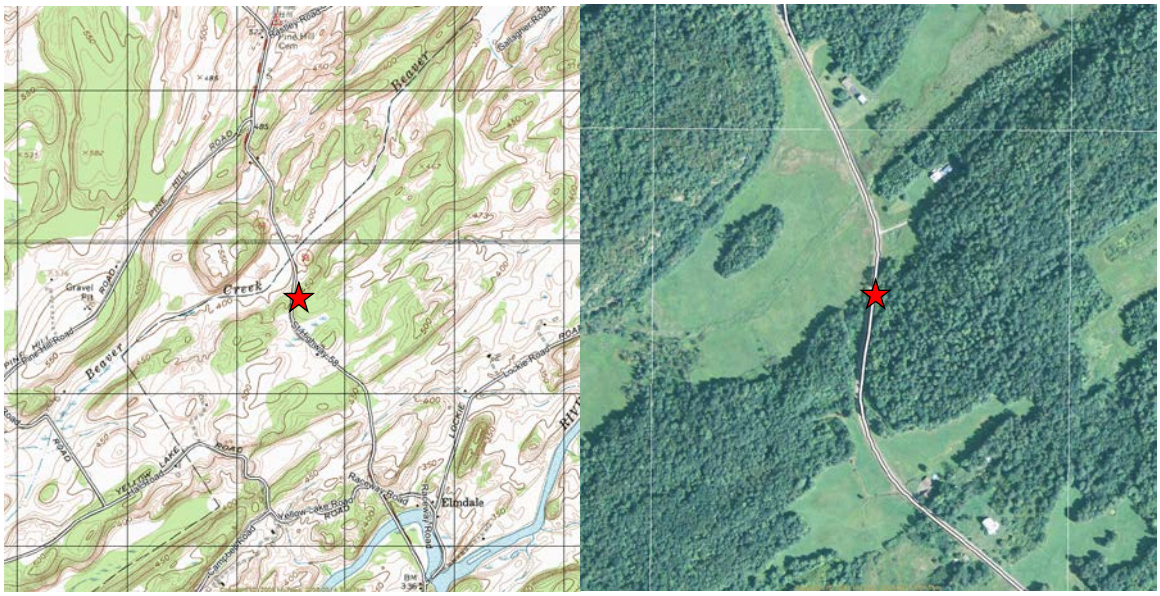

Stop 4 Contact between Pyritic gneiss and Ultramafic Rocks along the Grasse River
Dirt trail on right just after crossing the Grasse River on County Route 21 when headed east ; Latitude 44°31'24.7", Longitude 75°11'28.5"

Stop 5 Enel Hydropower Station on Grasse River at Pyrites
Entrance to Hydrostation is sharp right turn on to a dirt road which follows the penstock when headed south towards Pyrites on Churchill Street; Latitude 44°31'18.5", Longitude 75°11'17.1"

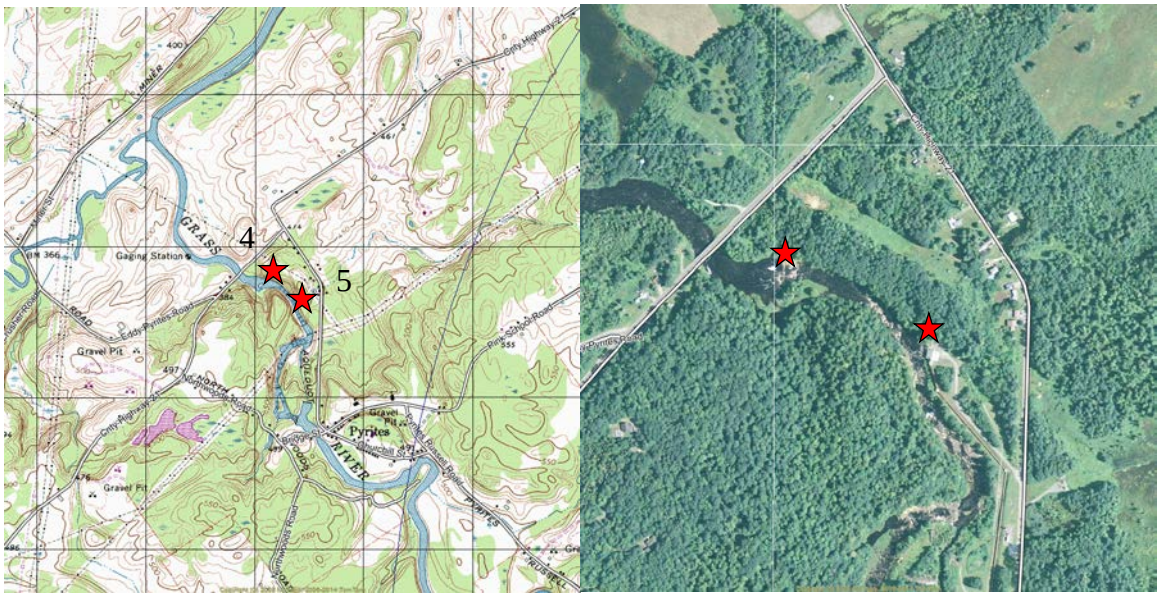

METAMORPHIC PETROGRAPHY BETWEEN TUPPER LAKE AND BLUE MOUNTAIN LAKE

ROBERT BADGER, JAMES CARL, AND KYLE ASHLEY*

Department of Geology, SUNY Potsdam
Potsdam, NY 13676
*Dept. of Geology, Virginia Tech

INTRODUCTION

This trip was led for the 2004 NYSGA. Since that time students have examined two additional outcrops on the trip, so we now have additional probe and petrographic data.

This trip examines the petrography and petrology of roadside outcrops along Route 30 between Tupper Lake and Blue Mountain Lake. As with most Adirondack rocks, these have been intensely metamorphosed. Lost during the metamorphism are the features which distinguish sedimentary rocks from extrusive and intrusive igneous rocks. Their intrusive igneous textures and/or content of fossils, clay minerals, layers of volcanic lava and ash, have long since been transformed. We will visit outcrops of marble and quartzite that clearly represent metamorphosed limestone and sandstone, and amphibolites that most likely were basaltic dikes. Most rocks, however, are gneisses with varying proportions of feldspars, quartz, amphibole, pyroxene and garnet. Without geochemical analysis, it is sometimes difficult to determine if their protolith was an igneous or sedimentary rock. We draw your attention to features at the outcrop that support our interpretations; color microphotographs will be provided at most stops. We anticipate lively discussion of interpretations about the outcrops.

Our understanding of the geologic history of the Adirondacks is an ever-evolving project that involves the work of hundreds of researchers. We offer a brief summary, and refer you to more detailed studies by Isachsen et al. (1991), Chiarenzelli and McLelland (1991), McLelland et al. (1996), Hamilton et al. (2004).

The oldest rocks in the Adirondacks are 1.2 to 1.3 billion year old metasedimentary rocks that include marbles and gneisses seen on this trip. Included are gneisses that carry a geochemical signature of island-arc complexes, suggesting that northern New York consisted of a marine environment fed with materials from a nearby island arc. These rocks were metamorphosed during the Elsevirian Orogeny about 1210 to 1160 million years ago (Hamilton et al., 2004). Intruded into this sequence were the anorthosites, mangerites, charnockites and granites comprising the AMCG suite of McLelland at al. (1996). The ages of many of these plutonic rocks cluster around 1155 million years; the rocks at stop 1 are younger. A second orogenic event, the Ottawan, occurred between 1090 and 1030 million years ago (Hamilton et al., 2004). It was associated with the supercontinent of Rodinia and the formation of the Grenville Mountain range, whose heights were similar in magnitude to the present-day Himalayas. By the time Rodinia broke up, between 600 and 550 million years ago, the Grenville Mountains had been eroded to a gently rolling landscape, not unlike the present-day Adirondack lowlands, except barren of vegetation. Detailed apatite fission-track thermochronology by Mary Roden-Tice (Roden-Tice et al., 2000) at SUNY Plattsburg indicates that uplift and unroofing of the central Adirondacks began during the late Jurassic.

THE FIELD TRIP

Convene at the Tupper Lake public boat launch on Route 30, about 2.6 miles south of the junction of Routes 3 and 30 in the center of Tupper Lake Village. Set your odometer to 0.0 miles.

Meeting Spot. *Public boat launch*
The boat launch, with restrooms, was renovated in 2002 with $610,000 provided by the Department of Environmental Conservation and the Environmental Protection Fund. Access to the lake is considered essential to the region's enjoyment and economy, and the launch is a very busy place in summer.

Proceed south on Route 30 for 2.1 miles from the boat launch.

2.1 mi. **STOP 1.** Metamorphosed, fractured and mineralized meta-syenite.
A long roadcut of reddish-colored rock on the right (west) side of Route 30. This outcrop was the focus of a senior research project by SUNY Potsdam student Scott McDonald, whose data are presented here.

Meta-syenite. This dark reddish-brown stained rock contains abundant red to tan K-feldspar, albite, and quartz (Figure 1). The dark minerals are hornblende, but locally have been altered to chlorite. The k-feldspar shows marvelous perthitic textures. The minerals display pronounced parallel alignment. We believe the protolith was an igneous syenite and classify the rock as a meta-syenite or hornblende-alkali feldspar gneiss.

Figure 1. Meta-syenite gneiss at stop 1. Lighter colors are primarily potassium feldspar, with lesser amounts of albite and quartz; dark streaks were hornblende now altered to chlorite.

Microprobe data for albite are listed in Appendix 1, for potassium feldspar in Appendix 2, and for calcite and chlorite in Appendix 3. Data was obtained on the microprobe at SUNY Binghamton, with the help of probe guru Bill Blackburn. The data show that the plagioclase was almost completely altered to albite during metamorphism, and that the potassium feldspar contains very little sodium.

The rock probably was coarse grained to begin with. What once were randomly oriented, tabular crystals of alkali feldspar were later transformed by shearing into small, parallel-aligned grains. Some chunky feldspar crystals were deformed into lens-shaped grains or augen, (German for “eye”). On the east side of the road, the gneiss is brown and finer grained, but it grades into reddish meta-syenite and probably is the same rock. Zircon crystals, $ZrSiO_4$, were separated from similar rock at a nearby outcrop. They have a uranium-lead age of 1098+/-4 million years, which is the age of crystallization of the syenite magma (McLelland et al., 1988, p. 921, their rock sample #10). The meta-syenite is typical of younger granitic rocks of the Adirondack Highlands which have not been studied in detail.

Joint planes and rockfalls. This outcrop has many prominent joint planes. Note the geometric shapes of the large blocks at the south end on the west side. Produced by breakage along sets of intersecting joints, they resemble children's play blocks perched precariously on edge (Figure 2). A small rockfall occurred by breakage along joints on the east side of the road (Figure 3). In July, 2000, crushed green plants beneath the rubble indicated that the fall had occurred a few days prior to our visit.

Figure 2. Blocks of meta-syenite displaying joint surfaces.

Figure 3. Site of rock fall along joint surface in July 2000.

*Mineral deposition in breccia zones.*Pace off about one hundred feet from the north end of the outcrop, west side, and locate the zones of crushed, broken and angular rock fragments (Figure 4). The breccia formed long after cooling of syenite magma and long after the period of Adirondack metamorphism, perhaps during uplift of the Adirondack dome.The breccia zones are shown by the presence of irregular patches and stringers of low magnesium, Mn-bearing calcite, $CaCO_3$ (see microprobe data in Appendix 3).

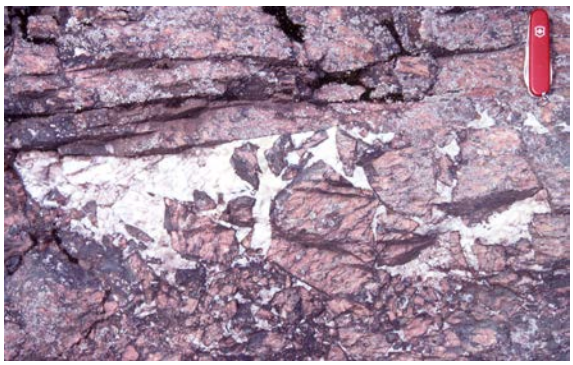

Figure 4. Brecciated meta-syenite with calcite zone. vein filling.

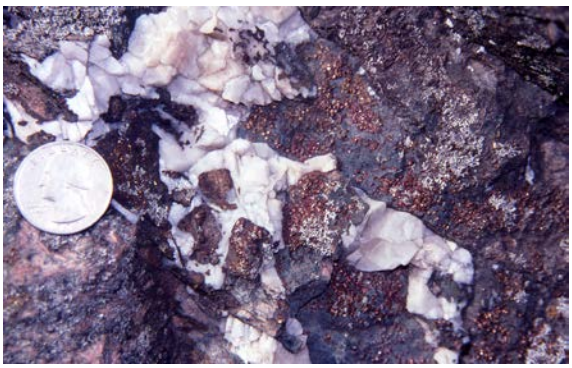

Figure 5. Pyrite crystals deposited in a breccia Pyrite occurs as small shiny crystals that cover surfaces of brecciated meta-syenite.

The calcite was deposited as cement in open spaces in the breccia. However, the calcite hides a sprinkling of tiny, brassy-yellow crystals of pyrite (FeS_2). The crystals occur as a coating on brecciated meta-syenite rock fragments (Figure 5). Magnified under a hand lens, the pyrite consists of millimeter-sized crystals of two types: (1) cubes with six square-shaped sides, and (2) pentagonal dodecahedrons, a geometric form consisting of twelve faces, each with the five sides of a pentagon.

The calcite could have originated in one of two ways. It could have precipitated from fluids that dissolved minerals from overlying rocks, or, less likely, it could be igneous calcite (carbonatite) with CO_2 derived by mantle degassing. To test these hypotheses, a sample of the calcite was sent to Steve Howe, stable isotope magician at the mass spectrometer lab at SUNY Albany. His analysis shows a delta ^{18}O value of –14.927 per mil (compared to PDB) or +15.474 per mil (compared to SMOW), and a delta ^{13}C value of –4.303 per mil (compared to PDB). These stable isotope numbers indicate a meteoric origin of the water and a bedrock source for the carbonate (Steve Howe, personal communication).

The carbon and oxygen isotope data therefore indicate that the calcite came from the dissolution of overlying layers of marble, the dominant carbonate rock in the Adirondacks. Calcite was dissolved in water to produce ions of calcium (Ca^{+2}), bicarbonate (HCO_3^{-1}), carbonate (CO_3^{-2}) and molecules of carbonic acid (H_2CO_3). The ions and molecules were transported downward by groundwater, perhaps traveling a considerable distance before crystallizing as calcite in the breccia. The marble source of these components, probably hundreds to perhaps thousands of feet above your head, was long ago removed by erosion.

The sulphur-bearing mineral, pyrite, is virtually insoluble in oxygenated groundwater. Reducing conditions are required for transport and deposition of iron sulfide. Such groundwater is generally deep-seated, oxygen-depleted and full of dissolved material. The point being made is that the kind of groundwater required to transport calcite is incompatible with water that transported the iron and sulphur. Separate solutions from different sources must have formed the minerals, the pyrite was first and the calcite later on.

Continue south on Route 30. *(3.6 miles between Stops 1 and 2)*

5.7 mi. **STOP 2**. Calc-silicate metasediments

Park in the large, paved pullover on the right (west) side of Route 30. We are located on South Bay at the south end of Tupper Lake. Examine the roadcut opposite the middle of the parking area (Figure 6). This outcrop was discussed by Jim McLelland in the 1992 NYSGA Guidebook.

Figure 6. Calc-silicate outcrop at Stop 2. Jim Carl for scale.

Figure 7. Diopside-feldspar gneiss. Dark grains are diopside, light grains are potassium feldspar and quartz.

We have left metamorphosed igneous rocks and entered a domain of metamorphosed sedimentary rocks. This outcrop is a slice through the steep west side of a bedrock hill, and the steeply inclined rocks include pale green gneisses with abundant diopside, $CaMgSi_2O_6$ (Figure 7). These metasediments must be older than the meta-syenite and other igneous rocks that intruded them.

The mineral assemblage of diopside, quartz, K-feldspar, plagioclase feldspar and sphene formed during the metamorphism of impure limestone. A chemical reaction occurred among minerals that commonly occur in limestone—calcite, $CaCO_3$, dolomite, $CaMg(CO_3)_2$, and the so-called impurity—a little quartz sand, SiO_2. Note that the formula of diopside, $CaMgSi_2O_6$, contains elements derived from each of them.

A difficulty with the presence of diopside at this outcrop is the scarcity of carbonate minerals, calcite and dolomite, that were needed to make it. Note the presence of light colored seams and veins that help to define the gneissic banding. At first glance, they might be mistaken for calcite, but the minerals do not fizzle in acid and cannot be scratched with a knife. The light-colored mineral is potassium feldspar, not calcite. We suspect that calcite and dolomite of the impure limestone protolith were completely used up in metamorphic reactions to produce diopside.

Before leaving, examine the outcrop from a distance and note the color change where green, diopside-bearing gneiss gives way to gray hornblende-biotite-feldspar gneiss as you look from right (south) to left (north). The gray gneiss was interpreted by McLelland (1992, p. 40-41) as an igneous intrusive rock, even though its contact with the diopside-bearing gneiss appears gradational over a distance of a few feet. McLelland's interpretation is that this is a highly sheared contact between two very different rock types, one igneous and one sedimentary. Another interpretation is that both are sedimentary and that the gray gneiss represents a facies change in the original sedimentary protolith, an impure limestone, to perhaps to a shale or mudstone that was metamorphosed to a hornblende-biotite gneiss. A few tens of feet north of the contact between diopside gneiss and the gray hornblende gneiss is another much smaller zone of diopside gneiss, interpreted as either a sheared fragment of the diopsidic gneiss or another facies change. You may form your own opinion.

Continue south on Route 30.

6.1 miles Junction with Route 421 on right

8.7 miles Intersection with the north entrance road to the William C. Whitney Wilderness Area on Little Tupper Lake.

The William C. Whitney Wilderness Area

Called the "most significant Forest Preserve acquisition in twenty five years," the estate of Mary Lou Whitney was purchased by the State of New York in December, 1997. The purchase consisted of 14,700 acres surrounding Little Tupper Lake, once the largest privately owned lake in the northeast. The eight mile-long lake is relatively shallow (less than twenty five feet deep), drains into the Bog River and is home to a native strain of fish called the Little Tupper brook trout. Canoeists were pleased with a land purchase that connected major canoe routes throughout a vast region of wetlands, lakes, bogs and cut-over timberland. In March, 2000, the area was classified as wilderness.

The road leads to an eighty acre site on the lake's north shore, once used as the headquarters for Whitney Industries. Now classified for "administrative use," the site includes a ranger station in a grove of tall pine trees, a parking area and a canoe launch. The lake has become one of the most widely used, flat water canoe routes in the East, and several tens of primitive camping sites have been constructed around its perimeter.

9.4 mi. **STOP 3.** Marble and other metasediments

Drive beyond the outcrop and park beyond the guard rail at the south end. Walk north and examine three outcrops on the west side. These outcrops were studied by SUNY Potsdam student Aaron Fiaschetti for his senior research.

Here's a good example of diopside-bearing marble, an easily recognized metamorphic rock that once was a limestone (Figure 9). The marble lies between gneissic layers of debatable origin. Separated by intervals of soil, the three parts of the outcrop include (1) garnetiferous biotite gneiss with quartzite layers at the south end, (2) marble outcrops in the middle, and (3) garnet-bearing gneiss at the north end.

Figure 9. Impure marble outcrop at stop 3. Rob Badger for scale.

Figure 10. Banded hornblende-biotite gneiss at south outcrop, Stop 3. Thin dark seams are biotite.

South outcrop

The dark gneiss contains alkali feldspar, quartz, hornblende, seams of biotite and locally garnet (Figure 10). The mica seams are close together and locally give the gneiss a schistose appearance. Some of the biotite appears to have been altered to bronze colored phlogopite. Non-geologists have misidentified such grains as flakes of gold. Thin layers of quartzite that broke away from weathered mica seams give the rock a slab-like appearance. The hornblende gneiss contains pods of quartz with small grains of garnet (Figure 11) whose lavender color indicates a small spessartine (i.e. manganese, Mn) component.

Figure 11. Pod of quartz with reddish-lavender garnet, quartz and feldspar, within hornblende gneiss.

Middle outcrop. The white marble and calc-silicate rock are easily recognized in the center outcrop (and across the road) (Figure 9). They consist of coarse calcite grains that were recrystallized from limestone during metamorphism. Most likely, the marble is much lighter in color than the original limestone. Finely dispersed coloring agents such as organic matter, clay minerals and iron oxides, were either expelled from the limestone or incorporated into the crystal structure of another mineral during metamorphism.

Glassy grains of green diopside are present, but there are fewer of them than at Stop 2. Also present are muscovite, brown sphene, shiny black flakes of graphite (pure carbon), tiny grains of pyrite, smoky to clear grains of quartz, and light colored seams of chunky alkali feldspar that, at first glance, can be mistaken for calcite. Look for veins of milky quartz. The graphite is probably the recrystallized remains of primitive algae that once lived in the warm marine environment in which the original limestone was deposited. A breccia zone at the south end of the outcrop may have formed at the same time as the breccia zone at stop 1.

North outcrop. This hornblende-biotite-garnet gneiss has more hornblende and less biotite than gneiss at the south outcrop. There are layers and lenses of pink alkali feldspar, as well as quartz veins that parallel the gneissic layering. Some layers were deformed into ragged and elongate stringers, whereas others were pulled apart into sausage-like boudins. Garnets in the boudins are iron-rich and reddish in color.

Layers of quartzite in the south outcrop and the proximity of the intervening marble lead us to interpret the gneisses at both ends of this outcrop as shales or mudstones prior to deep burial and metamorphism. There's a certain chemical "richness" to shale, thanks to the presence of sheet-structured clay minerals such as illite, chlorite, kaolinite and montmorillonite. They became unstable and decomposed during high temperature metamorphism, and their elements were re-combined to form a variety of high-grade metamorphic minerals. Imagine the conversion of compact and drab mud into an attractive crystalline aggregate of garnet, hornblende, biotite mica and feldspars (Figure 11). Hence, the well known saying, "There's nothing wrong with a sedimentary rock that 10 kilobars can't cure."

Continue south on Route 30.
(1.1 miles between Stops 3 and 4)

10.5 mi. **STOP 4.** Multiple igneous intrusive rocks?

Park beyond the guard rail and examine the rocks on the opposite (east) side of the road. This outcrop was studied by SUNY Potsdam student Kyle Ashley for his senior research and presented at the NE GSA meeting in 2009. The chemical data and interpretations come from his study and were updated this year reflecting his current graduate training at Virginia Tech.

Description

This outcrop contains a variety of metamorphic rock types, from pink, garnetiferous gneiss to gray garnet-poor gneiss to pegmatite with coarse, black hornblende crystals. Clearly, multiple protoliths are called for. From south to north, seventeen different units were differentiated which can be divided into six different rock types.

Units	Description
1, 2, 15	Hornblende gneiss with crosscutting pegmatite
10, 12, 14	Hornblende-biotite amphibolite dike
3, 9, 16	Garnetiferous gneiss with small pockets of qtz-gar-ksp pegmatite. Garnet is small and scattered.
6	Hbld-ksp-qtz pegmatite with euhedral hbld
4, 13	Garnetiferous gneiss with large scattered garnets
5, 7, 8, 11, 17	Ksp-plag-qtz gneiss with little to no other major minerals present

Table 1. Characteristics of rock varieties at stop 4.

The massive, pink and gray gneisses that predominate at the south end of the outcrop (Fig. 4-1) contain abundant quartz and potasssium feldspar with lesser amounts of plagioclase feldspar, biotite and a few small garnets scattered here and there. In thin section, the potassium feldspar contains a wide range of excellent examples of perthitic textures. The rock has a fairly uniform grain size. It lacks the pronounced banding and segregation of minerals that we observed at Stop 3. It also lacks dark colored minerals, but chemical reactions that produced the garnet may have used them up. Most likely this rock was originally a granite.

Garnet compositions throughout the outcrop are almandine (Table 2), and plagioclase feldspars have An compositions between 23 and 40.

Bed #	n	Fe	Mg	Ca	Mn	Al	Si	O
3	16	2.18	0.31	0.28	0.17	1.97	3.05	12
4	19	2.30	0.25	0.28	0.13	1.95	3.05	12
9	10	1.96	0.23	0.64	0.16	1.96	3.05	12
13	19	2.29	0.28	0.27	0.08	1.99	3.04	12

Table 2. Garnet compositions from units 3, 4, 9 and 13.

Bed #	n	K	Fe	Mg	Ti	Al	Si	O	OH
4	2	1.03	1.82	0.91	0.31	1.36	3.04	10	2
9	2	1.03	1.87	0.81	0.32	1.44	3.00	10	2

Table 3. Biotite compositions from units 4 and 9.

Present in the light colored granitic gneiss is a distinctive 10-15 inch wide layer of amphibolite (Figure 12), composed predominantly of black hornblende and plagioclase feldspar. This rock probably was a basaltic dike that intruded the granite prior to metamorphism.

The mafic content of the gneiss increases towards the north end of the outcrop, and the rock becomes an orthopyroxene-bearing granitic gneiss, or "charnockite" (see discussion of charnockites at Stop 9). Much of the opx has been altered to chlorite and other alteration minerals, but the persistence of relict cleavage indicates that the mafic grains were originally pyroxenes (table 4). Other portions of the rock contain significant amounts of hornblende. Again, an igneous protolith is called for, but the high mafic content suggests this intrusive rock unit differs from the mafic-poor granite gneiss at the south end of the outcrop. The prescence of pyroxene suggests crystallization deep in the crust at higher temperatures. The melt is derived from orogenic collapse of an over-thickened Grenville continental crust.

Bed #	n	Ca	Mg	Fe	Si	O
10	3	0.01	0.34	0.77	1.12	3
10	2	0.45	0.26	0.34	1.08	3

Table 4. Pyroxene compositions from amphibolite in bed #10. Opx on top, cpx on bottom.

The hornblende in the amphibolite of bed #10 has a composition as follows:

$$Ca_{1.9}Na_{1.67}K_{0.35}Ti_{0.24}Mn_{0.04}(Mg_{1.83}Fe_{3.19}Al_{1.02})Al_{0.95}Si_{7.05}O_{22}(OH)_2 \quad (n = 2)$$

A coarse grained pegmatite occurs near the north end of the outcrop (Figure 13). It contains coarse grains of potassium and plagioclase feldspar, hornblende and two varieties of pyroxene – one a pale green with second order interference colors of clinopyroxene, the other a pale pink with first order interference colors of orthopyroxene. The opx shows more alteration than cpx, which is typical in Adirondack rocks with co-existing pyroxenes. Apatite is also a significant component. The coarse minerals are randomly oriented as though crystallized from a silicate melt in the presence of a watery fluid. The pegmatite appears to be a late igneous intrusion that post-dates metamorphism. Or, given the compositional similarity to the surrounding rock, it could be recrystallized gneiss in the presence of hot, watery fluids of late stage metamorphism.

Figure 12. Amphibolite dike cutting garnetiferous pink and light gray granitic gneiss.

Figure 13. Coarse hornblende and feldspar in pegmatite dike, north end of outcrop at Stop 4.

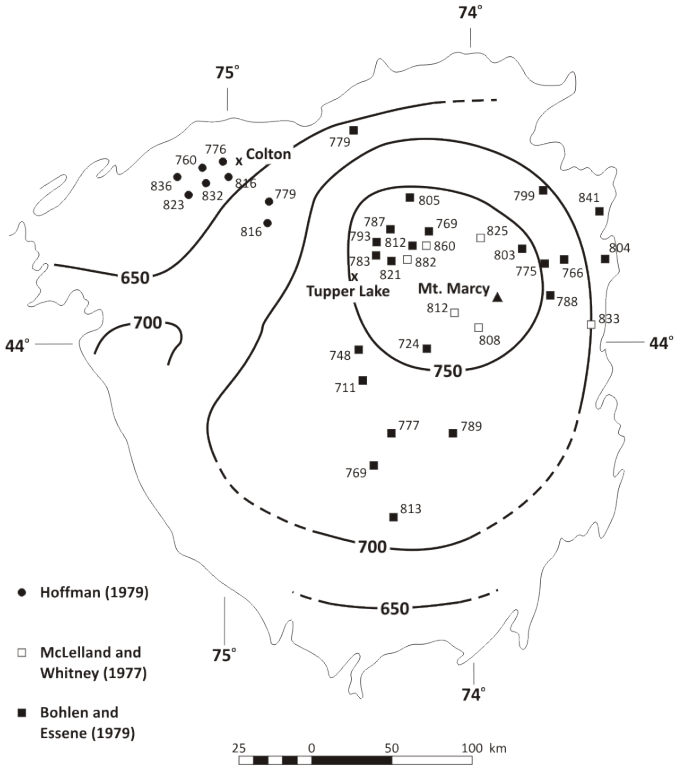

Figure 14. Map of the Precambrian Adirondack highlands of Northern New York State showing calculated temperatures from the two-pyroxene geothermometer (using Fe^{3+} estimates calculated from stoichiometry) with studies by Hoffman (1979), McLelland and Whitney (1977), and Bohlen and Essene (1979). Predicted isotherms are from oxide and feldspar geothermometery data (Bohlen and Essene, 1977; Bohlen et al., 1979, 1985). Modified from Bohlen and Essene (1979).

In thin section, quartz extensively exhibits chessboard extinction, which indicates the combined operation of prism [c] and basal <a> slip systems active in quartz, occuring at minimum deformation temperatures of ~630 °C (Blumenfeld et al., 1986; Mainprice et al., 1986). Garnet-biotite exchange thermometry considering the effects of Mn partitioning from Holdaway (2000) constrains peak metamorphic temperatures at ~750 °C – consistant with 2-pyroxene thermometry results from Hoffman (1979), McLelland and Whitney (1977), and Bohlen and Essene (1979) (Figure 14).

11.5 mi. **STOP 5.** The granite quarry outcrop.

Park at the south end of this long roadcut, beyond the guard rail, and examine the outcrop on the right (west) side (Figure 15).

Quarries. No, they don't quarry the granite for building stone here. In a sense, however, all road cuts are quarries because rock was removed to make room for the roadbed. The Department of Transportation blasted through the massive rock, and much breakage occurred along the natural fractures (joints). Breakage along prominent near-horizontal sheeting joints has provided some flat and narrow surfaces that resemble crude stair steps in the face of the outcrop, similar to the working face of an active stone quarry.

Metamorphosed granite. The finely foliated meta-granite or alkali feldspar-quartz-hornblende gneiss, has small grains of dark hornblende aligned as parallel stringers (Figure 16). Some of the hornblende has altered to chlorite, but most is intact. A little plagioclase feldspar is present, along with apatite and a few grains of zircon. Cutting diagonally across the outcrop is a dark amphibolite layer (Figure 15) that once was a tabular dike of basalt that intruded the granite. A small fault extends from the granite into the dike about midway up. See if you can find it. The top part of the dike was displaced a few inches to the right of the bottom part. Also note whether the dike lies parallel to, or cuts across the gneissic layering in meta-granite.

Small faults in meta-granite are often coated with fault gouge. Slickenlines in the gouge indicate the direction of fault movement (Figure 17). The fractures are coated with green hydrous alteration minerals, probably chlorite and serpentine.

Figure 15. Granitic gneiss at Stop 5 showing horizontal sheeting joints. Jim Carl is pointing to a thin mafic dike that cuts diagonally across the outcrop.

Figure 16. Alkali feldspar-quartz-hornblende gneiss at Stop 5. Note parallel alignment of hornblende grains.

Figure 17. Slickenlines parallel to pen indicate direction of movement along small fault.

Continue south on Route 30.
(3.1 miles between Stops 5 and 6)

12.4 mi. Intersection on the right (west) side with the south road (Sabattis Road) to the William C. Whitney Wilderness Area.

14.6 mi. **STOP 6.** The marble cake outcrop (that only has a little marble). Evidence for igneous intrusive origin.

SUNY Potsdam student Christopher Mack studied this outcrop for his senior research, and presented his data at NEGSA in 2013.

Examine the outcrop on the left (east) side of Route 30. The rock is cream and black mottled gneiss that reminds us of a marble cake. The light portions are composed primarily of plagioclase (An_{36}, optically determined) and perthitic alkali feldspar, with very little quartz, while the dark zones are predominantly composed of clumps of hornblende, plagioclase and diopside, with minor garnet, orthopyroxene, magnetite and scattered apatite. Some of the hornblende contains relict orthopyroxene cores. At the south end of the outcrop and on the west side of the road is a different type of rock. Thus, our "marble cake" rock may be of small volume and confined to this outcrop, but we think it is the most unusual rock on this field trip.

To make a marble cake, one takes a yellow cake batter and divides it into two parts. Chocolate is added and thoroughly blended in one part. Spoonfuls of the chocolate batter are then dropped into the remaining yellow batter, and a spatula is used to swirl the blobs about. This outcrop is the result. Or so it seems. The dark, steeply inclined layers contain abundant hornblende and pyroxene (Figure 18). The "free form" pattern of layers, ribbons, loops and swirls, however, was not produced by stirring. The pattern results from the intersection of the viewing surface with the plane of gneissic banding, whether parallel to it, perpendicular, or somewhere in between. Marble cakes and rocks that resemble them have beautifully convolute patterns, but the anticipation of eating is absent here.

An early effect of metamorphism was to segregate a coarse-grained igneous rock into light and dark layers. The rock then became "mobile" and began to flow. Some of the dark layers behaved rather stiffly. They were ruptured and shredded while the light-colored, feldspar-rich layers flowed plastically around them (Figure 19).

Figure 18. Mottled feldspar-hornblende-quartz gneiss at stop 6.

Figure 19. Dark bands of hornblende gneiss segregated from lighter feldspar rich zones.

Figure 20. Calc-silicate xenolith (to right of knife) in contact with its meta-intrusive host.

Evidence that the swirled gneiss was an igneous rock includes a large fragment of diopside-bearing marble in the gneiss (Figure 20). The marble is typical of marble found throughout the Adirondacks, consisting of coarse calcite with green diopside and brown sphene. The fragment is a xenolith whose presence is a powerful argument that the gneiss was once magma and that the fragment was caught up in it.

Another xenolith is composed of green diopside and red garnet (Figure 21). Note that the gneissic layering is deflected around it. The swirled gneiss also contains large feldspar crystals up to eight inches across (Figure 22). Minerals of that size generally have crystallized from low viscosity silicate melts, often in the presence of watery fluid. The question is how such large crystals survived the metamorphism, especially the shearing that produced the gneissic banding.

Our explanation is not very profound. A wide range in grain size is expected if the shearing had been a hit and miss operation. Some parts of the rock were reduced in grain size, whereas other parts were left undisturbed. Primary igneous textures are preserved elsewhere in the Adirondacks, including anorthosite outcrops near Saranac Lake which contain single plagioclase feldspar grains more than 12 inches long.

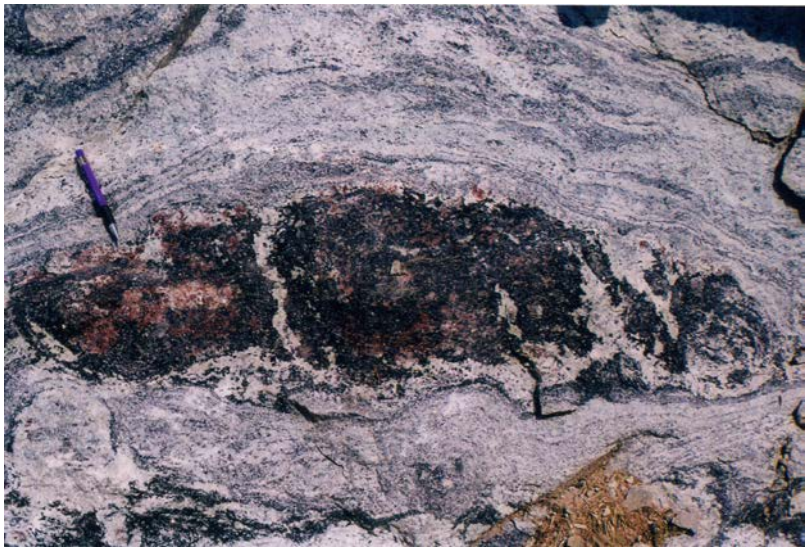

Figure 21. Xenolith of garnet-diopside gneiss within its intrusive host.

Figure 22. Feldspar phenocryst between pencil and dark border below knife.

We note that angular fragments make up a breccia zone parallel to the gneissic banding (Figure 23). This post-metamorphic breccia zone may be synchronous with the one seen at Stop 1.

A change in rock type occurs at the south end of the outcrop. The banded rock gives way to a pinkish and green, faintly foliated syenitic gneiss whose minerals include pink alkali feldspar, quartz, biotite, a little hornblende, and locally significant amounts of red brown garnet (Figure 24). Some garnets are up to 4 cm in diameter.

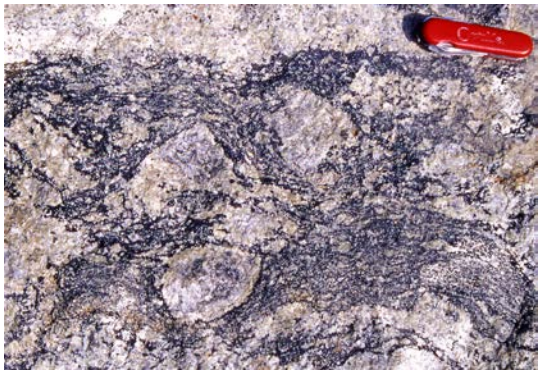

Figure 23. Fragments of broken rock (breccia) within a foliated matrix.

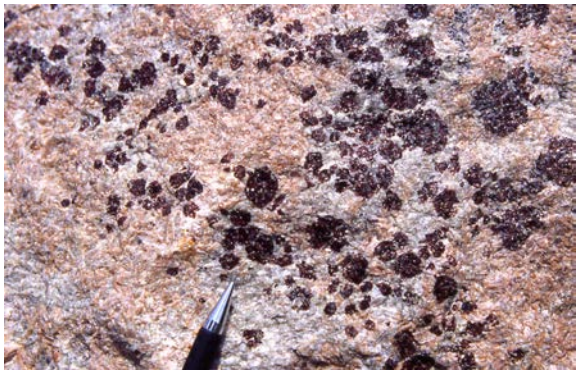

Figure 24. Garnet grains in pink feldspar gneiss at south end of outcrop at Stop 6.

Continue south on Route 30.
(1.6 miles between Stops 6 and 7)

16.2 mi. **STOP 7.** Layered "gray gneiss," a common metamorphic rock.

Examine the left (east) side of the road. Please no hammers here – it is a small outcrop and with only a couple of the large, interesting hornblendes in the pegmatite.

Welcome to the "gray gneisses," a common and widespread rock type in Precambrian age rocks throughout the eastern United States and Canada. This medium grained example has fewer surprises than the last outcrop. It, too, contains plagioclase and alkali feldspar, hornblende, pyroxene, garnet, quartz and a little biotite mica. The gneissic banding consists of stringers and seams of cream-colored alkali feldspar. Some bands are convoluted and pinch out, and all are vertical or steeply inclined (Figure 25). The gneiss is peppered with garnets, and the large ones are prominently displayed in the light colored seams. The rocks at this outcrop lack the large feldspar crystals and marble xenoliths seen at the previous stop, and may not be intrusive in origin.

Figure 25. Vertical gneissic layering in hornblende-garnet-biotite gneiss at Stop 7.

This gray gneiss may have been volcanic ash, an extrusive igneous rock. Similar-looking rock underlies a belt more than seventy miles across in the Adirondack Lowlands to the northwest. Published geological studies suggested that the original rock was sedimentary in origin, a shale or an arkose, but the chemical data were a good match for dacite volcanic rocks (Carl, 1988). We have not analyzed the rock at this outcrop but it, too, could represent a thick pile of volcanic ash.

Note the presence of a fifteen inch-thick pegmatite vein that cuts across the gneiss (Figure 26). It consists of smoky quartz and coarse, chunky grains of alkali feldspar, cream to gray in color. The vein also contains dark and tabular hornblende crystals about three quarters of an inch wide and up to four inches long (Figure 27). The crystals are randomly oriented as expected from growth within a low viscosity, water-bearing silicate magma. Such magma would promote the growth of large crystals, as well as the crystallization of the hydrous minerals hornblende and biotite observed along the vein margins.

Figure 26 Coarse pegmatite dike at Stop 7. Hornblende-garnet-biotite gneiss on right.

Figure 27. Hornblende grain in pegmatite of previous figure.

Continue south on Route 30.
(8.4 miles between Stops 7 and 8)

16.9 mi. Lake Eaton campground on the right (east) side.

18.8 mi. Bridge, beach and floatplane dock at Long Lake

19.5 mi. The junction of Routes 28N and 30. Turn right (west) on Route 28N and 30.

Turnoff to Buttermilk Falls
22.5 mi. Turn right (south) onto North Point Road. The turnoff occurs on a sharp left curve. Drive 2.1 miles west to the parking area for Buttermilk falls.

24.6 mi. **STOP 8**. Buttermilk Falls on the Raquette River.
Park near a small sign on the right (north) side of North Point Road. Walk the short distance to the waterfall. We are located upstream less than a mile from Long Lake.

This relatively steep stretch of the Raquette River lies east of Forked Lake and southwest of Long Lake. The river drops 116 feet in five miles, and Buttermilk Falls is the third of three canoe carries from Forked Lake. Rapids here extend for about one hundred yards before ending in a waterfall, and the total drop in elevation is about forty feet.

The bedrock at the falls is a highly weathered, dark brown, metamorphosed granite. One can see pods and veins of milky quartz that crop out near the shore. The bedrock is covered with pine needles and shallow soil. Trees are shallow-rooted and unstable in high winds.

Figure 28. Prominent jointing at outcrops near Buttermilk Falls. Joint planes intersect at nearly right angles, and blocks have broken away to leave vertical walls.

Figure 29. Potsdam student taking advantage of stairsteps produced by jointing at Buttermilk Falls. The river has removed blocks between joints and deposited them downstream.

Unless many rock hammers improve the quality of fresh outcrop exposures, this is a structure stop, and the petrography of the rock is best examined at Stop 9. Two prominent directions of jointing are present here (Figure 28), with one extending across the river. The joint planes had little influence in creating the stream channel, in contrast to joints that lie parallel to stream courses. But "cross joints" like these are partly responsible for the presence of rapids. Blocks were removed from the downstream side of a joint, resulting in stair steps that decline in the downstream direction. The river spills over them. People who sit in spaces where the blocks once sat will either enjoy a shower or a bouncing ride downstream (Figure 29).

The same joint spacing, often outlined by pine needles caught in the grooves, can be observed in the bedrock surrounding the falls. The origin of jointing is unclear. Is it due to isostatic rebound following glacial retreat? Or is it much older, related to uplift of the Adirondacks and erosion of the overlying bedrock? Or is it older still, caused by tectonic forces shortly after metamorphism?

The falls and spray sparkle in the sunlight, and our geology field trips get bogged down when the college students disperse among the rocks. They sit at the falls and perch with the demeanor of poised herons, legs crossed, patiently waiting for a stray fish. They relax, get wet and cannot hear their professor's voice over the roar of the falls. If the timing is right, this is a good place for lunch.

Turn around and drive 2.1 miles back to Route 30.
(6.3 miles between Stops 8 and 9)

26.7 mi. Intersection of North Point Road with Route 30. Turn right (south) on Route 30 towards Blue Mountain Lake.
(4.2 miles from this intersection to Stop 9)

30.9 mi. **STOP 9.** Dark brown meta-granite with pegmatite.
Park on the shoulder of Route 30, before the curve and near the center of a long outcrop on the right side.

The dark brown colored meta-granite (Figure 30) is similar to the bedrock at Buttermilk Falls. This type of rock was quarried and used as a building stone in handsome but very dark-walled churches in Saranac Lake, Lake Placid, Tupper Lake and elsewhere. The major minerals are alkali feldspar, hornblende and orthopyroxene with lesser amounts of quartz, plagioclase feldspar, clinopyroxene, garnet, magnetite and apatite. Gneissic banding is faint, steeply inclined and hard to see when the outcrop is wet.

Figure 30. Pegmatite dike pointed out by Jim Carl at Stop 9.

Figure 31. Pods of crystallized melt that probably moved very little from their point of origin.

The presence of pyroxene is unusual for granite, and geologists have a special name for orthopyroxene-bearing granite: charnockite. The name honors Job Charnock, the founder of Calcutta, India, who died in 1693. Charnock was not a geologist and may not have appreciated this particular rock, but his memory is preserved among geologists because the first described example of charnockite was his tombstone.

Charnockites are igneous rocks that were subjected to high grade metamorphism. The presence of hypersthene pyroxene, $(Mg,Fe)SiO_3$, raises a question. Did the mineral crystallize in the magma and, therefore, is of igneous origin? Or did it form much later during metamorphism when water-bearing silicate minerals, such as biotite and hornblende, dehydrated and converted into hypersthene? If so, hypersthene would be a metamorphic mineral. Adirondack charnockites are widespread igneous rocks that make up the "C" part of the AMCG suite of intrusive rocks.

Look closely along the outcrop, before the right bend in the road, for a pegmatite vein consisting of quartz and alkali feldspar (Figure 30). Also of interest are mottled patches of light colored, slightly coarser grained rock that lack hypersthene (Figure 31). The patches are best seen on dry surfaces around the bend towards the south end of the outcrop. The pegmatite and mottled patches are generally interpreted as having formed by partial melting of the charnockite.

During metamorphism, the temperatures were hot enough to melt some of the biotite, hornblende, quartz and feldspar. Most likely, the break-down of biotite and hornblende supplied enough water to lower the melting temperatures of the other minerals. Where appreciable quantities formed, the melt migrated into fractures to form pegmatite veins, like the one seen here, that may have migrated several tens or even hundreds of feet. The patches, on the other hand, appear to be small quantities of melt that did not migrate very far. The patches are sometimes

called “sweats,” a reminder of efforts by the human body to cool itself. The sweats at this outcrop solidified near where they formed.

If you have time, continue 2.4 miles on Route 30 to the Adirondack Museum at Blue Mountain Lake.

ADIRONDACK MUSEUM AT BLUE MOUNTAIN LAKE

The Museum honors the people of the Adirondacks. There are exhibits about the lives of Native Americans, early settlers, wealthy tourists who joined them in summertime, the unique architecture of Adirondack camps, and the intricate transportation networks that brought people into the woods. One learns about farmers, hunters, miners, loggers, guides, artists, writers, furniture makers and, most of all, tourists like you, drawn here for more than 150 years by the natural beauty of the mountains, lakes and forests.

The museum itself is a mountainside courtyard of large and small buildings, some serving to house a collection of artifacts, and others to illustrate a distinctive style of Adirondack architecture. All are clustered on a mountain side, the site of a former hotel and resort. The center of the grounds is a courtyard with an artificial pond and the steam engine from the Marion River Railroad. People climb on the engine, sit on Adirondack chairs, and leisurely stroll about, enjoying a spectacular view of mountains that overlook Blue Mountain Lake. The lake and its inflowing streams are the source of the Raquette River that we encountered at Tupper Lake, Long Lake and Buttermilk Falls.

Be sure to visit the log cabin of the Buck Lake Club and examine the mineral specimens mounted in the stone fireplace that include agate, garnet, rose quartz, flint, obsidian, feldspar, tourmaline and magnetite.

END OF TRIP

REFERENCES

Bohlen, S.R., and Essene, E.J., 1977, Feldspar and oxide thermometry of granulites in the Adirondack Highlands: Contributions to Mineralogy and Petrology, v. 62, p. 153-169.

Bohlen, S.R., and Essene, E.J., 1979, A critical evaluation of two-pyroxene thermometry in Adirondack granulites: Lithos, v. 12, p. 335-345.

Bohlen, S.R., Essene, E.J., and Hoffman, K.S., 1980, An updated on feldspar and oxide thermometry in the Adirondack Mountains, New York: Geological Society of American Bulletin, v. 91, no. 2, p. 110-113

Bohlen, S.R., Valley, J., and Essene, E.J., 1985, Metamorphism in the Adirondacks, 1. Petrology, pressure, and temperature: Journal of Petrology, vo. 26, p. 971-992.

Blumenfeld, P., Mainprice, D., and Bouchez, J.L., 1986, C-slip in quartz from subsolidus deformed granite: Technophysics, v. 127, p. 97-115.

Carl, James D., 1988, Popple Hill Geniss as dacite volcanics, northwest Adirondacks, N.Y.: Geological Society of America Bulletin, v. 100, p. 841-849.

Chiarenzelli, J.R., and McLelland, J., 1991, Age and regional relationships of granitoid rocks of the Adirondack Highlands, New York: Journal of Geology, v. 99, p. 571-590.

Hamilton, M.A., McLelland, J., and Selleck, B., 2004, SHRIMP U-Pb zircon geochronology of the anorthosite-mangerite-charnockite-granite suite, Adirondack Mountains, New York: Ages of emplacement and metamorphism, *in* Tollo, R.P., Corriveau, L., McLelland, J., and Bartholomew, M.J., eds., Proterozoic tectonic evolution of the Grenville orogen in North America: Boulder, Colorado, Geological Society of America Memoir 197, p. 337-355.

Hoffman, K.S., 1979, A reevaluation of the orthopyroxene isograd in the northwest Adirondacks (M.S. thesis): Ann Arbor, University of Michigan, 70 p.

Holdaway, M.J., 2000, Application of new experimental and garnet Margules data to the garnet-biotite geothermometer: American Mineralogist, 85, 881-892.

Isachsen, Y.W., Landing, E., Lauber, J.M., Rickard, L.V., and Rogers, W.B., editors, 1991, Geology of New York: a simplified account: New York State Museum/Geological Survey Educational Leaflet No. 28, 284 p.

Mainprice, D., Bouchez, J. L., Blumenfeld, P., and Tubia, J.M., 1986, Dominant C-slip in naturally deformed quartz: Implications for dramatic plastic softening at high temperature: Geology, v. 14, p. 819-822.

McLelland, J., 1992, Geological relationships of the anorthosite-mangerite-charnockite-granite (AMCG) suite and related ore deposites: New York State Geological Association Field Trip Guidebook, p. 1-46.

McLelland, J., 1995, Geochronology and Petrogenesis of Adirondack igneous and metamorphic rocks, *in:* Garver, J.I., and Smith, J.A., eds., Field Trip Guide for the 67th Annual Meeting of the New York State Geological Association, p. 205-225.

McLelland, J., Daly, S., and McLelland, J.M., 1996, The Grenville orogenic cycle (ca. 1350-1000 Ma): an Adirondack perspective: Tectonophysics, v. 265, p. 1-28.

McLelland, J., Chiarenzelli, J., Whitney, P. and Isachsen, Y.W., 1988, U-Pb zircon geochronology of the Adirondack Mountains and implications for their geologic evolution: Geology, v. 16, p. 920-924.

McLelland, J., and Whitney, P., 1977, The origin of garnet in the anorthosite-charnockite suite of the Adirondacks: Contributions to Mineralogy and Petrology, v. 60, p. 161-181.

Roden-Tice, Mary, Tice, S. J., and Schofield, I.S., 2000, Evidence for differential unroofing in the Adirondack Mountains, New York State, determined by apatite fission-track thermochronology: The Journal of Geology, v. 108, p. 155-169.

APPENDICES

Sample #	tlb141	tlb142	tlb143	tlb145	tlb146	tlb147	tlb148	tlb149	tlb150	tlb1410
SiO_2	65.6	65.12	64.53	67.33	66.38	67.07	66.73	67.78	68.03	68.03
Al_2O_3	20.00	21.10	20.66	20.02	20.03	20.11	20.00	20.02	20.08	20.08
TiO_2	0.00	0.02	0.00	0.01	0.01	0.01	0.03	0.00	0.00	0.00
FeO	0.24	0.17	0.09	0.16	0.16	0.03	0.12	0.03	0.00	0.00
MgO	0.00	0.01	0.00	0.02	0.00	0.00	0.01	0.00	0.01	0.01
MnO	0.03	0.03	0.02	0.00	0.02	0.00	0.00	0.00	0.02	0.02
CaO	0.20	1.57	1.23	0.08	0.05	0.05	0.03	0.10	0.06	0.05
Na_2O	12.96	12.19	12.15	12.80	13.12	13.15	13.01	13.01	12.98	12.98
K_2O	0.09	0.14	0.09	0.10	0.04	0.08	0.07	0.11	0.06	0.06

Appendix 1. Microprobe analyses of albite grains in the meta-syenite at Stop 1.

Sample #	tlb131	tlb132	tlb133	tlb134	tlb135	tlb136	tlb251	tlb252	tlb253
SiO_2	61.21	64.09	60.96	61.11	61.28	61.81	62.23	62.06	61.72
Al_2O_3	18.85	18.32	18.12	19.08	18.95	18.81	18.61	18.60	18.57
TiO_2	0.00	0.00	0.00	0.03	0.00	0.01	0.00	0.04	0.01
FeO	0.02	0.09	0.05	0.01	0.00	0.05	0.05	0.10	0.15
MgO	0.00	0.00	0.00	0.00	0.00	0.00	0.00	0.00	0.00
MnO	0.00	0.01	0.00	0.01	0.00	0.06	0.01	0.00	0.00
CaO	0.20	0.00	0.55	0.10	0.13	0.10	0.01	0.02	0.03
Na_2O	0.81	0.12	0.11	1.54	1.50	1.75	0.49	0.54	1.02
K_2O	19.05	19.87	20.54	17.56	17.70	17.74	19.16	19.38	18.56

Appendix 2. Microprobe analyses of potassium feldspar grains in the meta-syenite at Stop 1.

Sample #	tlb137	tlb138	tlb1310	tlb1311	tlb241	tlb242	tlb243	tlb424	tlb425	tlb426
	cc	cc	cc	cc	chl	chl	chl	chl	chl	chl
SiO_2	0.00	0.00	0.00	0.00	24.66	24.93	24.78	28.54	28.25	29.11
Al_2O_3	0.01	0.00	0.01	0.00	21.13	20.96	21.18	14.98	14.98	15.02
TiO_2	0.00	0.00	0.01	0.00	0.04	0.01	0.02	0.05	0.02	0.03
FeO	0.20	0.34	0.13	0.20	28.11	28.14	28.25	26.44	27.51	26.25
MgO	0.07	0.06	0.06	0.07	11.73	12.24	11.77	15.70	14.28	15.73
MnO	1.09	1.11	1.07	1.11	0.28	0.28	0.33	0.09	0.06	0.14
CaO	58.65	58.47	60.09	59.50	0.00	0.01	0.01	0.09	0.08	0.14
Na_2O	0.00	0.00	0.03	0.00	0.01	0.00	0.02	0.00	0.02	0.01
K_2O	0.02	0.08	0.00	0.01	0.01	0.01	0.02	0.03	0.00	0.02

Appendix 3. Microprobe analyses of calcite and chlorite grains in the meta-syenite at Stop 1.

STRATIGRAPHY AND TERRESTRIAL TO SHALLOW MARINE ENVIRONMENTS THE POTSDAM GROUP IN THE SOUTHWESTERN OTTAWA EMBAYMENT

DAVID G. LOWE
Department of Earth Sciences, University of Ottawa, Ottawa, Ontario, Canada

INTRODUCTION

This field trip showcases the stratigraphy and sedimentology of the Potsdam Group exposed along the southwestern Ottawa Embayment, south of the St. Lawrence River in Jefferson and St. Lawrence County of New York State (Figures 1, 2). The trip will highlight some important regional unconformities which have been used to correlate the Potsdam Group from this area to the north and east, as well as two contrasting fluvial styles in the Potsdam Group: braided perennial fluvial and sheet-like perennial fluvial. Refer to figure 2 for stop locations. We will begin at Wellesley Island and travel a loop that covers some classic Potsdam sections along Highways 37 and 12.

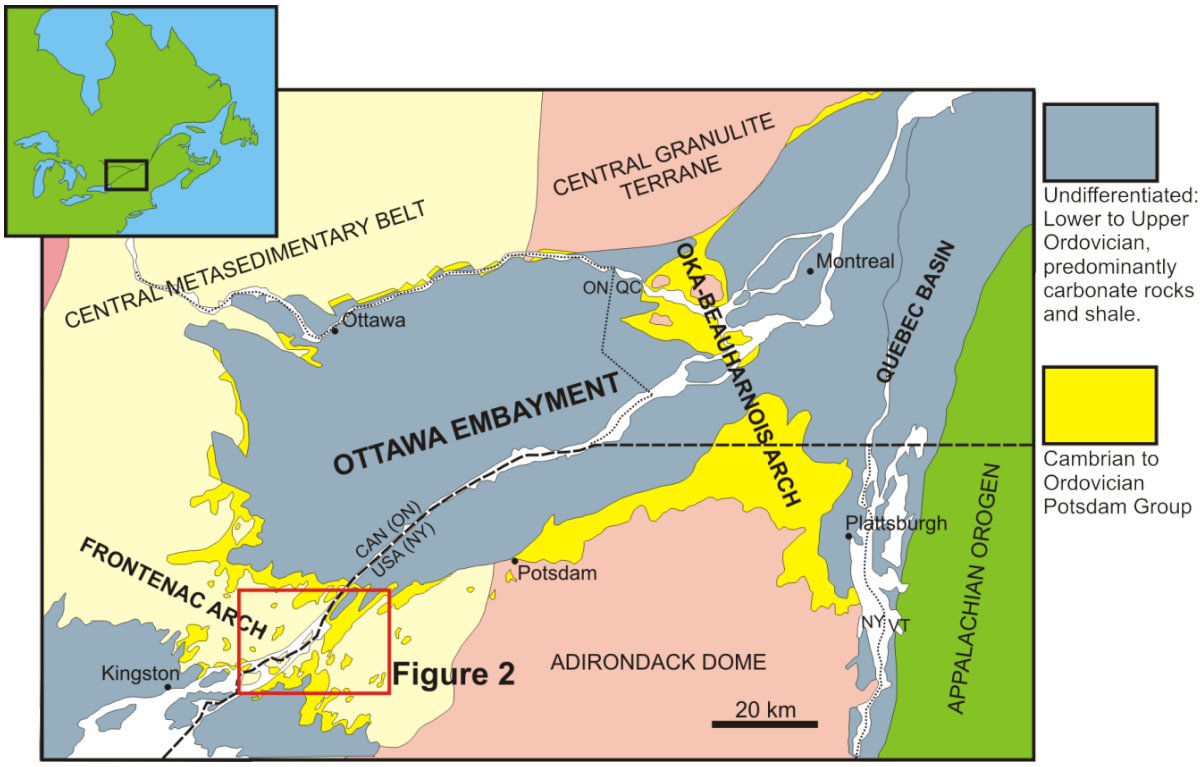

Figure 1. Base geologic map of the Ottawa Embayment-Quebec Basin and surrounding areas showing the outcrop distribution of the Potsdam Group. Today's trip will focus on the stratigraphy and sedimentology of the Potsdam Group in the southwestern margin of the Ottawa Embayment, along the southeastern extension of the Frontenac Arch (see Figure 2).

REGIONAL SETTING

The Cambrian to Ordovician Potsdam Group is a composite siliciclastic unit dominated by sandstone with subordinate conglomerate and exposed on the along the edge of the Ottawa Embayment and Quebec Basin, an east-west extension of the St. Lawrence platform in eastern Ontario, northern New York and western Quebec (Figure 1). Today we will be focusing on outcrops exposed along the Frontenac Arch in the southwestern Ottawa Embayment. The Potsdam Group is ≤ 25 m thick in this area, but thickens to ~ 700 m in the Quebec Basin along the Oka-Beauharnois Arch.

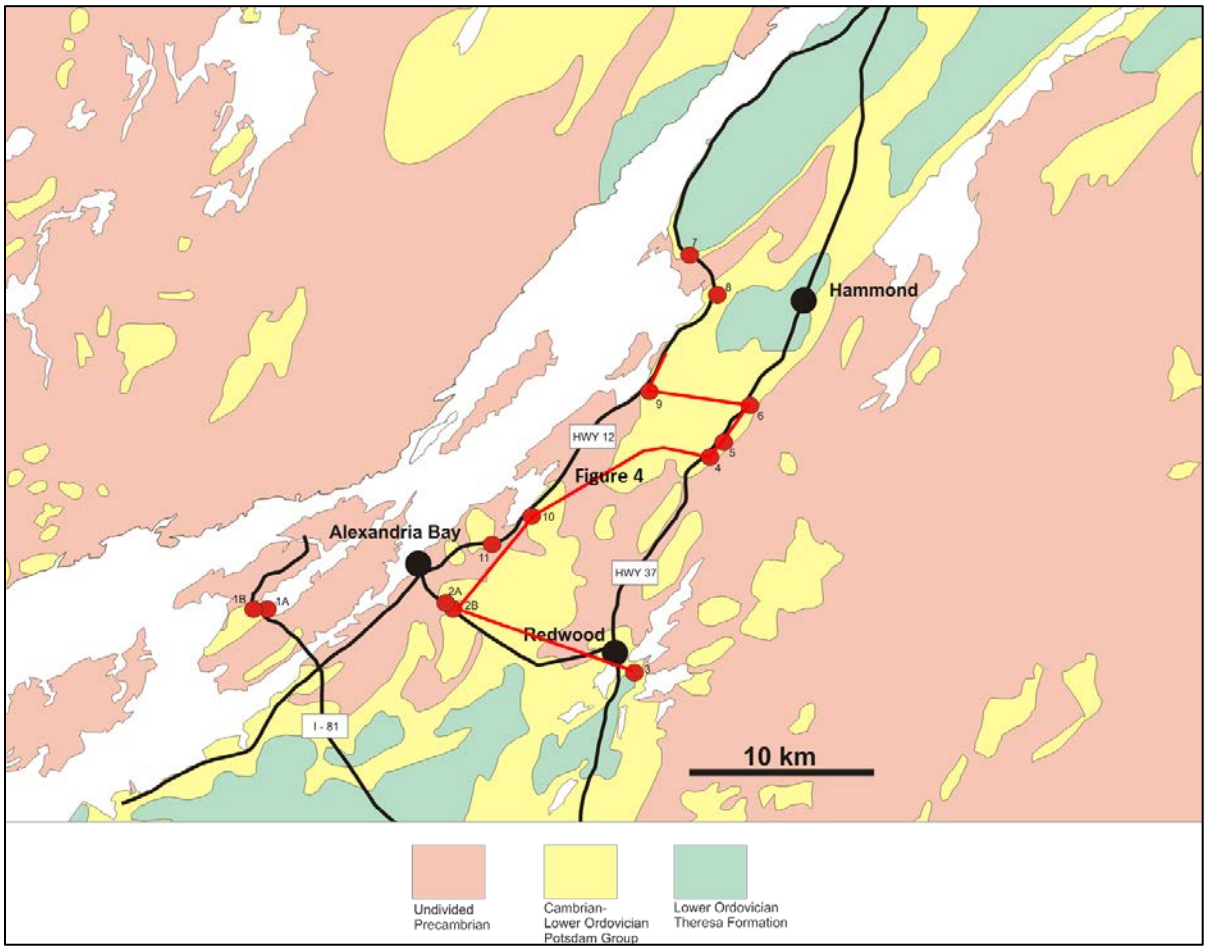

Figure 2. General geologic map focussing on the southwestern margin of the Ottawa Embayment along the southeastern extension of the Frontenac Arch, and showing today's field trip stops (red dots). The red outline shows the outcrops used to generate the more detailed cross-section in Figure 4.

AGE

The depositional age of the Potsdam Group is poorly resolved due to a general paucity of age diagnostic fossils. In the western Ottawa Embayment there is no age limit on the lowermost Potsdam strata due to the absence of any age diagnostic fossils, but farther east the lowermost Potsdam Group is no older than latest Early Cambrian, and it has been suggested that this is the oldest age of deposition regionally (Landing et al. 2009).

It has been suggested that the age of the uppermost Potsdam is not younger than Late Cambrian based on the interpretation of a regional Potsdam-Theresa unconformity and correlation to other unconformities in the Laurentian Platform succession (Salad Hersi et al., 2002; Dix et al. 2004). However, new biostratigraphic analyses from this study (Nowlan, 2013) indicate that an interval stratigraphically below the uppermost Potsdam Group (the Riviere Aux Outardes Mb of the Covey Hill Fm) is Lowermost Ordovician (Early Tremadocian) (Figure 3). We therefore consider the uppermost Potsdam in the western Ottawa Embayment to be of Lower Ordovician age (e.g. Greggs and Bond, 1971; Brand and Rust, 1977; Sanford and Arnott, 2010).

STRATIGRAPHY

This study uses allostratigraphy (correlation of unconformity-bound units) to subdivide and correlate the Potsdam Group. A correlation scheme is shown on Figure 3, with proposed lithostratigraphic revisions superimposed on the allostratigraphy to reconcile existing cross-border inconsistencies with the nomenclature, following the North American stratigraphic code. Also shown are the depositional environments determined from detailed facies analysis. Four allomembers are recognized in the Potsdam Group. Correlations are in part aided by characterization of detrital zircon assemblages, but those are not discussed in detail in this field trip guide.

Allomember 1: Altona Formation: uppermost Early Cambrian to Middle Cambrian: is only recognized in the Quebec basin, along and to the east of the Oka-Beauharnois Arch (Figures 1, 3). It consists of wave/storm-dominated marine shoreface/shelf deposits. We will not visit outcrops of allomember 1 today. The Altona Formation is described in more detail by Landing et al. (2009).

Allomember 2: Ausable Formation (proposed revision): Middle to lower Upper Cambrian: consists of fluvial arkose that reach a thickness of ~600 m along the axis of the Oka-Beauharnois Arch and is exposed as outliers elsewhere (the Covey Hill Member, proposed) and of red bed aeolian quartz arenites, primarily present as locally preserved outliers, ≤ 20 m thick, along the southern and southwestern Ottawa Embayment (Hannawa Falls Member, proposed). We will see a few outcrops of the Hannawa Falls Member today that highlight the unconformity between allomembers 2 and 3 (Stops 3 and 9). This unconformity is correlated to the Sauk II – Sauk III boundary, representing a major early Late Cambrian lowstand on the Laurentian margin and adjoining Michigan and Appalachian basins (Lavoie, 2008; Sanford and Arnott, 2010).

Allomember 3: Chippewa Bay and Riviere Aux Outardes Members of the Keeseville Formation (proposed revision): Upper Cambrian to Lowermost Ordovician: consists of widespread but thin (≤ 20 m) quartz arenites and quartz cobble-boulder conglomerates of fluvial origin (Chippewa Bay Member, proposed) overlain in the northern Ottawa Embayment by marine sandstones with local mudstone and carbonate interbeds (Riviere Aux Outardes Member, proposed). The fluvial Chippewa Bay member of allomember 3 makes up the thickest part of the Potsdam in this area (Figure 4), and consists of braided perennial (Stops 1, 2, 6 and 10) and ephemeral (Stops 2 – 6 and 8 – 11) depositional facies associations. The Riviere Aux Outardes Member is not present here, but constrains the age of allomember 2, which is otherwise terrestrial and devoid of fossils. A nodular to massive silcrete horizon of probable groundwater origin and intraclast breccias within the horizon of probable tectonic origin is present at the top of allomember 3 in this area.

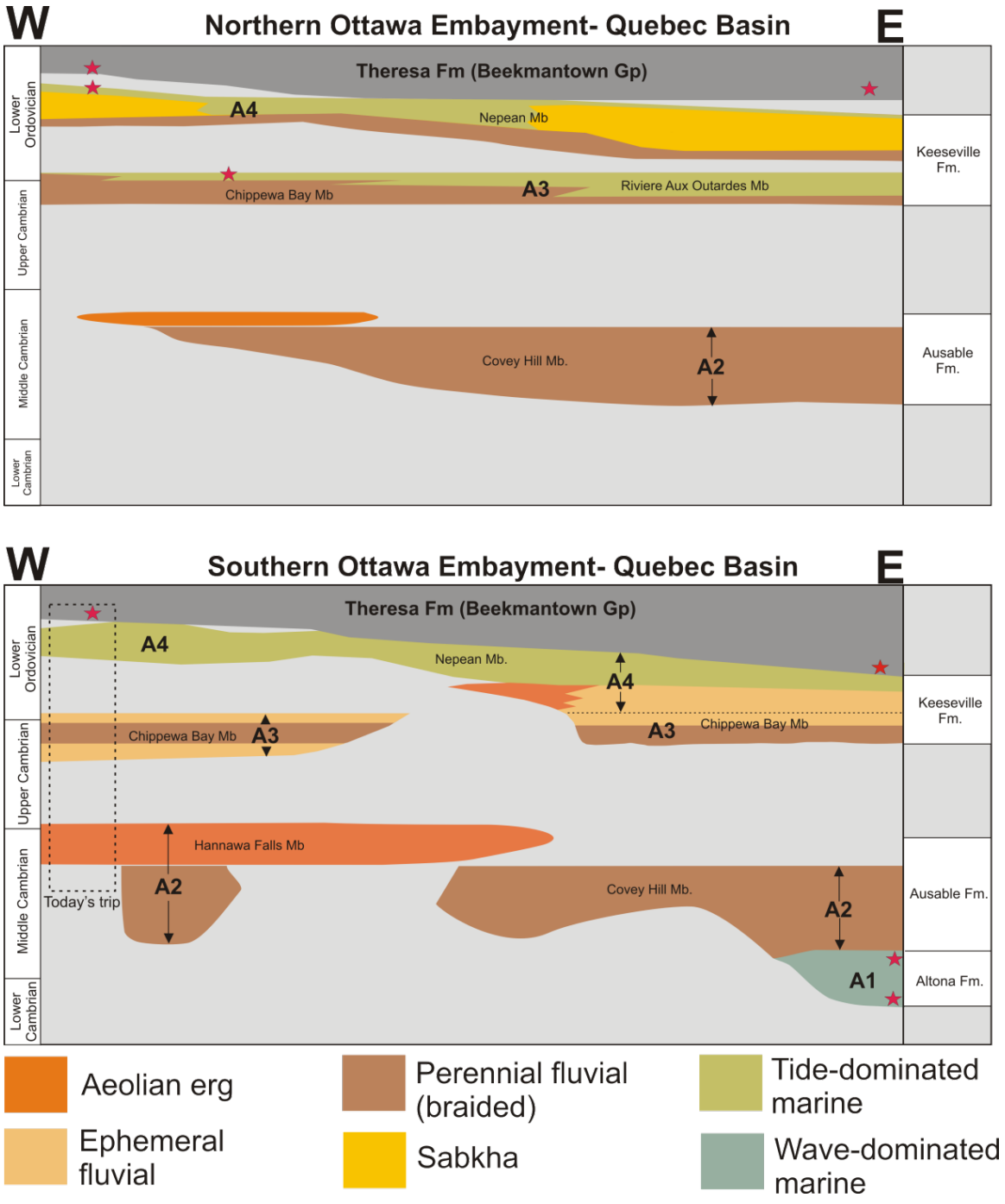

Figure 3. East-west allostratigraphic correlations of the Potsdam Group in the northern and southern Ottawa Embayment-Quebec Basin. Existing biostratigraphic age controls are shown by the red stars. Depositional environments, interpreted from detailed facies analyses, are overlain on the stratigraphy. Four allomembers (A1-A4) are recognized in the Potsdam Group (see text for more detail).

Allomember 4: Nepean Member of Keeseville Formation (proposed): Lower Ordovician: consists of basal terrestrial and overlying marginal marine and tide-dominated shallow marine quartz arenite that forms the uppermost Potsdam. Allomember 3 is locally conformably but abruptly overlain (Wilson, 1946; Brand and Rust, 1977; Selleck, 1993) or unconformably overlain (Salad-Hersi et al., 2002; Dix et al., 2004) by the mixed carbonate and siliciclastic Theresa Formation. Existing and new ages of the basal Theresa Formation indicate that the switch from pure siliciclastic (Potsdam) to mixed siliciclastic-carbonate (Theresa) was diachronous, younging from the southwest to the northeast (Figure 3).

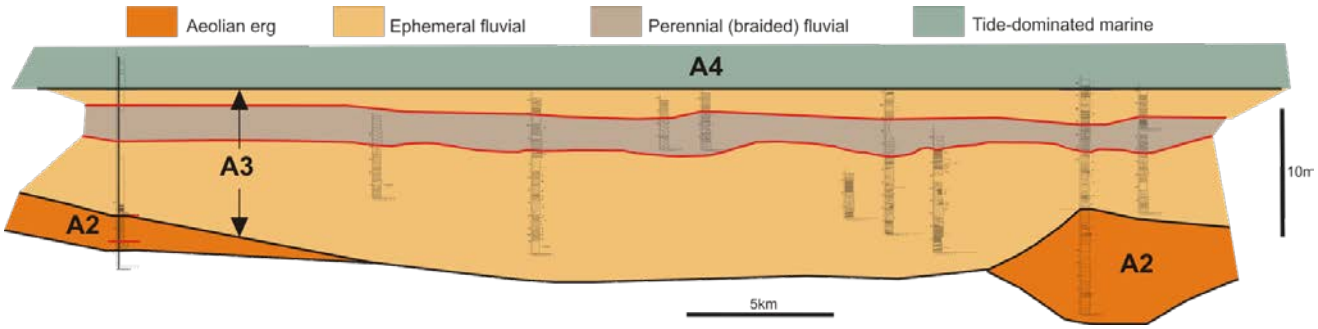

Figure 4. Cross-sectional correlation Potsdam allomembers (A2-A4) and facies associations in the Southwestern Ottawa Embayment (the exact location of this correlation is given in Figure 2). Allomember 3 makes up most of the Potsdam in this area, and is dominated by sheet-like ephemeral fluvial facies.

DEPOSITIONAL FACIES ASSOCIATIONS

Four Depositional facies associations, each recoding deposition by unique depositional environments and depositional processes, are recognised in this part of the Potsdam Group. These include: aeolian erg, ephemeral fluvial, perennial (braded) fluvial and tide-dominated marine (Figure 4). Of these, aeolian erg and tide-dominated marine are well described from previous work in the Potsdam (Bjerstedt and Erickson, 1989; Selleck, 1993; MacNaughton et al., 2002; Hagadorn et al., 2008, 2011), and do not make up a large part of the Potsdam succession in this area, so they are not summarized in detail here. Ephemeral and perennial fluvial deposits make up the bulk of the Potsdam Group in this area (Figure 4) and have not previously been described in detail. Also, these facies associations are present at most of the stops today. The following is a summary of facies analysis and criteria for the recognition of these depositional environments in the Potsdam Group.

Perennial (braided) fluvial facies association: braided fluvial deposits are recognized by a dominance of coarse-grained trough cross-stratified sandstone, locally with tractional conglomerates, as well as the presence of lateral, downstream and upstream accreting architectural elements and channel elements (Figures 5, 9 – 10, 16a), and a lack of trace fossils. The most common elements are lateral, downstream, and upstream accretion elements, interpreted as the products of solitary and compound mid-channel and point bars formed by sequential and gradual accretion during successive channelized flood events in a braided river setting (Figure 5). Internally, these elements are made up of trough cross-stratified coarse-grained sandstone interpreted to have been deposited by the migration of subaqueous dunes. Other common elements include tractional conglomerates and channel elements (Figure 5). Tractional conglomerates are recognized by imbricated, oriented and sometimes graded conglomerate beds, interpreted as a number of gravel bedforms including chutes and lobes, bed load sheets and clusters forming at mid-channel positions at the base of compound bar deposits or near bar tops. Channel elements (Figure 5) vary in size and are filled either with dune cross-stratified

sandstone or draping or concordant bedding. The largest of these are interpreted to form at the base of channel by scouring due to the confluence of channels around mid-channel compound bars, while smaller channel elements are interpreted as bar-top channels (Figures 5, 10 and 16b). A hierarchy of bounding surfaces are present, and the highest order surfaces subdivide braided fluvial strata into channel belts successions, which are differentiated by changes in average paleoflow, grain size and sedimentary character. Good examples of this facies association will be shown at Stops 1A and B.

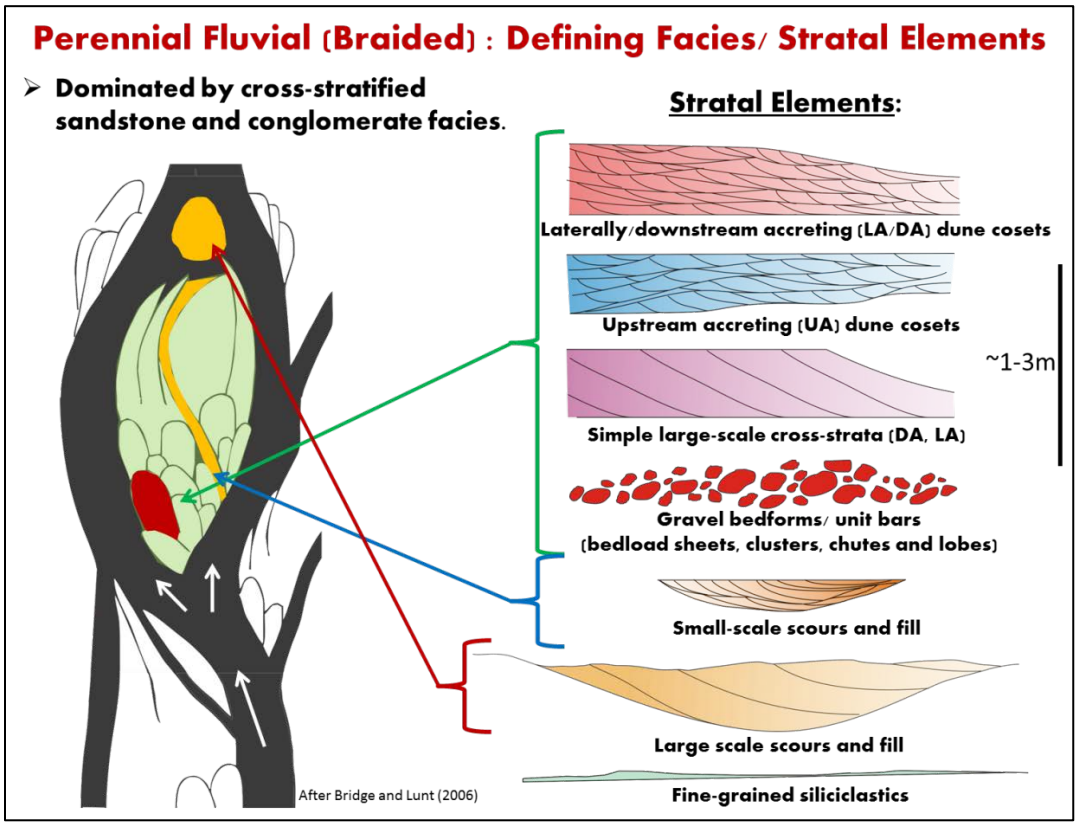

Figure5. Architectural elements and facies typifying braided fluvial systems in the Potsdam Group. The most abundant deposits are of laterally, downstream and upstream accreting dune cross-stratification, formed by the migration and accretion of bars. Channel elements are also recognized. Large Channel elements are interpreted as confluence scours that form in front of large compound bars, and smaller scours are interpreted as bar top channels and their fill.

Ephemeral fluvial facies association: Ephemeral fluvial systems are distinguished from perennial fluvial systems in that they are characterized by a very different set of conditions- specifically, deposition during catastrophic and episodic high discharge events that are prompted by uncharacteristically high precipitation rates in a semi-arid climate. Such discharge overwhelms existing dry channel networks (if present), resulting un-channelized very high energy and shallow sheet flood conditions. Deposits of ephemeral fluvial systems are common in this part of the Potsdam and are interpreted to have formed a north-facing fan system. They are recognized by a predominance of planar stratification formed by upper stage plane bed, with less common but highly diagnostic cross-stratification formed by supercritical bedforms (antidunes, chutes and pools and cyclic steps), and occasional wave and current ripples, erosionally-based subaqueous dune cross-stratified cosets,

desiccation cracks, adhesion structures and stratification and minor aeolian strata (Figure 6). Architectural elements are mostly simple and sheet-like (upper flow regime (UFR) bars, Figure 6), and are interpreted to have formed by rapid aggradation during high energy and short-lived sheet floods (perhaps as short as a day, e.g. Stear 1984). Packages bound by high-order bounding surfaces are interpreted as the deposits of depositional lobes in a distributary fan type of system, rather than channel belts as in perennial (braided) fluvial systems (e.g. Hampton and Horton, 2007; Figure 7).

The most diagnostic sedimentary structures are antidunes, chutes and pools and cyclic steps, and are primarily recognized by low- to moderate-angle cross-stratification with dips generally opposing that of associated dune cross-stratification; all of which form under supercritical flows (Froude # >1) with higher velocities and shallower (< 20 cm) depths than the subaqueous dunes that characterize perennial fluvial deposits. Although poorly recognized in the sedimentary record and relatively rare due to rare due to the conditions required for their deposition, their recognition in fluvial outcrops has been highlighted in a review paper by Fielding (2006) and their depositional constraints and mechanisms have been outlined recently by experimental studies by Cartigny et al. (2013).

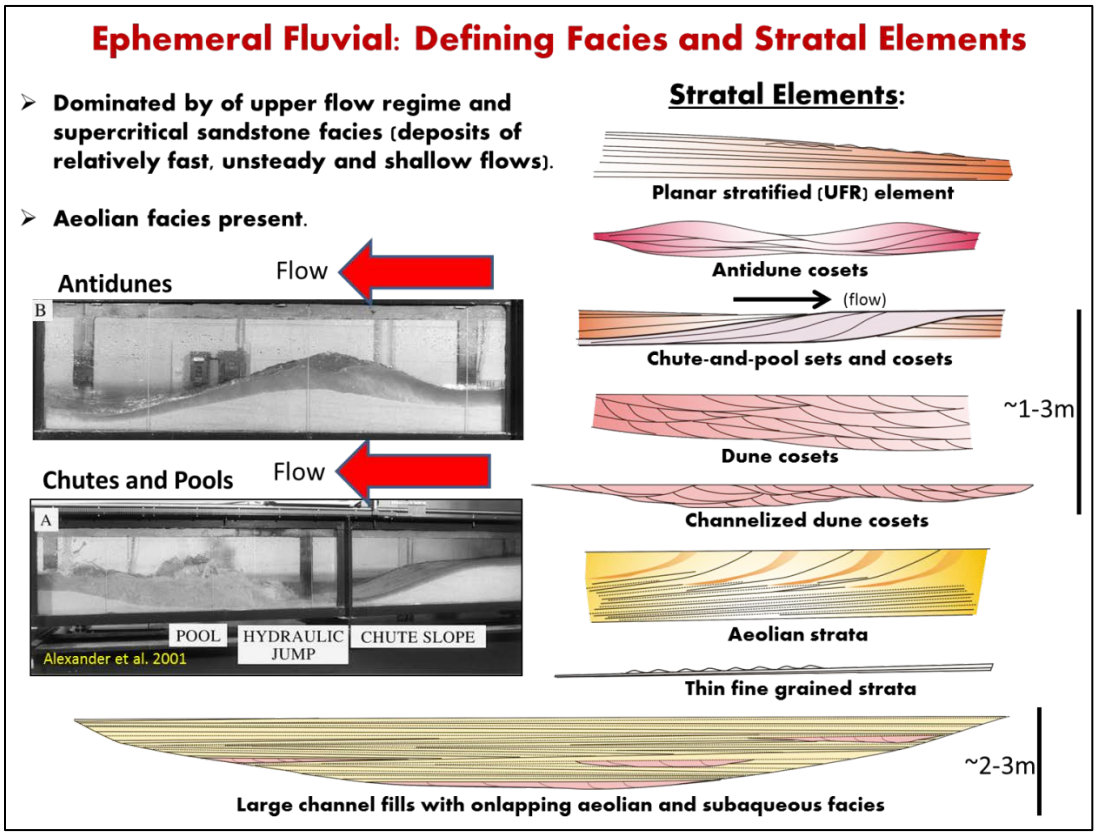

Figure 6. Architectural elements and facies typifying ephemeral fluvial depositional systems in the Potsdam Group. The most common element is low angle to horizontal upper flow regime (UFR) elements, dominated by upper stage plane bed. However, the most diagnostic elements are those formed by supercritical bedforms, typifying very fast and violently energetic relatively shallow sheet flood conditions (antidunes and chutes and pools, but also cyclic steps (see Figure 8)).

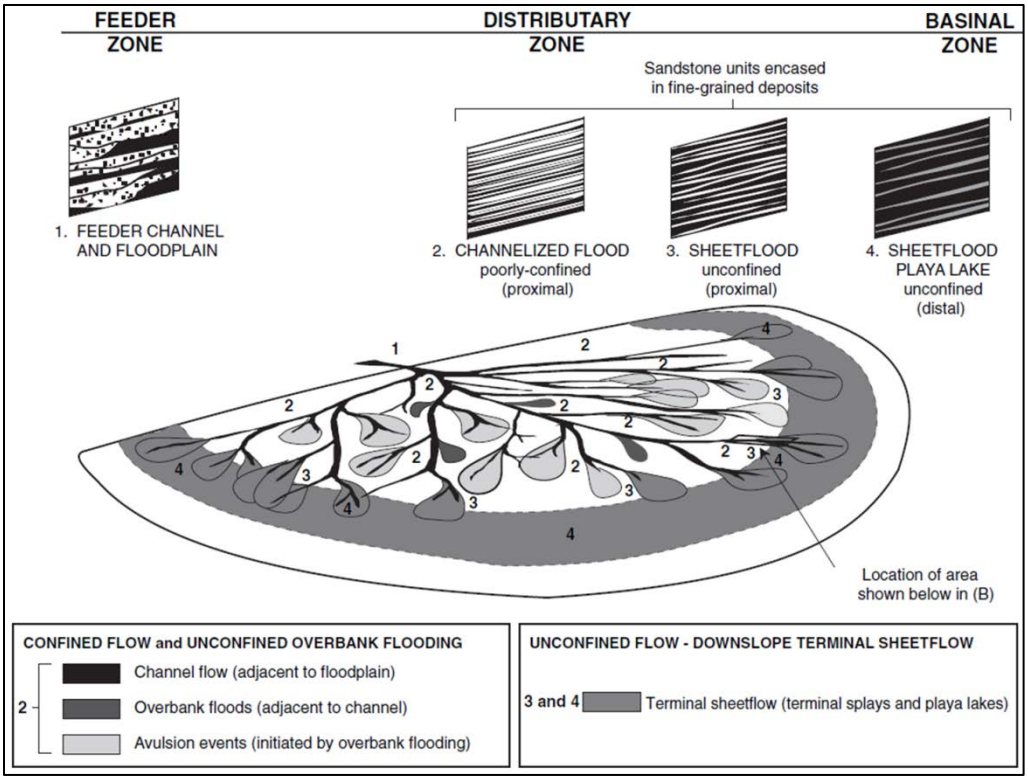

Figure 7. Schematic depositional model of a sheetflood-dominated ephemeral fluvial distributary fan system, from the Eocene-Oligocene Potoco Formation in the Altiplano plateau of Bolivia (from Hampton and Horton, 2007). The sheet-like ephemeral fluvial exposures we will view today are interpreted to have been part of a similar system in a north-facing distributary fan, probably deposited in the unconfined and proximal sheetflood environment (#3).

Antidunes are recognized by thin (2 – 15 cm) lenticular sets of low angle ($\leq 20^o$) cross-laminated lower medium to upper coarse grained sandstone bounded by low-angle ($5 – 15^o$) concave-upward scours (troughs), with occasional low angle ($10 – 15^o$) convex-upwards symmetrical formsets (Figures 8 and 14). These form under shallow supercritical flows (Froude number >1) in which upstream-migrating surface waves are in-phase with the bed (Figure 8). The breaking of surface waves causes the erosion of antidune crests and the deposition of backsets into antidune troughs, which is the most common type of stratification preserved. The preservation of convex-upwards antidune formsets (as at Stop 4) indicates higher rates of aggradation and therefore high sediment concentrations (Cartigny et al., 2013).

Chute and pool stratification is recognized by upstream-dipping scours filled by upstream-dipping sigmoidal cross-stratification (Figures 6, 8, 15b-c, 16b). These are formed
under flows with even higher Froude numbers (and therefore higher velocities and/or shallower depths) than antidunes in which upstream-migrating surges and hydraulic jumps form (turbulent rapid flow expansions from supercritical to subcritical conditions). Low angle backsets at the base characterize the upstream migration of the surge, while overlying, higher angle backsets formed during the development of a stationary hydraulic jump, and relatively planar laminations at the top formed after the hydraulic jump subsided and shallow, supercritical sheet flow conditions resumed (Figure 8). Chutes and pools are not stable bedforms, but instead represent deposits of the transition between more stable antidunes and cyclic steps (Cartigny et al., 2013). Their presence

therefore probably records highly unstable flow conditions, during either the waning or waxing stage of supercritical flows.

Cyclic steps are recognized by thin to thick (15 cm - 1.2 m) low to high angle (10 – 35^{o}) boundary-conform backsets (Figures 8, 16b and 17a). They form at higher Froude numbers than antidunes and chutes and pools, and under the highest velocities for a given flow depth of any known bedform. Essentially, they are upstream-migrating bedforms in which the lee-side is erosional and the stoss-side is depositional, due to the presence of regularly-spaced hydraulic jumps in their troughs and flow acceleration over their crests (Figure 8).

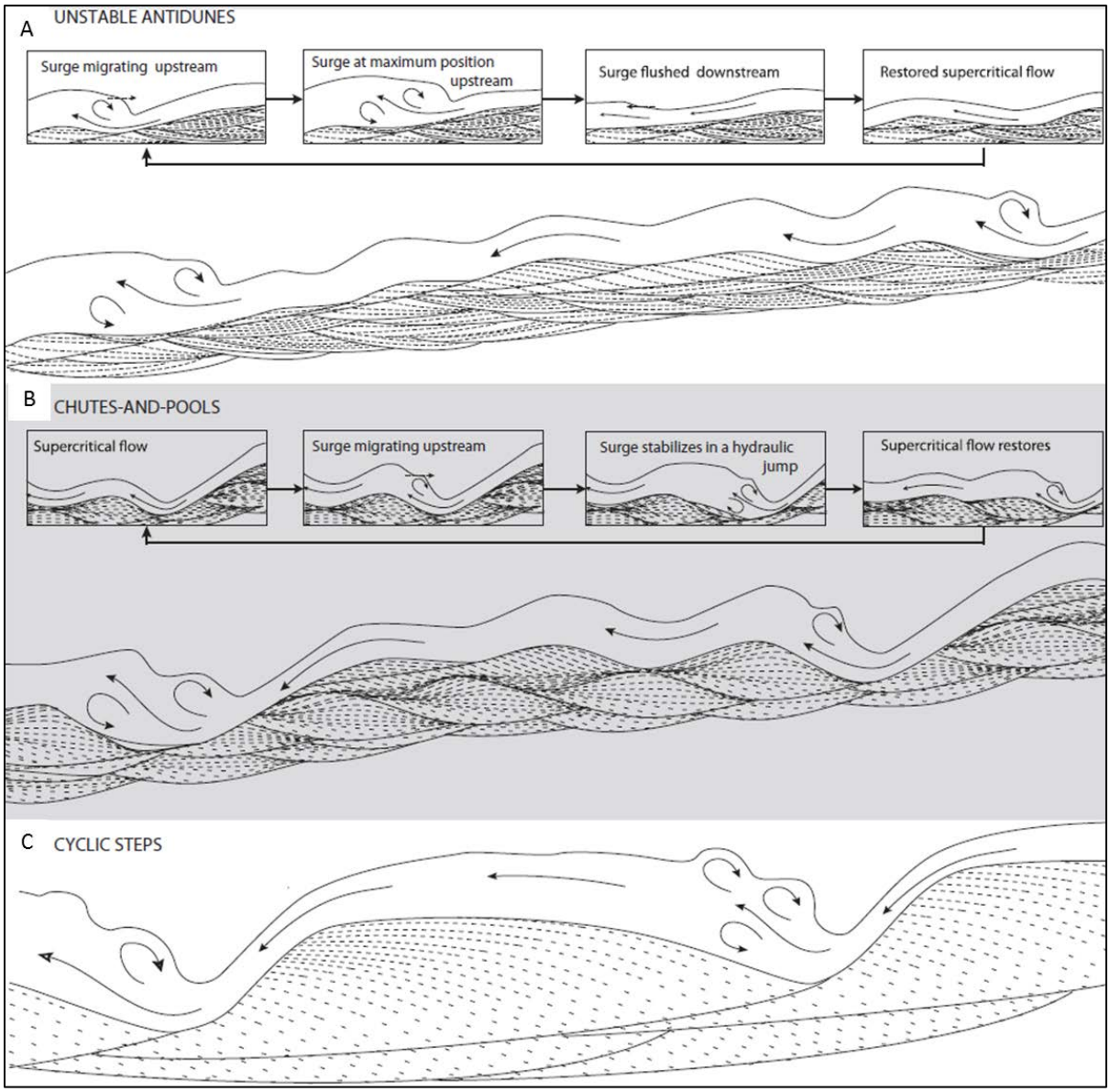

Figure 8. Schematic summary of the depositional processes and products of supercritical flows in which surface waves, surges and hydraulic jumps interact with the bed, from Cartigny et al., 2013. The bedforms resulting from such flows (antidunes, chutes-and-pools, cyclic steps) migrate in the upstream direction and the preserved cross-laminations dip in the opposite direction of the paleoflow direction.

FIELD TRIP STOPS

Stop 1A: Braided fluvial architecture, interactions with active basement topography and an Early Ordovician marine transgression**.** *Wellesley Island Route 191 (44.31640 N; -76.00551 W).* This section consists of perennial fluvial deposits of allomember 3 (Chippewa Bay Mb of the Keesville Fm) overlain by tide-dominated marine strata of Early Ordovician allomember 4 (the Nepean Mb of the Keeseville Fm). This section contains good braided fluvial architectures, interesting stratigraphy and evidence of interaction with the adjacent basement ridge directly to the south (Figure 9).

Perennial fluvial deposits of allomember 3 are present at the base of the outcrop. On the west side of the road, 2 - 3 channel belt successions are present, and are differentiated by abrupt grain size and paleoflow direction changes and by sharp bounding contacts. The lower channel belt (Figure 9A) consists mainly of tractional conglomerate facies and was a ~WNW paleoflow. This is overlain by a sharp contact and a 1 – 1.5 m thick lateral accretion bar deposit at the base of the second channel belt succession (Figure 9A). Boulder debris increases upward and these thin debrites thin to the north. Clasts are presumably derived directly from the ridge to the south (Figure 9B). A laterally-discontinuous boulder debrite characterizes the base of the third channel belt, underlain by a sharp, angular erosional contact (Figure 9C). This "progradation" of boulder debris in the upper part of the second channel belt succession and base of the third is interpreted to represent the presence (possibly active) of the basement ridge directly to the south during deposition of allomember 3 (Figure 9B).

The contact between Allomember 3 and 4 is best viewed some 50 m north, and is present on both sides of the road. Early silcrete nodules of probable groundwater origin are present 1 – 1.5 m from the top of Allomember 3. The base of Allomember 4 is marked by an erosional contact overlain by coarse-tail graded conglomerate. Approximately 1 m above this are gutter casts (visible on the west side of the road) above which fully marine strata onlaps underlying transgressive lag deposits (this onlap is very low angle and is best viewed at the next stop).

Stop 1B: *Wellesley Island, I-81 (44.31725, -76.01024)*: **SAFETY NOTE**: This section gives a broader view of the previous section, and is located only ~200 m to the west. The best view is from the west side of the I-81, looking east across the I-81.

The Allomember 3-4 contact is well displayed here (Figure 10a). The base of Allomember 3 is a north-dipping erosional contact overlain by a ~50 – 75 cm thick conglomerate. The conglomerate is onlapped by tabular-bedded tide-dominated marine strata of Allomember 4. The lower contact and conglomerate are interpreted as a transgressive surface of erosion and transgressive lag, respectively (Figure 10A). Although marine strata appear to onlap the lag deposit here relatively passively, this contact was accompanied by erosional gutter casts at the previous stop, suggesting local erosion by waves and tides.

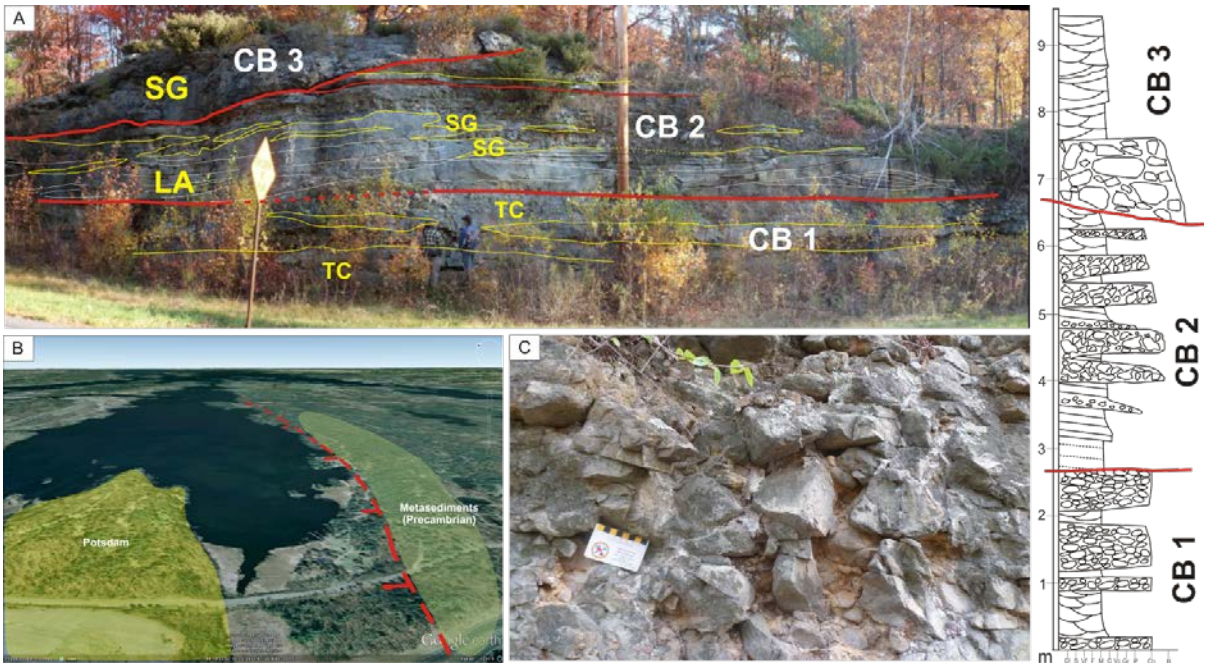

Figure 9. Fluvial architecture and progradation of boulder debris at Stop 1A. A: 3 channel belts are identified here, separated by high order bounding surfaces (CB 1-3). TC= tractional conglomerate, SG= Sediment gravity flow (debrite), LA= lateral accretion element. B: This section is located adjacent to a normal fault and basement ridge. The increasing progradation of debris flow (A and C) indicates that this ridge was present during sedimentation.

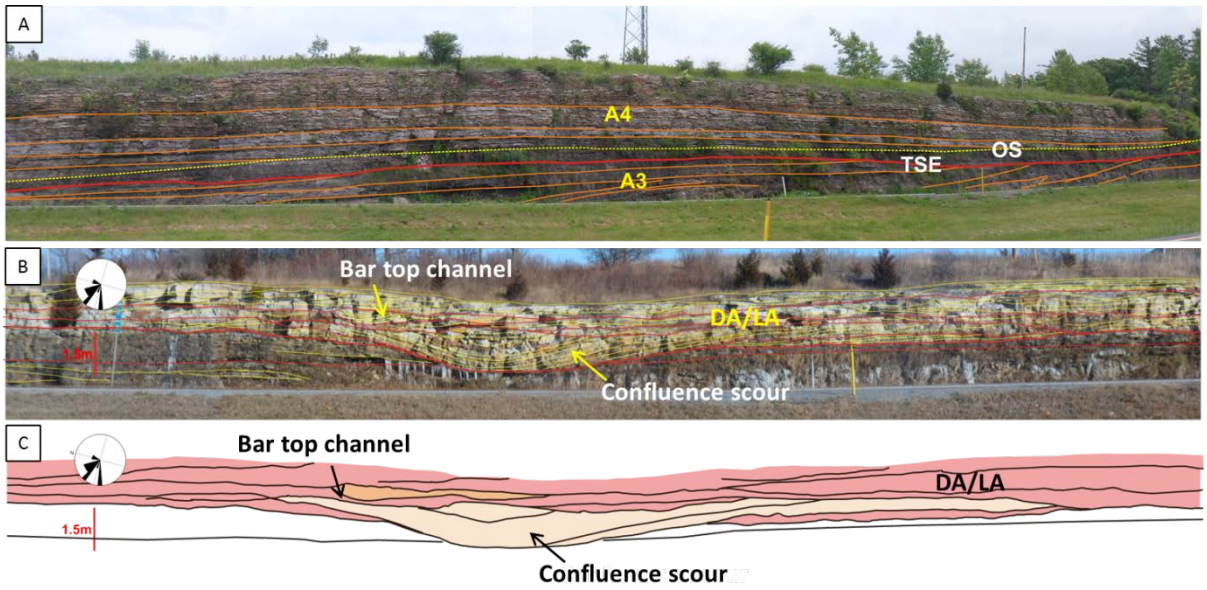

Figure 10. Stop 1B: A: contact between allomembers 3 and 4 (A3, A4). A3 is overlain by a transgressive surface of erosion (TSE) and a conglomerate lag. Marine strata of A4 onlaps the lap (OS= onlap surface). B, C: braided fluvial architectures in A3, exposed farther to the north along I-81. Paleoflow is to the NW.

Some instructive braided fluvial architectures can be seen farther north that demonstrate the initiation of a new channel belt succession and subsequent bar migration (Figure 10b, c). Again, we should be looking east across the I-81. The paleoflow here is to the NW to the N, generally coming out of the outcrop. A broad but very obvious confluence scour marks the base of the second channel belt succession from the previous stop (Figure 10b-c). Low to moderate angle dune cross-stratified laterally to downstream accreting elements (DA/LA on Figure 10b-c), interpreted as the deposits of bars- are built up into a compound bar deposit. A smaller scour element is present near the top of this compound bar succession, and is interpreted as the deposit of a cross-bar channel.

Stop 2: Ephemeral and perennial fluvial contact. *Route 26, south of Alexandria Bay (44.32148, -75.90305):* This stop shows the contact between ephemeral fluvial and perennial fluvial systems in Allomember 3 (Chippewa Bay Mb of the Keeseville Fm). The ephemeral fluvial section is best viewed in the northern part of this section (stop 2A), and the ephemeral –perennial contact is exposed just 100 m to the north (Stop 2B).

Stop 2A: Ephemeral fluvial strata are exposed here, and diagnostic architectural elements include UFR bars and antidune cosets. These architectures are better exposed at later stops (stops 4, 5 and 6).

Stop 2B: The contact between ephemeral and perennial fluvial systems is exposed here, 100 m to the south of 2A along route 26 (Figure 11). The contact is sharp and horizontal (with minor, cm-scale incision). The lower ephemeral fluvial deposits are characterized by their tabular bedding, whereas the overlying perennial fluvial deposits are clearly trough cross-stratified, dominated by dune-cross stratification with mean paleoflow to the north. This contact is correlated elsewhere (Figures 4, 16a and 18c) and is interpreted to record a change in climate from semi-arid to humid.

Figure 11. Ephemeral – perennial fluvial contact exposed at Stop 2B. Minimal incision is present along this contact, in contrast to the same contact exposed at stop 6.

Stop 3: Allomember 2-3 contact: *Near Millsite Lake on Cottage Hill Road, east of Redwood, NY (44.29374, -75.79057).* Precambrian basement as well as Allomembers 2, 3 and 4 are exposed here (Hannawa Falls Mb of the Ausable Fm; and the Chippewa Bay and Nepean Mbs of the Keeseville Fm, respectively). All of these are exposed on the south side of the road, uphill from the Millsite Lake access parking. Grenville basement and the Precambrian unconformity are visible from the road. A ~50 cm regolith is present just above the basement.

Overlying that is a 2 m section of aeolian red beds of the early Late Cambrian Allomember 2 (Hannawa Falls Mb of the Ausable Fm). An excellent exposure of the allomembers 2 – 3 unconformity is exposed on a small ridge just a small way (~10 m) south over the ditch and into the wooded area. The unconformity is erosional and lithified rip-up clasts of allomember 2 are present in

the lower few cm of Allomember 3 (Figure 12a-b). Lithification of allomember 3 is characterized by hematite rims and kaolinite cementation (Figure 13), interpreted to have formed pedogenically by the formation of a laterite paleosol. This contact is correlated to others in the Ottawa-Embayment and Quebec Basin, and represents a long period of time (possibly ca. 10 Myr) and significant changes in provenance, depositional setting and paleogeography (from basin –wide correlations, detrital zircon analysis and regional paleoflow analysis).

Allomember 2 (Latest Cambrian – Earliest Ordovician Chippewa Bay Mb of the Keeseville Fm) is relatively thick (~10 m) and consists mainly of ephemeral fluvial facies. Specific architectures and divisions of facies associations into ephemeral and perennial fluvial deposits are not differentiated here due to poor exposure of the section.

Allomember 3 (Early Ordovician Nepean Mb of the Keeseville Fm) is exposed in the upper ~2.5 m of the section (near the top of the hill) and consists of medium-scale tabular dune and ripple cross stratification that is locally bioturbated by a filter-feeding *Skolithos* ichnofacies (including *Skolithos*, *Diplocraterion*, and *Arenicolites*).

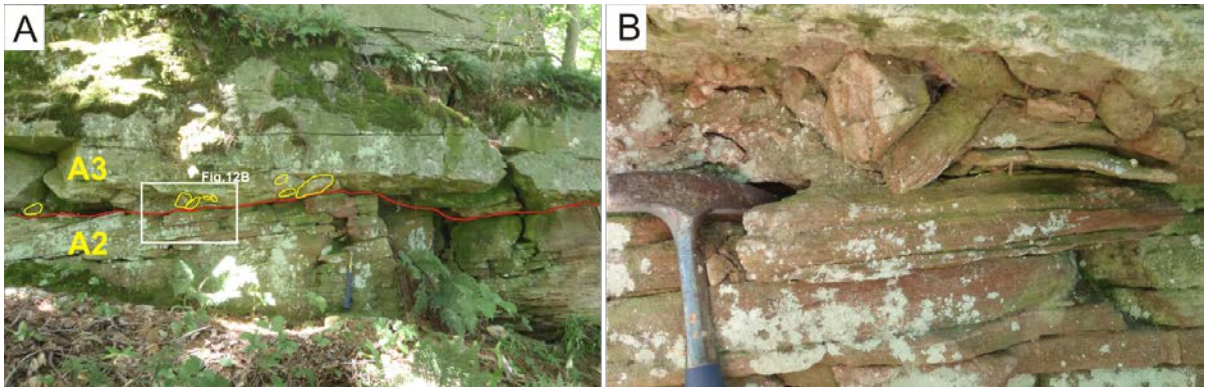

Figure 12. Allomembers 2-3 (A2-A3) contact exposed at Stop 3. A: the contact is sharp and erosional with undulating relief and several cm. A-B: lithified clasts of A2 are present at the base of A3, suggesting that A3 was lithified before deposition of A3. This contact is correlated to outcrops to the south Theresa (~10 km to the south), as far north as Perth, ON (~70 km to the north) and east as Pope Mills (~30 km).

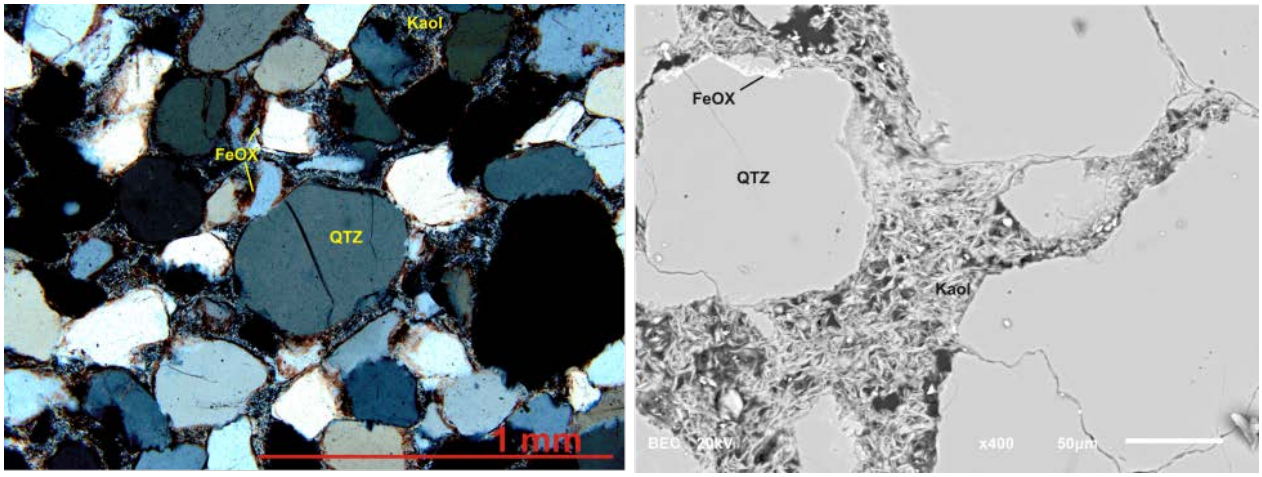

Figure 13. Photomicrograph and backscattered SEM image of A2 at Stop 3. Detrital quartz grains (QTZ) are rimmed by hematite (FeOX) and cemented by pore-filling kaolinite (Kaol).

Stop 4: Antidune cross-stratification: *North ledge outcrop on the north side of Highway 37: between Redwood and Hammond, NY (44.38048, -75.75508).* This is a relatively small outcrop of ephemeral fluvial strata from Allomember 3 (Chippewa Bay Mb of the Keeseville Fm). Here one of the most diagnostic elements indicating sustained deposition by supercritical flows is present: antidune cosets and convex-up formsets (Figure 14). This is interbedded with UFR bar form elements, dominated by upper flow regime plane bed indicative of fast-moving and probably shallow unidirectional flows (Figure 14).

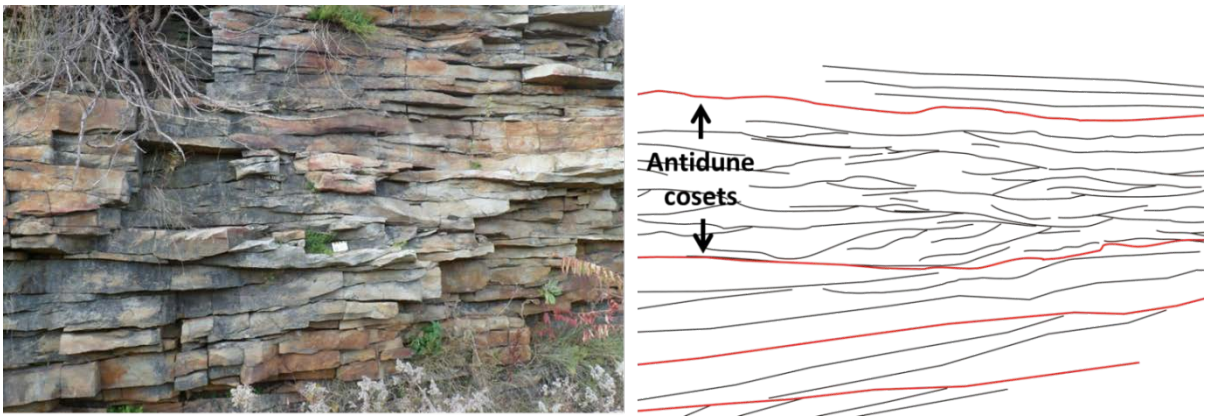

Figure 14. Antidune cross-stratification exposed at Stop 4. The small card is 10 cm across.

Stop 5: Aeolian and chute-and-pool stratification in an ephemeral fluvial setting: *North and south of Highway 37, between Redwood and Hammond, NY (44.38696, -75.74568).* This is another exposure of Allomember 3 (Chippewa Bay Mb of the Keeseville Fm) that highlights some aeolian and upper flow regime facies of the ephemeral fluvial facies association. On the north side of the road is a small outcrop that contains the remains of an aeolian dune, complete with lee-side grain flow deposits and "pinstripe" wind ripple stratification (Figure 15a). On the south side of the road is a natural pavement, with rib-and furrow structures formed by the intersection of 3D dune cross-strata, showing a paleoflow of 355^{o} (~N). Past this and down a steep slope of rubble (beware of broken glass here! – proceed with caution) is an outcrop exposing the same interval as at the last stop. This outcrop exposes some of the best examples of up-flow dipping chute and pool and cyclic step stratification (Figure 15b-c) recoding the deposition from extremely fast-moving highly-concentrated supercritical flows.

Stop 6: Perennial-Ephemeral fluvial contact (again!) and cyclic steps: *North and south of Highway 37 and on Cemetery Road, near Hammond (44.40248692, -75.72873119).* This is another exposure of the ephemeral – perennial fluvial contact within allomember 3 (Chippewa Bay Mb of the Keeseville Mb) and one that also showcases some thick cyclic step supercritical bedform stratification. On the north and south of Highway 37, the ephemeral fluvial deposits with moderate angle upper flow regime macroforms are incised by dune cross-stratified channel elements of perennial fluvial deposits (Figure 16a). On the east branch of Cemetery Road, south of Highway 37, a ~N-S oriented section reveals the "macroforms" actually consist of thick, up flow-dipping cyclic step stratification (Figure 16b). Incredibly, cross-stratification formed by dunes is preserved on the stoss-side of cyclic steps, climbing and dipping in the opposite direction of the upflow-dipping chute and pool backsets (Figure 16b). On the south part of this exposure, antidune cross-stratification and formsets are present (Figure 16b).

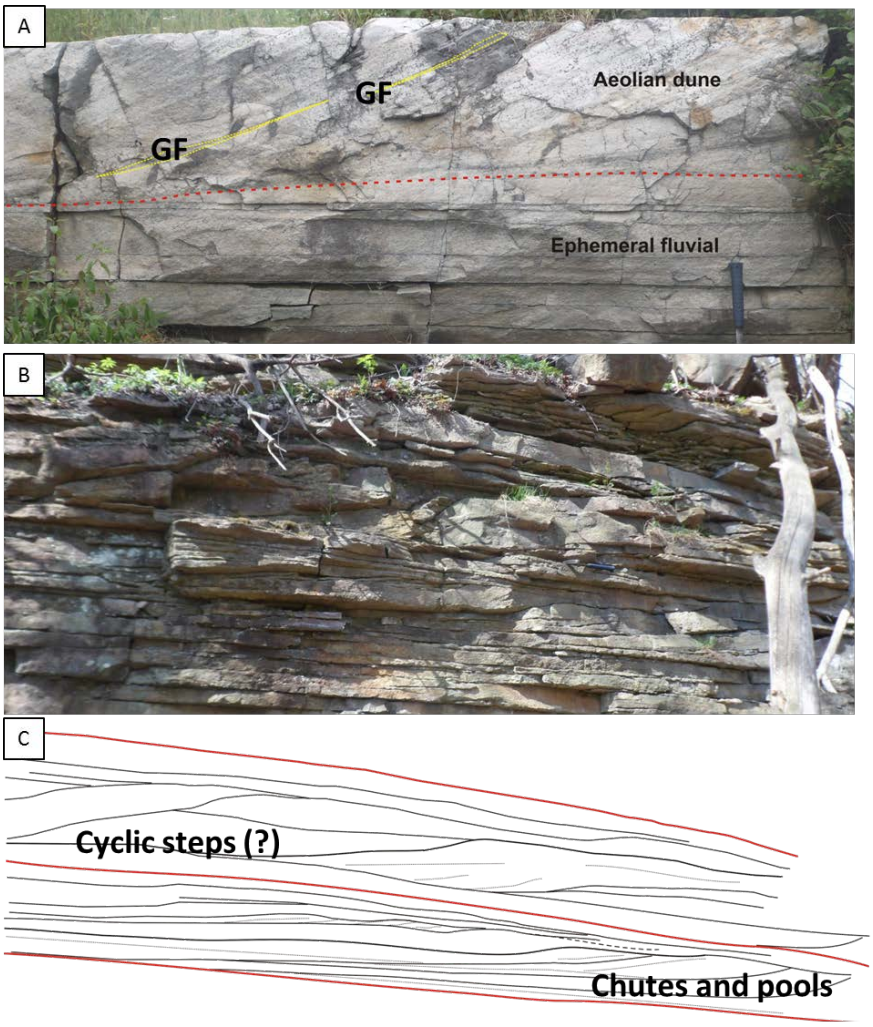

Figure 15. Stop 5: A: aeolian dune cross-stratification is exposed on a small outcrop on the north side of the road. B, C: in the wooded area south of Route 37 is a ledge that exposes some upstream-dipping cyclic step and chute-and-pool cross-stratification. This exposure is at roughly the same stratigraphic position as the antidunes exposed at Stop 4. Fig 15C is a traced sketch of Fig 15B.

Stop 7: Potsdam-Theresa contact: *Highway 12, just north of Pleasant Valley Road (44.46609, -75.76102).* This is a classic stop, showing the Potsdam—Theresa contact. The uppermost Potsdam is the typical tide-dominated marine facies association characterizing Allomember 4 in the area. The contact at this location is interpreted as a probable conformable but drastic facies change, into deeper water, storm- and tide- dominated shelf setting. The Theresa here is largely characterized by dolomite cemented fine- to medium-grained sandstone (locally coarse) with normally-graded beds, 2 -15 cm thick, consisting of sharp to diffuse upper plane bed laminations overlain by wave and/or combined flow ripples and bioturbated fine argillaceous sandstone. These beds are interpreted as tempestites (e.g. Selleck, 1993). Hummocky cross-stratification (HCS) in the Theresa is probably largely inhibited due to a relatively strong unidirectional flow component caused by reinforcing ebb tides. Experiential work has shown that only small unidirectional velocities mixed with strong oscillatory wave-generated currents are needed to inhibit HCS (Dumas et al., 2005).

Stop 8: Marine flooding and a groundwater silcrete linked to the Black Lake Fault. *Highway 12 near Chippewa Bay (44.44787, -75.74829).* This stop consists of two small outcrops on either side of Highway 12. These outcrops show the contact between Allomembers 3 and 4, characterized here by a sharp erosional discontinuity and a flooding surface separating ephemeral fluvial strata below from marine strata above. A massive silcrete horizon is present here at the very top of allomember 3, with conical intraclast breccias, originally described by Selleck (1978). A recent honours study focusing the genesis of this silcrete was undertaken by Ed DeSantis at the University of Ottawa. Ed's findings were that: (a) the silcrete is of groundwater origin, rather than pedogentic origin due to the preservation of primary sedimentary structures, occurrence of nodules and lack illuviation features; (b) multiple generations of silica overgrowths are present, indicating multiple precipitation-dissolution events; (c) the silica was likely derived from feldspars in basement rocks, given that the underlying Potsdam contains no evidence of feldspar dissolution; and (d) movement of fluids along, and movement of the Black Lake fault itself contributed silica and also stresses that generated the conical breccias in these relatively well-indurated horizons. The close spatial relationship between the distribution of the pervasive silica horizon, the conical breccias and the Black Lake fault provide good evidence for this relationship (DeSantis, 2014). The stratigraphic location of the silcrete (at the top of allomember 3) although suggestive of a pedogentic origin, is interpreted to have resulted from transgressive erosion down to the well-indurated and erosionally-resistant horizon.

Stop 9: Stratigraphy, sedimentology and diagenesis- this stop has it all! *Highway 12 just south of Schermerhorn Landing (44.41019, -75.78736).* Allomembers 2, 3 and 4 are all exposed in this section. Allomember 2 is present at the westernmost part of this exposure, where it is at least ~8 m in thickness (the base is not exposed, Figure 4), which contrasts with the thin preservation of this unit at Stop 3 and lack of preservation elsewhere, and attests to the variable preservation of allomember 2 in this area. Here it consists of large-scale cross-stratification formed by the migration of aeolian dunes. Inversely graded grain flow avalanche cross-strata are present, and can be found on the south side of the highway. Allomember 2 also has a blocky structural fabric, which appears to be truncated by the allomember 2-3 contact (Figure 17A).

Allomember 2 (~10 m thick) consists of planar-tabular stratified ephemeral fluvial deposits, with a few ~west dipping cyclic step deposits towards the top of the unit, and some ~NE-dipping subaqueous dune cosets as well as aeolian sand sheet deposits. The massive silcrete at the top of allomember 3 is well-developed here. It is coincident with bedding in the western part of the exposure, but towards the east it cuts across the bedding at a low angle, dipping east (Figure 17B). Minor conical autoclastic breccias are present here within the silcrete, and appear to be spatially associated with vertical fractures in the underlying sandstone.

At the very easternmost part of this outcrop and on the south side of the road, the eastward-dipping silcrete horizon is onlapped by marine strata of allomember 4 (Figure 17B). Elsewhere, allomember 4 has been eroded, which shows that the silcrete horizon is currently more resistant to erosion as it probably was in the Latest Cambrian- Earliest Ordovician.

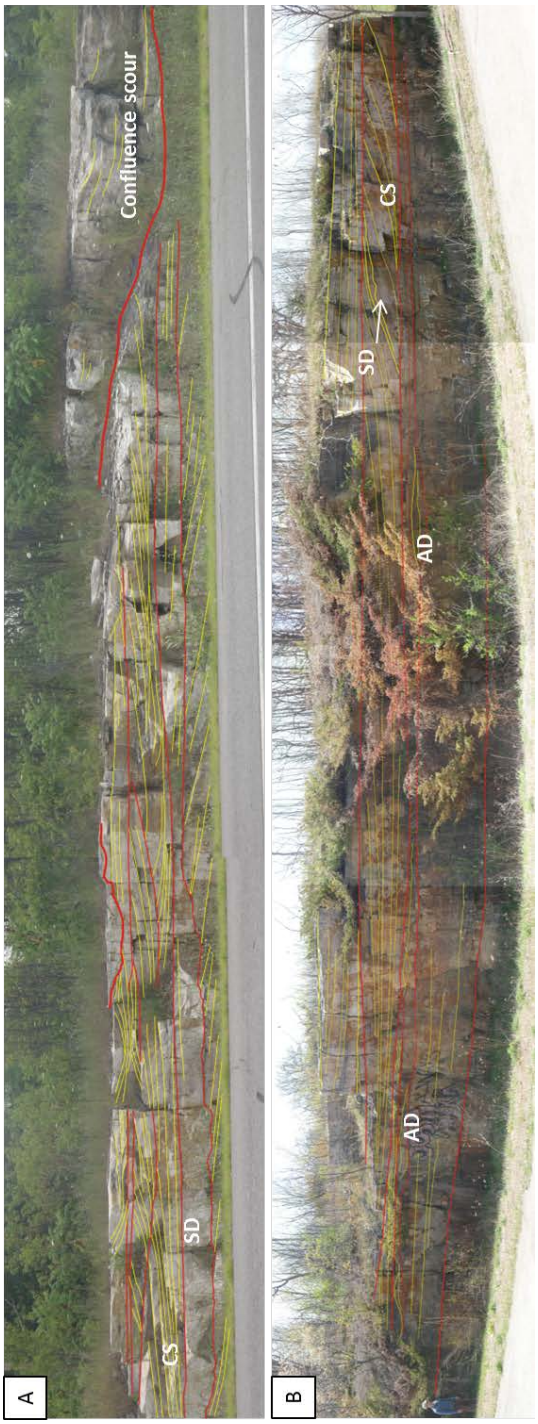

Figure 16: Ephemeral and perennial fluvial architectures and facies preserved at Stop 6. A: outcrop on the south side of Route 37 showing high and low angle upper flow regime elements such as cyclic steps (CS) and channelized subaqueous dune cross-stratification (SD). Overlying braided fluvial deposits deeply incise the ephemeral deposits to the west, where they form a confluence scour. B: Same outcrop viewed from Cemetery road. Cyclic steps (CS) are present at the northern part of the section and are draped by subaqueous dune cross-strata (SD) and sheet-like upper flow regime elements. Antidunes (AD) occur in an underlying bed.

Stop 10: Cyclic steps and the ephemeral-perennial fluvial contact. *Highway 12, south of Goose Bay (44.35967, -75.85242).* This outcrop exposes a thick (~12 m) section of allomember 3, including a lower section of ephemeral fluvial strata dominated by upper plane bed stratification, with some ~SW dipping cyclic steps and chute and pool stratification, and an upper perennial fluvial section dominated by ~N – NE dipping dune and current ripple cross-stratification with an overall "sheet-like" architecture. Thick (up to 1 m) sets of SW-dipping cyclic step cross-stratified sandstone are exposed at the western part of the outcrop on the south side of the road (Figure 18A). Farther to the east, where the outcrop thins on the south side of the road, low angle and sigmoidal cross-stratification is present, interpreted to have formed by chutes and pools (Figure 18B). Moving east again, the outcrop thickens and exposes a sharp contact between the ephemeral and perennial fluvial deposits (Figure 18C). The large-scale cross-stratification beneath the contact was originally assumed to be from an aeolian dune; however, it lacks the characteristic inversely graded grain flow strata and it shallows to the west, grading into upper flow regime facies. Possible interpretations for this feature include: (a) a large cyclic step deposit, (b) an asymmetric or oblique channel element filled with upper plane bed strata, or (c) it is in fact an aeolian dune that has been onlapped by upper flow regime strata. The contact between the ephemeral and perennial deposits is sharp, but without significant incision. The "sheet-like" nature of the perennial fluvial deposits is interpreted to record deposition and accretion in very wide and shallow channels.

Figure 17: Stop 9: A: Allomember 2-3 (A2-A3) contact. There is a small amount of erosion on this contact, and near-vertical joint fabric is truncated. It is correlated to the A2-A3 unconformity present at Stop 3 and elsewhere (see caption of Figure 12). B: The A3-A4 contact is visible farther east, viewed from the south side of Route 12. The silcrete horizon at the top of A3 dips to the east and is onlapped by marine strata of A4.

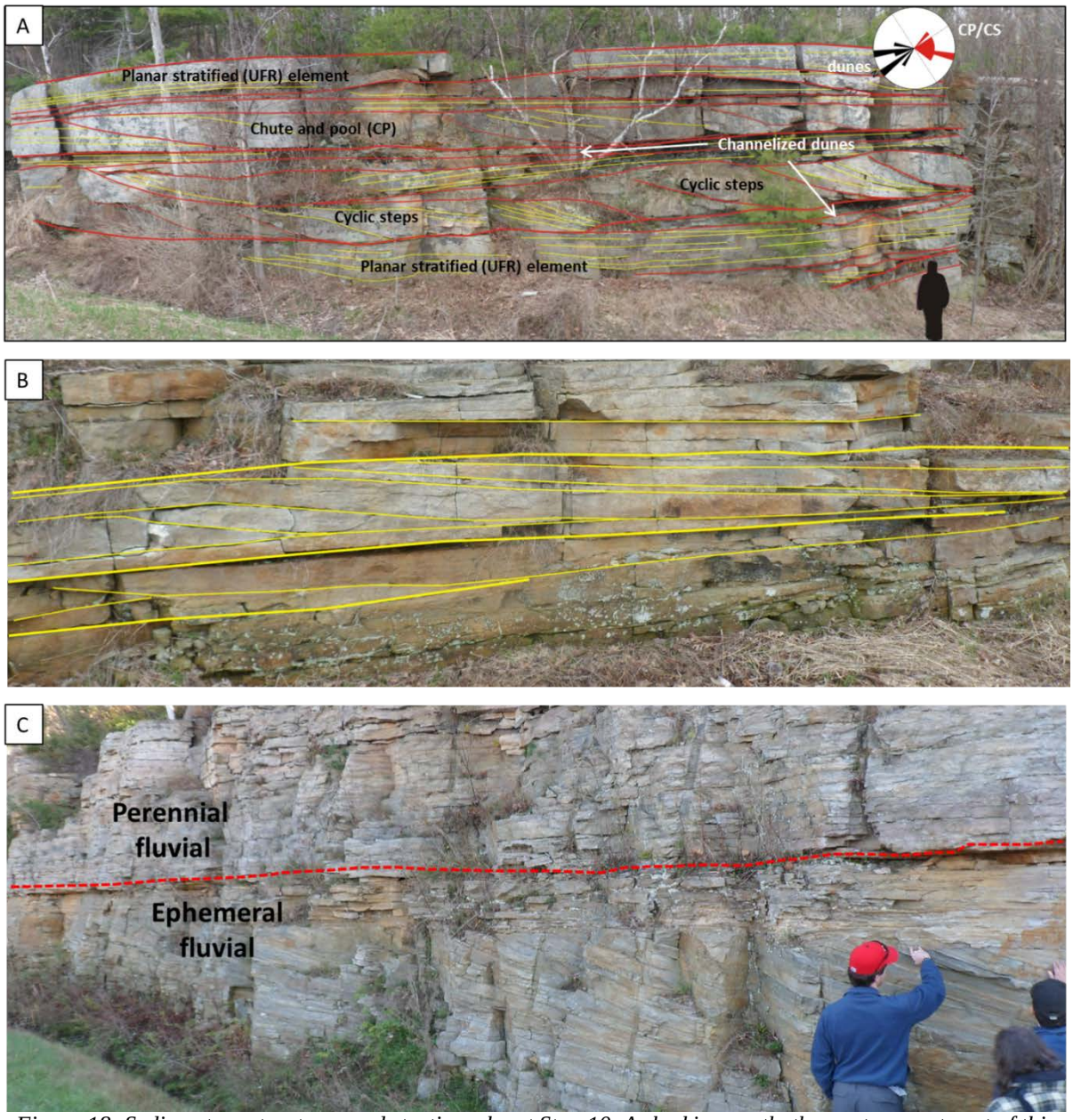

Figure 18: Sedimentary structures and stratigraphy at Stop 10. A: looking south, the westernmost part of this outcrop exposes stacked deposits of ephemeral fluvial origin. Upstream-dipping cyclic step stratification is relatively well-developed here, interbedded with upper flow regime elements and channelized subaqueous dunes. B: farther east is a sigmoidal-cross-stratified feature interpreted as the deposit of a chute-and-pool. C: The ephemeral – perennial fluvial contact of A3 is prominent farther east, defined by a change from upper flow regime- to subaqueous-dune dominated deposition. The origin of the inclined cross-strata at the top of the ephemeral fluvial package is up for debate (see related text).

Stop 11: The Great unconformity and ephemeral fluvial architecture. *Highway 12, east of Alexandria Bay (44.34598, -75.87674).* This is another "classic" Potsdam outcrop, exposing the basal unconformity with Precambrian basement rocks. At this location, all of the Potsdam strata unconformably overlying the Precambrian is correlated to allomember 3, and interpreted as ephemeral fluvial in origin. Allomember 3 appears to onlap a basement knoll at the easternmost part of the outcrop; however, some structural tilting of the lower ~4-6 m of allomember 3 is also vaguely evident above the basement feature. The architecture is sheet-like and dominated by planar laminations with occasional isolated west-dipping cross-beds and scour fills. Sheet-like packages generally 1.5 – 2 m thick are interpreted as discrete deposits of depositional lobes in an ephemeral fluvial setting. The best way to explore this outcrop is to walk from the west to the east, essentially moving up section. Many subtle features can be observed moving up-section; including aeolian wind ripple stratification and lags, isolated aeolian dune cross-stratification, upper flow regime plane bed, minor scour fills, possible cyclic steps and chutes and pools, ripples and adhesion structures and stratification. Near the top of the section is the contact between ephemeral and perennial fluvial facies associations.

REFERENCES

Bjerstedt, T.W. and Erickson, J.M., 1989. Trace fossils and bioturbation in peritidal facies of the Potsdam-Theresa formations (Cambrian-Ordovician), northwest Adirondacks. Palaios, v.4, p.203-224.

Brand, U., and Rust, B. R., 1977. The age and upper boundary of the Nepean Formation in its type section near Ottawa, Canada. Canadian Journal of Earth Sciences, v. 14, p. 2002–2006.

Bridge, J.S. and Lunt, I.A. 2006. Depositional models of braided rivers; *In* Braided Rivers: Process, Deposits, Ecology and Management. Edited by Gregory H. Sambrook Smith, James L. Best, Charlie S. Bristow and Geoff E. Petts. 390 p.

Cartigny, M.J.B., Ventra, D., Potsma, G., and Jan Den Berg, J.H., 2013. Morphodynamics and sedimentary structures of bedforms under supercritical-flow conditions: New insights from flume experiments. Sedimentology, v.61, p. 712-748.

DeSantis, E., 2014. Silcrete formation in the Potsdam Group and its relation to faulting in Northern New York. Unpublished BSc. Thesis. University of Ottawa.

Dix, G. R., Salad Hersi, O. and Nowlan, G. S., 2004.The Potsdam–Beekmantown Group boundary, Nepean Formation type section (Ottawa, Ontario): a cryptic sequence boundary, not a conformable transition. Canadian Journal of Earth Sciences, v. 41, p. 897–902.

Dumas, S., Arnott, R.W.C.; and Southard, J.B., 2005. Experiments on oscillatory-flow and combined-flow bed forms: Implications for interpreting parts of the shallow-marine sedimentary record Source: Journal of Sedimentary Research, v. 75, p. 501-513.

Fielding, C.R., 2006. Upper flow regime sheets, lenses and scour fills: Extending the range of architectural elements for fluvial sediment bodies. Sedimentary Geology, v. 190, p. 227–240.

Greggs, R.G., and Bond, I.S., 1971. Conodonts from the March and Oxford Formations in the Brockville area, Ontario: Canadian Journal of Earth Sciences, v. 8, p. 1455–1471.

Hagadorn, J.W., and Belt, E.S., 2008. Stranded in Upstate New York: Cambrian Scyphomedusae from the Potsdam Sandstone. Palaois, v. v. 23, p. 424–441.

Hagadorn, J.W., Collette, J.H., and Belt, E.S., 2011. Eolian-Aquatic Deposits and Faunas of the Middle Cambrian Potsdam Group. Palaios, v. 26, p. 314-334.

Hampton, B.A., and Horton, B.K., 2007. Sheetflow fluvial processes in a rapidly subsiding basin, Altiplano plateau, Bolivia. Sedimentology, v.54, p.1121–1147.

Landing, E., Amati, L., and Franzi, D.A. 2009. Epeirogenic transgression near a triple junction: the oldest (latest early–middle Cambrian) marine onlap of cratonic New York and Quebec. Geological Magazine, v.146, p. 552–566

Lavoie, D., 2008. Appalachian Foreland Basin of Canada. *In* Sedimentary Basins of the World, Vol 5, The Sedimentary Basins of the United States and Canada. Edited by Andrew D. Miall. 610 p.

MacNaughton, R.B., Cole, J.M., Dalrymple, R.W., Braddy, S.J., Briggs, D.E.G. and Lukie, T.D., 2002. First steps on land: Arthropod trackways in Cambrian-Ordovician eolian sandstone, southeastern Ontario, Canada. Geology, v. 30, p. 391–394.

Nowlan, G.S., 2013. Report on two samples from Lower Ordovician strata in the vicinity of Rockland in eastern Ontario submitted for conodont analysis by David Lowe and Bill Arnott (University of Ottawa); NTS 031G/11; CON # 1777. Geological Survey of Canada, Paleontological Report 004-GSN-2013, 3 p.

Salad Hersi O., Lavoie, D., Mohamed, A. H. & Nowlan, G.S., 2002. Subaerial unconformity at the Potsdam–Beekmantown contact in the Quebec Reentrant: regional significance for the Laurentian continental margin. Bulletin of Canadian Petroleum Geology 50, 419–40.

Sanford, B.V., and Arnott, R.W.C. 2010. Stratigraphic and Structural Framework of the Potsdam Group in eastern Ontario, western Quebec and northern New York State. Geological Survey of Canada Bulletin 597. 84 p.

Selleck, B.W., 1978. Syndepositional Brecciation in the Potsdam Sandstone of Northern New York State. Journal of Sedimentary Petrology, v. 48, p. 1177 – 1184.

Selleck, B.W. Sedimentology and diagenesis of the Potsdam Sandstone and Theresa Formation. *In* Field Trip Guidebook, New York State Geologic Association; 65th Annual Meeting.

Wilson, A. E., 1946. Geology of the Ottawa-St. Lawrence Lowland, Ontario and Quebec. Geological Survey of Canada, Memoir 241, 66p.

ST. LAWRENCE COUNTY, NEW YORK: NO LONGER AN AREA PRODUCING QUALITY MINERAL SPECIMENS?

MICHAEL R. WALTER
Nicholville, New York 13672

INTRODUCTION

It is so often said when describing the localities available to mineral collectors, "*That location is exhausted"*. One might get the impression that there are no longer places where fine mineral specimens can be collected. This statement could not be further from the truth when it concerns St. Lawrence County, New York. As one of the most mineralogically productive counties in our country it continues to offer field collectors ample opportunity to find exceptional mineral specimens. Numerous localities described as *exhausted* have produced significant finds (often better than historic specimens in museums) in contemporary time. *Exhausted*, "I say not"!

Participants on this field trip will be led to two sites often referred to as exhausted but still available to collectors: Powers farm in Pierrepont, St. Lawrence County, New York and the Wolf property near Edwards, St. Lawrence County, New York will both be visited. There will be approximately three hours of collecting time at each site.

To participate meet Mike Walter at the Pierrepont Highway Department parking lot at 9 am on Saturday October 11th, 2014. The Highway Department is found at the intersection of county routes 24 and 29 in the town of Pierrepont. From there participants will be taken to the first site, the Powers farm approximately two miles away.

STOP 1 POWERS FARM, PIERREPONT, ST. LAWRENCE, COUNTY, NEW YORK

(44^{o} 33' 32" N by 75^{o} 01'12"W)

Common Mineral Species: Dravite, Quartz, Calcite, Phlogopite, Pyrite, Fluorapatite, Talc

Less Common Mineral Species: Chalcopyrite, Magnetite, Tremolite, Actinolite, Marcasite, Goethite, Diopside, Microcline, Malachite, Sphalerite, Synchysite-(Ce), Vermiculite, Gold
*many unusual pseudomorphs are found at this location, as well.

The tourmaline species from this location is now being described as dravite, as per new International Mineralogical Association (I.M.A.) guidelines. Previously known as uvite these lustrous black crystals can reach impressive dimensions. Individuals of large size are uncommon but have been known to reach 30 cm. More commonly they are in the one to three cm range. Although the target species is normally the these fine dravite crystals other species can be desirable. The mica, phlogopite, can form beautiful, large, double terminated crystals to 15 cm in size. Quartz can be found in two distinct generations. First generation quartz is found in unattractive milky to gray colored tessin habit crystals. The second generation quartz is highly prized by collectors forming in prismatic crystals to 10 cm in length of alpine quality.

Many other species can be found in well-formed crystals but most are less common. Pseudomorphs are numerous and include talc after quartz and scapolite, quartz after phlogopite, pyrite after pyrrotite, and quartz after diopside, to name a few.

The reality is that land owners are being more restrictive in allowing access to their land but many locations remain accessible if collectors simple ask for access and act responsible when it is granted. This location, however, has been open to the public since the mid 1800's as a fee site. The land owner, Bower Powers, Jr. charges five dollars and visitors may keep all the mineral specimens they find. Field trips from area colleges, high schools, and mineral clubs frequent this location and often and fine specimens are collected with regularity (fig. 1). There will be no fee charged for our visit.

Figure 1. An attractive dravite cluster collected by a 10th grade high school student on May 16th, 2014. He had never been mineral collecting before! It was found loose on the soil and measures 8.8 cm with individual crystals reaching 4.8 cm.

STOP 2 THE WOLF PROPERTY (also known as the Morgan Farm), EDWARDS, ST. LAWRENCE, COUNTY, NEW YORK

(44° 19'01" N by 75° 14'21"W)

Common Mineral Species: Diopside, Microcline,Tremolite, Mica

Less Common Mineral Species: Pyrite, Apatite, Molybdenite

It seems that this site has been seldom visited over the past 40 years. It is on private property and we will have permission for this one time collecting effort. It has the reputation as being "exhausted" but that is not true. A large feldspar vein and the road cut where enormous diopside crystals were collected in the early 1960s are now likelydepleted but other diggings at this location will produce specimens. There has been very little collector activity at the site in the past 40 years and the location holds strong potential for further finds of quality specimens.

HISTORY AND GEOLOGY REVIEW OF MAGNETIC IRON MINING IN THE WESTERN ADIRONDACKS

JEROME ZAYKOSKI C. P. G.

Jefferson Community College
Coffeen Street, Watertown, NY 13601
jzaykoski@sunyjefferson.edu

INTRODUCTION

Today when people talk about mining, they generally have an adversarial opinion of this industry. In addition, many fail to recognize the importance mining provides to today's economy. There is an old saying that goes "if it can't be grown, it must be mined". Today, most mining in New York State revolves around the sand, gravel and construction aggregates industry. However, New York has a rich history of mining that goes back into the early 18th century and the dominant material mined was iron. Much of this iron was mined in the Adirondacks and, not only an important commodity to the early colonists for everyday use, it also played a critical role in the fight for independence from Great Britain.

The purpose of this trip is to examine the history of western Adirondack iron mining, along with an overview of the regional and site specific geology. We will visit and discuss the mine history and limiting factors that governed the life of the Clifton Iron Ore, Jayville and Benson Mines.

GENERAL IRON MINING HISTORY

Iron was most likely discovered by Native Americans as a result of their fire pit coals contacting rocks containing iron. The heat from the fire caused the iron to deoxidize into crude steel. They later found that they could pound this material into various useful shapes (Farrell, 1996). One of the earliest known iron mining and forging operations in New York occurred in 1736 when Cornelius Board and Timothy Ward formed the Sterling Forge and Furnace Company in Rockland County (Levine, 2012). Initial reference of Adirondack iron discovery is made by Swedish naturalist Peter Kalm, who in 1749 noted the magnetic "iron sands" in the Crown Point area of Lake Champlain. Little did he know he was virtually standing on ore deposits which would be mined for over one and a half centuries (Farrell, 1996).

In colonial times, early American settlers were forced to purchase many manufactured products from the British. They were prevented from manufacturing goods, thus providing a market for British wares. Though smelting of raw iron for further refinement by the British was allowed, production of final products was outlawed. Yet there was a need for finished goods by the colonialists and, with the scattered colonial populations, these laws were largely ignored (Farrell, 1996).

Early Adirondack mining most likely began along the shores of Lake Champlain where forces and arms were mustered to fight the British. Philip Skene built a forge with hammers at Skenesborough (now Whitehall) in 1761 and used boats to transport ore from an area north of Port Henry. Benedict Arnold's regimental book records in June 1775 that he ordered men to dig ore from what was to become the Cheever mine, located north of Port Henry. This ore was refined to make implements and arms (Farrell, 1996). This iron was also used to build a fleet of ships that Arnold used to battle General Carlton and his well-armed fleet of British ships around Valcour Island in September 1775. Though badly beaten in this day long fight, Arnold was able to slip his fleet past the British under the cover of darkness and sailed toward Crown Point. These actions by Arnold successfully held the British from attacking again for almost a year (Farrell, 1996).

After the war of independence, iron mining and manufacturing continued to develop around Lake Champlain. Forges were used to process the ore and in 1798 the first Catalan forge was built around Plattsburgh (Hyde, 1974). Additional forges were built around the Lake Champlain area, including several at Ticonderoga prior to

1800. Typically, these forges were an open hearth construction with a two and a half to three foot opening (Farrell, 1996). This type of forge or bloomery used charcoal to heat the ore to a semi-molten state called a bloom or loupe, which was then removed and hammered to expel impurities. The iron mass was then reheated and hammered multiple times and then shaped into a billet of wrought iron (Dawson, et al., 1988).

As the demand for iron increased, the size of the furnaces grew to increase capacity. Stack heights were raised and water power was used to increase the blast capacity. This increased blowing capacity allowed for more contact between the ore and fuel, carburizing the metal. The metal melted into a mass, which allowed for separation from the gangue and permitted the iron to be poured into casts of various shapes (Farrell, 1996).

The population continued to grow and the demand for iron products, such as farm implements and utensils, continued to provide a market for the Lake Champlain iron industry. With the completion of the barge canal system, transportation was improved and allowed for additional forges and furnaces to be built in support of new iron mine development (Farrell, 1996). This growth extended westerly from the Lake Champlain area to areas that had plentiful resources of magnetite, forests for wood, marbles and limestone for flux, and water to drive air compressors and trip hammers. Ore deposits were rather easily detected when surveyor's compasses were perturbed by the magnetic fields. The location and size of these deposits could be further defined later by dip-needle surveys (Dawson et al., 1988). In fact, the Benson Ore body, what would later become the largest open pit iron mine in the world, was discovered in 1810 by engineers surveying a road from Albany to Ogdensburg when their compasses were affected by the magnetic ore. Both large and small operations became plentiful in all areas and more than two hundred mines and forges operated during the 1800's (Hyde, 1974).

Expansion of the iron industry did not come without some difficulty. Most of the areas west of Lake Champlain were unsurveyed, mountainous and wilderness. New York Surveyor General Simon DeWitt ordered that the unappropriated lands in Essex County be surveyed. This survey of what was later to become the Iron Ore Tract was completed in March 1812. Survey compasses were affected by ore deposits and several of the lots were later developed. In 1824, while preparing fields for planting, ore was discovered very shallow to the surface on the D.E. Sanford Lot 25 of the Iron Ore Tract. Harry Sherman and Elijah Bishop arranged to pay Sanford to explore and develop the ore on this property. A short time later, a large ore vein was discovered and later referred to as the Sanford or Old Bed Deposit. The magnitude of the size of this vein was not realized at first and would eventually be mined for over a century and a half (Farrell, 1996).

Other lots within the Iron Ore Tract were developed, including Lots 21, 23, 24 and 25. Eventually Lots 24 and 25 were purchased by the firm of Lee, Sherman and Withersbees, later to become Withersbee Sherman and Company, who, along with The Port Henry Iron Ore Company and the Chateauguay Iron Ore Company, became major iron ore players through the nineteenth century in Essex and Clinton counties (Farrell, 1996). By 1842, iron production in Essex and Clinton Counties exceeded any other county in the state and perhaps the world and the quality of the iron produced rivaled the ores from Sweden (Hyde, 1974).

EXPANSION TO THE WESTERN ADIRONDACKS

The iron mining history of the western Adirondacks includes several small pyrite (FeS_2) mines. One notable pyrite mine was in Stellaville. The Stella Mines were located along County Route 17, a few miles north of the Hamlet of Hermon, NY. However, due to the sulfur, pyrite is not mined for iron production rather than for the making of sulfuric acid (Carl, 2007). In addition, there were numerous small magnetic iron developments near Colton, Russell and Fullerville (Leonard & Buddington, 1964). This report and field trip will focus on three major iron mines that were within the St. Lawrence County Magnetite District, Clifton Iron Company, Jayville and Benson Mines.

Around 1810, engineers in the process of surveying the route for a military road from Albany to Ogdensburg surveyors had their compasses affected by a magnetic ore body located just easterly of Star Lake. Some thirty years later, State Geologist Ebenezer Emmons referenced this "Chaumont" deposit in his annual report on mineral resources of the state. The remoteness of this ore body did not make it a viable resource until 1889, when logging activity brought the railroad into the neighborhood of the deposit (Crump and Beutner, 1968).

Clifton Iron Company. Located roughly 3.5 miles southeast of DeGrasse, the Clifton deposit was likely discovered prior to 1840 (Leonard and Buddington, 1964). John Worden while surveying lands in the area is credited with discovering the ore body (Palmer and Thomas, 1969). The mine was first opened in 1858 (Linney, 1943), however operations here did not move forward until 1863 when the Clifton Iron Company was founded by Zebulon T. Benton, John B. Morgan, Samuel B. Smith and Charles G. Myers (Palmer and Thomas, 1969). Significant mining operations then began around 1865 with several small pits and shafts (Leonard and Buddington, 1964). The firm of Myers Steel and Iron Wire built forges, furnaces and miscellaneous machinery for use in the production of steel (Palmer and Thomas, 1969) and, in 1866, built a charcoal furnace at Twin Falls on the Grasse River in Clarksboro (figure 1) (Leonard and Buddington, 1964). Evidence at the site suggests that the ore was refined into pig iron by the "Bessemer Process" with waterpower from the adjacent sluiceway powering the bellows (Palmer and Thomas, 1969). In 1868, a new furnace was built at the mine (Leonard and Buddington, 1964) with its famous 160 foot high brick chimney bearing the date "1868" on all four sides (Palmer and Thomas, 1969).

The Clifton ore deposit is located approximately 2 miles southwest of Clarksboro and several roads were built around the area. Huftle Road was built from the mine to the Clarksboro furnace. Horse and oxen drawn wagons were initially used to haul ore and were eventually replaced by railroad. The main workings at the mine were the Dodge, St. Lawrence, Dannemora and Sheriden veins and analysis of the ore showed that it was very pure (Palmer and Thomas, 1969).

In April 1864, the New York State legislature passed a bill allowing Clifton Iron Company to construct a 23 ½ mile railroad from the mine to the Rome, Watertown and Ogdensburg Railroad at East DeKalb. The scarcity of iron after the Civil War made it impossible to use iron rails and maple timbers were used instead (Palmer and Thomas, 1969).

Figure 1. Remains of Clarksboro furnace at Twin Falls (photo by J. E. Zaykoski, 2013). Inset shows charcoal fragments found on-site.

Construction of this railroad presented engineers with many challenges and unique solutions. Rather than build the railroad from the mainline in East DeKalb, construction began at the mine. The terrain along the route is very rugged and special four wheeled engines and cars were built in order to navigate the tight turns. The track was standard gauge and constructed using spruce ties with notches cut near the ends. Maple rails were attached using wedges driven into the spruce notches and no rail spikes were used in initial construction (Thompson n.d.). The rail is said to have been completed by January 1, 1868 (Palmer and Thomas, 1969). Once in operation, problems with the rail began soon after. Polished rail surfaces were used and were then sanded to allow for climbing uphill grades. Continued use created large splinters that were torn from the rails, some of which broke through the floors of the engines. To solve this problem, many iron straps were spiked to the rails around curves and road crossings. This created another problem as train traffic drew out the metal spikes and the plates would wrap around a wheel and break through the floor of ore cars causing derailments. The combination of the track problems and the crooked terrain made for slow train travel and, at peak use only 3 to 4 trains made the trip from Clarksboro to East DeKalb daily (Thompson n.d.). See Figures 2 and 3.

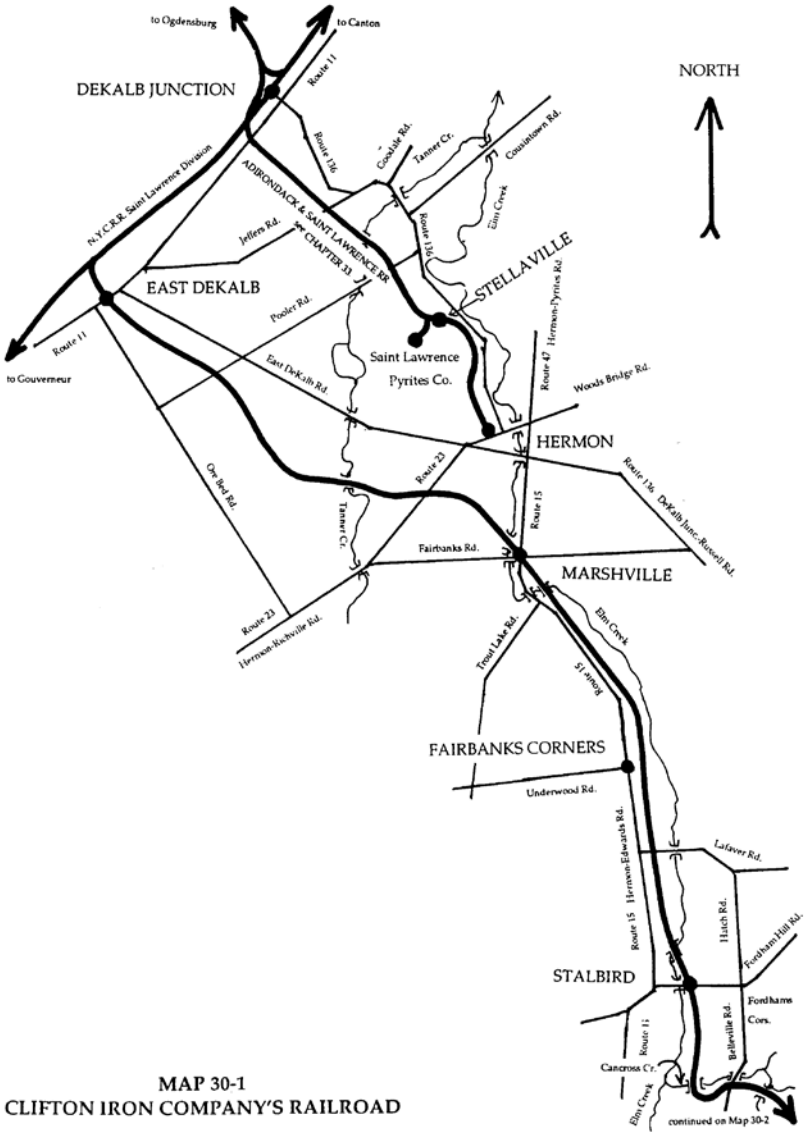

Figure 2.Clifton Iron Company's Railroad (Kurdish, 1996).

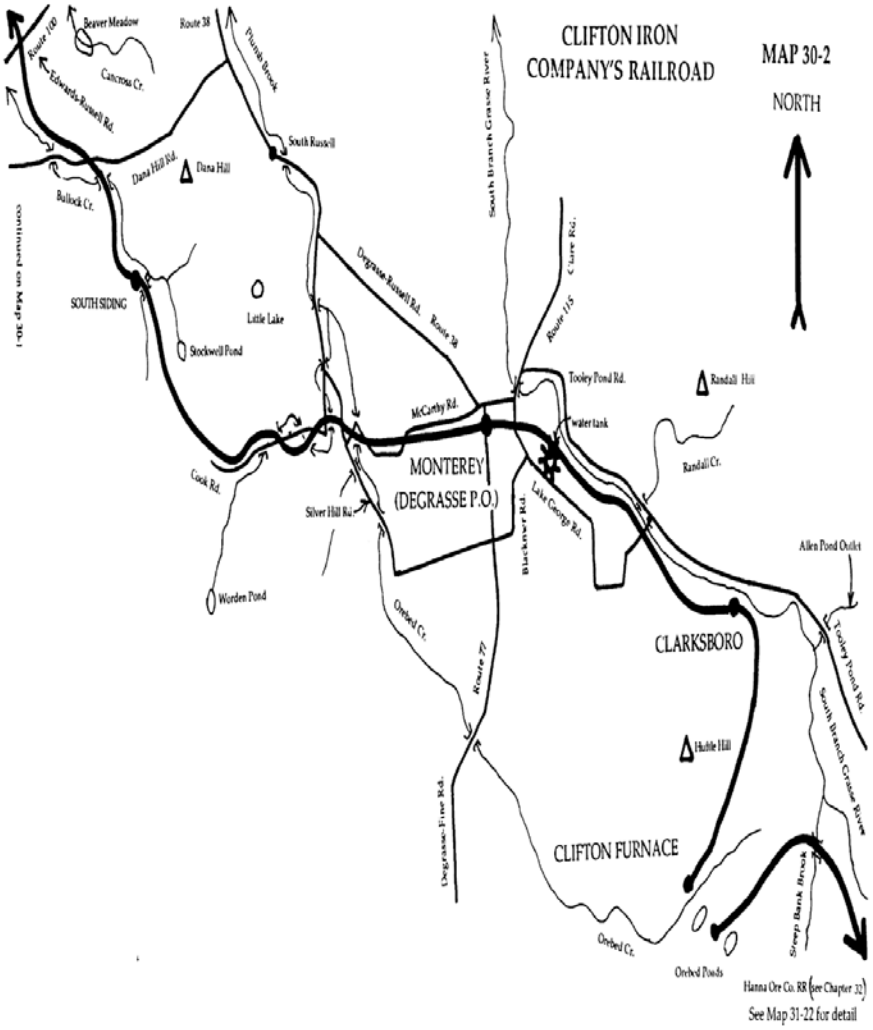

Figure 3. Clifton Iron Company's Railroad (Kurdish, 1996).

Mining operations by The Clifton Iron Company brought the first white settlers to the area and Clarksboro became a boom town with a population reaching close to 700 people. On April 21, 1868, the Town of Clifton was organized. The new town contained 61,930 acres taken from the town of Pierrepont and was described as largely forest covered and a popular area for sportsman. Early 1869 was said to be a very busy period for Clifton and Clarksboro. However, on September 4, 1869, fire destroyed the steel mill at the mine and caused $140,000.00 in damages that were only partially insured. This tragedy and the illness of mine developer George Clark left the mine idled. Clark intended to resume operations at the mine, but was informed the company was in troubled financial condition owing $ 55,000.00. With the mine operations suspended, the population of Clarksboro dwindled down to less than 50 people. The loss of the Clifton operations did not slow down Clark as the nearby Benson Mines operations were an extension of his interests (Palmer and Thomas, 1969).

Figure 4. Aerial View of Clifton Iron Mine taken by Dwight Church St. Lawrence Historical Society

The Clifton Mine lay idle for decades until 1940, when the M.A. Hanna Company of Cleveland performed a dip needle and diamond drill surveys of the ore body. The results showed an ore body of sufficient size to allow for further development (Leonard and Buddington, 1964). The Hanna Ore Co., Clifton Mine Division (a subsidiary of The M.A. Hanna Co.) was formed and purchased the mine properties in 1941 (Linney, 1943) and mining production began in June, 1942 (Hunner, 1943; Leonard and Buddington, 1964).

With the purchase of the properties, the Hanna Ore Co. began to develop the property (Figure 4). Due to the remoteness of the mine a new road had to be constructed, which followed the original trail and became known as the Lake George Road. The railroad was extended from Newton Falls to the mine and telephone power lines run from Edwards. Stripping operations took place during the winter of 1941-1942. The first shipment of lump ore took place on June 3, 1942. Lump ore shipments continued while the new facility was constructed. A benefication plant was built and housed crushers, magnetic separators, a wet grinding mill, separators and sintering plant. While surface mining operations continued, underground mining plans were put into action and the sinking operations of the vertical shaft began in July, 1942 (Hunner, 1943) in order to intersect the ore 500 feet underground (Linney, 1943).

Mining operations were conducted by a work force of roughly 175 men, who mostly came from the surrounding farms and, with no experience in mining, they required several months of training to develop them into skilled miners (Hunner, 1943). Due to the remote location of the mine, Hanna Ore Co. was responsible for maintaining the roads, including snow plowing responsibilities in the winter. The mine produced around 900 tons of ore daily until operations ceased in 1952 (Barnes, 1962). Reports cited the ore was exhausted and deeper operations were too costly to continue. In all from 1942 through 1952, a total of 2 to 2 1/2 million long tons of ore averaging 38% iron were mined (Leonard and Buddington, 1964). All structures were demolished and little remains of the mine today, other than some remnant foundations (Barnes, 1962).

Jayville Mine. Jayville is located in the Town of Pitcairn, roughly 1.25 miles east of the former hamlet of Kalurah (Leonard and Buddington, 1964) and 29 miles east of Carthage by rail (Newland, 1908). The mine, located on the eastern and western flanks of a north trending hill, was originally opened in 1854 by Zebulon H. Benton. However, little mining activity occurred at that time. The mine contained ores made up of Magnetite and Vonsenite (Ferris Ferric Borate – $Fe_2Fe\ (BO_3)O_2$) (Leonard and Buddington, 1964). The ore was mined and drawn by wagons some 15 miles to the blast furnaces at Fullerville (Ingalls, 1914). In 1886, with financing by Byron Benson, the Carthage and Adirondack railroad was completed to Jayville (Carl, 2009). Mining operations resumed under the name of the Magnetic Iron Ore Company and continued to 1888, when the property was abandoned (Leonard and Buddington, 1964).

Iron mining in the western Adirondacks cannot be examined without a discussion about railroads. The rugged and remoteness of the terrain made ore transportation difficult at best and this was the case in the remote community of Jayville. With the completion of the Black River Canal and the tracks of the Utica and Black River Railroad reaching Carthage in 1872, prominent business men knew of the magnetic ore resources to the east and began efforts to build a railroad to the western Adirondacks. In 1868, the NY legislature passed a bill authorizing the issuance of bonds for capital stock in the Black River and St. Lawrence Railway Company. The proposed railroad would be constructed with the cheaper wooden rails that were acceptable for short local runs. The railroad was completed from Carthage only to Natural Bridge in 1869 and operated for less than a year before its failure. Local communities lost money and the blame was placed on the use of wooden rather than iron rails (Carl, 2009).

Byron Benson was born in Fabius, New York in 1823 and left home as a young man to operate a stave mill. After the Civil War, Benson and friend Robert Hopkins moved to Pennsylvania to make their fortune in the oil industry. Forming the Colorado Oil Company they later partnered with D. McKelvey to drill several oil wells in Butler and Wardwell Counties. Later Benson and several partners organized the Tide Water Pipe Line Company Ltd. and built a 100 mile long pipeline from Corryville to Williamsport (Carl, 2009).

There is speculation as to why Benson moved his interests to northern New York, though there is an account suggesting he had been investigating the prospects of the Jayville deposit. In 1873, Benson's younger brother, Caldwell Belden Benson, and others were scouting an iron deposit in Jayville (Lupulescu etal, 2014). On March 23, 1883, the Carthage and Adirondack Railroad was chartered and construction began later that year. The rail followed the right-of-way of the former Black River and St. Lawrence Railroad and steel rails were used. Construction of the railroad to Jayville was completed and it was formally opened on January 1, 1887 (Carl, 2009).

With the railroad complete, mining efforts at Jayville intensified. Byron Benson leased the property from Benton and mined the ore under the name of the Magnetic Iron Ore Company. Ore was removed from several pits and underground workings accessed by shaft or drift. Estimates are the mine yielded 25,000 to 200,000 tons of ore, ranging in grade from 40 to 60 percent iron (Leonard and Buddington, 1964).

Mining operations at Jayville ended in 1888 and, for a period of time, the railroad supported some logging. In 1917 the Watertown Herald reported that J. W. Hughes of Rochester had reopened up the Jayville mine. Money was spent pumping out water in an effort to mine under Twin Ponds where the mother lode of ore was suspected. However, the water filled the mine as fast as it could be pumped and, after 3 years, the operation was shut down (Miller and Carvell, 2010). Little remains of Jayville today. In 1929, dairy farmer Frank Hall purchased what buildings that were left in Jayville and had them torn down. The old Jayville boarding house was relocated and used as a hunting camp, which later burned down (Carl, 2009).

Benson Mine. Benson Mine was at one time the largest open pit iron mine in the world (Hyde, 1974), yet its discovery was quite by accident. Around 1810, engineers, while in the process of surveying the route for a military road from Albany to Ogdensburg, had their compasses affected by a magnetic ore body located just easterly of Star Lake in an area known as Little River. Some thirty years later, State Geologist Ebenezer Emmons referenced this "Chaumont" deposit in his annual report on mineral resources of the state (Crump and Beutner, 1970). In 1888, the Carthage and Adirondack Railroad was extended eastward from Jayville to Little River and its potentially large iron deposit. With the prospects of this new mine, The Magnetic Iron Ore

Company abandoned its Jayville operations and moved their equipment to this new location (Carl, 2009). See figure 5.

The Benson Mine main deposit is 2.5 miles long (Figure 5), averaging 400 feet in width and 90 feet deep, containing a low grade magnetic and nonmagnetic ore that is roughly 23% iron. However, what made this deposit attractive for development is the ore is at the surface and no underground mining methods were needed (Lupulescu etal, 2014). The mine operated at a low level for several years until 1893, when the United States suffered an economic depression. This, combined with low cost of the Mesabi Range ores, led to the mine being abandoned (Crump and Beutner, 1970). The mine briefly reopened in 1900, shipping 67,000 tons of concentrate (Tillinghast, 1948) and, in 1907, the Benson Mines Company was formed and open pit operations began. The mine operated sporadically through World War I and was again abandoned in 1919 (Crump and Beutner, 1968).

Figure 5. Google Earth View of Benson Mines showing former flooded strip mine and tailings.

In 1941, the Jones and Laughlin Ore Company leased the Benson Mineral lands and, in the fall of 1942 the Defense Plant Corporation undertook construction of a modern plant facility (Tillinghast, 1948; Crump and Beutner, 1970). With the new modernized plant, open pit production began in 1944, shipping ore to Pittsburgh furnaces (Crump and Beutner, 1970). Production briefly halted in 1946, due to a strike. The strike ended in July 1946. However production did not resume until September of that year in order for extensive plant repairs to be completed (Tillinghast, 1948). In December, 1946 the holdings of the Defense Plant Corporation were purchased by Jones and Laughlin (J & L) Steel Corp and operated under the name of Jones and Laughlin Ore Company (Crump and Beutner, 1970). In 1952, Jones and Laughlin Ore Company merged with the parent corporation and became the New York Ore Division of Jones and Laughlin (J&L) Steel Corporation (Crump and Beutner, 1970) and operated continuously through 1978 (Lupulescu etal, 2014). Major expansion of the mine occurred during the 1950's and, by 1960, the company reportedly had 840 workers and had the capacity to produce 1,800,000 long tons of ore concentrate (Lupulescu etal, 2014).

REGIONAL GEOLOGY

The St. Lawrence Magnetite District lies within the Adirondack Highlands portion of the Adirondack Mountains and is the southernmost extension of the Grenville Province (McLelland, Daly and McLelland, 1996; Lupulescu et al., 2014). Tectonic activity formed the Adirondacks, with major activity occurring between 1.3 and 1.0 billion years ago that can be broken down into three periods of orogenic (mountain building) activity: the Elzevirian (1,245-1,225 Ma), Shawinigan (1,190-1,145 Ma) and ending with the Grenvillian' which is separated into the Ottawan (1,090-1,020 Ma) and Rigolet (1,000-900 Ma) pulses (Lupulescu etal, 2014). The rocks of the Adirondacks are further divided into the orthogneissic Highlands and the northwest lying Lowlands characterized by metasediments, particularly marbles. The Highlands and Lowlands are separated by a high strain shear zone known as the Carthage–Colton mylonite zone (CCMZ) (McLelland, Daly and McLelland, 1996).

A quick look at the Adirondack Lowland rocks (Figure 7) show they are dominated by marbles, gneisses and quartzite metamorphosed from limestone, shale and sandstones. Though highly metamorphosed, these rocks show metamorphic grades ranging to upper amphibolite conditions. By contrast, the Highlands are comprised of sedimentary rocks laid down on preexisting basement, intruded by younger igneous rocks that were all metamorphosed to granulite facies (Lupulescu etal, 2014). Tonalites are the oldest metamorphosed igneous rocks found in the Highlands, with emplacement roughly between 1,330-1,300 Ma (McLelland and Chiarenzelli, 1990b, p.181). Rocks of the anorthosite-mangerite-charnockite-granite (AMCG) suite were emplaced around 1155 Ma and later intruded by rocks such as the Hawkeye Granite (1,100-1,090 Ma). The last magmatic episode emplaced the Lyon Mountain Granite (1,070-1,040 Ma) and the mangerites in the northern Highlands around 1,080 Ma. Magmatic rocks of the AMCG suite were intruded into older metasediments that can be correlated to comparable rocks exposed in the Lowlands (Lupulescu et al, 2014). Both regions show evidence associated with strong ductile strain, including multiple events of intense deformation and strong penetrative fabrics (McLelland, Daly and McLelland, 1996).

The rocks of the St. Lawrence County magnetite district are characteristic of Adirondack geology. The bedrock is roughly 80 - 85% igneous rocks with about 15% metasedimentary and roughly 5% metagabbro and amphibolite (Figure 7). Potsdam sandstone also outcrops in the northwestern part of the district. Metasomatic skarn is present in many parts of the district and is closely associated with magnetite bodies. Also notable is the relationship of magnetite to granite, with all magnetite deposits within the district being adjacent to younger granites. Deposits occur within the narrow belts of metasedimentary rocks that are surrounded by granitic or granitic gneiss rocks. In some areas of alaskite or microcline granite, magnetite has replaced skarns (Leonard and Buddington, 1964).

The origin of magnetite deposits is a topic that has been debated amongst geologists for many years. There have been several lines of thought on the origin of the ores that can be grouped into three categories: 1) metamorphism of iron-rich sedimentary rocks; 2) movement and concentration of iron from silicates rich in iron and magnesium during metamorphism; and 3) replacing and depositing ore by hydrothermal solution after metamorphism. Currently there is support for the first process described above (Lupulescu et al, 2014; Chiarenzelli, 2014, Personal Comm.).

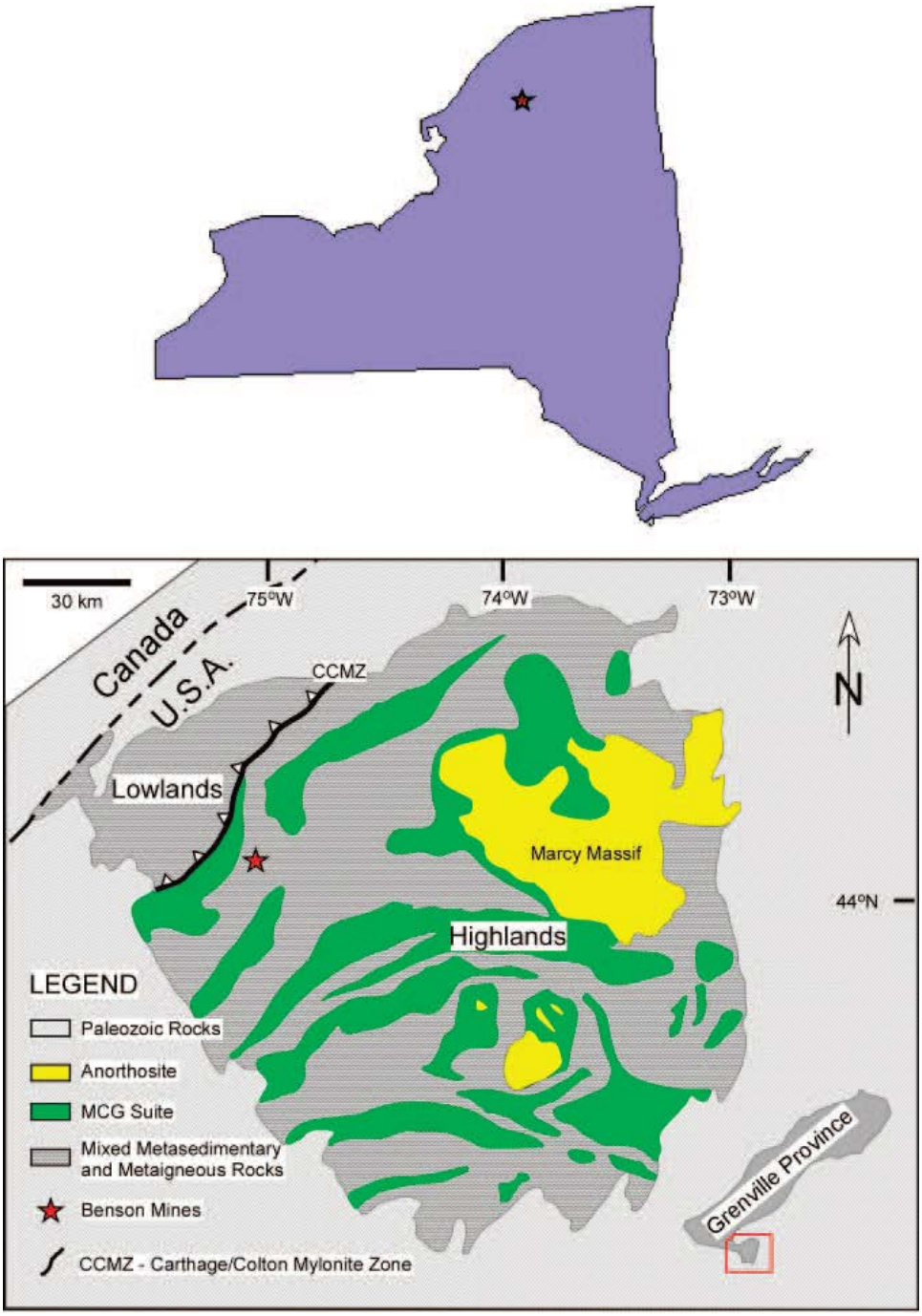

Figure 6: Simplified geological map of the Adirondacks, prepared by Jeffrey Chiarenzelli (Lupulescu et al, 2014).

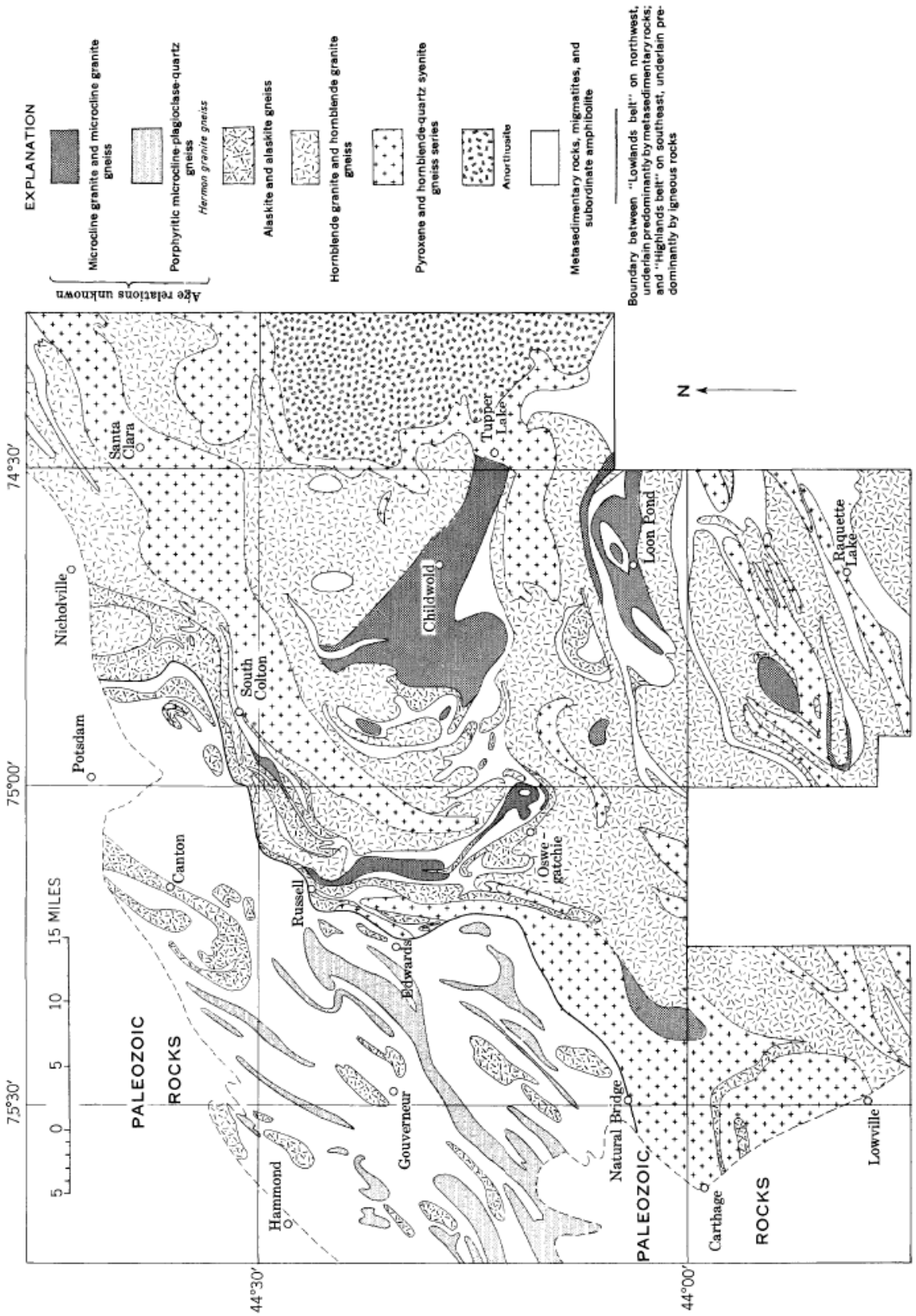

Figure 7. Geologic map of the northwest Adirondacks (Buddington and Leonard, 1962)

Clifton Deposit. Located roughly 3.5 miles southeast of DeGrasse, the Clifton deposit was likely discovered prior to 1840 (Leonard and Buddington, 1964) and John Worden, while surveying lands in the area, is credited with discovering the ore body (Palmer and Thomas, 1969). The mine was first opened in 1858 (Linney, 1943). However operations here did not move forward until 1863 when the Clifton Iron Company was founded by Zebulon T. Benton, John B. Morgan, Samuel B. Smith and Charles G. Myers. Mining took place until late 1869, when fire destroyed the mill (Palmer and Thomas, 1969).

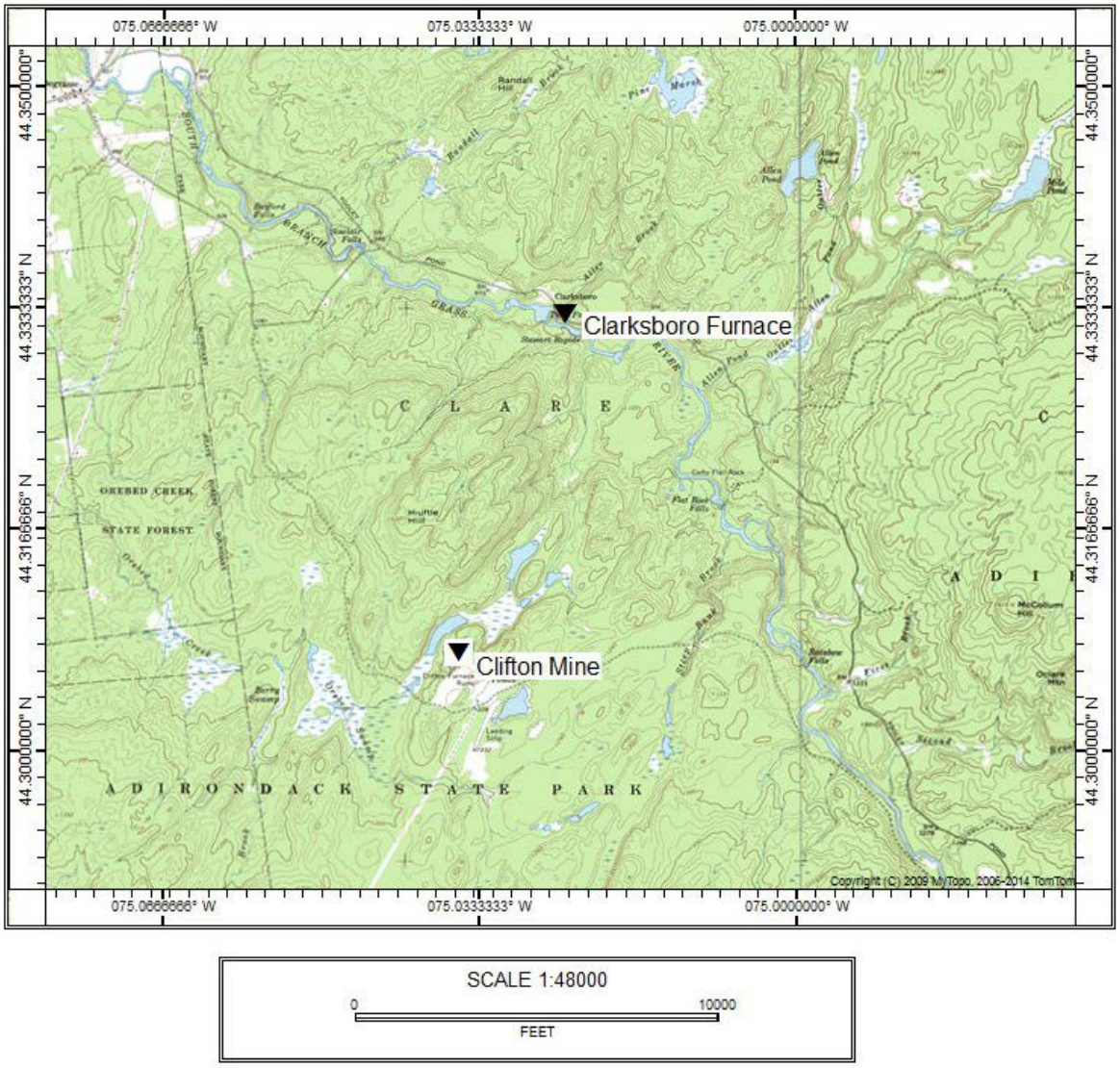

Figure 8. Location of the Clifton Iron Mine and Clarksboro Furnance near Twins Falls on the Grass River.

The Clifton ore deposit is located within a narrow belt of metasedimentary rocks on the east flank of the northeasterly trending Stark anticline. These rocks include a large phacoidal granite gneiss, along with many thin sheets of the same. Hypersthene metadiabase dikes intrude this complex and sheets of alaskite and alaskite gneiss are located within and near the metasedimentary rocks. Specifically, the ore is hosted within skarn, quartz feldspar granulites and gneisses, along with phacoids of hornblende granite gneiss and the associated quartz syenite series, metadiabase and granites and granite gneiss series. Skarn ores contain only magnetite ore

and deposits are usually small to medium in size and compact. Ore grade is extremely variable. (Leonard and Buddington, 1964). Chiarenzelli (2014 Personal Comm.) revealed that ore specimens were recently dated by U-Pb zircon method of Laser Ablation Inductively Coupled Plasma Mass Spectrometry (LA-ICP-MS), giving an age of 1052.8+/- 3.0 Ma. This age is likely either for the time of igneous intrusion or the time of zircon growth in rocks which originally had none. He further states that, due to the scarcity of zircons, their size, U/Th ratio and morphology, he believes they are likely metamorphic.

Structurally, the Clifton deposit has a complex habit unlike the fishhook patterns of many of the magnetite bodies in the district. At the location of the mine the Stark anticline is upright with its axis gently dipping southward (Figure 9). The major rock in the hanging wall is a quartz feldspar granulite (Leonard and Buddington, 1964).

Jayville Deposit. Operations at the Jayville mine began in 1854 and continued to 1888, shipping ore with a grade ranging from 40 to 60 percent. Located on the flanks of a north, trending hill, magnetite is the prominent mineral mine here. However, it is accompanied by Vonsenite and supergene hematite in places. Similar to the Clifton deposit, the ore is hosted in a pyroxene amphibole skarn and a quartz-bearing amphibole skarn rich in fluorite. Adjacent to the skarn are alaskite gneisses and sodic granite (Leonard and Buddington, 1964). Using U/Pb zircon methods (LA-ICP-MS), an age of 1045.7 +/- 8.9 Ma was recently obtained (Chiarenzelli, 2014 Personal Comm.).

The main ore body has been described by Leonard and Buddington (1964) as a shoot on the northwest limb of an isoclinal syncline which has been overturned. The ore shoot plunges to the northwest in rocks that are steeply dipping at angles up to 60° (Smock, 1889).

The Benson No. 1 working probably provided the most ore for the mine (Leonard and Buddington, 1964), due to the size of the ore body, which is said to be twenty feet wide and 400 feet long (Smock, 1889). Ore was shipped to Fullerville furnaces (Ingalls, 1914), Scranton and Bethlehem (Smock, 1889).

In 1947, an unknown metallic mineral was collected from two drill holes at Jayville. Initially, this mineral was thought to be ilvaite but later identified, as vonsenite (Ferrous ferric borate). Lab analyses gave not only high B_2O_3, content but also showed a high soluble Fe content of the nonmagnetic fraction, making vonsenite a major constituent of the ore zone. When comparing hand samples of magnetite and vonsenite, they cannot be distinguished from one another though Vonsenite has a slightly bluish appearance. Vonsenite is weakly magnetic. However where these minerals constitute ore, this property is not of much use in identifying one from another (Leonard and Vlisidis, 1961).

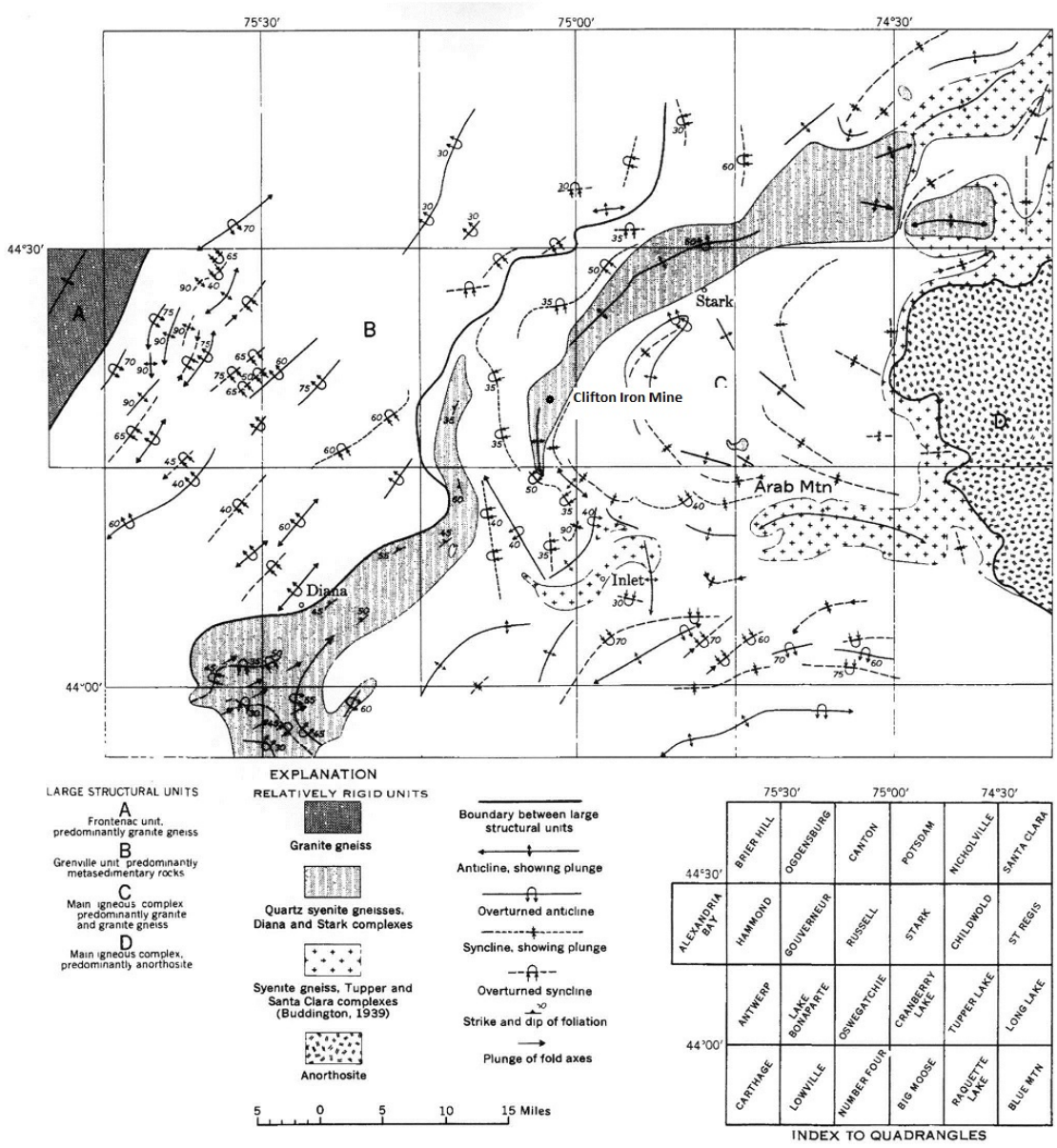

Figure 9. Map of the northwest Adirondack area showing relations of structure axes and isoclinal folds overturned toward more rigid units (Buddington and Leonard, 1962). Clifton Iron Mine Label by J.E. Zaykoski, 2014

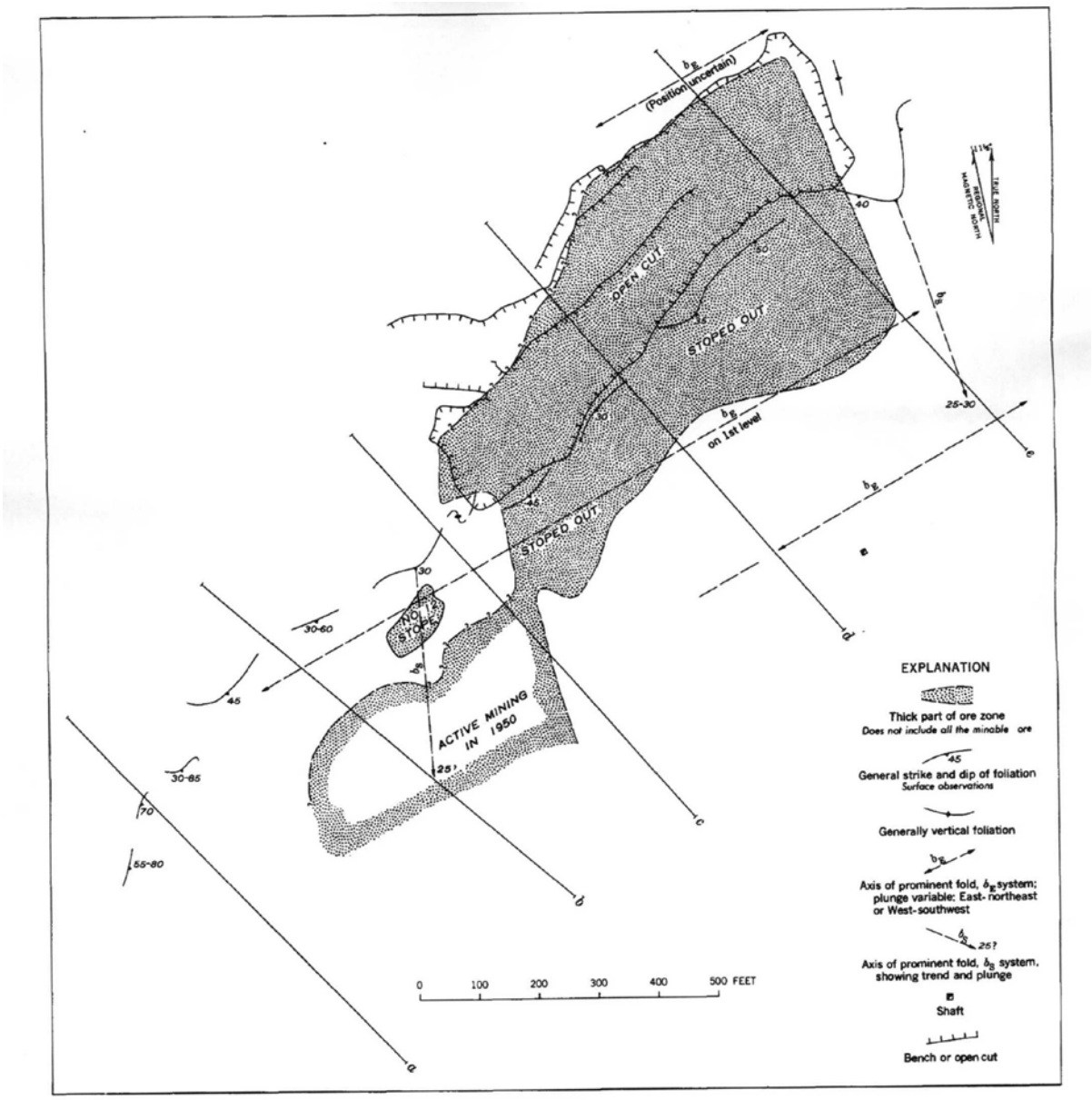

Figure 10. Key structural features and horizontal projection of main ore shoots, Clifton mine (Leonard and Buddington, 1964)

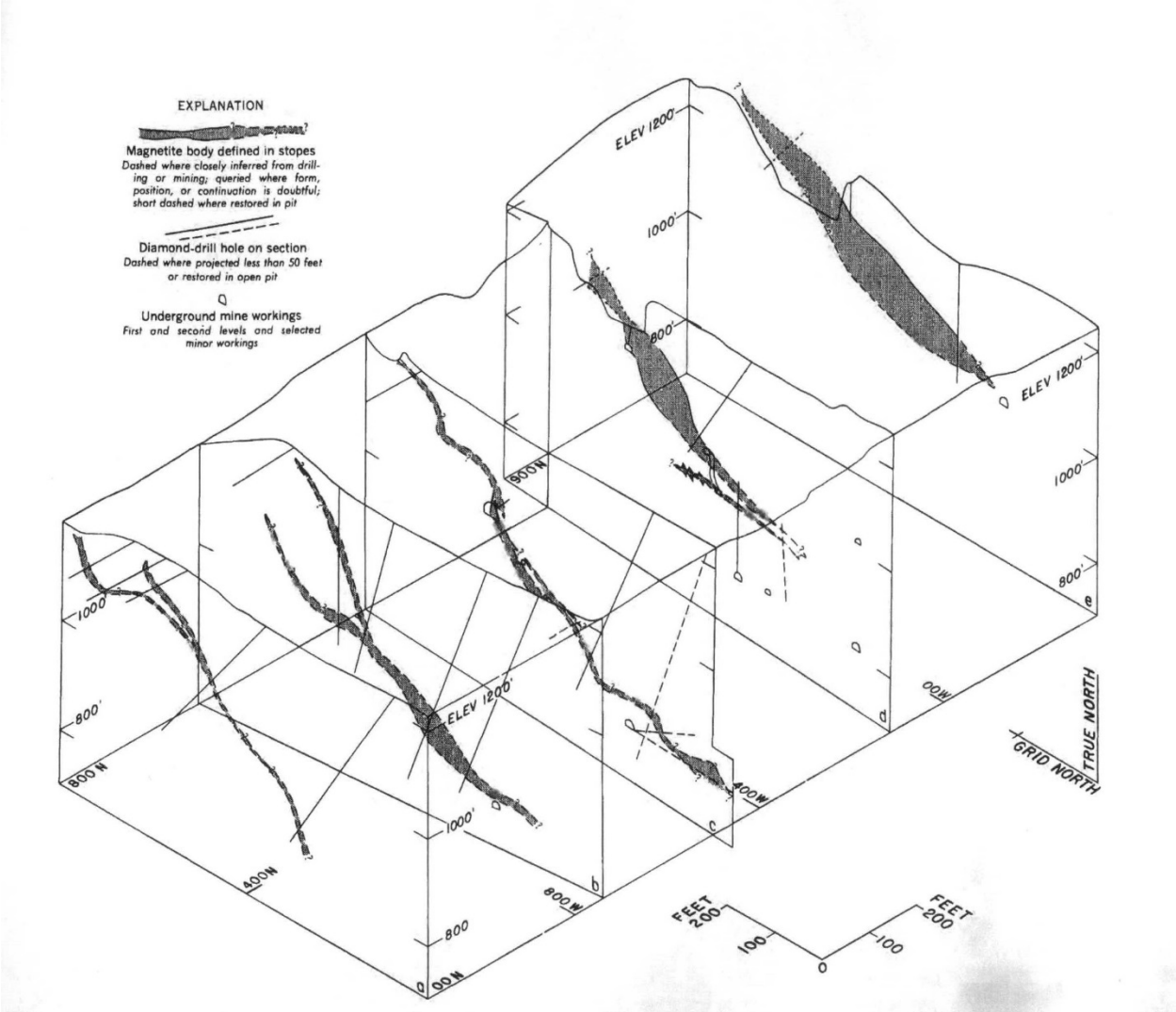

Figure 11. Skeleton block diagram of Clifton ore body (Leonard and Buddington, 1964).

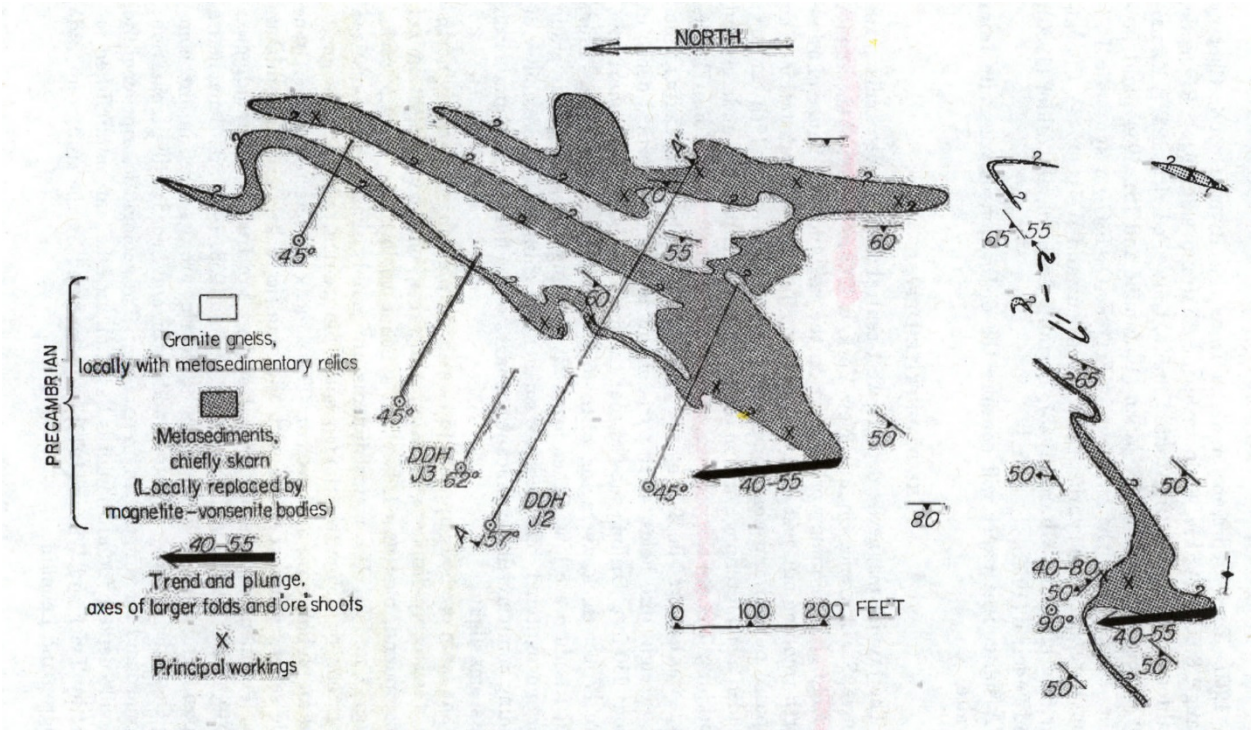

Figure 12. Geologic sketch map of the Jayville magnetite deposit (Leonard and Vlisidis, 1961).

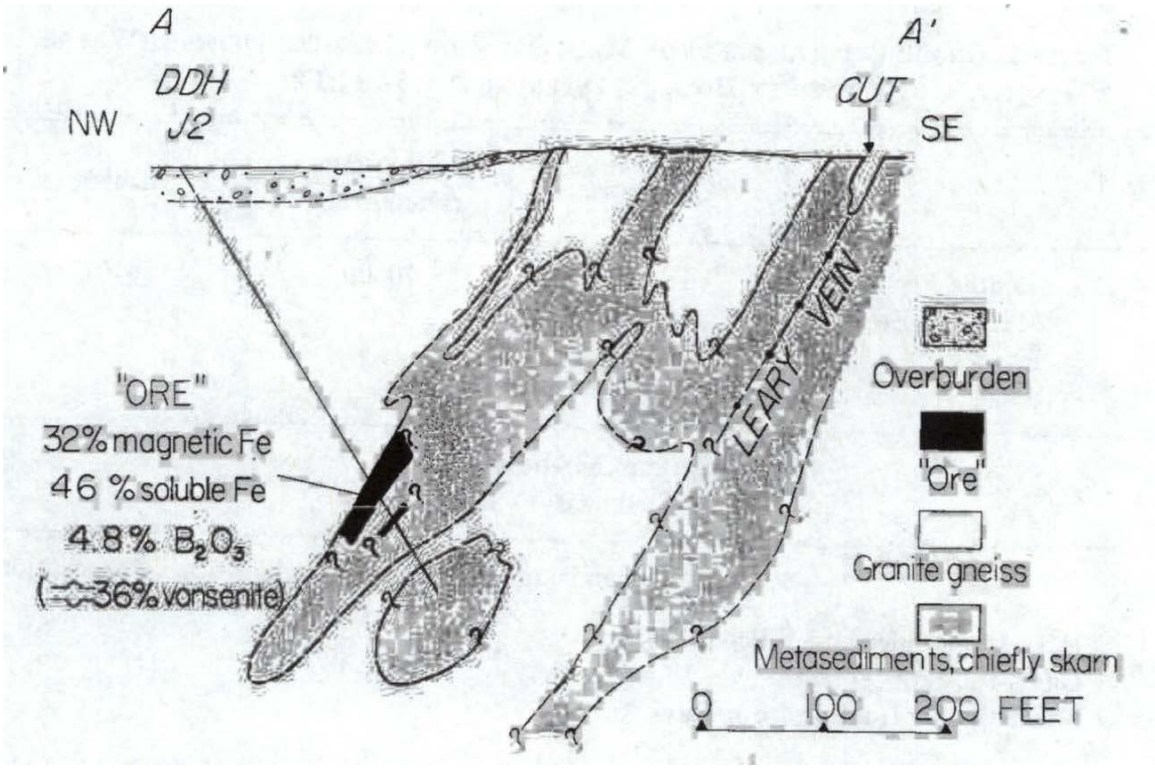

Figure 13. Cross section of Jayville magnetite deposit (Leonard and Vlisidis, 1961).

Benson Mines. Benson Mine was at one time the largest open pit iron mine in the world (Hyde, 1974) yet its discovery was quite by accident. Around 1810, engineers, while in the process of surveying the route for a military road from Albany to Ogdensburg, had their compasses affected by a magnetic ore body located just easterly of Star Lake in an area known as Little River. The main deposit is 2.5 miles long, averaging 400 feet in width and 90 feet deep, containing a low grade magnetic and nonmagnetic ore that is roughly 23% iron (Figure 14). That the ore is located at the surface made this deposit attractive for development (Lupulescu etal, 2014) and allowed the Magnetic Iron Ore Company to abandon the Jayville operation in favor of this location (Carl, 2009).

The Benson mines ore is mined in the main pit and the smaller Amoeba pit, located west of the main workings (Crump and Beutner, 1970). The ore is hosted within a sequence of gneissic metasedimentary rocks with varying amounts of garnet, pyroxene, microcline, albite, sillimanite, calcite, quartz and magnetite (figure 14) (Lupulescu et al, 2014). Structurally, the ore is contained within a syncline that has been overturned to the west and plunges roughly 20° to the north with a secondary roll on the east limb. The Amoeba pit is thought to be at the bottom of a roll forming an anticline and syncline on the east limb of the main syncline. The Benson ore is only found where the stratigraphic footwall has been overturned, becoming the hanging wall (Figure 15). At the southern end of the structural trough, the ore stops where the hanging wall is no longer the hanging wall (Crump and Beutner, 1970).

The ore at Benson mines is a low titanium magnetite, similar to other Adirondack magnetites. Origin preference is metamorphism of an iron rich sedimentary protolith. Lupulescu et al (2014) argues for this origin based on 1) the appearance that ore is conformable for more than 3 kilometers in the same sequence of the metasedimentary rrocks; 2) large scale replacement is not very abundant or not seen at all; 3) microscopic ore grain textures suggest that some were present during the silicate development; 4) the abundance of the high aluminum and potassium minerals sillimanite and potassium feldspar imply a clastic sedimentary protolith; 5) experimental work has shown that the silicate and ore minerals were stable at 640° $\pm$ 50° C.

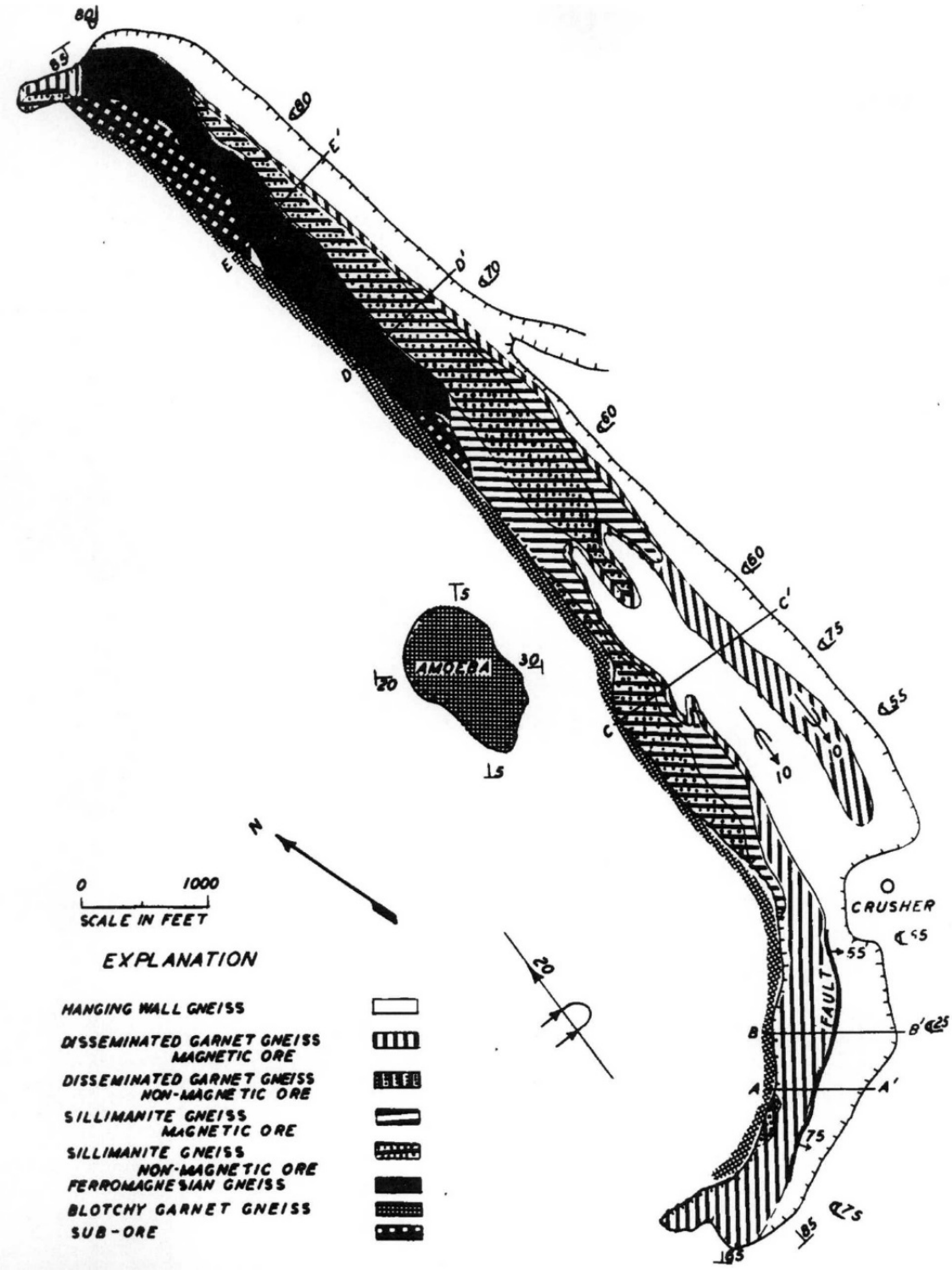

Figure 14. Benson Mines Pit Diagram (Crump and Beutner 1970)

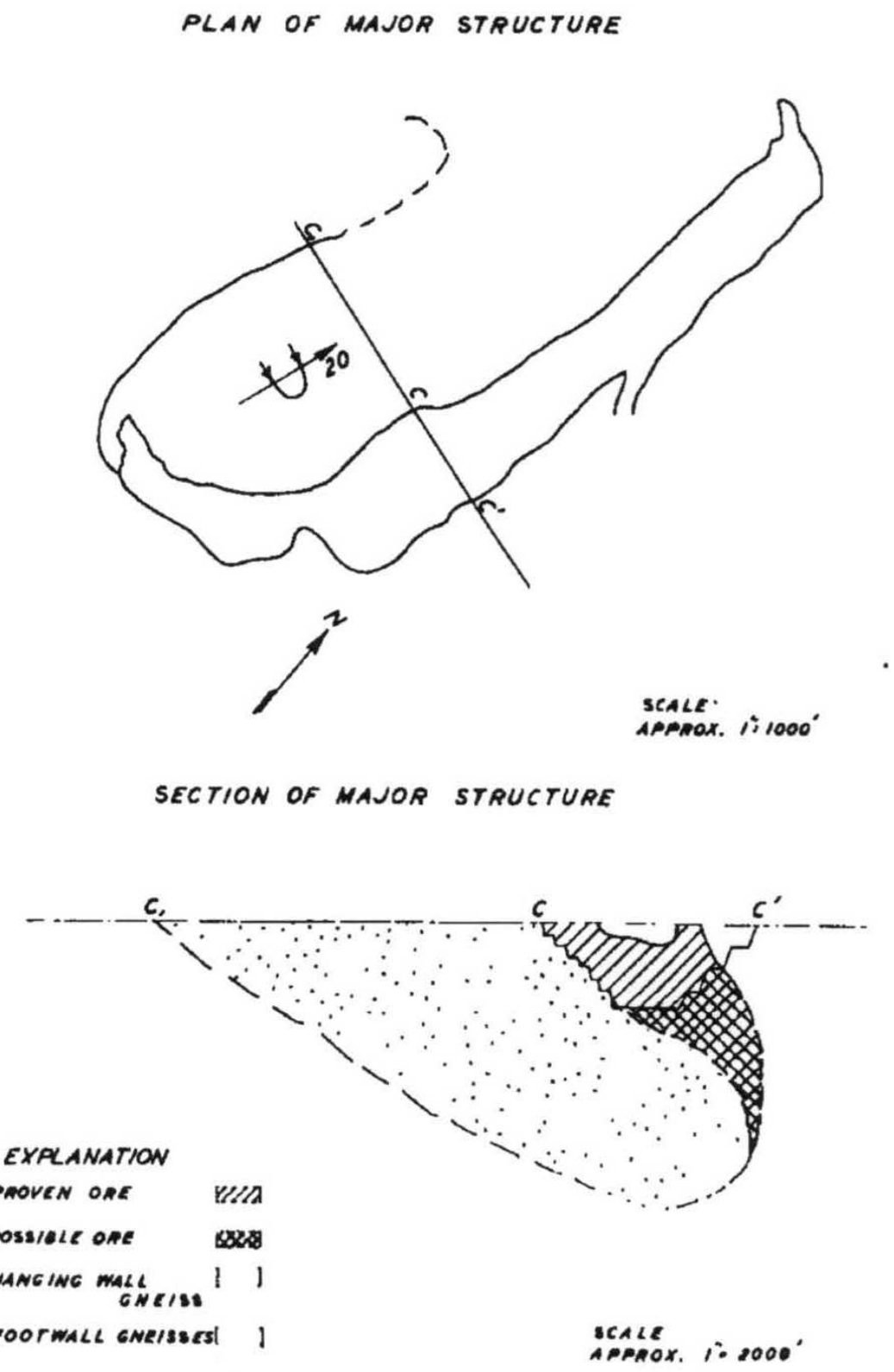

Figure 15. Major Structure of Benson Deposit (Crump and Beutner, 1970)

REFERENCES

Barnes, J. B., 1962. Clifton Mines. The St. Lawrence County Historical Association Quarterly 7 (1): p. 13-14.

Buddington, A. F., and B. F. Leonard. 1962, Regional geology of the St. Lawrence County magnetite district, Northwest Adirondacks, New York. Geological Survey professional paper 376.

Carl, J. D. 2007. Mines, Immigrants and Railroads: Stellaville in the Early Twentieth Century. The St. Lawrence County Historical Association Quarterly 52 (1): 3-3-29.

Carl, J. D. 2009. Opening the western Adirondacks—Part I: How Byron Benson financed iron mines and the Carthage & Adirondack Railroad. The St. Lawrence County Historical Association Quarterly 54 (4): 7–28.

———. 2009. Opening the western Adirondacks—Part II. The St. Lawrence County Historical Association Quarterly 55 (4): 4–18.

Crump, M. R., and E. L. Beutner. 1970. The Benson Mines ore deposit, Saint Lawrence County, New York. In Ore deposits of the United States, 1933–1967, ed. J. D. Ridge, 49–71. New York, NY: The American Institute of Mining, Metallurgical, and Petroleum Engineers, Inc.

Curtis, G., editor, 1894, Our County and its People. A Memorial Record of St. Lawrence County, New York, The Boston Company. P. 713-714.

Dawson, J. C., J. R. Moravek, M. F. Glenn, G. C. Pollard 1988. Iron Industry of the Eastern Adirondack Region: NYSGA Guidebook, 60th annual meeting, Trip A7, 26p.

Farrell, P. F., (1996). Through the Light Hole. Utica, New York: North Country Books.

Hunner, G. B., 1943, Development and operation of Clifton Mines, Hanna Ore Co.: Mining and Metallurgy, v. 24, p. 517-519.

Hyde, F. S., (1974). Adirondack Forests, Fields, and Mines. Lakemont, New York: North Country Books.

Ingalls, W. R. (ed.). (1914). Engineering and Mining Journal, Volume 97. New York: Hill Publishing Company.

Jones & Laughlin Steel Corporation. (n.d.) Benson Mines brochure

Kudish, M., (1996). Railroads of the Adirondacks: A History. Fleischmanns, New York: Purple Mountain Press, Ltd.

Leonard, B. F., and A. F. Buddington. 1964. Ore deposits of the St. Lawrence County magnetite district, northwest Adirondacks, New York. Geological Survey professional paper 37.

Leonard, B. F., and A. C. Vlisidis, 1961, "Vonsenite at the Jayville magnetite deposit, St. Lawrence Count, New York," American Mineralogist, vol. 46, p. 786-811.

Levine, D., 2012. Hudson Valley Iron-Ore Mining Industry: A History of Sterling Forest. Hudson Valley Magazine, September 2012.

Linney, R. J. 1943. A century and a half of development behind the Adirondack iron mining industry. Mining and Metallurgy 24:480–87.

Lupulescu, M. V., D. G. Bailey, M. Hawkins, J. D. Carl, J. R. Chiarenzelli. 2014. The Benson Mines, St. Lawrence County, New York: History of the Discovery, Mining, and Mineralogy of the Deposit: Rocks & Minerals, Vol. 89, p 118-131.

McLelland, J. M., and J. R. Chiarenzelli. 1990a. Geochronology and geochemistry of 1.3 Ga tonalitic gneisses of the Adirondack Highlands and their implications for the tectonic evolution of the Grenville Province. In Middle Proterozoic crustal evolution of the North American and Baltic shields. Geological Association of Canada special paper 38, 175–96.

———. 1990b. Geochronological studies of the Adirondack Mountains, and the implications of a Middle Proterozoic tonalite suite. In Mid-Proterozoic Laurentia-Baltica, ed. C. Gower, T. Rivers, and C. Ryan, 175–94. Geological Association of Canada special paper 38.

McLelland, J. M., J. S. Daly, and J. McLelland. 1996. The Grenville Orogenic Cycle (ca. 1350–1000 Ma): An Adirondack perspective. Tectonophysics 265:1–28.

Miller, R., and M. Miller Carvell. 2010. Lumbering in the Aftermath of Mining: Who Lived in Jayville and Kalurah? The St. Lawrence County Historical Association Quarterly 55 (4).

Newland, D. H., and J. F. Kemp. 1908 Geology of the Adirondack Magnetic Iron Ores with a Report on the Mineville – Port Henry Mine Group. New York State Museum bulletin 119.

Palmer, R. F., and J. Thomas. 1969. Wooden Rails in the Wilderness. Part I – Clarksboro. The St. Lawrence County Historical Association Quarterly 14 (2) 3, 11, 14, 22.

Palmer, R. F., and J. Thomas. 1969. Wooden Rails in the Wilderness. Part II. The St. Lawrence County Historical Association Quarterly 14 (3) 11, 14, 22.

Palmer, R. F., and J. Thomas. 1969. Wooden Rails in the Wilderness. Part III – Conclusion. The St. Lawrence County Historical Association Quarterly 14 (4) 11, 14.

Smock, J. C., 1889, First Report on the iron mines and iron ore districts in the State of New York: New York State Mus. Bull. 7

Thompson, B., (n.d.). The Clifton Mines Railroad. The Historians Office, Town of DeKalb, NY

Tillinghast, E. S., 1948, New York's Benson Mines: Mining World, v. 12, no. 12, p. 27-30

Walker, A.E., 1943, Geology of the Clifton and Parish ore deposits: Mining and Metallurgy, v. 24, p. 519-520.

Road Log for the Trip

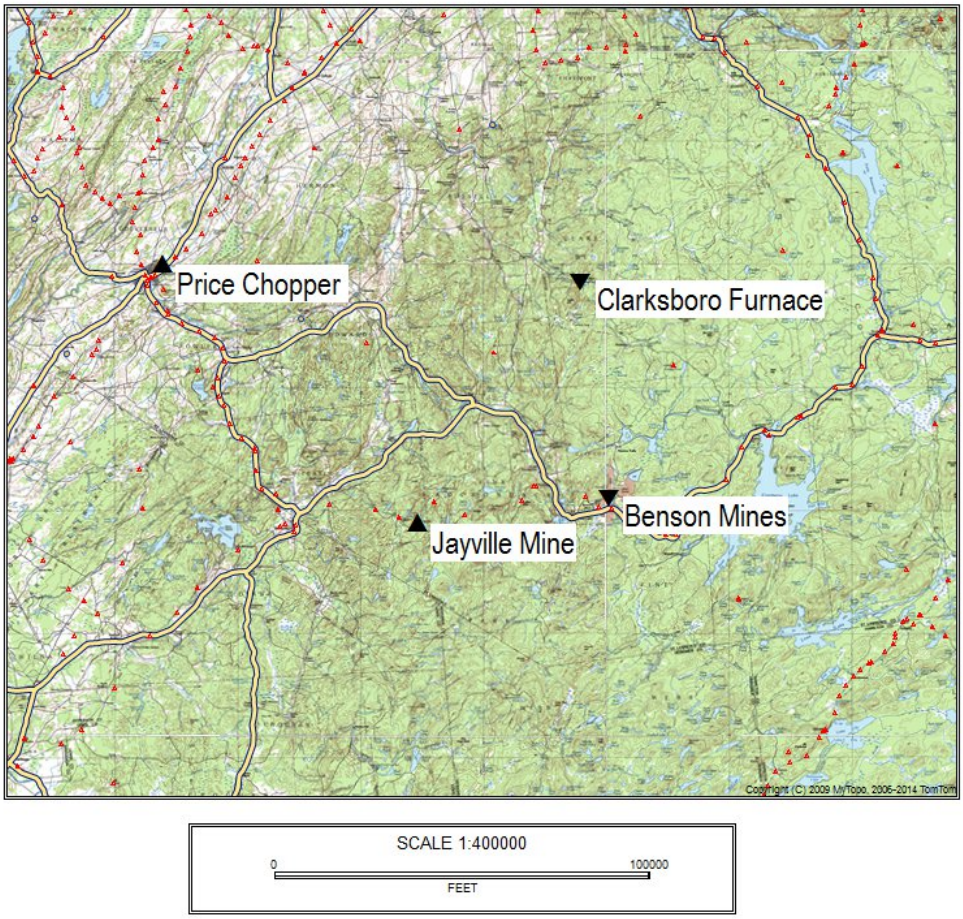

Figure 16. Road map of the field trip. The trip begins in the Price Chopper parking lot in Gouverneur.

The field trip begins at the Price Chopper parking lot, located on the west side of E. Main Street (US Route 11) in the northeast portion of the village (Figure 16). The address is 389 E. Main Street, Gouverneur, NY 13642. (N 44.15983°, W75.19078°). Please note the coordinates are in DECIMAL DEGREES.

Cumulative Mileage	Miles from last point	Route Description
0	0	Leave parking lot and turn right at the light onto E. Main Street.
0.8	0.8	Turn left onto NYS Route 58/812.
6.9	6.1	turn right onto NYS Route 812
16.8	9.9	turn left onto NYS Route 3
19.2	2.3	turn right onto Jayville Road
23.4	4.3	Kalurah. Bear left at the intersection.
24.6	1.2	Arrive at Jayville Mine. Park at gravel pit.

We will park at the gravel pit and walk around to the various stops at this old mine. We will visit several different shafts and drifts. Please use caution as these areas are not well marked and all are flooded.

Stop 1. Jayville Mine (N 44.16062°, W 75.18896°)

Leonard and Buddington (1964) describe eleven principal workings at the mine with the Benson No. 1 shaft (N 44.16032°, W 75.18929°) located on the northwest side of the hill believed to have supplied most of the ore shipped from Jayville (Figures 17 and 18). This shaft is inclined about 65° NW and has a slope length of 350 feet. There was no processing of the ore at the mine, other than hand sorting with low grade ore being cast aside. Ore was loaded onto rail cars and shipped to furnaces in Scranton and Bethlehem.

Leonard and Buddington (1964) describe the other workings as follows. The author has provided the Latitude and Longitude information for each;

> Fuller No. 1 (Open Cut) (N 44.15938°, W 075.18979°): Located roughly 180 feet south southwest of Benson No. 1, the cut is roughly 100 feet deep with ore analyses showing 47 and 52 percent Fe.
>
> Benson No. 2 (N 44.15960°, W 075.18960°): Located less than 100 feet southwest of Fuller No. 1, the shaft is inclined at 55° W, 60 feet deep through 12 feet of ore ranging in grade from 37 to 49 percent.
>
> Adit (N 44.16000°, W 075.18958°): Located about 150 feet south of Benson No. 1 shaft, this adit opens up a lens of ore 60 – 70 long and 20 feet wide.
>
> Fuller No. 2 Shafts (N 44.15813°, W 075.19044°): Located roughly 400 feet southwest of Benson No. 2 and is said to be 50 feet deep, with ore averaging 54 percent Fe.
>
> Fuller No. 3 (N 44.15803°, W 075.19029°): Located roughly 100 feet southeast of Fuller No. 2 shafts, a 30 to 40 foot opening accessed by a drift.
>
> New York No. 1 (N 44.15951°, W 075.18842°): This shaft is located roughly 170 feet due south of the Leary shaft, inclined to the northwest and 300 feet deep with short drifts at the bottom. Ore averaged 47 percent Fe.
>
> Hart No. 2 (N 44.15787°, W 075.18842°): Located slightly north and west of the former train station, this shaft is 60 feet deep.

Hart No. 1 (N 44.15685°, W 075.18890°): This shaft is located just to the west of the former railroad station and is roughly 300 feet deep, with ore shoots 10 feet thick. Ore analyses averaged 55 percent Fe.

New Find (Hustler mine): This small pit is located off the map, but contained ore analyzed at 52 and 58 percent.

Leary (New York No. 2) (N 44.16016°, W 075.18910°): Located roughly 120 feet southerly of the building foundation in the gravel pit, this shaft is roughly 50 feet deep with ore analyses ranging 22 to 38 percent Fe.

The Jayville mine lacked any ore processing facilities other than simple hand separation of low grade ore. There are many old shafts and drifts around the site and caution is advised as all are flooded.

We will walk around and visit several shafts and drifts that accessed the mine, as well as look at some of the few foundation features found at the mine.

.

Figure 17. Bedrock Geologic and Magnetic Map for Jayville Mine (Leonard and Buddington, 1964).

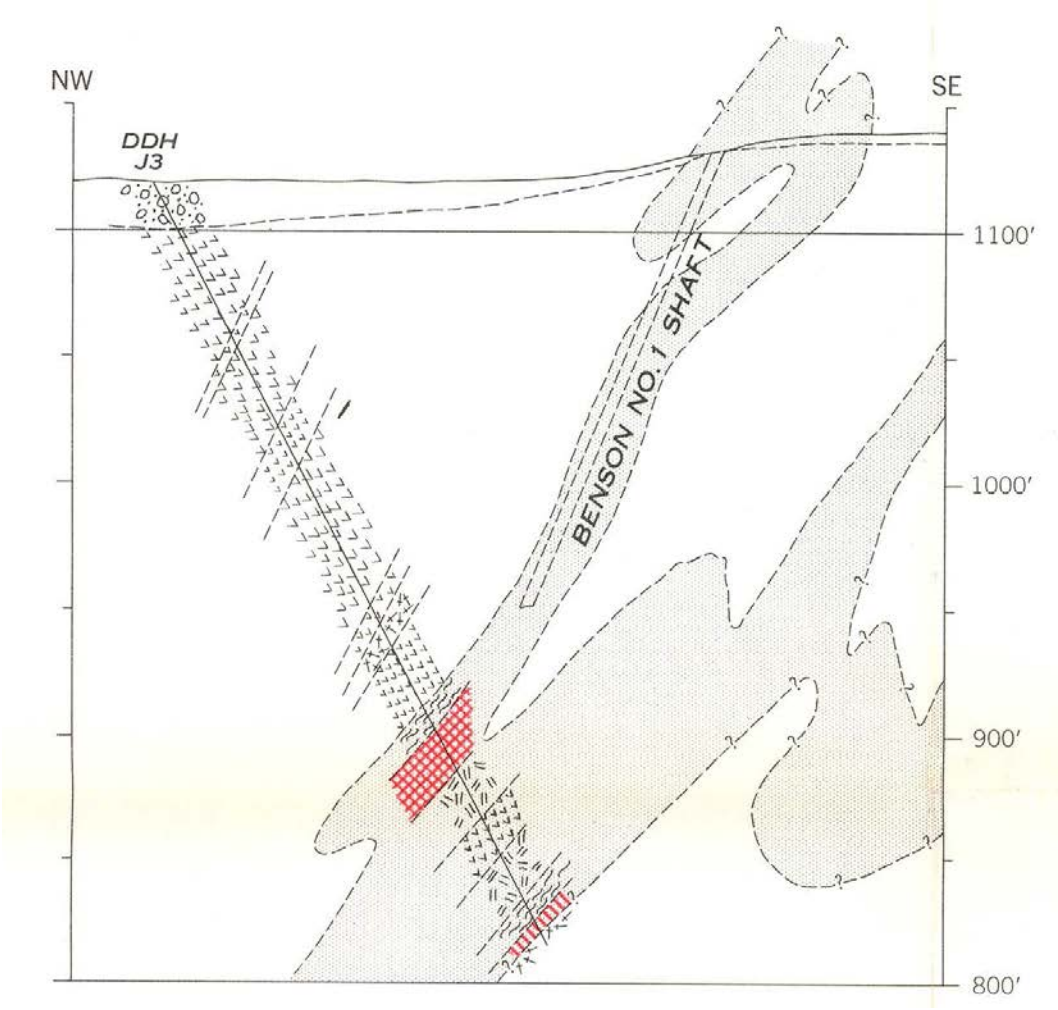

Figure 18. Cross Sectional View for Benson No. 1 Shaft (Leonard and Buddington, 1962).

Jayville stop 1. Benson No. 1 shaft: This working provided most of the ore that was transported from this mine. Presently flooded and not sealed.

Jayville stop 2. Adit (drift): This drift opens to a 60-70 foot seam of ore. Do not walk in as it becomes a decline and is flooded.

Jayville Stop 3. Fuller No. 3 working: This is another drift leading to ore that is flooded. Do not enter.

Jayville Stop 4. Gravel pit area. Here, the foundations of a couple buildings remain. Perhaps a loading dock for ore onto rail cars and a building housing machinery.

Jayville Stop 5. Train station location and water tower foundation.

Jayville Stop 6. Hart No. 1 shaft.

Return to cars to travel to the Clifton Furnace ruins at Clarksboro.

Cumulative Mileage	Miles from last point	Route Description
30.1	5.5	Return to Route 3. Turn right going east.
38.8	8.7	Turn left onto Route 58.
39.1	0.3	Turn right onto County Route 27A.
40.9	1.8	Turn left onto CR 27 towards DeGrasse.
48.7	7.8	Turn right staying on CR 27.
49.1	0.4	Turn right onto Tooley Pond Road.
52.1	3.0	Twin Falls. Pull off the road and park.

Stop 2. Clifton Furnace at Clarksboro (N 44.33314°, W 75.02531°)

Clifton Iron Company was founded by Zebulon Benton and sporadic mining operations began in 1863 (Leonard and Buddington, 1964). In April, 1864, the New York State legislature passed a bill allowing Clifton Iron Company to construct a 23 ½ mile railroad from the mine to the Rome, Watertown and Ogdensburg Railroad at East DeKalb. The scarcity of iron after the Civil War made it impossible to use iron rails and maple timbers were used instead. Major mining operations then began in 1865 and a charcoal furnace was constructed at Twin Falls on the Grasse River. Later in 1868, a new furnace was constructed at the mine, located roughly 2.0 miles southwest of Twin Falls. The mill at the mine succumbed to fire in September, 1869, forcing the mine to be shuttered (Palmer and Thomas, 1969).

In 1940 the M. A. Hanna Company purchased the mine and operated it until 1952 when it closed for good. All structures were torn down at the mine.

At this stop we will carefully cross the sluiceway and visit the old furnace, ore and charcoal piles. The access to the island is a hemlock log that must be shimmied across. You may or may not wish to access the island.

Today, the mine itself, located 2.0 miles south southwest of Twin Falls is owned by the Clifton Hunting Club. The club has a strict no entry policy and therefore we will not be able to visit the mine.

After visiting the remains of the 1863 furnace, carefully turn around and return to NYS Route 3.

Cumulative Mileage	Miles from last point	Route Description
55.1	3.0	Return to County Route 27.
58.5	0.4	Turn left and remain on County Route 27.
66.3	7.8	Turn left and remain on County Route 27.
67.1	0.8	Turn left onto NYS Route 3.
75.1	8.0	Turn left and enter Benson Mines gate.

Stop 3. Benson Mines at Star Lake (N 44.17045°, W 74.99963° - crusher site)

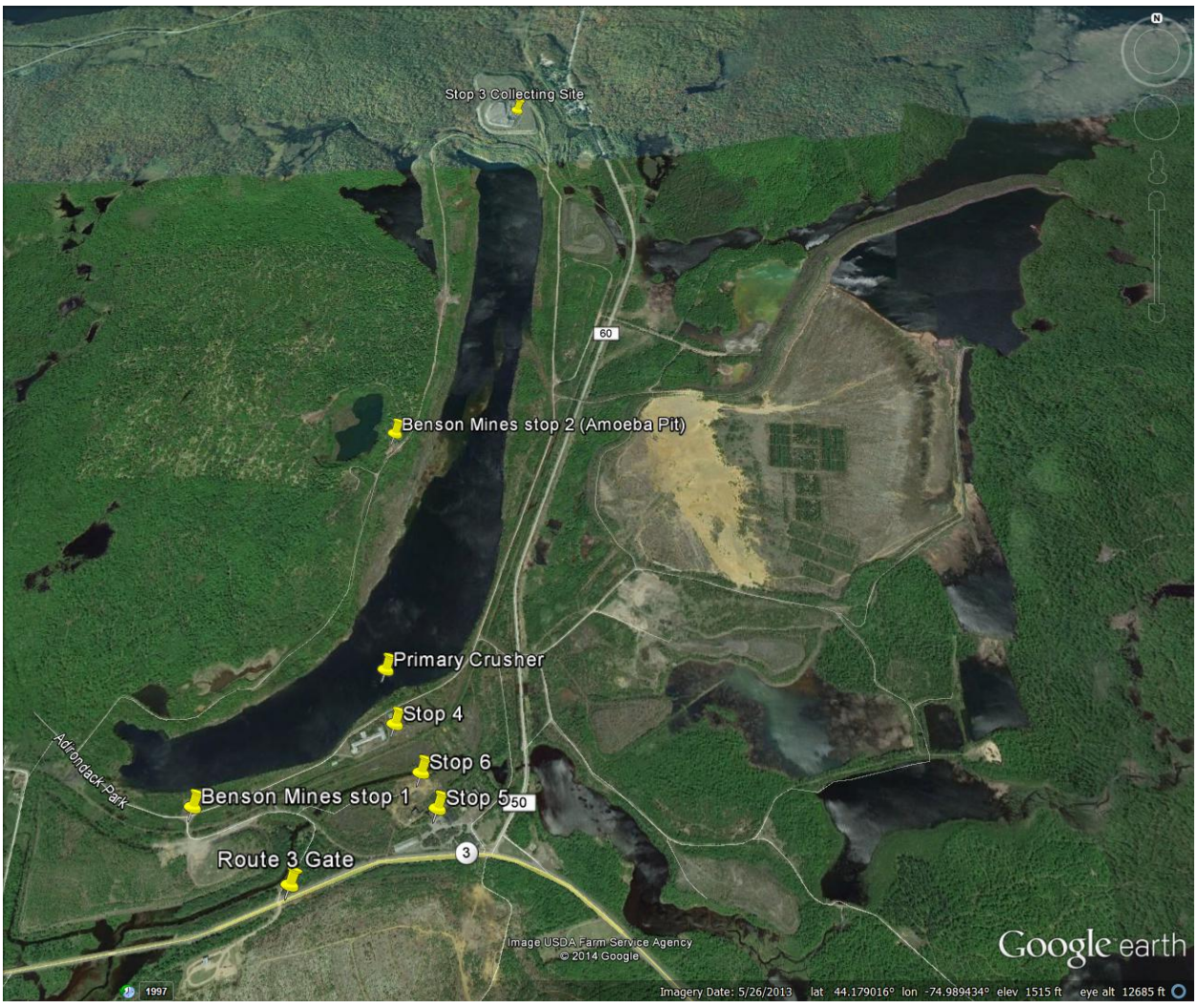

Figure 19. Benson Mines stops.

MINING AND CONCENTRATING METHODS

The open pit mine is now flooded (Figure 19). When in operation it utilized standard quarry methods to remove ore. A standard bench used nine inch holes drilled to a depth of 55 feet. The ore required roughly one half pound of explosives per long ton. Once broken, the muck pile is excavated with large 5 cubic yard electric shovels, loading an average of 25 tons into large dump trucks. The ore is then hauled to the 54 inch primary gyratory crusher located in the pit (Figure 20). The ore is then carried via conveyor belt to two 18 inch secondary gyratory crushers and then discharged into 500 ton silos that act as surge bins to feed the fine crushers (Tillinghast, 1948).

Originally, only magnetic ore was concentrated. However methods were later developed to process the nonmagnetic ore known as martite (Figure 21). Magnetic ore travelled from storage silos to one of three rod mills, where it was ground to pass a 20-mesh screen. From here, the ore was fed to three magnetic separators, with the waste then cycled back through for additional grinding and magnetic separation. From here, the concentrate is dewatered and transferred to the sintering plant. Tailings are pumped to a waste pond (Tillinghast, 1948).

The martite was concentrated in two sections, a rod mill section and an aerofall section, with the difference being the method of reducing the ore to a liberation size. In the rod mill, ore is ground to 18 mesh and the oversize is returned to the rod mill. The 18 mesh ore is sent to a set of rougher spirals that utilize the different specific gravities. The concentrate from the rougher moves to a cleaner spiral and the middlings return to the rougher spiral feeder tank. The tailings are classified and the minus 100 mesh portion sent to a floatation section (Jones & Laughlin, n.d.).

The concentrate is then sent to storage silos at the sintering plant. Here the roughly 64 percent concentrate is mixed with five percent coal, one percent lime and 30 percent fine sinter that is obtained from screened finished sinter. The mix is ignited and passed through an oil fired chamber where suction is applied. The entire sintering process is completed in eleven minutes when the sinter is sent to be screened and cooled. Once cooled to around 350° F., sinter is loaded onto railroad cars and shipped to steel plants at Pittsburgh and Aliquippa, Pa., and Cleveland, Ohio (Jones & Laughlin, n.d.).

BENSON MINES EPILOGUE

The mine continued operations until 1978 (Lupulescu et al, 2014). However problems, from the past industrial activity began to show in 1987 (Jesmore, 2014 NYSDEC, Personal Comm.). After almost ten years of inactivity, the quarry water rose to a level that began to float spilled petroleum to the surface and an oil sheen was discovered on the Little River. New York State Department of Environmental Conservation undertook an investigation and found that the network of underground pipes that carried fuel oil to various parts of the plant had corroded to the point where large volumes of petroleum were leaking directly to the ground. In all, it is estimated that roughly 1,000,000 gallons of fuel oil was lost. A groundwater dam was erected between the spill area and the Little River. Recovery wells were sunk and pumping activity has recovered about 350,000 gallons to date. In addition, the investigation revealed a number of PCB issues as well as a solvent spill and mercury problem (Figure 19), (Jesmore, 2014, NYSDEC, Personal Comm.).

Stop 1. View of the flooded mine looking northward. Here we will discuss the overall geology of the mine.

Stop 2. Amoeba Pit. This is a brief look at the small pit located westerly of the main workings.

Stop 3. Northern waste rock piles. The waste rock in this area was removed from the northern end of the mine where pegmatites intruded. Magnetite and martite can be found around the mine. This waste rock dump is a good location to collect minerals. Some minerals such as sillimanite, calcite, garnet, bornite, hornblende, tourmaline and molybdenite can be found. Dark green fluorite cubes have been found, though these are rare.

Stop 4. Here we will stop and discuss the processing of the ore and look at the remains of the plant.

Stop 5. A continued look at what is left of the mill.

Stop 6. Remediation site.

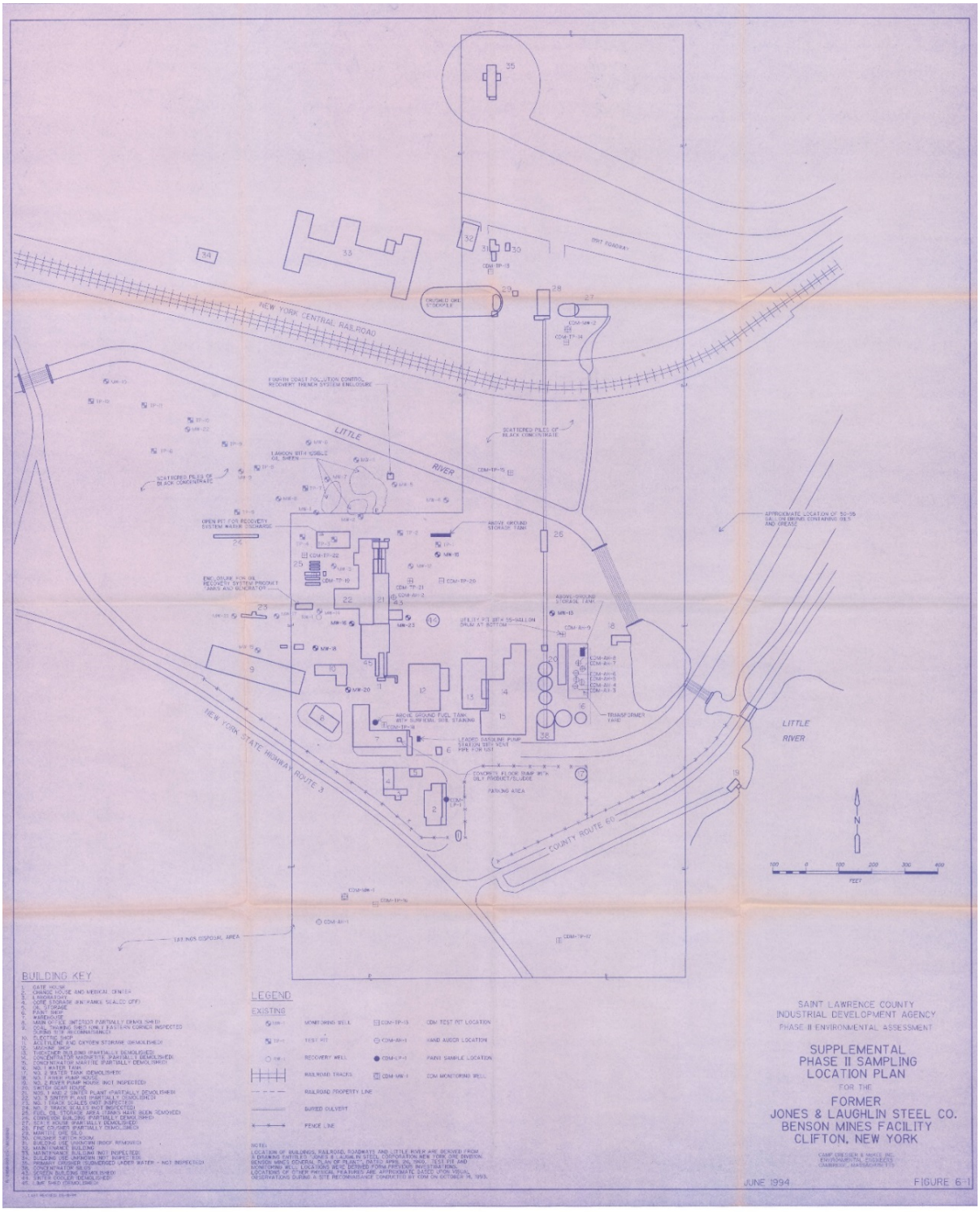

Figure 20. Processing Plant Layout Benson Mines (NYSDEC).

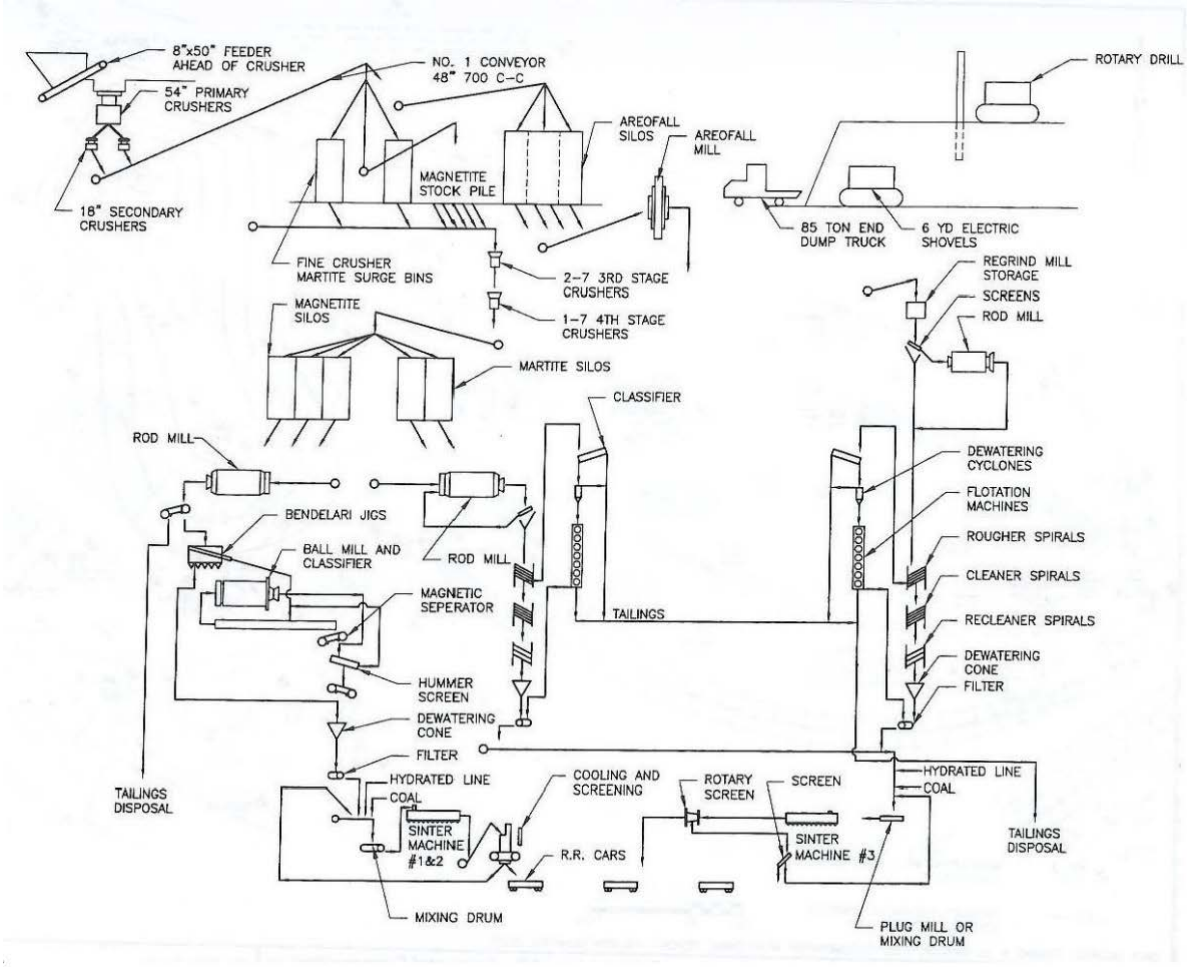

Figure 21. Benson Mines Ore Processing Flow Diagram (Jones & Laughlin Steel Corp, n.d.).

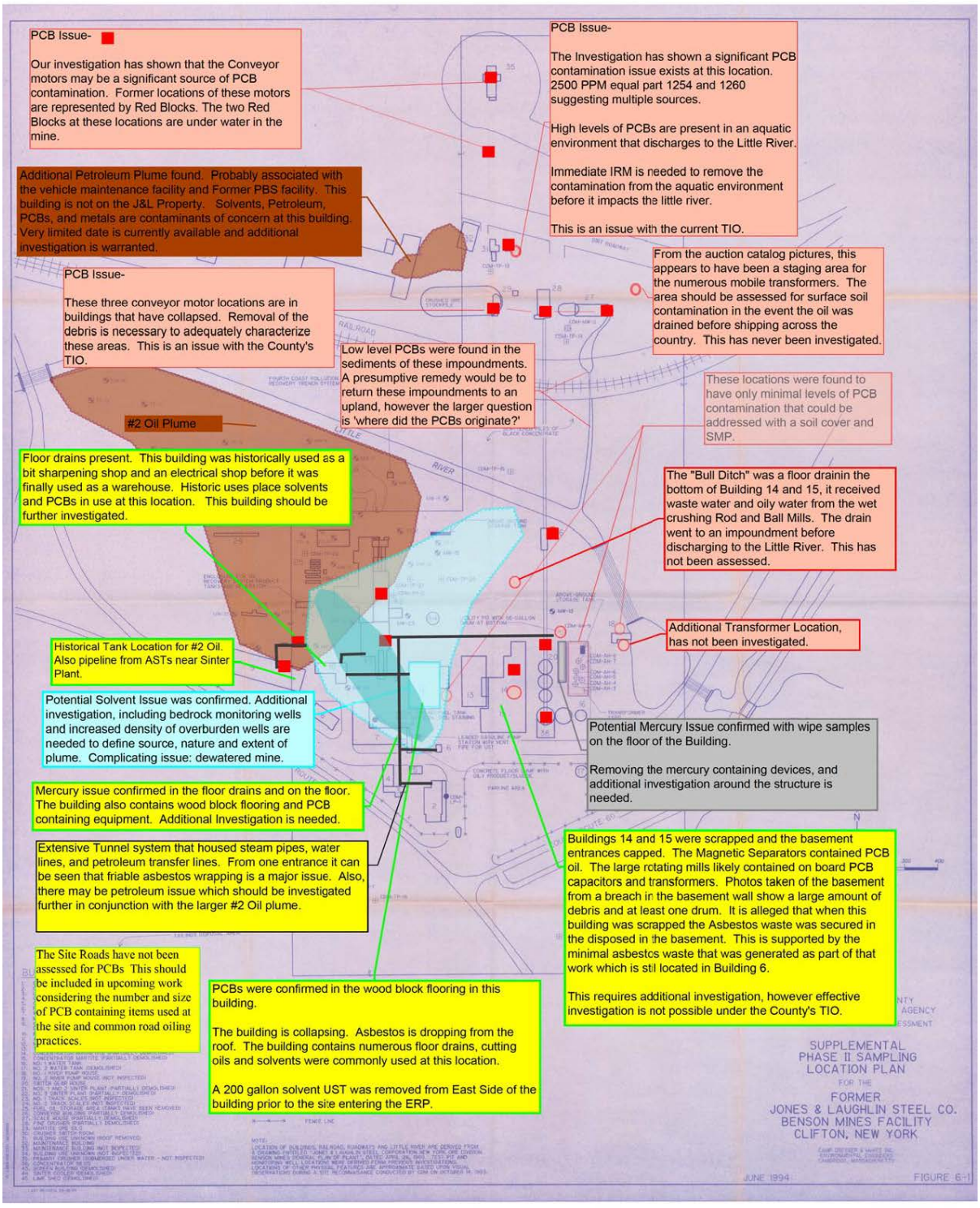

Figure 22. Environmental Investigation Map (NYSDEC).

WATER QUALITY TESTING BASICS FOR WORK IN THE ENVIRONMENTAL FIELD

ADRIENNE C. RYGEL

Department of Civil and Construction Technology, State University of New York at Canton, Canton, New York 13617

INTRODUCTION

Many geologists have careers in the environmental field. The Bureau of Labor Statistics predicts a 15% growth rate for careers in the environmental industry over the next decade, therefore there will not be a shortage of job opportunities for those looking to apply their background in geology to improve the natural environment for human use and consumption. The environmental sector is a diverse field, both in terms of the professionals who work in it and what they do. Professionals with backgrounds in geology, chemistry, biology, physics, or engineering will work to prevent, control, and remediate environmental problems that relate to surface water, groundwater, soil, air, and waste materials. Depending on the position, a professional may be responsible for quality testing, assessment, remediation, treatment, and/or management of these natural resources and human related waste materials. Most entry level positions will require field and/or laboratory work including collection and sample management and handling, sample testing for any number of analytical parameters, and then data analysis and assessment. This knowledge and skill set goes beyond basic chemistry classes and typically can be gained in an aqueous geochemistry course or water quality course.

The objective of this short course is to provide participants with either an initial exposure to or a refresher of basic water and wastewater quality tests that are commonly used in the environmental industry. This is a hands-on short course that will be run in the new Environmental Technology laboratory at SUNY Canton. Participants will be instructed on how to properly test for common water and wastewater quality parameters such as pH, temperature, conductivity, turbidity, dissolved oxygen, alkalinity, hardness, inorganics, and biochemical oxygen demand (BOD). The test procedures and equipment are those commonly used in environmental field sampling, drinking water treatment plants, and wastewater treatment plants. Using surface/ground water samples collected from around the region participants will learn how to calibrate and use the equipment, execute the analytical test procedures, and interpret the results. Participants will also learn about proper sample collection, handling, and preservation techniques. A variety of equipment/approaches will be used in the analytical tests: probes, meters, titrations, and color spectrophotometers. All methods and procedures are after industry standard and practice found in the ASTM Book of Standards, Volume 11 for Water and Environmental Technology (ASTM International) and Standard Methods for the Examination of Water and Wastewater (APHA, AWWA, and WEF); and in accordance with equipment specific standard operating procedures.

BASIC LAB SAFETY

Safety is of utmost importance and is not something to be taken lightly. Some of the equipment and materials that are used in water and wastewater testing can be potentially very harmful. It is therefore important to know how to properly use and handle these materials and equipment in the field/laboratory setting. Creating and maintaining a safe and healthy environment is a shared responsibility of everyone. This is something that must be taken seriously by all participants. Industry requires training and certifications to address such issues (e.g. OSHA 10hr safety training, OSHA 40 Hour HAZWOPER). The following subsections review key laboratory safety procedures that participants will follow in today's short course. It is not intended to be a fully comprehensive laboratory safety training course.

Protective Equipment

- *Lab Coat*:

  Lab coats will be required. They act as a barrier to protect skin and clothing from potentially harmful chemicals, dyes, or other substances encountered in the lab. Be aware of sleeves as they can knock equipment over. Lab coats must be removed if leaving the lab room, so as to not contaminate areas outside of the work space.

- *Safety Glasses or Goggles*:

  Eye protection is required when working in the lab. Prescription eyeglasses may be worn instead of safety glasses, provided that they adequately shield the eyes. Some safety glasses will fit over prescription eyeglasses. This is recommended if adequate protection cannot be offered from regular glasses alone. It is strongly encouraged that contact lenses not be worn in the lab. If something is splashed into the eye, it is more difficult to rinse the eye properly with a lens in the way. Trying to remove the lens could cause a delay in rinsing the eye and result in serious damage. Some chemicals will adhere a contact lens directly to the eyeball making it next to impossible to remove.

- *Protective Gloves*:

  Gloves should be worn when working with chemicals and potentially infectious materials. Gloves should be replaced if they develop a tear or perforation. When gloves are removed, take them off while turning them inside out and do not touch the exterior of the glove. Properly dispose of the used gloves in a trash can, do not set them down on a counter, table, or workbooks as this may contaminate the surface. If you must leave the lab area, gloves must be removed so as to not contaminate areas outside of the work space.

- *Clothing:*

  Proper clothing should be worn at all times. Loose fitting clothing, especially loose shirt sleeves, should be avoided. Long sleeve shirts and pants will provide more protection for your skin than T-shirts and shorts.

- *Footwear:*

  Proper footwear should be worn at all times. In particular, no sandals, flip-flops, slippers, ect. should be worn, since they provide no protection should equipment/chemicals be dropped on them.

Chemicals

- *Labeling and Safety Information*:

  All chemicals and solutions should be properly labeled so it is clear what they contain. The phone number and web address to obtain the Material Safety Data Sheets (MSDs) are posted in the work area.

- *Handling and Transport:*
  Chemical/solution containers should be kept well away from the edge of the workbench and any equipment that generates a flame or excessive heat. When working with chemicals on the workspace the containers should be covered and sealed whenever not in use to prevent spillage. It should not be necessary to transport any chemicals during the short course. However, if chemicals must be moved it should be done carefully, in a fashion that minimizes the chance of a spill or leak. No chemicals should be moved without the permission and supervision of the overseeing faculty member or laboratory assistant. Other participants should be made aware that a chemical is "on the move". While being moved the container should be properly sealed, should possibly be contained in a secondary containment vessel, and the person moving the chemical should be wearing all necessary protective covering.

- *Disposal:*

Not all wastes (chemicals, solutions, containers, disposable equipment, ect) can be disposed of in a normal trash can or down the sink – special secondary containment or pre-disposal treatment may be required. Do not dispose of any wastes down the sink or in the trashcan until you have consulted with the short course instructor.

Equipment

- *Handling of equipment:*

  Treat all equipment with care and respect. Most of this equipment is expensive and to varying degrees – fragile. Use equipment only for what it is intended for, do not move equipment unless you are told to do so, and follow the instructors use and handling of the equipment.

- *Cleaning:*

  Keep a clean workspace. Each group and individual is responsible for cleaning the equipment and workstation space as instructed. Glassware typically requires a multi-step cleaning – soap wash, 3x tap water rinse, and 3x distilled water rinse. Be careful when handling wet glassware as it becomes very slippery and can easily be dropped into the sink. Should glassware break the instructor will clean and dispose of the broken pieces.

Emergency Response

At the start of the short course the instructor will point out the location of the following:

- Fire extinguishers
- Eye wash fountains
- Emergency showers
- First aid supplies
- MSDS sheet contact information
- Laboratory exits

Miscellaneous Rules

- Follow the instructions provided to you by the instructor at all times. If you are unsure of part of the procedure do not hesitate to ask for assistance.
- *Food and Drink:* Absolutely NO food or drink is allowed in the laboratory area. All food and drink should be consumed prior to coming to the laboratory session. Water is available down the hall at water fountains.
- *Jewelry:* Rings, watches, and bracelets may catch on equipment. Some articles will react negatively with protective gloves and certain chemicals, causing discoloration or staining. In the event that there is a chemical spill, the material may become trapped under the jewelry, making it difficult to remove the chemical and prevent injury. Use precaution when wearing these items in the laboratory.
- *Hair:* Long hair should be kept tied back, especially when working with open flame or when leaning over the bench to work as it may knock equipment or get into chemicals.
- *Hand Washing:* Hands should be washed and dried thoroughly with soap prior to the start and at the end of the lab. Antibacterial soap can be found at each of the work stations.

BASIC WATER QUALITY PARAMETERS

Introduction and Background:

Environmental assessment typically will include measurement of basic water quality parameters such as pH, temperature, conductivity, dissolved oxygen, and turbidity. These parameters are important as they drive most physical, chemical, and/or biological reactions that impact water and wastewater quality and are important factors in treatment/remedial systems. In this section of the short course, participants will learn about the probes and meters used to measure these parameters, how to handle and calibrate the equipment, and how to use the instrumentation to obtain analytical values for pH, temperature, conductivity, dissolved oxygen, and turbidity. Participants will be divided into four (4) groups and each group will be assigned a different source of water. Analytical results from each group will be shared with all participants to allow for comparison and discussion of the results. The same work groups and water sample will be used for the other three short course modules as well.

In water, hydrogen ions, H^+, are directly or indirectly involved in numerous chemical reactions; and are often driving factors in these reactions. The concentration of hydrogen ions is measured as pH, or acidity, where pH is the negative log concentration of hydrogen ions:

$$pH = -\log [H^+]$$

A solution that is acidic will have a low pH (thus a high concentration of hydrogen ions) and a solution that is basic will have a high pH (a low concentration of hydrogen ions). In order to measure pH a meter and probe are used. The pH scale ranges from values of 0 to 14, with a value of 7 being neutral, pH values less than 7 are considered acidic, and pH values greater than 7 are considered basic. As reference, vinegar has a pH of 2.5, milk has a pH of 6.7, and Pepto Bismol has a pH of about 10. The pH of natural waters (surface and groundwater) can be quite variable depending on overall water quality, bedrock/soil types, seasonal variation, the types of chemical reactions that are occurring, etc. Commonly pH levels of streams in the North Country (e.g. the Grasse River and Raquette River) are close to neutral (6.8-7.2). Municipal drinking water treatment plants have a target pH of about 7.0 in their effluent stream. In water and wastewater treatment systems, some chemical and/or biological reactions require a particular pH in order to proceed or be most efficient (time it takes for a particular treatment process and/or degree to which a reaction will occur). For example, the alum coagulation/flocculation process in a conventional drinking water treatment plant requires a pH of 6. In passive treatment systems for iron acid mine drainage a high pH (8-10) is required to optimize iron oxidation.

Temperature is a factor in both natural and engineered systems as it is one factor that impacts the rate in which many reactions proceed. Both chemical and biological reaction rates typically increase as temperature increases. Water samples are collected and put on ice in the field and stored in a cold refrigerator (< 4°C) in order to slow both chemical and biological reactions. A temperature probe is typically part of the pH meter and probe.

Conductivity measures the solutions ability to conduct an electronic charge. It is a reflection of the number of ions present in the sample. These ions are charged particles and the electron activity that they produce is a reflection of the ions concentration. The greater the number of ions present in the sample, the greater the conductivity. A probe is used to measure conductivity.

Oxygen is found in water and is referred to as dissolved oxygen (DO). It is typically consumed in many chemical and biological reactions and is an important factor in 1) assessing the water quality for ecological systems, 2) system components of wastewater treatment systems, and 3) assessing water quality of treated

wastewater streams (as participants will learn in the biochemical oxygen demand module of this short course). Dissolved oxygen is measured with a DO meter and probe. A healthy, natural stream would typically have DO concentrations of 7-9 mg/L.

Turbidity is the measure of clarity of water and is used in treatment design tests (e.g. jar test to determine chemical coagulant dose in drinking water treatment) and for monitoring effectiveness of treatment systems. Turbidity is measured with an instrument called a turbidimeter, which measures the amount of light that is able to pass through a sample. The more material that is present in a sample (e.g. solids, metals, bacteria, organics), the less light is able to pass through the sample, and the higher the turbidity of the sample. Turbidity is reported in units of NTU or nephelometric turbidity units. Finished treated drinking water should have a turbidity of 0.1 to 1.0 NTU according to the US Environmental Protection Agency (EPA).

Objectives:

- *Overview of Field Work*: review sample collection, preservation, and handling techniques
- *Analytical tests*: learn how to operate meters and probes used to measure pH, temperature, conductivity, DO, and turbidity, conduct analytical tests for these basic water quality parameters (pH: ASTM D1293-99R05, APHA 4500-H+; temperature: ASTM D6764, APHA 2550; conductivity ASTM D1125-95RR99, APHA 2510; dissolved oxygen ASTM D0888-03, APHA 4500-O; turbidity ASTM D1889-00, APHA 2130), and discuss results from varying water sources

Overview of Field Work:

In the environmental engineering profession, quality control is of the utmost importance. Reducing error and producing repeatable data sets is essential to proper analysis and evaluation. It is therefore necessary to learn the appropriate method in which to collect a water sample so that you can be assured that your data represents the conditions of the water/wastewater source as accurately as possible. The main goal is to collect a number of samples that are a good representation of the water/wastewater source. To ensure that a representative sample is obtained, one must minimize the sampling bias that could arise during collection by having a routine that deals with sample site selection, sample handling, sample preservation, the frequency of collection, and the equipment and method(s) used to collect the sample. Prior to sampling it needs to be determined what parameters are going to be tested. It should then be determined by what method they will be analyzed. The standard procedure for that method should be carefully reviewed. In the standard procedures for that method it should indicate how the sample should be collected: type of sample container, sample volume, sample preservation, and allowable sampling holding time and conditions. Any or all of these may vary depending on the source type (e.g. stream, lake, groundwater well, tap/pipe). All of this should be carefully reviewed to ensure that all of the proper equipment has been acquired and all procedural steps are accurately followed.

As an introduction to measurement of basic water quality parameters, the instructor will give a brief overview of the topics outlined below that relate to field work:

- *Typical field kit*: cooler, ice, clip board, chain of custody forms, sample labels, field book, sample bottles, filtration equipment, preservation materials, samplers (sample bottle, sample cup on arm, bailer, peristaltic pump+tubing), field meters and probes (e.g. pH probe, DO probe, turbidimeter), calibration standards and reagents, distilled/deionized water, gloves, safety glasses, markers, hip boots, water level tape, measuring tape, camera, site map.
- *Sample collection*: containers and collection method
- *Sample preservation*: filtration, chemicals, cooling agent

- *Sample handling*: coolers, chain of custody, arrival in lab, holding times (**Exhibit 1** – Example Chain of Custody form)

Materials for Analytical Tests:

The following materials will be used to determine pH, temperature, conductivity, DO, and turbidity of the water sample.

- pH/temperature probe
- Mulitparameter field probe (can test for pH, temperature, conductivity, total dissolved solids, and salinity)
- pH standard solutions
- Conductivity standard solutions
- DO probe
- DO calibration sleeve
- HACH turbidimeter
- HACH turbidity calibration standards and verification sample
- Bottle of distilled water
- 250 mL beakers
- Kim wipes
- Protective gloves
- Water samples

Procedures for Analytical Tests

The following procedures will be used to determine pH, temperature, conductivity, DO, and turbidity of the water sample. Record the results in the data table found in **Exhibit 2**. These results will be shared with the group for discussion of variation in water quality between the different sources.

- Measuring pH, Temperature, and Conductivity

    1. Turn on the pH/temperature/conductivity multimeter probe.
    2. Temperature does not require any calibration.
    3. To calibrate the probe for pH make sure it is reading pH by pressing the "Mode/Ent" button
    4. Rinse the probe with distilled water into a rinse beaker.
    5. Obtain the container with 7.00 standard solution and pour a small amount into the probe cap.
    6. Place the probe into the 7.00 standard solution.
    7. Hit "Cal".
    8. Wait until the reading is stable and then hit "Mode/Ent".
    9. Remove the probe from the 7.00 standard solution.
    10. Rinse the probe with distilled water into the rinse beaker.
    11. Dump the calibration standard from the cap into the rinse beaker and repeatedly rinse the cap with distilled water.
    12. Repeat steps 3-9 with the 4.01 and 10.00 pH standard solutions.
    13. To calibrate for conductivity press "Mode/Ent" until the probe is in the conductivity mode.
    14. Rinse the probe with distilled water into a rinse beaker.
    15. Obtain the container with 84 μS standard solution and pour a small amount into the probe cap.
    16. Place the probe into the 84 μS standard solution.
    17. Hit "Cal".
    18. Wait until the reading is stable and then hit "Mode/Ent".
    19. Remove the probe from the 84 μS standard solution.
    20. Rinse the probe with distilled water into the rinse beaker.

21. Dump the calibration standard from the cap into the rinse beaker and repeatedly rinse the cap with distilled water.
22. Repeat steps 15-21 with the 1413 μS and 12.88 mS conductivity standard solutions.
23. The probe is now calibrated.
24. Pour approximately 100mL of water sample into an empty 250mL glass beaker.
25. Rinse with probe with distilled water into the rinse container.
26. Place the probe into sample, holding it off the bottom of the beaker and away from the sides of the container.
27. Gently stir the sample with the probe.
28. Monitor the parameters on the screen of the probe, allowing them to equilibrate before taking a reading. Record your results in the table found in **Exhibit 2**. Pressing the "Mode" button will cycle the meter through the different parameters.
29. Remove the probe from the water, rinse with deionized water into the rinse container, gently dry the exterior of the probe with a Kim wipe, replace the end-cap, and turn off the probe.

- Measuring DO

1. Prior to the start of the lab, the DO meter was turned on to allow the probe to polarize. If the meter has automatically shut itself off turn it on.
2. The water-saturated air method is used to calibrate the meter and probe.
3. Take the white calibration sleeve, remove the cap from the one, and take out the gray sponge.
4. Saturate the sponge with distilled water, squeeze out the excess water, replace the sponge into the end of the calibration sleeve, and replace the cap.
5. Make sure there are not water drops at the end of the DO probe – if any are present, gently blot dry with a Kim wipe.
6. Insert the DO probe into the calibration sleeve.
7. Select calibrate ("Cal") on the DO meter. The meter will cycle through a few readings, should obtain a reading close to 102.3%, and then go back into measurement mode, reading DO at mg/L or %. Press the "Mode" button until the meter reads DO in units of mg/L.
8. To measure DO of the sample, remove the DO probe from the calibration sleeve and suspend it in the beaker that contains the water sample. Holding the beaker in one hand and the probe in the other, gently stir the sample with the probe to get the water sample flowing past the membrane at the end of the probe. Press "Measure" and continue to slowly stir the sample until the DO reading stabilizes. Record the result in the data table found in **Exhibit 2**.

- Measuring Turbidity

1. Turn on the turbidimeter with the On/Off button that looks like a circle with a vertical line through the top.
2. Push the calibration key, which looks like a two point scatter plot with a best fit line.
3. Follow the instructions on the display. Three standard solutions will be used to calibrate the meter. The first calibration standard has a turbidity of 20 NTU, the second of 100 NTU, and the third of 800 NTU. For each calibration standard, carefully remove it from its storage place, hold it at the top being sure not to touch the sides of the vials. Carefully wipe the sides with a Kim wipe to remove any marks. Gently invert each standard several times to stir up the "sediment" that is creating the turbidity for the sample. Do not shake as it may introduce air bubbles that will cause error in the calibration. Insert the vials into the holding cell with the arrow head facing to the front, close the lid, and press "Read". The display will show the meter stabilizing, will present the result, and will then ask for the next standard. Repeat these steps for each calibration standard.
4. After the 3rd calibration standard has stabilized, press "Done" and then "Store" to save the results.

5. The meter will then require a verification sample to be read. Gently wipe and invert the verification sample cell, place it into the meter's hold cell, close the lid, and press "Read". If the verification sample reads correctly the meter is calibrated and it will automatically re-enter the measurement mode.
6. Once the machine is calibrated test the water sample provided to the group.
7. Obtain the water sample. Gently invert the sample container to mix, but not vigorously as you don't want to add air bubbles as this may impact the results.
8. Rinse the turbidity sample cell two or three times with a small portion of sample.
9. Pour the sample into the sample cell up to the fill line and put on the cap.
10. Using a KimWipe, wipe the entire cell free of fingerprints, water drops, or other marks. Holding the call up to a source of light is useful for this.
11. Gently invert the cell a couple of times to mix the contents. Again, do not shake as tiny air bubbles can alter readings.
12. Place the sample cell into the turbidimeter with the arrow head facing front, close the lid, and press "READ".
13. Records the turbidity value (units are NTU) in the provided data table found in **Exhibit 2**.

ALKALINITY AND HARDNESS TITRATIONS

Introduction and Background

Alkalinity is defined as the ability of water to neutralize acids. This is commonly referred to as buffering capacity and works to prevent a drop in pH. Alkalinity is the sum of all bases found in water that are titratable with a strong acid. It is essentially the opposite of acidity, which can be defined as the presence of a weak acid preventing a rise in pH upon the addition of a strong base. Typically, alkalinity in surface waters is derived from carbonates, bicarbonates, and hydroxides. These carbon sources may or may not be naturally occurring. If they are naturally occurring, it is usually due to the presence of a certain rock type (e.g. limestone, dolomite, ect.). When one makes the assumption that only the inorganic carbon is significantly impacting alkalinity, it can be defined as follows in equivalents/liter (eq/L):

$$\text{Alkalinity} = [HCO_3^-]+[CO_3^{2-}]+[OH^-]$$

Anions such as borates (e.g. $B_4O_5(OH)_4^{2-}$), phosphates (e.g. PO_4^{3-}, HPO_4^{2-}, H_2PO^{4-}) and silicates (e.g. $SiO(OH)_3^-$) may also affect the alkalinity of water. If concentrations of these ions are significant, they must be included in the above equation. Water bodies with high alkalinity (acid neutralizing capacity) are capable of maintaining a pH near neutral pH during environmental events such as acid rain, spring runoff, and acidic or caustic chemical spills. Water with low alkalinity tends to be corrosive, which can bad for pipes in distribution systems or structures made of reinforced concrete or steel.

While alkalinity could be determined by measuring the ions that are contributing to it, the most common method to determine alkalinity is a titration called the Gran Method. According to the Gran Method, alkalinity can be calculated using the following equation:

$$\text{Alkalinity} = 5000*(V_e * N_t) / V_s = \#\ \text{mg/L as } CaCO_3$$

Where V_e = volume of titrant at the equivalence point (L), N_t = normality of titrant in equivalents per liter (eq/L), V_s = sample volume (L), and the 5000 converts from eq of $CaCO_3$ to mg of $CaCO_3$. The normality of the titrant and the volume of sample are predetermined, so the only value that needs to determined is the volume of titrant at the equivalence point.

The equivalence point is the point in the titration where an equivalent or stoichiometric amount of titrant has been added to the sample water to complete the acid-base reactions that are occurring, thus depleting the sample of all of the alkalinity. There are several ways to determine the volume of titrant at the equivalence point. The simplest method to determine V_e, is to add an indicator dye to the water sample. An indicator dye, such as Bromphenol blue indicator solution, will be added to the water sample at the beginning of the titration. As the titration proceeds, the equivalence point will be reached when there is a persistent color change. The volume of titrant used at the point of this color change is the V_e needed to calculate alkalinity. See **Table 1** below for an example of a data set recorded from an alkalinity test.

Table 1. Example data set from an alkalinity test.

Example Alkalinity Test Data		
Vs (L) =	0.2	
Nt (eq/L) =	0.1	
Volume of Acid Added (mL)	**pH**	**Gran Function (F1)**
0.5	7.33	9.37809E-09
1.0	7.19	1.29777E-08
1.5	7.00	2.015E-08
2.0	6.91	2.48514E-08
2.5	6.69	4.13452E-08
3.0	6.52	6.1305E-08
3.5	6.41	7.91707E-08
4.0	6.15	1.44421E-07
4.5	5.76	3.5538E-07
Color Change 5.0	3.98	2.14661E-05
5.1	3.81	3.17662E-05
5.2	3.72	3.91001E-05
5.3	3.57	5.52572E-05
5.4	3.49	6.64661E-05
5.5	3.44	7.46125E-05
5.6	3.38	8.57083E-05
5.7	3.32	9.84542E-05
5.8	3.26	0.000113096
5.9	3.23	0.000121243

The second way to determine the volume of titrant at the equivalence point is to add incremental volumes of titrant, recording the pH change with each addition, and create a titration curve from this data set (cumulative volume of acid added vs pH). If a strong acid is added to a sample with alkalinity and the sample is not complex (i.e. having many species contributing to the alkalinity), a graph similar to **Figure 1** can be generated. As more and more acid is added, the alkalinity buffers the water sample from initially dropping quickly in pH. However, around the equivalence point there is a rapid change in pH where the moles of weak base converted equals the moles of strong acid added and all of the alkalinity is exhausted. The point where there is a change

in curvature from convex to concave, or visa versa, is termed the equivalence point. The volume of titrant used to reach this point is the V_e needed in the alkalinity equation.

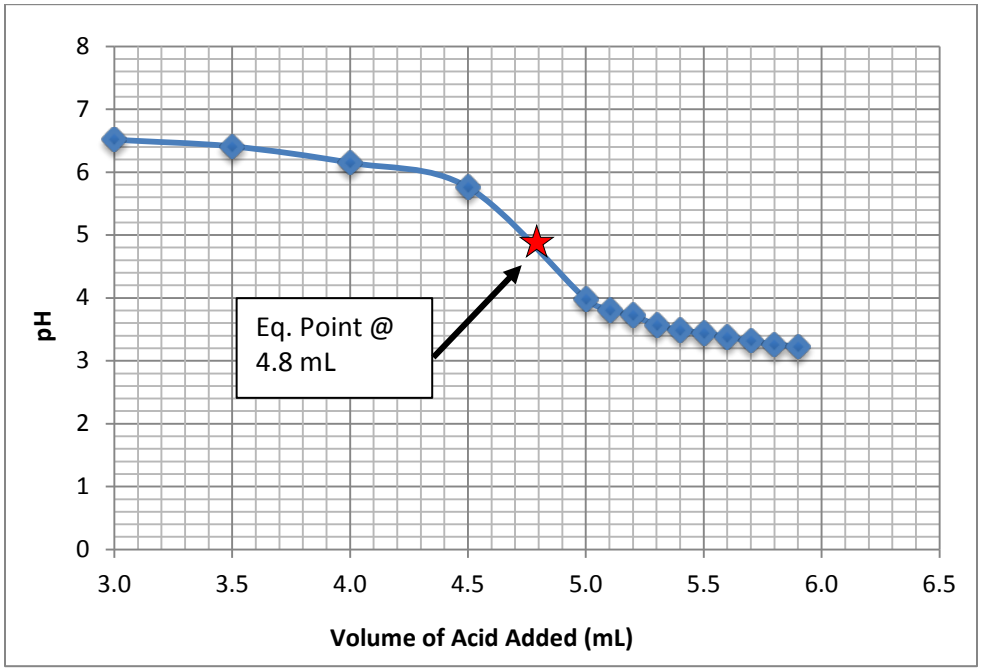

Figure 1: Example alkalinity titration curve.

There are a number of reasons why developing a titration curve can become difficult. One difficulty lies with the type of acid and based found in the water being titrated. When dealing with monoprotic acids and bases (accepts one H^+), the titration curve will look like the one drawn in **Figure 1**. However, if the acid or base accepts more than one hydrogen ion, the curve will become more complex, with multiple equivalence points, creating "steps" in the titration curve. In complex water samples where there are multiple influences on the alkalinity, or if the system is buffered, the equivalence point can become difficult to find or non-existent. In addition, if the alkalinity is very low, it may be difficult to locate the equivalence point on the titration curve. There are multiple ways in which these difficulties can be overcome to determine the volume of titratant used to reach the equivalence point in order to solve for alkalinity. One method requires calculating what is referred to as the first Gran function (F_1). This function is calculated with the following equation:

$$F_1 = (V_s + V_t) * 10^{(-pH)}$$

The first Gran function is determined for each volume of added titrant. Then a plot of F_1 vs volume of added titrant is created. **Figure 2** below is an example of a Gran plot. Note how there is a significant change in slope just as the data approaches a F_1 value of zero. The linear regression line is only plotted through the points on the portion of the data that has a high slope. The linear regression line will intercept the x-axis at the volume of titrant used to reach the equivalence point (V_e). An arrow is used in the plot below to show where the linear regression line intersects the x-axis. This value is the volume at the equivalence point (V_e).

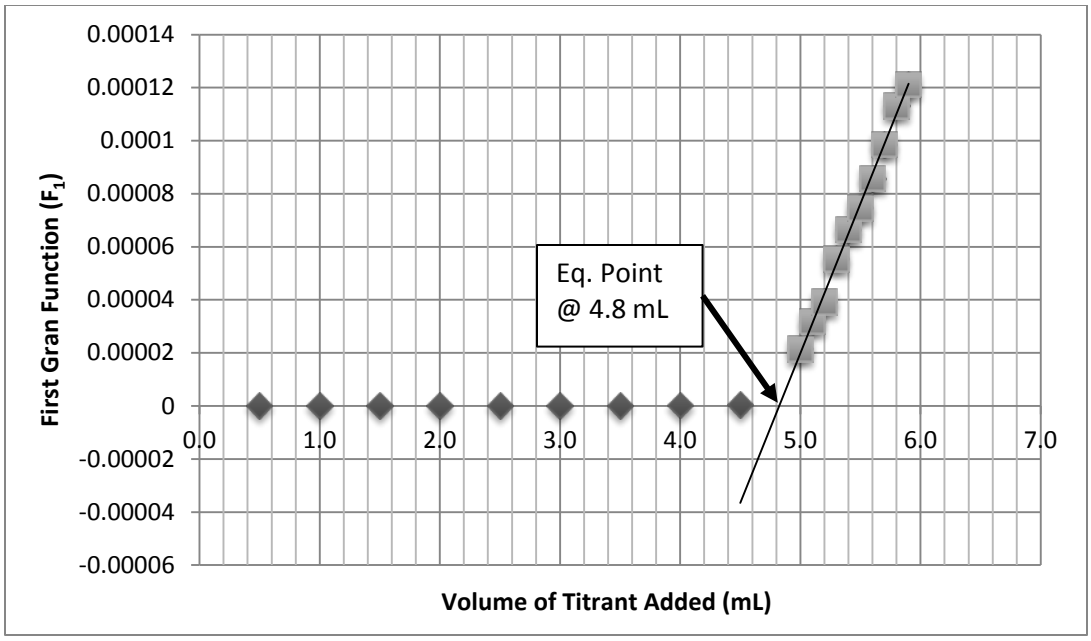

Figure 2. Example of a first Gran function plot for alkalinity.

For natural waters, the equivalence point usually occurs around a pH of 4.5, but this will depend greatly on the geology of the region. It is worth saying that larger volumes of titrant can be added at pH values higher than 5.5, but after this point, smaller volumes should be titrated so as not to miss the equivalence point. Once the volume of titrant at the equivalence point has been determined, it and the sample volume and titrant concentration can be used to calculate alkalinity. Alkalinity is a very important water quality parameter in several remedial/treatment processes. Many treatment process require controlling/driving certain chemical reactions by manipulating pH and alkalinity. For example, passive treatment systems for iron acid mine drainage contamination requires using limestone channels before and between oxidation and settling ponds in order to increase alkalinity, increase pH, and as a result oxidize ferrous and ferric iron into settleable iron oxide compounds.

Hardness was originally associated with the capacity of water to precipitate soap. The polyvalent metal ions associated with water hardness (chiefly Ca^{2+} and Mg^{2+}) can cause the precipitation and buildup of carbonate or the formation of soap scum. In current practice, the hardness of water is defined as the sum of the magnesium and calcium concentrations and is expressed as mg/L of $CaCO_3$. When the hardness is greater than the sum of the carbonate and bicarbonate alkalinity, that amount of hardness equivalent to the total alkalinity is called the carbonate hardness. Hardness in excess of this is called non-carbonate hardness. Water is considered soft when the measured hardness is less than 60 mg/L as $CaCO_3$ and is considered very hard when great than 180 mg/L as $CaCO_3$. The hardness of the water can be impacted by many factors, soil and/or bedrock type being two of the more significant contributing factors. Groundwater typically is hard whereas surface water bodies tend to be softer. This is why most residences with private wells have water softener systems installed as the general consumer tends to prefer soft water as is reduced carbonate scaling, can prevent soap scum, and can produce a good lather with soap. However, excessively soft water can be corrosive to pipes.

The preferred method of hardness determination is through the separate quantification of calcium and magnesium concentrations where:

$$\text{Hardness (mg/L as } CaCO_3) = 2.497\ (\text{Ca in mg/L}) + 4.118\ (\text{Mg in mg/L})$$

This method is more accurate in determining a hardness concentration, but requires two separate analytical techniques. If the results do not warrant this level of accuracy, a single titrimetric technique can be applied that determines the calcium and magnesium hardness simultaneously. The theory behind this technique is outlined briefly below.

Ethylenediaminetetraacetic acid and its sodium salts (EDTA) are added to the solution were they form a complex compound that bonds to metal cations, essentially removing them from the solution as free ions. The amount of EDTA that must be added to remove all of the Ca^{2+} and Mg^{2+} directly correlates to the concentration of these cations – regardless pf valence it is always a 1:1 reaction of EDTA:cations. EDTA is titrated into the sample which contains an indicator die (either Eriochrome Blakc T or Calmagite). The endpoint of the titration is identified where there is a color change in the solution, indicating that all of the Ca^{2+} and Mg^{2+} have been removed.

The sharpness of the titration endpoint improves with increasing pH. To prevent $CaCO_3$ and/or $Mg(OH)_2$ precipitation, the pH for this method is set at a maximum of 10.0 with the stipulation that the titration be completed within 5 minutes. In addition, Mg^{2+} ions must be present in solution to provide a sharp end point. To accomplish this and eliminate the need for Mg^{2+} correction, a small amount of EDTA-Mg complex is added to the buffer solution (although this step can prove problematic in very soft waters where this small volume of EDTA can induce an immediate color-change). The EDTA hardness is determined using the following equation:

Hardness (EDTA) as $CaCO_3$/L = {A*B*1000}/{mL sample used}

Where A = volume of titrant used in the titration and B = mg $CaCO_3$ equivalent to 1.00 mL of titrant.

The variable B depends on the concentration of the titrant: the higher the concentration, the higher the value of B. This value is determined by titrating a standard concentration (1.000 g/L) of reagent-grade $CaCO_3$ with the titrant to be used in the laboratory. This value is often provided on the EDTA solution bottle.

Objectives

- Learn how to perform a titration.
- Quantify the alkalinity (ASTM D1067-02, APHA 2320B) and hardness (ASTMD1126-02, APHA 2340) of a water sample and discuss results from different water sources.

Materials for Measuring Alkalinity

The following materials will be used to determine alkalinity of the water sample.

- Mixing plate and magnet
- Stand with burette clamp
- Burette
- pH probe
- 500 mL beaker
- Graduated cylinder
- DI water
- Bromphenol Blue Indicator solution
- 3 mL dropper pipette
- 0.1N Hydrochloric Acid (HCl) titrant
- Safety gloves
- Safety goggles
- Lab coats

Procedure for Measuring Alkalinity

The following procedure will be used to determine alkalinity of the water sample. Record the pH and titrant volumes in the alkalinity data table found in **Exhibit 3**. The final calculated alkalinity value can be recorded in the data table found in **Exhibit 2**. The final alkalinity value will be shared with the group for discussion of variation in water quality between the different sources.

1. Obtain a graduate cylinder and measure 200 mL of sample water.
2. Transfer sample into a 500 mL beaker.
3. Place a magnetic stirrer into the beaker, place on stir plate under burette found in the fume hood, turn on stirrer. The setup should be positioned beneath the burette.
4. Add 7+ drops of Bromphenol blue indicator solution (note that more may be required to add a noticeable blue color to the solution – check with the instructor).
5. Rinse pH probe with deionized water from squirt bottle and place into sample, submerging the end, but not allowing it to touch the bottom/sides of the beaker.
6. Record the initial volume of acid titrant and initial pH.
7. Slowly add acid titrant in small volumes (0.5 mL), unless pH change is greater than 0.2 units, then adjust accordingly. With each addition of titrant, record the cumulative volume of titrant added and the new pH value.
8. At a pH of about 5.5, decrease the volume of titrant, adding only 0.1 mL or as little as a few drops at a time. With each addition it titrant, record the new cumulative volume of titrant added and the pH.
9. When color change remains constant (blue changes to yellow), record the titrant volume and pH – you have reached the equivalence point.
10. Continue to add titrant in 0.1 mL increments, recording the volume and pH, until you've reached a pH of about 3.
11. Calculate V_e (in L) based on the Bromphenol Blue Indicator dye color change:

    V_e = (titrant volume at color change) – (initial titrant volume)

12. Calculate the alkalinity (in mg/L $CaCO_3$):

    Alkalinity = $5000*(V_e * N_t) / V_s$

    Where V_e = volume of titrant at the equivalence point (L), N_t = normality of titrant in equivalents per liter (eq/L), V_s = sample volume (L), and 5000 converts from eq to mg.

13. Should time permit the groups may collectively work with the instructor to calculate alkalinity using the graphical methods.

Materials for Hardness

The following materials will be used to determine hardness of the water sample.

- Stand with burette clamp
- Burette
- Mixing plate
- Magnet

- 250 mL beaker
- Graduated cylinder
- DI water
- Eriochrome Black T Indicator solution
- Buffer Solution
- EDTA titrant
- 3 mL dropper pipettes
- Safety gloves
- Safety goggles
- Lab coats

Procedure for Hardness

The following procedure will be used to determine hardness of the water sample. Record the titrant volumes in the hardness data table found in **Exhibit 4**. The final calculated hardness value can be recorded in the data table found in **Exhibit 2**. The final hardness value will be shared with the group for discussion of variation in water quality between the different sources.

1. Use a graduated cylinder to measure the water samples. Obtain 100 mL of sample water and place it in a 250 mL beaker.
2. Place the beaker on the mixing plate below the burette found in the fume hood.
3. Place a magnet bar in the beaker and turn on the mixing plate.
4. Add 4 to 8 drops of indicator solution (either Eriochrome Black T) to the sample (note that more may be required to add noticeable color to the solution – check with the instructor).
5. Add 2 mL of the buffer solution. Note – the titration must be completed within 5 minutes of buffer addition. This is to minimize the tendency of the $CaCO_3$ to precipitate from solution. Should the addition of the buffer solution result in a color change – get a new sample volume, follow steps 1 through 4, and skip step 5 (do not add buffer solution).
6. Record the initial volume of EDTA by reading the volume on the burette.
7. Add EDTA titrant slowly (a rate of 1-2 drops per second is ideal), until the last pink tinge disappears. Add the last few drops at 3 to 5 second intervals. At the end point, the solution is normally blue. The indicator dye changes from pink to blue over the span of one drop so care is required. If the endpoint color change is missed the titration will have to be repeated.
8. Records the final volume of EDTA titrant.
9. Calculate the volume of EDTA titrant used.
10. Calculate the hardness (in mg/L $CaCO_3$).

INORGANIC ANALYSIS

Introduction and Background

Metals (inorganic ions, such as iron, manganese, aluminum, arsenic, uranium, and lead) are found in varying concentrations in natural waters. Typically these metals are released from bedrock via dissolution from contact with water. Initially these metals will be present in their dissolved, ion state. In groundwater the metals typically will remain in a dissolved state as groundwater typically has low oxygen concentrations and so oxidation reactions do not occur. In surface water these metals tend to oxidize to some extent, due to high oxygen, microbial oxidation, and reactions with organic material. Presence and concentrations of these

minerals can be quite variable depending on rock type, degree of exposure to water, and water quality. In areas where there has been industrial mining for metal-bearing minerals (e.g. pyrite releases iron), surface water runoff over mine tailings piles can often result in concentrations higher than typical background levels due to natural exposure. Some of these metals may also make their way into waterways from other industrial processes wastewater discharges.

The presence of these metals may or may not be a water quality issue depending on the metal type and concentration. When considering metal concentrations for drinking water purposes, metals like iron, manganese, and aluminum are regulated for aesthetic purposes, not health related concerns. The secondary maximum contaminant levels (SMCL) for these metals is not enforced by the EPA, but in areas where these compounds are found at higher levels drinking water treatment plants will treat for these metals and will meet the SMCL. Metals like arsenic, uranium, and lead do cause health problems, have enforceable maximum contaminant levels (MCLs), and must be treated for in drinking water treatment plants. Metals analysis can be routine in water quality assessment, remediation/treatment design, and remedial/treatment quality control testing. Therefore, it is important to have an understanding of how these materials should be properly sampled and analyzed.

In this module participants will analyze water samples for iron. As mentioned above, iron is a nuisance compound that leads to problems such as red water, staining of laundry and food, pipe fouling and interference of other technical equipment. The drinking water standard for iron is 0.30 mg/L. Iron can be present as ferrous iron (Fe^{2+}), ferric iron (Fe^{3+}), or any number of iron compounds (e.g. $Fe(OH)_3$ or Iron(III) hydroxide). Ferrous and ferric iron are dissolved ions, whereas the iron compounds are considered particulate material. In order to determine the concentrations of ferrous iron, ferric iron, and general iron compounds the water samples must be collected and handled in a particular way. These samples require filtration (0.45 μm filter paper) and acidification (pH < 2 with Nitric Acid) in the field. Filtration separates the free ferrous and ferric ions from the particulate, solid compounds. The acidification forces the iron reactions in such a direction that preferentially the iron remains in a dissolved state – thus not accumulating on the sides of the sample bottle which would lower the iron concentration levels. Additionally, there should be no headspace left in the sample bottles as the presence of atmospheric oxygen could result in oxidation of the dissolved iron species. Once the samples are in a lab and ready for analysis, the concentrations can then be measured in a number of ways, with a: color spectrophotometer, atomic adsorption, iron chromatograph, or gas-chromatography-mass-spectrometry. Should the metal concentrations be over range for the color spectrophotometer, dilution may be required.

Objectives:

- Learn to filter and acidify samples for metals analysis.
- Learn to use a color spectrophotometer to measure total and total dissolved iron concentrations (ASTM D1068-03, APHA 3500-Fe), calculate the concentration of particulate iron, and discuss results from different water sources.

Materials:

The following materials will be used to determine the iron concentration of a water sample.

- 1 beaker
- 1 filtration setup
- Tweezers
- Filter paper
- HACH colorspectrophotometer
- FerroVer Iron power packets
- Scissors

- KimWipes
- Distilled water

Procedure:

The following procedure will be used to determine the concentrations of total, particulate, and dissolved iron for a water sample. Record the results in the data table found in **Exhibit 2**. The results will be shared with the group for discussion of variation in water quality between the different sources.

- To measure total iron:
    1. Turn on the HACH and enter program # 265 (US EPA Ferro Ver Method, Method 8008, Range = 0.02 – 3.00 mg/L).
    2. Obtain a numerically matching pair of 10 mL cuvettes. Fill both of the 10 mL cuvettes with sample water. The bottom of the meniscus should fall just about the 10 mL marker line.
    3. Place the two sample cells on the benchtop in front of the spectrophotometer. The sample cell on the left will serve for the blank and the second sample cell on the right will serve as the sample.
    4. To the second sample cell on the right, add the contents of one FerroVer powder packet to the sample cell. Hold the powder packet at the top, give it a few flicks with a finger to get the powder to the bottom of the packet, use scissors to cut off the top along the black dashed line, pinch either side of the packet and push inwards to open the packet, and invert the packet over the sample cell to dump the contents. Swirl to mix. Push the timer button to start the instrument timer for a reaction time of 3 minutes.
    5. Wipe the sides of sample cells with a KimWipe, removing any spots or smudges.
    6. Once the timer has sounded place the first, blank sample cuvette into the holding chamber of the HACH, close the lid, and hit Zero.
    7. Once a reading of 0.00 mg/L Fe is displayed, remove the blank sample cell from the HACH. Insert the second sample cuvette into the holding chamber, close the lid, and hit Read.
    8. Record your results, which are displayed in mg/L Fe, in the data table found in **Exhibit 2**.
    9. Dump the contents of the sample cell into a waste container, dump the contents of the blank into a sink, and place the cuvettes in a designated wash tray to cleaned later by the instructor. Please be careful when handling the cuvettes as they become very slippery when wet and can be easily dropped and broken.
    10. Note: If the sample's concentration blinks at 3.0 mg/L the sample is over range and will need to diluted. To prepare a x10 dilution, use a pipette to draw 1 mL of sample. Extrude the 1 mL of sample water into a washed and rinsed cuvette. Using the pipette with a clean tip, add 9 mL of distilled water. Both the blank and sample should be prepared in this manner. If you need a clean pair of cuvettes ask the instructor for assistance. Depending on the iron concentration of the sample – further dilution may be required. To prepare a x100 dilution, 1 mL of the x10 solution should be drawn and added to 9 mL of distilled water. To prepare a x1000 dilution, 1 mL of x100 solution should be drawn and added to 9 mL of distilled water.
- To measure total dissolved iron:
    1. To measure total dissolved iron, and then calculate the amount of particulate iron, the sample must be filtered. Typically samples are filtered ahead of time in the field, but in some cases if they are immediately taken to the laboratory after collection they may be filtered in the lab. Filtering may be done with a syringe and screw-on filter or with a larger filter assembly that is hooked up to one of a variety of vacuum systems. A filter setup has been pre-prepared for each group with a 0.45 μm filter paper

2. Turn on the vacuum pump.
3. Pour approximately 200 mL of distilled water onto the middle of the filter. Leave the vacuum on until the entire sample has been pulled through the filter paper.
4. Turn the vacuum off. Remove the bottom portion of the filter apparatus from the collection flask. Transfer 10 mL of the filtrate to a clean cuvette – this will serve as the "blank".
5. Dump the remaining filtrate and reconnect the collection flask to the filter apparatus. Turn on the vacuum pump.
6. Pour approximately 200 mL of sample water into the middle of the filter. Leave the vacuum on until the entire sample has been pulled through the filter paper.
7. Turn off the vacuum pump. Remove the bottom portion of the filter apparatus from the collection flask. Transfer 10 mL of the filtrate to a second clean cuvette – this will serve as the "sample".
8. Follow the same procedure used to measure total iron to measure the amount of dissolved iron.
9. Record the result in data table provided in **Exhibit 2**.

- <u>To calculate particulate iron</u>:
    1. To calculate the amount of particulate iron, subtract the amount of dissolved iron from total iron.
    2. Record this result in the data table provided in **Exhibit 2**.

BIOCHEMICAL OXYGEN DEMAND (BOD) ANALYSIS

<u>Introduction and Background:</u>

The biochemical oxygen demand (BOD) test is used to determine the amount of dissolved oxygen utilized for the degradation of organic matter in waters such as wastewater effluents and polluted waters. It is one of the primary parameters used by wastewater treatment plants and various industries to determine if their treated waste stream is of acceptable quality to be pumped into a fresh surface water source like a river. This form of BOD is termed the carbonaceous demand.

BOD exertion (and utilization) is a complex process and can be affected by the following factors:

- **Microbial population:**
  For degradation of the organic matter in the sample to occur, a microbial population must be present. A suitable population may already be present in the sample itself, as is the case with most wastewater samples. However, other types of water being tested may not contain a sufficient level of microorganisms on their own, requiring that the sample be "seeded" with a microbial population. In their natural environment, the seed microbial population becomes adapted to utilizing the nutrients that are available; however, when they are placed in a different environment with different biodegradable organics, it may take some time for the metabolic machinery to become adapted to the new food source. As an alternative to using a natural seed, laboratory prepared seed is available that includes a wide variety of microbial types this ensuring that biological growth of some type can occur without an acclimation period.

- **Environmental conditions:**
  Factors such as pH, temperature, and availability of nutrients can affect BOD. It is important that analysis is started within 24 hours of collecting the water sample and that it is kept at 4ºC until then. The pH of the sample water should lie between 6.5 and 7.5 and can be adjusted to this range with

sulfuric acid or sodium hydroxide, depending on whether the water is alkaline or acidic. Once the samples have been prepared, they should remain at approximately 20ºC for the duration of the test period.

- **Type of Organic Matter:**
  Organic matter such as simple sugars and amino acids can be degraded faster than polysaccharides and complex proteins, potentially influencing the rate at which oxygen is consumed.

- **Inhibiting and toxic compounds**

The organic matter that is initially utilized is classified as readily or easily biodegradable organic matter. The bacterial population is the first to utilize the organic matter, resulting in a rapid depletion of available oxygen and substrate. This results in the rapid growth of the bacterial population. As the oxygen becomes scarce, bacteria begin to die and are preyed upon by other bacteria and protozoans. The protozoans become the dominant microbe and continue until the amount of organic matter becomes negligible or the oxygen drops below a threshold level and the aerobic bacteria die. A new stage can then begin where anaerobic bacteria begin to grow (assuming that they are present at this stage in the BOD utilization cycle).

The BOD measure, in a BOD_5 determination, is a measure of the oxygen consumed in the first five (5) days of bacterial and protozoan growth. If the dissolved oxygen does not get totally consumed, then most of the growth in the experiment has been bacterial. Because the growth of biomass in the BOD experiment is highly variable, BOD determinations are often difficult to reproduce even between replicates of the same sample. BOD measures should therefore be interpreted with caution.

A different class of microbial cells called algae can also influence the results of the BOD test, especially if the sample is taken from a natural water stream such as a lake. Algae act as a source of oxygen due to their photosynthetic metabolism which produces oxygen as a by-product. To minimize the impact of algae, BOD bottles are stored in the dark during the five-day incubation period. The results of any BOD test on waters where algal growth is significant or where light is allowed to shine on the BOD bottles should be considered faulty.

The carbonaceous oxygen demand is the oxygen used by microorganisms in the breakdown of organic matter. However, oxygen may also be used to oxidize reduced forms of nitrogen. This is termed the nitrogenous demand. The oxidation of reduced forms of nitrogen requires the presence of microorganisms capable of carrying out this oxidation. In many waters, including raw sewage and primary effluent, these microorganisms are not present in sufficient enough numbers to have much influence during a 5 day BOD test. Usually, they will not exert a significant oxygen demand until day seven or eight (at 20ºC). Under these circumstances, the BOD_5 measured will be the carbonaceous BOD_5 because the decrease in oxygen is attributable to bacteria using carbon compounds as a nutrient source. As the BOD test reaches the seventh or eighth day, nitrifying bacteria begin to exert a measurable amount of oxygen demand (3.76 mg O_2/mg NH_3). Measurements of BOD that include both carbonaceous and nitrogenous demand are not a true measure of the oxygen required to degrade organic matter and it is often desirable to inhibit the nitrogenous demand. Inhibition of nitrogenous demand can be achieved by using a chemical inhibitor.

BOD_5 levels in waste streams can be quite variable depending on the source of the waste and other water/wastewater quality parameters (e.g. water at lower temperatures can hold more oxygen). Animal manure may have a BOD level as high as 20,000 mg/L, sewer water is approximately 150-250 mg/L, and treated municipal sewer waste is approximately 20 mg/L.

Objectives

- To quantify the five-day carbonaceous biochemical oxygen demand (BOD_5) (ASTM D6238, APHA 5210) of a water sample and discuss results from different water sources.

Materials

The following materials will be used to determine the BOD_5 of a water sample.

- Sterile BOD bottles
- Water sample
- Sterile deionized water
- Labeling tape
- DO probe
- Squirt bottle of sterile deionized water
- Kim Wipes

Procedure

The following procedure will be used to determine the BOD_5 for a water sample. Record the results in the data table found in **Exhibit 5** and **Exhibit 2**. The results will be shared with the group for discussion of variation in water quality between the different sources.

First, each group will learn how to prepare BOD bottles for analysis. Then, the groups will analyze BOD bottles prepared 5 days ago in order to determine the sample's BOD_5. Note that we will not be diluting the samples or adding a seed or nitrogen inhibitor.

- Preparing the sample bottles:

    1. Obtain 4 sterilized BOD bottles.
    2. Prepare and adhere labels. All labels should include the Sample ID, date at t = 0, initials of the person(s) conducting the test, BOD day number (BOD_t, where t = 0 or 5), and indicate whether the bottle is the blank or sample. There should be a blank bottle and sample bottle for day 0, and a blank bottle and sample bottle for day 5.
    3. Vigorously shake the jug of sample water in order to aerate the sample, saturating the water with dissolved oxygen.
    4. Immediately upon aerating the sample water, fill the BOD bottles to the top with sample water. Place the stoppers in the bottles. When the caps are put on the bottles, they should displace water. If they do not displace water, add some more sample water. This will ensure a tight seal and prevent air from being trapped in the bottles (which could potentially alter the dissolved oxygen readings).
    5. Start a timer for 15 minutes.
    6. Vigorously shake the jug of sterile, deionized water (with the same vigor and for the same period of time as the sample water).
    7. Immediately upon aerating the deionized water, fill the blank water bottles to the top with deionized water. Place the stoppers in the bottles. When the caps are put on the bottles, they should displace water. If they do not displace water, add some more sample water. This will ensure a tight seal and prevent air from being trapped in the bottles (which could potentially alter the dissolved oxygen readings).

8. Start a second timer for 15 minutes.
9. Place all bottles for sample day 5 in the designated dark storage compartment.
10. Put the samples aside that you just prepared; you will now work with the samples prepared for you five, 5, days prior to this short course.
11. Turn on and re-calibrate the DO probe, following the instructions from the "Basic Water Quality Parameter" section above.
12. After the 15 minutes has passed for the Day 0 blank and sample bottles, measure and record the DO concentration in the data table found in **Exhibit 5**. To measure DO in the BOD bottle, Remove the stopper from the BOD bottle, carefully insert the probe into the bottle until it is at a medial depth. Holding the bottle very carefully as it is wet and very slippery, gently swirl the bottle so that water is flowing past the membrane at the end of the probe.
13. The instructor will provide each group with the DO readings for the Day 0 sample and blank of each group's source water. Enter these values in BOD Analysis Data Table (**Exhibit 5**).
14. Measure the amount of dissolved oxygen for the prepared blank and sample bottles for the group's sample source, for Day 5. Enter these values in BOD Analysis Data Table (**Exhibit 5**).
15. Determine the BOD_5, show your work and final result in the BOD Analysis Data Table (**Exhibit 5**):

    $BOD_t = \{(D_1-D_2) – (B_1-B_2)\}/P$

    Where 1= initial (t=0) and 2 = final, D = sample, B = blank, and P = dilution factor (e.g. 1mL/300mL). Note: if the sample was not diluted – 300mL sample/300mL = 1.

REFERENCES CITED

American Public Health Association (APHA), 1998. Standard Methods for the Examination of Water and Wastewater, 20th edition. American Public Health Association, Washington, D.C.

American Society For Testing and Materials (ASTM), 2004. Annual Book of ASTM Standards, Section 11, Water and Environmental Technology. ASTM, West Conshocken, PA.

Drever, J., 1997. The geochemistry of natural waters surface and groundwater environments: Upper Saddle River, Prentice Hall.

Droste, R., 1997. Theory and practice of water and wastewater treatment: New York, John Wiley and Sons, Inc.

Langmuir, D., 1997. Aqueous environmental geochemistry: Upper Saddle River, Prentice Hall.

Stumm, W. and Morgan J.J., 1996. Aquatic Chemistry: Chemical Equilibria and Rates in Natural Waters, third ed., New York, John Wiley and Sons, Inc..

Tchobanoglous, G. and Schroeder, E.D., 1987. Water Quality: Reading, Massachusetts, Addison Wesley Longman.

US Environmental Protection Agency (EPA), 1974, Safe drinking water act, US EPA.

US Environmental Protection Agency (EPA), 1979, Federal register secondary national drinking water standards – final rule, 44FR 42195.

US Environmental Protection Agency (EPA), 1992, Secondary drinking water regulations: guidance for nuisance chemicals, EPA 180/K-92-001.

vanLoon, G.W. and Duffy, S.J., 2000. Environmental chemistry: New York, Oxford University Press.

Exhibit 1: Example Chain of Custody form

CANTON
STATE UNIVERSITY OF NEW YORK

SUNY CANTON CHAIN OF CUSTODY

Page ____ of ____

Department of Civil and Construction Technology
Canino School of Engineering Technology
Nevaldine North 105, 34 Cornell Drive, Canton, New York 13617

TEL: 315-386-7411
FAX: 315-386-7928

Date Rec'd in Lab: _____
SUNY Canton Job #: _____

Client Information

Client:
Address:
Phone:
Fax:
E-mail:

Project Information

Project Name:
Project Location:
Project Manager:
Send Report to:
Send Invoice to:

SUNY Canton ID	Client Sample ID	Date Sampled	Time Sampled	Sample Matrix	Sampler's Initials	Analysis: Alkalinity	Hardness	Inorganics - Iron (total and dissolved)	BOD				
SC-NYSGA-10122014-1	Raquette River	10/7/2014	3:45pm	SW	ACR	√	√	√	√				
SC-NYSGA-10122014-2	Potsdam Tap Water	10/7/2014	4:00pm	DW	ACR	√	√	√	√				
SC-NYSGA-10122014-3	Private Well	10/7/2014	5:00pm	GW	ACR	√	√	√	√				
SC-NYSGA-10122014-4	Mine tailing runoff	10/7/2014	2:00pm	SW	ACR	√	√	√	√				

Matrix Code: DW = Drinking Water, GW = Groundwater, SW = Surface Water, WW = Wastewater, RW = Raw Water, SE = Sediment, SL = Sludge, S = Soil, SD = Solid, W = Wipe, Oil = Oil, B = Bulk, L = Liquid

Preservation Code: A = None, B = HCl, C = HNO3, D = H2SO4, E = NaOH, F = MeOH, G = NaHSO4, H = Na2S2O3, I = Ascorbic Acid, J = NH3CL, K = Zn Acetate, O = Other

Container Code: P = Plastic, A = Amber Glass, V = Vial, G = Glass, B = Bacteria Cup, C = Cube, D = BOD Bottle, O = Other

Filtered (Y/N):	
Preservation	
Container Type	

Special Instructions, Comments, Requests:

Relenquished By:	Date/Time:	Received By:	Date/Time:

Time:

Standard: ____
Rush: _____
Due Date: _____

Arrival Conditions of Samples:

Cooler (Y/N): ____
Coolant (IPK, Ice, Dry Ice, None): _____
Temperature (°C): _____
Other: _____

Exhibit 2: Summary Data Table for Water Quality Parameter Analytical Results

Water Quality Testing Analytical Results Summary Table		
Sample ID: **Source:**		
Parameters	**Results**	**Comments**
pH		
Temperature		
Conductivity		
Turbidity		
Alkalinity		
Hardness		
Total Iron		
Particulate Iron		
Dissolved Iron		
BOD_5		

Exhibit 3: Data Table for Alkalinity Analysis

Alkalinity			
Sample ID: **Source:**			
N_t of titrant **(Hydrochloric Acid, HCl, eq/L)**			
V_s (volume of sample, L)			
Volume of Titrant (mL)	**pH**	**Volume of Titrant (mL)**	**pH**

Exhibit 4: Data Table for Hardness Analysis

Hardness	
Sample ID: **Source:**	
Initial Volume of EDTA (mL)	
Final Volume of EDTA (mL)	
Volume of EDTA used in the titration (mL) - A	
mg $CaCO_3$ equivalent to 1.00 mL of titrant - B	
Volume of Sample Used (mL)	
Hardness (mg/L as $CaCO_3$)	

Exhibit 5: Data Table for BOD Analysis

Biochemical Oxygen Demand (BOD)		
Sample ID: **Source:**		
Day 0 Results for Bottles Prepared During the Short Course		
Sample Day	**Sample DO Concentration (mg/L)**	**Blank DO Concentration (mg/L)**
0		
Pre-Prepared BOD Bottle Results		
Sample Day	**Sample DO Concentration (mg/L)**	**Blank DO Concentration (mg/L)**
0 (provided)		
5		
Calculated BOD_5 for Pre-Prepared Bottles		
BOD_5 (mg/L)		

GEOLOGY OF THE CAMBRIAN NONCONFORMITY AT THE WELLESLEY ISLAND STATE PARK NATURE CENTER

Courtesy of Dr. DAVID VALENTINO, SUNY Oswego, 13126

INTRODUCTION

Wellesley Island straddles the international border between the USA and Canada within the Saint Lawrence Seaway, and in the heart of the Thousand Islands region (Figure 1). The island is underlain by Mesoproterozoic gneisses of the Frontenac Arc with a thin veneer of the Cambrian Potsdam sandstone. Bedrock exposures are abundant, with easy access to most rock types. Wellesley Island State Park nearly spans the distance between the two channels of the Saint Lawrence River. This self-guided field trip is a walking tour of the geology within the Minna Anthony Common Nature Center, located on the southwestern corner of the island within the state park (Figure 2).

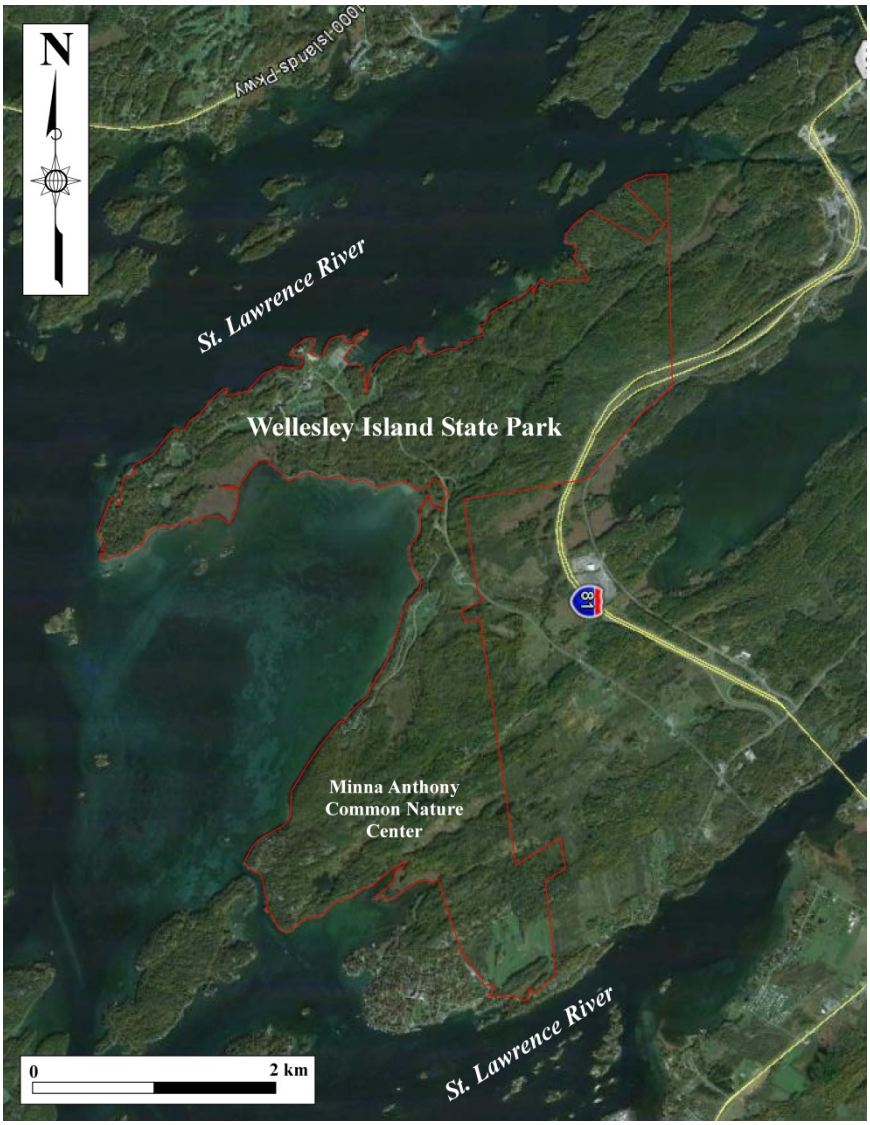

Figure 1. Air photograph of the southwestern end of Wellesley Island showing the location of the state park and the Minna Anthony Common Nature Center.

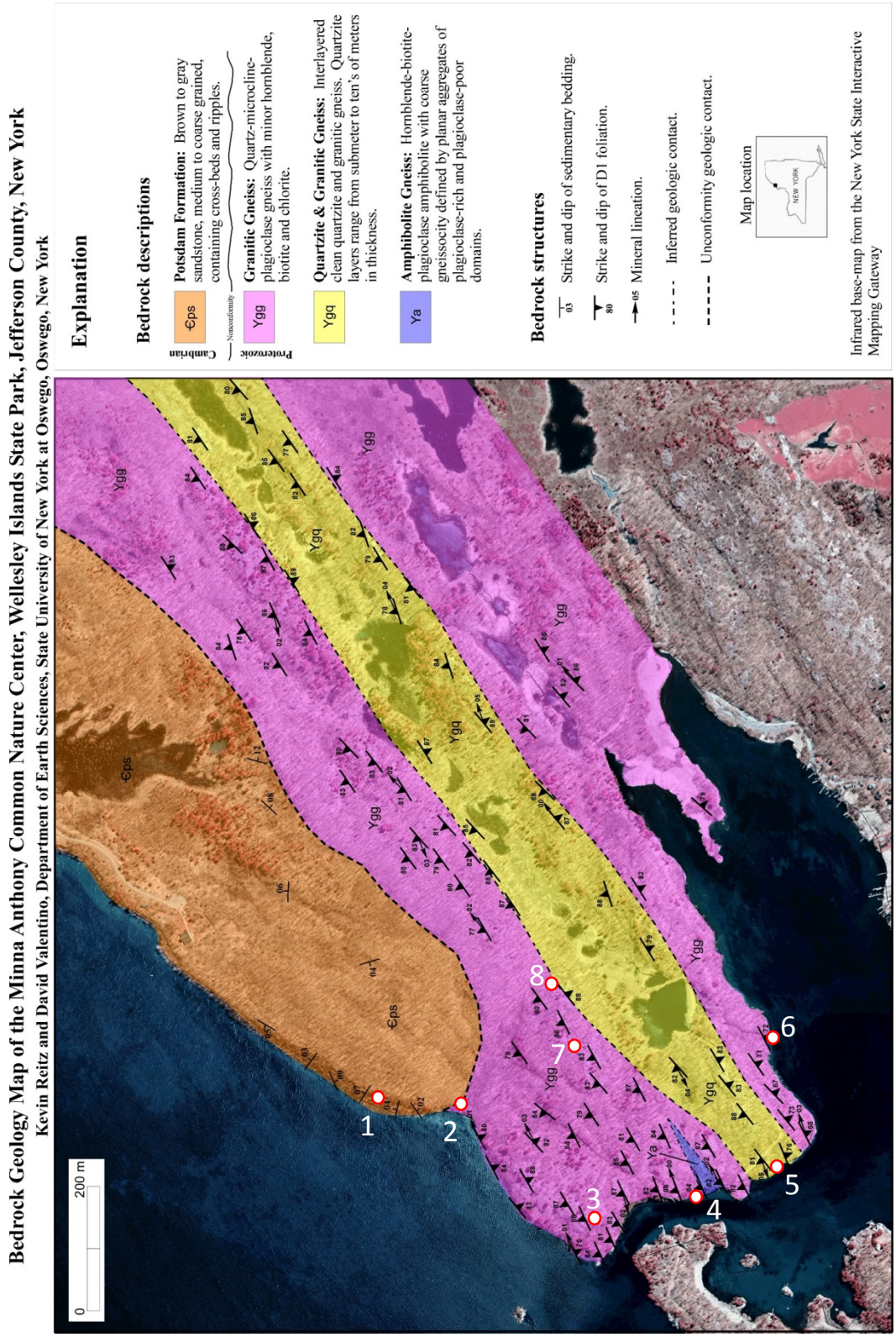

Figure 2 – Bedrock geology map of the Minna Anthony Common Nature Center, Wellesley Island, New York.

GEOLOGY OF MINNA ANTHONY COMMON NATURE CENTER

A series of well-marked trails lead from the parking area, across and around the wooded peninsula that makes up the Minna Anthony Common Nature Center. There is no specific trail to follow for this self-guided tour, however, a few key outcrop locations are marked on Figure 3 that will illustrate the different rock units and contact relations between units. Under no circumstances should anyone use a rock hammer or collect any samples in the nature center unless you have obtained a permit from NYS DEC in advance. There are many fresh bedrock exposures that can be studied without a hammer.

Location 1 – A series of deeply weathered outcrops of the Potsdam formation occur along the trail that follows the north shore of the island. At these locations, the Potsdam formation is a brown to gray, thin to medium bedded, medium to coarse grained sandstone with well-developed ripple marks and cross beds. The overall bedding attitude dips a few degrees northeast.

Location 2 – The trail traverses down-hill into a small cove. As you walk down the hill, note the transition in the bedrock. There are exposures of granitic gneiss at lake level on the west side of the cove. This is good place to stand on the gneiss and talk about the nonconformity contact relationship with the Potsdam sandstone.

Location 3 – There are many fresh exposures of the granitic gneiss as the trail winds around the southwestern end of the peninsula. The gneiss contains recrystallized quartz, microcline and plagioclase with minor hornblende and biotite. In places, the biotite has been replaced by chlorite. The gneiss contains a weakly- to strongly- developed foliation and mineral lineation. The foliation is defined by planar aggregates of the recrystallized feldspars and quartz, it generally strikes ENE and dips steeply to the north. Subhorizontal mineral lineations are defined by elongate hornblende and biotite grains in the foliation plane. Some exposures exhibit well developed lineation with very weak foliation (L>>S tectonite).

Location 4 – This location requires leaving the trail and is difficult to access. It is not recommended to take a larger group of people to this location at the same time. A thin amphibolite body is exposed in the rock ledge that overhangs the water. It contains planar aggregates of hornblende, biotite and plagioclase that define foliation that is concordant with the local foliation in the other rock units. The contact with the granitic gneiss is parallel to the foliation.

Location 5 – Outcrops along the river edge contain foliated quartzite that is interlayered on the meter-scale with the granitic gneiss. The quartzite contains quartz with accessory grains of biotite.

Location 6 – A glacier polished outcrop at river level at this location shows excellent field relations between the quartzite and granite intrusions. The well foliated quartzite is cross cut by a coarse granite dike with the contact exposed. In turn, both of these units are cross cut by a second steeply dipping granite dike that is about 40 cm wide.

Location 7 – Although this location only includes more of the granitic gneiss, the excellent exposures on the glacier polished ridge allow for the study of the rock fabrics in detail.

Location 8 – The northeastern end of the granitic gneiss ridge has a series of outcrops that show the field relations with the quartzite. There are small to large blocks of quartzite that form xenoliths in the granitic gneiss. There are also places were small granite injections penetrated the quartzite blocks along fractures.

FIELD EXERCISE

After leading students through the suggested field locations as an introduction to the area, it is recommended that the students are turned loose to discover the geology in teams of two or three. An infrared false color image and a topographic map are provided herein. Individual outcrops can easily be located on the infrared image while in the field. This exercise has been used as a first mapping experience for classes in structural geology, petrology, historical geology and geophysics at SUNY Oswego. The well exposed rock units and the relative ease of access makes it possible for students to cover the 1 square kilometer area in an afternoon. Please

emphasize that rock hammers are not to be used and samples should not be collected. Once the mapping exercise is over, it has been instructive to take students to the noncomformity outcrop located on Route 12, about 2 km north of Alexandria Bay. This world-class exposure can serve as the answer-key to the mapping exercise.

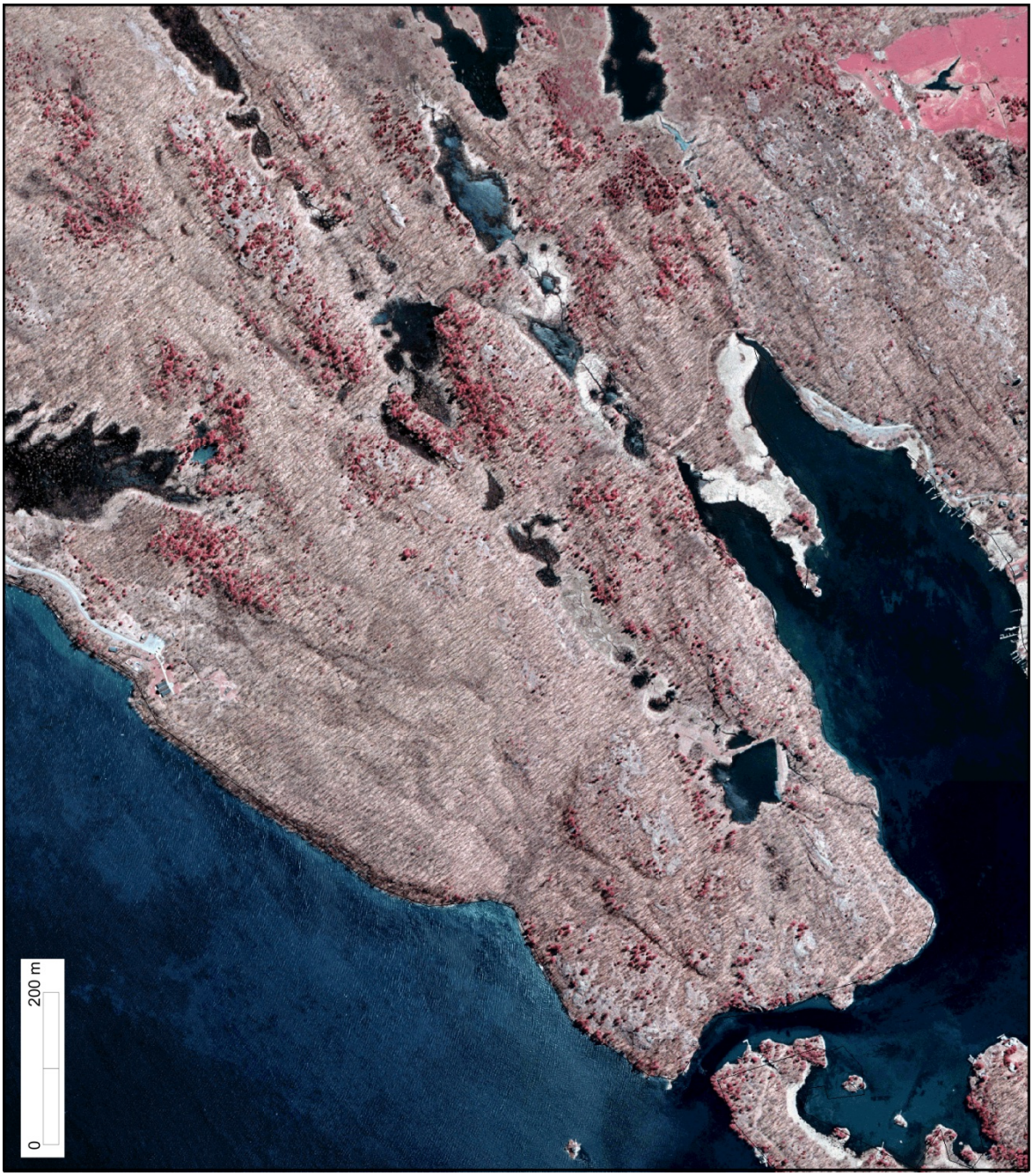

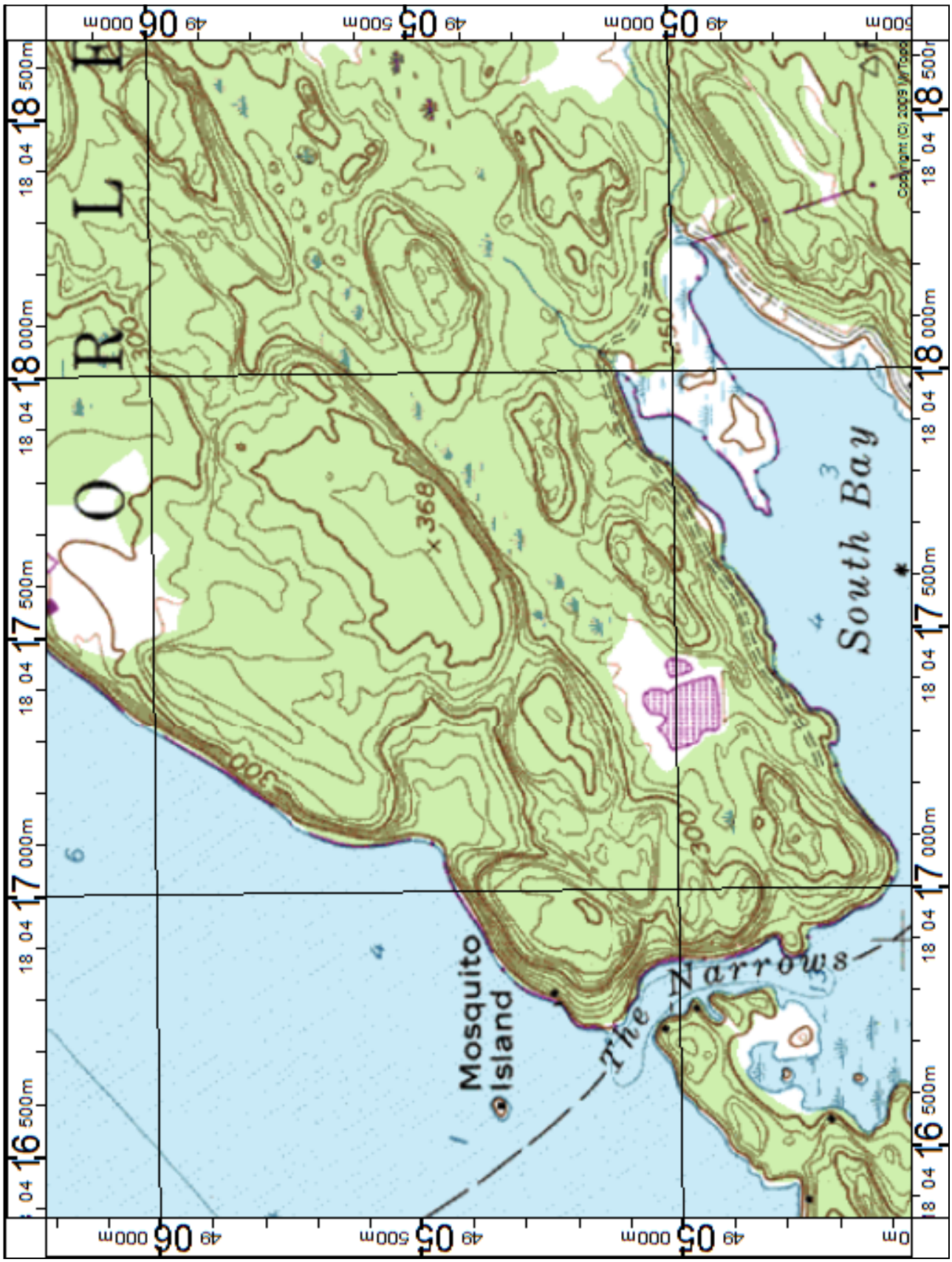
South Bay
Mosquito Island
the Narrows
368